Adsorption of plasma and blood elements onto hydrogel coated silicone rubber of different filler concentration

by

Katherine Ann Schwen

A Thesis Submitted to the
Graduate Faculty in Partial Fulfillment of the
Requirements for the Degree of
MASTER OF SCIENCE

Major: Biomedical Engineering

Approved:

Signatures have been redacted for privacy

Iowa State University
Ames, Iowa

1984

TABLE OF CONTENTS

LIST OF TABLES

LIST OF FIGURES

INTRODUCTION

Small diameter (5mm inside diameter, or less) polymeric arterial prostheses have shown limited success when implanted. Small caliber vascular prostheses are needed in situations in which the recipient's autologous veins are not adequate for grafts for use in coronary bypass or femoropopliteal bypass operations. This limited success of small diameter vascular prostheses is due to the foreign body nature of the implant. The possibility of protein accumulation and thrombosis is always present for a prosthesis exposed to biological fluids of high protein content (i.e., blood).

A number of investigators believe that one of the most important criteria in determining the biocompatibility of polymers is the protein film adsorbed onto polymers exposed to flowing blood (Jakobsen and Gendreau, 1978; Lyman et al., 1974). Platelet adhesion is believed to be promoted by the adsorption of specific proteins, thereby triggering the cascade sequence which leads to thrombus formation. The chemical nature of the surface has in turn been found to selectively influence the composition of the adsorbed protein layer (Lyman et al., 1974; Kim and Lee, 1975).

The physical properties of hydrogels resemble those of living tissue more so than any other class of synthetic biomaterial (Ratner and Hoffman, 1976). Andrade (1973) found these acrylic gels to be compatible with many types of biological tissue, including blood. The potential use of these materials in blood contact environments is of interest in this study in view of their many desirable characteristics.

The hydrogels hydroxyethyl methacrylate (HEMA) and N-vinyl pyrrolidone (NVP) were chosen as candidates for ex vivo biocompatibility testing. Various formulations of HEMA and NVP were copolymerized onto the interior surfaces of Silastic ® tubes which had been previously coated with silicone rubber with or without silica filler (0 and 24%). The silica filler content of silicone rubber was varied to test the hypothesis that filler free silicone rubber is less thrombogenic than silicone rubber containing filler. It is known that NVP penetrates the silicone rubber matrix, whereas HEMA localizes on the surface of the silicone rubber matrix. An hypothesis to be tested is that the impregnation from NVP and/or the buildup of a thin coating from HEMA onto the silicone rubber at different filler concentration may have a synergistic effect in that impregnations, coatings, or filler contents of silicone rubber affect the biocompatibility of the material, and certain of these treatments (alone or in combination) may offer improvement in blood compatibility. The initial blood-foreign material interactions of these composite materials were sampled at blood exposure time periods of 0.25, 0.5, 5, 15, and 75 minutes. They represent a range of material properties of interest including critical surface tension and hydrophilicity. They were characterized using scanning electron microscopy for microstructural information and a Fourier Transform infrared/attenuated total reflectance (FT-IR/ATR) technique for monitoring protein buildup.

OBJECTIVES

The objectives of this study are to investigate what effects certain implant variables have on short-term blood-biomaterial interactions. The biomaterial formulations chosen for this study consist of HEMA and NVP polymerized alone and copolymerized onto 0% silica filler and 24% silica filler content substrates. The specific objectives include the following:

1) To evaluate the effects of silica filler by comparing the results from silica containing substrates with those from substrates which do not contain filler.

2) To monitor the relative buildup of protein and cellular material with time of blood exposure.

3) To monitor the character of the buildup of material (i.e., the microstructural features of the thrombi).

4) To identify patterns of blood-material interaction.

5) To note if the responses are consistent with, or can be related to, the chemical characteristics of the sample and/or to the texture of the surface.

LITERATURE REVIEW

Thrombosis

The sequence of events which leads to possible thrombus formation on foreign materials exposed to whole blood is generally agreed to be the following: adsorption of plasma proteins, platelet adhesion, platelet release and aggregation, fibrin formation, and subsequent thrombus formation (Lyman et al., 1975). Other investigators have found white blood cells (leukocytes) to play a role in thrombosis (Van Kampen et al., 1979); Barber et al., 1979). The thrombotic growth can lead to total or partial blockage of the lumen unless the thrombus is shed off by shear forces (Madras et al., 1971) or released from the surface as an embolus in some other way (for instance, by a nonadhesive surface as proposed by Ratner et al., 1979). Tissue infarction can be caused by emboli which may lodge in organs such as the heart, lung, brain, and kidney.

Adsorption of plasma proteins

The noncellular portion of blood, the blood plasma, consists of approximately 90% water and 10% organic and inorganic solutes. Three-fourths of the solutes are plasma proteins, which consist of the following three major fractions: albumin, globulin, and fibrinogen. Serum albumin, which is the most abundant plasma protein, functions in osmotic regulation and the transport of important nutrients such as fatty acids and bilirubin. The globulin fraction is further subdivided into many components. The gamma globulins, which function as antibodies, are glycoproteins (conjugated proteins which contain carbohydrate prosthetic group components) and

have been the most studied globulins in relation to their adsorption onto polymer surfaces. Fibrinogen is also a glycoprotein and functions in blood clotting.

The major reason for studying the nature of protein adsorption onto polymer surfaces is the strong and frequently specific influence of adsorbed proteins on cellular reactions (Horbett, 1982). In fact, the film of adsorbed protein which deposits onto a polymer surface in contact with whole, flowing blood has been demonstrated by previous studies to be the first, and perhaps most important, step in determining the biocompatibility of the polymer (Jakobsen and Gendreau, 1978; Lyman et al., 1974). The composition of the adsorbed protein film (Roohk et al., 1976; Lyman et al., 1975; Young et al., 1982), as well as the conformation of the proteins adsorbed onto a surface (Jakobsen and Gendreau, 1978), are factors which various investigators have postulated to be of importance in determining biocompatibility. All surfaces, except possibly thin hydrogels, are spontaneously coated with protein upon exposure to whole blood or plasma (Bruck, 1973). Under physiologic flow conditions, a protein layer of approximately 200 Å is adsorbed onto foreign material surfaces before platelets attach to these surfaces (Baier, 1978a).

Specifically, the adsorption of albumin, fibrinogen, and gamma globulins onto polymer surfaces has been shown to affect the thrombogenicity of the polymer. It has been consistently shown that surfaces which preferentially adsorb, or are precoated with fibrinogen, promote thrombus formation (Packham et al., 1969; Lee and Kim, 1974; Roohk et al., 1976). On the other hand, albumin coated surfaces are likely to attract fewer platelets

and become passivated (Barber et al., 1979; Lyman et al., 1974; Packham et al., 1969). Gamma globulins also appear to be thrombus formation promoters since they have been shown to attract an increased number of platelets (Roohk et al., 1977; Kim et al., 1974).

Many investigators believe that the mode of protein adsorption is important (Baier, 1972; Bruck, 1973). Bagnall (1977) stated that protein adsorption onto hydrophobic surfaces will involve molecular distortion since a globular protein consists of a hydrophobic core with a hydrophilic outer surface, and the protein is attempting to optimize both nonpolar amino acid-surface and polar amino acid-water interactions. To minimize interfacial tension, the adsorbed protein attempts to present as nonpolar a surface as possible to the hydrophobic substrate. However, steric constraints make it necessary that some polar groups will be present at the substrate-protein interface. In contrast to what Bagnall (1977) stated, Lyman et al. (1968) and Brash and Lyman (1969) concluded that plasma proteins are not drastically denatured on nonwettable surfaces. Theoretically, denaturation and adsorption of proteins onto foreign surfaces will be caused by any condition which upsets the balance of forces controlling the conformation of a protein in solution (Cottonaro et al., 1981). Conditions which can cause conformational changes are osmotic pressure, pH, ionic balance, and temperature.

Several investigators agree that weaker surface-protein interactions occur at more hydrophilic surfaces than hydrophobic surfaces (Weathersby et al., 1977; Brash and Lyman, 1971). Brash and Lyman (1971) concluded that protein adsorption onto hydrophobic surfaces is generally irreversible,

whereas protein adsorption onto hydrophilic surfaces is reversible. In contrast, Ratner et al. (1979) suggested that purely hydrophilic (polar) surfaces may strongly interact with plasma proteins.

Platelet adhesion, release, and aggregation

Platelets (thrombocytes) make up less than 1% of the total cellular volume of whole blood. In adults, platelets originate in the red bone marrow by fractionation of the cytoplasm of megakaryocytes (giant cells). Platelets, which are 2-4 μm in diameter, contain two types of granules: α granules, which contain clotting factors and other proteins; and dense granules, which contain Ca^{+2}, serotonin, adenosine 5'diphosphate (ADP), and adenosine 5'triphosphate (ATP). Their membrane is extensively invaginated, and they have a canalicular system in contact with the extra cellular fluid. Platelets can change morphology, discharge their granular contents (platelet release), and collect at the site of injury (platelet aggregation). Platelets play a major role in thrombus formation.

Most investigators believe that platelets do not contact, or have very little contact, with a foreign surface but instead contact and adhere to a layer of deposited noncellular blood components (Dutton et al., 1969; Baier et al., 1971; Kim et al., 1977). Lee and Kim (1974) proposed a platelet adhesion model which involves reaction of the platelet membrane glycosyl transfurase (an enzyme) with surface adsorbed glycoproteins.

When the platelet release reaction is stimulated, the released ADP (from the platelet's dense granules) promotes release of granule contents from other platelets and makes platelets sticky which in turn promotes

platelet aggregation. The isovolumic shape change in which the platelets round up and put out pseudopodia presumably promotes platelet aggregation (Gordon, 1976; Lee and Kim, 1974). The release reaction can be induced in vitro by stimuli such as thrombin, collagen, or ADP (Gordon, 1976). Likewise, release has been shown to be stimulated by adhesion to foreign surfaces (Whicher and Brash, 1978; Packham et al., 1969). Whicher and Brash (1978) observed that collagen and gamma globulin were quite reactive in terms of mean adhesion and release and that two hydrophilic polyurethanes and albumin had negligible platelet adhesion.

Other cellular elements

Red blood cells (erythrocytes) and white blood cells (leukocytes) comprise the remainder of the cellular elements in blood. Red blood cells are approximately 7.5 μm in diameter and are usually associated with fibrin when involved in the clotting process. White blood cells consist of the granulocytes (polymorphonuclear leukocytes), lymphocytes, and monocytes. Polymorphonuclear leukocytes and monocytes have been observed to participate in the thrombotic process (Barber et al., 1978, 1979; Van Kampen et al., 1979). The thrombogenic powers of leukocytes have been known for some time (Niemetz and Fani, 1973). Neutrophils (polymorphonuclear leukocytes), which are the most abundant white blood cell, and monocytes are both phagocytic and attracted by chemotactic stimuli. Lymphocytes are the second most abundant white blood cell and play an important role in immunity. White blood cell adhesion has been observed to release a substance which interacts with the fifth component of complement to generate a chemotactic activity (Gordon, 1976).

Fibrin and thrombus formation

The blood coagulation process involves a complex series ("cascade") of reactions and is responsible for the formation of fibrin. The basic reaction in the coagulation of blood is conversion of the highly soluble plasma protein fibrinogen into insoluble fibrin monomer by thrombin (a proteolytic enzyme). The fragile fibrin clot that is formed by this aggregation of fibrin monomers is subsequently stabilized by covalent cross-links formed between the side chains of fibrin molecules. The latter reaction is catalyzed by factor XIII, the fibrin-stabilizing factor, and requires Ca^{+2}. There are two enzymatic pathways of blood clotting: the intrinsic and extrinsic pathways. The intrinsic pathway can be presumably activated in vivo when blood is exposed to collagen fibers underlying the endothelium in the blood vessels. The extrinsic pathway can be activated by tissue thromboplastin, a protein-lipid complex released from blood vessel walls and other damaged tissues. The adsorption of plasma proteins, platelets, and leukocytes onto artificial surfaces appears to activate the blood coagulation systems (Lindsay et al., 1980). Platelets and leukocytes that are activated appear to have the ability to trigger both the intrinsic and the extrinsic blood clotting systems (Lindsay et al., 1980). Coagulation promoted by a platelet near an aggregate depends on three reactions: (1) collagen activation of coagulation Factor XI on the membrane of the platelet; (2) the procoagulant phospholipid complex (platelet factor 3) unmasking at the surface of activated platelets; and (3) the release from platelet storage granules of fibrinogen and antiheparin (platelet factor 4).

The subsequent thrombus formation on a surface exposed to whole blood is therefore due not only to platelet activation but to the activation of the blood coagulation systems. The thrombi on a foreign surface can be composed largely of platelets containing an abundant amount of fibrin (Dutton et al., 1969). These thrombi are called white thrombi and are promoted at high shear rate (arterial) flow conditions (Hoffman, 1982). Dutton et al. (1969) observed columnar shaped platelet aggregates initiating at the foreign surface and extending into the blood for a variety of foreign surfaces exposed to whole blood. These columnar shaped platelet aggregates were surrounded by a red cell fibrin mesh as the thrombus grew in thickness.

For some polymer surfaces, the little thrombus accumulation on the surface may be due to a shedding of the material by a nonadhesive surface rather than good blood compatibility (Ratner et al., 1979). In other words, some surfaces are in fact thrombogenic but are not strongly thromboadherent. Thromboemboli can cause tissue damage and infarcts. However, if the emboli that are spewed off are small enough, the normal enzymatic processes in the flowing stream can handle the emboli in such a way that they cause no tissue damage or infarcts downstream (Baier, 1972).

Microstructural Features-Scanning and Transmission Electron Microscopy

Foreign material-induced thrombogenesis has been characterized utilizing scanning electron microscopy for microstructural information (Lelah et al., 1983; Barber et al., 1978, 1979; Van Kampen et al., 1979). The scanning electron microscope has been utilized to obtain temporal

information on the morphology of cells and thrombi present on polymer surfaces exposed to blood. Scanning electron microscopy (SEM) also provides the capability to survey thrombosis and embolization over large areas of surfaces. Transmission electron microscopy (TEM) provides the opportunity to visualize the internal morphology of thrombi.

Baier (1978b)

Baier reported his findings on the fate and consequence of blood exposure to different vascular interfaces. Intact endothelium-lined blood vessel lumens were observed (with SEM) to be essentially nonadhesive to platelets and very rarely had anything but a few red cells deposited on them. Similar arterial specimens which were deendothelialized (purposely stripped of the endothelium) and exposed to fresh whole blood *in vivo* for 10 minutes were observed to promote extensive platelet adhesion. However, no platelet aggregates or white blood cells were attracted to this surface. The initial consequences of blood exposure to other deendothelialized specimens under controlled *in vitro* flow conditions revealed that within 1 minute to 10 minutes of blood exposure, initial platelet adhesion and aggregation did occur. As blood exposure was increased, a more platelet-adhesive state was reached by shedding of the microthrombi, and eventually (probably through the participation of white cells) a platelet-free state was attained.

The degree of adhesion is a relative concept. A poor adhesive quality was predicted for both deendothelialized and endothelialized vessel surfaces by critical surface tension calculations (i.e., critical surface

tension values within the range of 20 to 30 dynes/cm) and was reflected in the lack of strong attachment of platelets and microthrombi to these vascular interfaces. In a variety of nonmedical applications (such as the separation of cured tires from the adhesive-coated steel molds in which they are formed), synthetic surfaces with such adhesive qualities have been called adhesive. As will be explained in detail later, Baier has designated a critical surface tension range of between 20 and 30 dynes/cm as being useful to predict biocompatibility of a material.

Barber et al. (1978)

Barber et al. have used an ex vivo canine arteriovenous shunt model to test the short-term interactions of blood with a few selected polymeric vascular graft materials. They used SEM, along with other techniques, to measure the transient ex vivo thrombus deposition and to determine the mechanics of thrombus deposition and release on the following polymeric surfaces: polyvinyl chloride (PVC), Silastic®, Biomer®, polyacrylamide, and polyhydroxyethyl methacrylate (poly-HEMA from Hydron Laboratories, New Brunswick, New Jersey). The latter two surfaces were polymerized as grafts onto silicone rubber by using ^{60}Co gamma radiation. The short-term interactions of blood with fibronectin-preadsorbed PVC and fibrinogen-preadsorbed PVC were also observed. The interactions which occur when polymers are exposed to blood in the range of 2 minutes to 2 hours were studied to determine if materials which seem to be nonthrombogenic, in that there is little thrombus buildup over long periods of time, are not in fact actually generating microemboli as platelet clumps are washed from their surfaces.

Both SEM and TEM were used to visualize the mechanisms of thrombus formation on the various surfaces. The thrombosis mechanism was found to be surface-dependent as seen by the differences among samples regarding fibrin absence or presence, cell types involved, thrombi size formed, and shunt surface area covered. On the various surfaces tested, dendritic platelets were occasionally seen after short periods of blood exposure (2-5 minutes) but were for the most part absent from samples collected after 10 minutes. Isolated platelets were often seen distributed over surface areas not covered by thrombi. The amount of fibrin involved was the most noticeable difference in thrombus structure among the various surfaces tested.

Fibrin deposition onto HEMA tended to be diffuse at first but eventually covered the whole lumen of the tube. The buildup of thrombus on HEMA was found to cover the entire inner surface of the tubing on samples collected from 30 minutes to 120 minutes. This thrombus covering was firmly attached basally to the fibrin layer formed on the surface of HEMA. Thrombi on the HEMA grafted silicone rubber surface were found to consist of a thick, continuous basal layer of fibrin, aggregates of platelets, and occasional red blood cells and polymorphonuclear neutrophils. Thrombi analyzed for composition were those cell or cell-fibrin aggregates that were 30 μm or greater in their largest dimension. By 15 minutes exposure, 87% of the HEMA surface was found to be covered by thrombus as calculated with a 2500 square transparent grid overlay on prints of 500x magnification. In the same way, percent of thrombus coverage was calculated at 120 minutes, and on HEMA the thrombus coverage at 120 minutes had fallen to

79%. The percent embolization was calculated as follows: (1-(thrombus coverage at 120 min./thrombus coverage at 15 min.))*100=percent embolization. The extent of embolization on HEMA was found to be 9%. The fact that little production of emboli by the HEMA surface had occurred was also indicated upon examination by TEM which showed that at the 15 minute and 120 minute exposure periods approximately the same thrombus structure was present. Only small amounts of fibrin had formed within thrombi on HEMA, and platelet degranulation and disintegration was quite a bit less on this surface than on PVC.

On the Silastic® surface, thrombi were composed of platelets, fibrin, and rarely, leukocytes. By 15 minutes of blood exposure, 11% of the Silastic® surface was covered by thrombus, which decreased to a 5% thrombus coverage by 120 minutes of exposure, indicating 55% embolization. On the Silastic® surface, polymorphonuclear neutrophils were often observed in clear areas.

Barber et al. (1979)

Using the same ex vivo arteriovenous shunt model as discussed previously, these investigators studied the effects of serum protein pre-adsorption onto silicone rubber (Silastic®, SR) and polyvinyl chloride (PVC) on short-term thrombosis. Using SEM and TEM, along with other techniques, their objective was to examine the thrombosis process on the polymeric materials by categorizing the flowing blood response to the polymeric systems being studied and by characterizing the mechanisms of thrombosis and embolization on such surfaces. PVC, which is a

thrombogenic surface, and SR, which is relatively more biocompatible than PVC, were coated with the following serum proteins: Fibronectin (FN), anti-fibronectin (AFN), von Willebrand factor (vWF), alpha-2-macroglobulin (α_2M), albumin (Alb), IgG, mixed gamma globulin (γIg), and FN followed by anti-FN (FN-AFN).

In general, it was found that enhancement of thrombosis or, conversely, surface passivation was dependent upon the protein-surface combination under consideration. Four categories of thrombi were observed based upon morphologic variations: (1) large spherical thrombi formed on a localized basal fibrin plaque, (2) small thrombi (50 μm or less in diameter) formed without a basal fibrin plaque, (3) large thrombi formed without a basal fibrin plaque, and (4) thrombi formed on top of leukocyte aggregates with or without a basal fibrin plaque. The PVC surface precoated with albumin had much less thrombotic activity than the PVC surface alone. Smaller thrombi than those on the uncoated surface, and no fibrin or polymorphonuclear neutrophils (PMNs), were found on the passivated surface. Thrombosis was modulated less by serum proteins precoated onto PVC shunts. However, FN did prove to be the most powerful modulator of thrombosis on both SR and PVC in that it evoked a severe thrombotic response in both cases. On both the FN precoated SR and PVC surfaces, very large thrombi with fibrin and numerous PMNs within and basal to the thrombus was seen.

The suggestion of the loss of thrombi into circulation was seen on all surfaces tested except uncoated SR and Alb/PVC surfaces by the occurrence of bare areas free of thrombus following the decline of platelet counts. Platelet counts were made by radiolabeling platelets from the dog 24 hours

prior to surgery. On most of the surfaces tested, a platelet count maxima occurred by 15 minutes, followed by a decline in the count rate due to embolization. The internal morphology of thrombi was found to change following the platelet count maxima in such a way as to strongly indicate embolization activity. The changes included the following: (1) extensive platelet degranulation and lysis, (2) loss of small platelet clumps from the thrombi, (3) occurrence of internal fibrin meshwork in thrombi, (4) occurrence of cytomuscular fibrillar material in intact platelets, and (5) breakage of thrombus basal fibrin strands when the cytomuscular fibrillar material appeared. Disruption of the basal fibrin strands of a thrombus was particularly noticeable by SEM.

The role of leukocytes in thrombosis on the surfaces tested appeared to be dependent upon the specific serum proteins precoated onto these surfaces. Monocytes (MNs) and PMNs, which are active phagocytes, were shown to be involved in the initial thrombus adherence, to be present in sizable numbers within thrombi, and (at times) to form aggregates (leukocyte thrombi) without fibrin or platelets on the tested surfaces. FN, AFN, and FN-AFN surface precoatings resulted in an increased adherence of PMNs and MNs on these surfaces. Also, IgG and γIg precoated SR attracted large numbers of MNs. On some shunt surfaces, leukocytes basal to thrombi appeared to anchor thrombi to the surface. Degranulation of PMNs was observed during the declining platelet count phase (after 15-30 minutes of blood exposure) in clear areas within thrombi. The occurrence of PMN aggregates on PVC and FN/PVC and MN aggregates on IgG/SR and γIg/SR surfaces, and subsequent thrombus deposition on top of these cells,

appeared to indicate that leukocyte adherence played a role in thrombosis on these particular surfaces. It was speculated that the degranulation of basal PMNs prior to maximum embolization suggests the release of fibrinolytic enzymes from the leukocytes to aid embolization processes.

Van Kampen et al. (1979)

In contrast to what the role of leukocytes in thrombosis appeared to be in the Barber et al. (1979) research, these investigators found leukocyte deposition to be a nonthrombogenic event. On hydrophilic and hydrophobic materials that remained patent, and eventually endothelialized, leukocytes were found to adhere and spread before extensive platelet aggregation.

A series of poly (α-amino acid) materials and Biomer (a polyurethane) were implanted against the inside wall of canine femoral and carotid arteries for periods of 30 seconds to 2 weeks. The thrombus deposits were examined by scanning and transmission electron microscopy. The series of poly (α-amino acid) materials ranged from hydrophilic to hydrophobic and consisted of the following: (γ-benzyl L-glutamate) which is a nonionic hydrophobic material and is abbreviated Glu(OBz), poly(γ-benzyl L-glutamate co L-leucine)-50/50 (Glu(OBz):Leu-1:1) which is a nonionic hydrophobic material, poly (L-glutamate co L-leucine-50/50 (Glu(OH):Leu-1:1) which is an ionic hydrophilic material, Glu(ONa):Leu-1:1 which is the sodium ionomer of Glu(OH):Leu-1:1, and poly (ω-N-hydroxypropyl L-glutamine) which is a nonionic hydrophilic material and is abbreviated Gln(PrOH). It was found that the changes in implant surface chemistry evoked responses ranging from

rapid vessel occlusion to little thrombus formation and eventual endothelialization.

Glu(OH):Leu-1:1, Glu(OBz), and Glu(OBz):Leu-1:1 all elicited intense thrombosis which led to vessel occlusion. The mechanism of thrombosis to vessel occlusion was similar on these three materials. On the Glu(OH):Leu-1:1 implant, substantial platelet adhesion and some platelet aggregation were present after 30 seconds of blood exposure, and at 1 minute platelet aggregation was extensive. Five minutes after implantation large platelet aggregates and thrombus deposits in piller formation were present. The pillars were composed of platelets, leukocytes (primarily polymorphonuclear leukocytes), and fibrin. In some areas between the pillars, red blood cells entrapped in fibrin had begun to accumulate. By 10 minutes after implantation, very large platelet-leukocyte pillars extended into the vessel lumen, and fibrin and red cells filled in the spaces between the pillars. By 15 minutes of blood exposure, about 90% of the vessel cross sectional area was covered by thrombus, and, on occasion, an artery was occluded at this time (a minimum of four implants at each time interval was studied). The thrombus consisted of platelets, leukocytes, fibrin, and red blood cells. The major cell type in the thrombus was polymorphonuclear leukocytes.

Thrombus deposition on Glu(ONa):Leu-1:1, Gln(PrOH), and polyurethane was minimal at first but gradually increased in thickness until the surface became endothelialized. By 15 minutes after implantation, small platelet-leukocyte pillars were observed on Glu(ONa):Leu-1:1, and a considerable amount of flattened out leukocytes was found directly on the implant

surface. Platelets, polymorphonuclear leukocytes, and fibrin were the components of the pillars. The pillars grew at a moderate rate, and by 4 hours the implant surface was covered by a somewhat even layer of thrombus composed of platelets, leukocytes, fibrin, and red blood cells. At this point, the layer of thrombus stopped increasing and eventually became covered with endothelial cells.

Platelet adherence and aggregation, followed by platelet-leukocyte pillar formation, were the initial thrombus deposition sequence of events on all the materials tested. In some cases, there was platelet and leukocyte competition during the initial stages of thrombus formation, and the rate and extent of thrombus formation on the materials were found to be directly related to this initial platelet and leukocyte interaction. The degree of direct leukocyte adherence to, and spreading on, the implant surfaces preceding considerable growth of pillars was found to be the major difference between implants that caused vessel occlusion and those that remained patent and eventually endothelialized. No simple relationship between a gross surface property (i.e., hydrophobicity) and the degree of thrombosis resistance was found to exist.

Vale and Greer (1982)

Four types of composite materials, which vary in hydrophilicity (consisting of HEMA alone or copolymerized with N-vinyl-2-pyrrolidone (NVP) and incorporated into silicone rubber tubing), and two silicone rubber types (of different size) were exposed to whole, flowing blood in a canine ex vivo femoral arterial-to-venous shunt configuration. The materials were

sampled at 5, 15, 30, 45, and 60 minute intervals. The type and amount of adhering cellular material were determined at these various time intervals with SEM. Whether or not enhanced hydrophilicity could have a desirable effect on blood-material interactions and whether or not a trend was developed in one hour by the blood-material interaction were two issues addressed in this study.

The distribution of platelets on the tubing surface was found to be homogeneous in most cases. An increase, followed by a decrease, in the platelet populations was found to occur on all the samples tested by 60 minutes. Vale and Greer found at least two kinds of responses to be indicators of shunt failure. In one case, a homogeneous layer of platelets with large aggregates forming led to the deposition of a fibrin mat with entrapped red blood cells which occluded the shunt. In another case, an initial variation in the blood-material interaction, as indicated by distinct areas of leukocyte and platelet adherence, led to shunt failure. The role of leukocytes was found to be both procoagulant and proendothelialization. Shunt failure in a few samples was preceded by initial leukocyte adhesion. In contrast, another sample retained its patency with little blood element covering even though leukocytes were found to adhere initially.

Lelah et al. (1983)

Lelah et al. have used an acute ex vivo femoral arteriovenous series shunt technique to investigate thrombus formation and embolization on the following surfaces: polyethylene (PE), oxidized polyethylene (OX-PE),

Silastic® (SR), polyvinyl chloride (PVC), and porous Gore-Tex® and Impra® expanded polytetrafluroethylene (PTFE). These samples were connected in the shunt in a series configuration. SEM was used to examine the sequence of thrombus formation and embolization on these surfaces for the blood contact period of 0.5 to 60 minutes.

The mechanism of thrombus formation and embolization on the SR, PE, and PVC surfaces was similar. For the blood contact periods of 0.5, 1, 2, 5, 10, 15, 20, 30, 45, and 60 minutes, the reaction to flowing, nonanticoagulated blood on PE was observed to be platelet deposition and activation, thrombus formation, and embolization. Platelets, with short cell extensions and discoid in form, were first noted to adhere by 0.5 minute of blood contact. Platelet deposition and activation (in the form of shape change) were found to increase between 0.5 to 5 minutes of blood exposure. Between 5 and 10 minutes of blood contact, a further increase in platelet adherence with subsequent activation, aggregation, and thrombus formation was observed. By 20 minutes of exposure, the thrombi, which consisted principally of platelets with few leukocytes (as seen with SEM), peaked in size. Embolization of most of the large thrombi occurred between 20 and 60 minutes, leaving behind a layer of individual platelets or small aggregates. Retraction during detachment was indicated by the form of some of the larger thrombi on PE which were surrounded by an area devoid of platelets. White or red blood cells were rarely associated with thrombi on SR, and platelet aggregates were quite a bit smaller on SR than those on PE. Thrombi on SR were of looser organization with less obvious retraction than those on PVC (which evoked a response to blood similar to that of SR).

A maximum in platelet and thrombus deposition was found to occur on all surfaces at approximately 15-20 minutes of blood exposure. A subsequent decrease in platelet and thrombus deposition was observed during embolization on all surfaces except PTFE and Gore-Tex®. The rapid growth of the thrombi on the surfaces tested was suggested to be due to large-scale platelet release of aggregating substances and to the thrombus mass presence in the bloodstream. In general, leukocytes were not found to be necessary for thrombus formation. However, leukocytes did appear to play a role in the embolization process on OX-PE, although their presence was not necessary for embolization in general as shown by the embolic process for PVC, SR, and PE.

Retraction and detachment of the thrombi as emboli followed thrombus formation on the PE, OX-PE, SR, and PVC surfaces. Platelet retraction, which results in the area basal to the thrombi to be almost devoid of platelets or sometimes surrounded by a "webbed" region, appears to be an important mechanism for embolization. Shear forces, caused by the flowing blood, were also speculated to play a larger role in the detachment of larger thrombi than smaller thrombi. Thrombi more exposed to the shear field and reduced surface-thrombus contact areas are both a result of clot retraction.

Protein Characterization-FT-IR/ATR

Fourier Transform infrared (FT-IR) spectroscopy coupled with attenuated total reflectance (ATR) is a technique for studying protein adsorption onto polymers (Jakobsen and Gendreau, 1978). The polymer, which has been

exposed to protein, is placed in intimate contact with a crystal such as germanium. Subsequent FT-IR analysis results in a spectrum consisting of information from less than the top 1000 nanometers of the sample.

General theory

In a Fourier Transform infrared spectrometer, there are no prisms, gratings, or slits. Unlike conventional infrared spectrophotometry, there is no need to establish a monochromatic beam. Instead, all the frequencies of a polychromatic source are analyzed simultaneously. The monochromator in a conventional infrared spectrophotometer is replaced by the Michelson interferometer in a FT-IR spectrometer, although the functions cannot be correlated. A monochromator divides a continuous bandwidth into its component frequencies, whereas an interferometer produces interference patterns of the bandwidth (De Haseth, 1982).

The Michelson interferometer consists of two mutually perpendicular plane mirrors, one of which can be made to travel uniformly in a direction perpendicular to its plane (see Figure 1). Between the two mirrors is a semi-reflecting film or "beamsplitter." An ideal beamsplitter reflects half of the incident light, transmits half of the incident light, and has zero absorption. It can be seen in Figure 1 that half of the source radiation is transmitted by the beamsplitter and goes to the movable mirror M2, while half is reflected and goes to mirror M1. At the beamsplitter, the two beams reconverge from M1 and M2, with half of the recombined beam being reflected towards the detector and half being transmitted back towards the source. As M2 is uniformly moved, the signal at the detector goes through

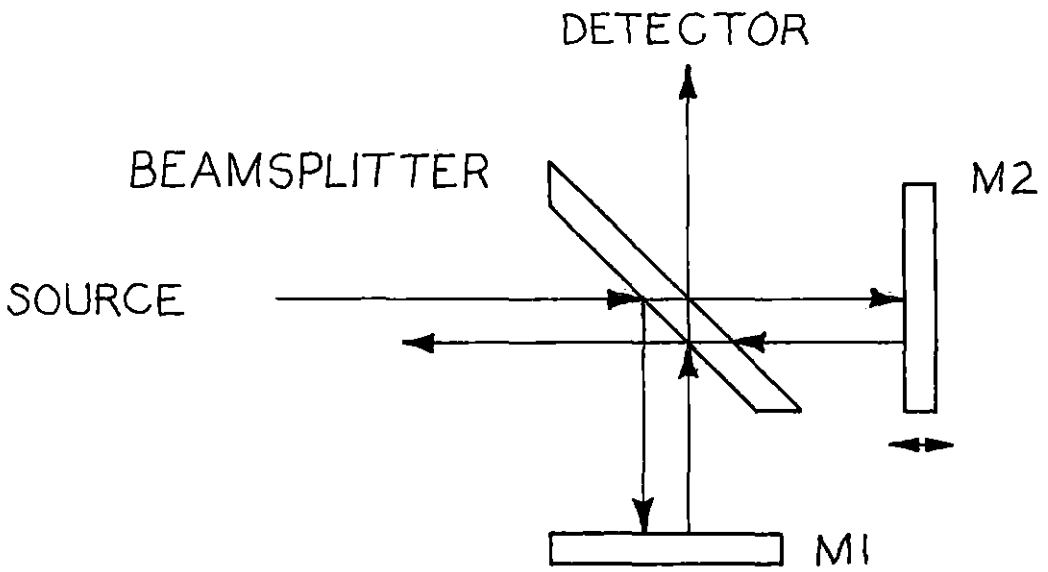

Figure 1. Michelson interferometer

a series of maxima and minima in a cosine fashion directly proportional to the velocity of the moving mirror. The sum of these cosine waves is the signal seen at the detector. This signal is called the interferogram. If a sample is placed in the path of the beam, the frequencies from the interferogram corresponding to the sample absorption modes are subtracted, and the resulting interferogram will be a synthesis of all frequencies except those absorbed by the sample. The signal at the detector, the interferogram, is mathematically transformed into a spectrum using Fourier Transform pairs.

The attenuated total reflection (ATR) effect may be explained as follows: when a beam of radiation enters a crystal, the beam will be reflected internally if the angle of incidence at the sample and crystal interface is greater than the critical angle (a function of refractive index). All of the energy is reflected on internal reflection. However, the beam does appear to penetrate slightly beyond the crystal into the sample.

When a material which absorbs radiation selectively is placed in contact with the reflecting surface (crystal), beam energy will be lost at those wavelengths where the material absorbs due to an interaction with the penetrating beam. When measured and plotted as a function of wavelength by a spectrophotometer, this attenuated radiation will give rise to an absorption spectrum characteristic of the material. The depth to which the radiation penetrates is a function of the angle of incident radiation, the refractive index of both the reflector and sample, and the wavelength of light. Typically, the internal reflector plate is a germanium or KRS-5

(which is composed of 42 mole % TlBr and 58 mole % TlI) crystal, and the angle of incidence is 45°, giving approximately 25 reflections. In theory, provided there are enough reflections, spectra of any desired intensity can be produced.

An advantage to using FT-IR spectroscopy to characterize adsorbed protein layers over conventional infrared spectroscopy is its sensitivity, which enables it to work with highly complex systems such as whole blood. This high sensitivity is due to the fact that the FT-IR spectrometer records data from the entire spectral region throughout the experiment. This leads to a signal-to-noise ratio on the order of 10 to 100 times greater than that of a conventional infrared spectrometer.

The ATR technique combined with the FT-IR technique (FT-IR/ATR technique) is very useful for studying protein adsorption onto polymer surfaces. With the sensitivity and the improved signal-to-noise ratio of the Fourier Transform technique over conventional infrared instrumentation, the usefulness of the ATR method is greatly enhanced. Higher internal reflection angles and crystal materials of high refractive index such as germanium (both of which reduce the depth of sampling) can be used with the increased signal-to-noise ratios of the Fourier Transform technique (Ratner, 1982). The FT-IR/ATR technique can detect changes in protein conformation or composition, but the problem lies in interpreting the resulting complex spectrum when whole blood is used as the protein source. A dedicated minicomputer is used in FT-IR spectroscopy for data processing and for performing spectral subtraction. Spectral subtraction is the mathematical subtraction of two similar spectra, with the end result being

a spectrum which is due to the differences between the two original spectra. The spectral subtraction method enables one to look solely at the protein layer adsorbed onto a polymer, since the technique eliminates the polymer infrared bands.

Wavenumber regions of interest

The amide I (1650 cm^{-1}) and amide II (1550 cm^{-1}) absorption bands are common to all proteins. The amide I band is mainly due to a carbonyl group (C=0) stretch, while the amide II vibration is due to -NH bending (Koenig and Tabb, 1980). The amide I band can vary as much as 10 cm^{-1} for different polypeptides in essentially the same extended conformation, whereas the amide II band can vary as much as 20 cm^{-1}, since it is even more conformation sensitive (Elliot and Bradbury, 1962). The kinetics or rate of adsorption of proteins can be determined by measuring the intensities of various infrared bands and plotting these intensities as a function of time of flow. This can be done only if the infrared bands used are not sensitive to conformational or structural changes. Two bands independent of conformational changes at constant pH and common to all proteins are the amide II band (as mentioned previously) and the 1400 cm^{-1} infrared band. Based on the preceding observations, the amide II and the 1400 cm^{-1} infrared bands were found to be linearly related to the total amount of protein adsorbed and, therefore, could be used to determine relative amounts of adsorbed protein (Gendreau et al., 1982). The amide III spectral region occurs at 1200-1350 cm^{-1}. The intense water infrared bands obtained from aqueous solutions (i.e., blood) usually need to be removed,

since they tend to mask important weaker bands (i.e., the amide I and II bands in blood). The amide I and II bands are easily resolved when the 1640 cm^{-1} bending vibration of water is removed from a whole blood spectrum. Absorption bands occurring near 1080 and 1160 cm^{-1} from plasma or serum are felt to be due to a blood plasma species of high carbohydrate content, for example, a glycoprotein like α_1-acid glycoprotein or fibronectin (Gendreau and Jakobsen, 1979).

Ratner and Hoffman (1975) used conventional infrared spectroscopy combined with attenuated total reflectance (ATR) to observe the infrared spectra of hydrogels grafted onto silicone rubber. The poly (NVP) amide-type carbonyl has an adsorption at 1689 cm^{-1} (5.92 μm), and the poly (HEMA) ester linkage has a carbonyl adsorption at 1754 cm^{-1} (5.70 μm). The absorption bands characteristic of silicone rubber which are of interest are the 1410 cm^{-1} band, the 1260 cm^{-1} band (due to the $Si-CH_3$ stretch), a broad doublet occurring at 1020 and 1090 cm^{-1}, and a band occurring at 800 cm^{-1}.

Gendreau and Jakobsen (1979)

Gendreau and Jakobsen investigated the adsorption of blood proteins onto polyvinyl chloride and germanium from flowing plasma or serum using FT-IR spectroscopy coupled with ATR. Human plasma or serum (fibrinogen poor) was diluted either 20:1 or 10:1 with unbuffered, isotonic saline prior to an experiment.

Spectra of blood serum collected under flowing conditions using a germanium crystal were used for kinetic studies. The amide I and II bands

were plotted as a function of time. The amide II band reached a plateau by 90 minutes, but the amide I band did not. Other factors which may function to increase the intensity of the amide bands, besides the total amount of protein adsorbed, were felt to be the cause of this difference. A compositional change of the layer with time, a conformational change of the adsorbed layer with time, or both of these factors were speculated to be responsible for the continuing increase of the amide I band, assuming that the total amount of surface protein had reached equilibrium by 90 minutes.

Jakobsen et al. (1981)

Blood protein adsorption onto germanium crystals was studied at the molecular level using an ex vivo FT-IR/ATR technique. Canine blood was pumped through an arteriovenous shunt (the energy of flow being provided by the dog's arterial pressure), to the ATR cell, and then back into the dog. FT-IR spectra were obtained in real time by this technique. Within the first minute of contact with a surface, most of the blood protein adsorption occurs. This rapid adsorption necessitates an experimental technique that is capable of monitoring events in this time frame (i.e., real time). The FT-IR/ATR technique is capable of monitoring events in real time. Scan sets of 25 scans were co-added at a scan speed of 0.2 seconds, resulting in a spectrum collected every 5 seconds. Subtraction between spectra was performed to detect changes in composition of the protein layer.

Most of the information about protein composition and structures is provided by bands in the 1500-900 cm^{-1} spectral region. By monitoring the

ratio of the 1300 to the 1250 cm^{-1} bands, Jakobsen et al. (1981) found that during the first 5-10 seconds, a mixture richer in albumin adsorbed, and a mixture richer in fibrinogen adsorbed during the last 50-55 seconds of the first minute. The rationale behind this conclusion will be explained later. Glycoproteins were also believed to be involved in the initially adsorbed protein layer by the appearance of the 1080 cm^{-1} band (which arises from the C-O vibration of the carbohydrate portion of the glycoprotein). The intensity of the 1080 cm^{-1} band is proportional to the glycoprotein carbohydrate amount. Spectral subtraction was found to cancel the 1400 cm^{-1} band in the time period from 4 to 10 minutes, indicating that little adsorption of protein occurred during this time. However, the bands near the 1230 and 1080 cm^{-1} range, which are protein frequencies, did not cancel, indicating that considerable replacement of proteins took place from 4 to 10 minutes.

Gendreau et al. (1982)

The dynamic adsorption of a 1:1 mixture of albumin and fibronogen in saline onto a germanium crystal was monitored for 222 minutes by the FT-IR/ATR technique. Several spectral changes were observed over this time period. The number, shapes, and frequencies of the infrared bands in the 1250 cm^{-1} and 1300 cm^{-1} region and the ratio of the 1300 to the 1250 cm^{-1} bands were all found to change with the time of flow. The 1300 cm^{-1} region spectral changes were found to be very similar to those spectral changes which occur with different concentrations of pure albumin solutions. From this observation, it was deduced that the spectral changes in the 1300 cm^{-1}

region follow the behavior of albumin. The 1250 cm^{-1} region spectral changes were found to coincide with frequencies assigned for conformers of fibrinogen; in other words, the 1250 cm^{-1} region spectral changes track the conformational behavior of fibrinogen. From the preceding arguments, it was reasoned that changes in the 1300-1250 cm^{-1} intensity ratio indicate changes in the albumin/fibrinogen ratio.

During the first 1.5 to 7.5 minutes, the ratio of the 1300/1250 cm^{-1} intensities indicated that the adsorbed layer was richer in albumin. However, after 7.5 minutes of protein exposure, the 1300/1250 cm^{-1} intensity ratio began to significantly decrease, indicating that the relative amount of albumin was decreasing. The fact that the 1400 cm^{-1} band (indicating total amount of protein) had not increased much at 7 minutes provided further proof that albumin was being replaced by fibrinogen at the surface of the germanium crystal as shown by the increase in fibrinogen intensity (1250 cm^{-1} band). At 222 minutes of adsorption, the total layer was observed to be rich in albumin.

Surface Characteristics-Implant Materials

Surface texture, surface chemistry, and surface energy phenomena of polymers and how these characteristics are related to biocompatibility are of interest.

Surface texture

Flow parameters are significantly affected by the texture of a surface. Blood stagnation points can be caused by micro- and macro-surface imperfections which may initiate the steps leading to eventual thrombus

formation (Cumming, 1980). The formation of a localized wedge-shaped thrombus may occur downstream from a surface imperfection (Herzlinger and Cumming, 1980).

The addition of silica (SiO_2) filler particles to silicone rubber improves the material's mechanical properties, but the silica particles have a high energy and could induce thrombosis if exposed (Nyilas et al., 1970). Filler free silicone rubber (FFSR) has been shown to be less thrombogenic than Silastic® (Chawla, 1978). By noting the number of cells adhering to the surfaces of Silastic® and of FFSR and the morphological changes of adhering cells, Chawla observed that FFSR is more biocompatible than Silastic® as far as platelet-foreign surface and leukocyte-foreign surface interactions are concerned.

Merrill and Salzman (1976) measured the criteria for roughness in terms of plasma proteins and formed elements. For a peak-to-peak distance (λ_1) and a peak-to-valley distance (λ_2), a λ of approximately 10^3 Å was considered rough to a protein, and a λ of between 10^2 μm to 10^4 μm was thought to be rough to cells.

By examination with transmission electron microscopy, injection molded medical grade Silastic® 372 (which contains approximately 30-33% filler by weight), as well as commercially available cured sheeting, were found to contain aggregates of silica particles (Nyilas et al., 1970). In areas on the injection molded Silastic® 372, the silica filler was found to be covered by only a monolayer of the poly (dimethylsiloxane) of the Silastic®. It was suggested that if the monolayer covering of the silica filler was imperfect, the relatively high energy nature of these particles

could cause denaturation of blood proteins. The commercially available, cured Silastic ® 372 was observed to be quite rough. Agglomerated silica particles approaching 1 μm in size were found to protrude from the commercial material, although the aggregates were still covered by the poly (dimethylsiloxane). A 10 μm layer of silica-free Medical Adhesive A cast over a cured Silastic ® 372 surface was found to completely cover any occurrence of partially or completely exposed silica filler particles (Nyilas et al., 1970). The silica-free Medical Adhesive A was prepared by filtering a solution of the gum. Surface roughness (the roughness attributed to the presence of filler in this case) was found to have an effect on blood compatibility if the filler particles were partially or totally exposed.

Surface chemistry

The hydrophilic/hydrophobic domain hypothesis presumes that to be biocompatible, a polymer should possess both hydrophilic and hydrophobic sites throughout its surface (Nakashima et al., 1977). It is known that the blood vessel wall has both hydrophilic and hydrophobic sites. Other investigators also found that a balance of hydrophilic and hydrophobic sites at a biomaterial surface may be important for blood compatibility (Ratner et al., 1979; Sasaki et al., 1976).

Gel chemistry, "pore" structure, and cross-linking density are factors that influence the water structure of hydrogels and should, therefore, be related to biocompatibility instead of mere water content according to "water structure" hypotheses (Bruck, 1973). In other words, how water is

structured and oriented at the interface of a hydrophilic material such as hydrogels is important and not the actual water content of the material (Garcia et al., 1980; Andrade et al., 1973). Jhon and Andrade (1973) and Garcia et al. (1980) hypothesized that there are at least three kinds of water in hydrogels: 1) bound and/or structured water (hydrated), 2) interfacial, and 3) bulk and/or normal water.

In contrast, Nakashima et al. (1977) concluded that there are at least two kinds of water in hydrogels, free water and bound water. The bound water was found to be bound to the polymer molecule either directly through hydrogen bonds or indirectly to other water molecules (which were bound to the polymer directly). Nakashima et al. (1977) suggested that at the blood/biomaterial interface, water may form the "iceberg" structure near the biomaterial's hydrophobic sites. Iceberg formation refers to the condition where water forms a continuous hydrogen bonded (cage-like) structure around a hydrophobic site of a hydrocarbon. The "iceberg" formation promotes platelet aggregation in blood. Nakashima et al. (1977) also suggested that near the hydrophilic sites of a polymer, water may be bound to the surface of the polymer, inhibiting "iceberg" formation and, therefore, playing an important role in blood coagulation inhibition.

Surface energy phenomena

Surface free energy is a measure of the unsatisfied primary or secondary bonding capacity of a surface. This energy term is a measure of the inward attractive force.

The phenomenon of surface tension can be described as follows (Andrade, 1973): the asymmetric force field present at the surface of any condensed phase results in an attraction towards the bulk. This net attraction towards the bulk displaces some surface atoms into the bulk, resulting in an atom depleted surface which is in tension. The surface tension is the tension created by the atom depleted surface and causes the surface area to be reduced. Surface tension is surface free energy and is expressed in dynes/cm or ergs/cm^2. Solids may have little or no surface tension due to the nondeformability of many solids, except at high temperatures.

The interfacial free energy between two phases A and B can be described as $\gamma_{AB} = \gamma_A - \gamma_{A(B)} + \gamma_B - \gamma_{B(A)}$, where γ_A, γ_B = the surface free energies of A and B, respectively, $\gamma_{A(B)}$ = the effect on A due to B, $\gamma_{B(A)}$ = the effect on B due to A, and γ_{AB} = the interfacial free energy between phases A and B (Andrade, 1973). The effects of $\gamma_{A(B)}$ and $\gamma_{B(A)}$ reduce the free energy at the interface. The unsatisfied bonding capacity of A is partially satisfied by the presence of B and vice versa. The minimum interfacial tension hypothesis proposed by Andrade (1973) states that interfaces with minimal interfacial free energy should be compatible with host tissues, including blood. Holly (1979) observed that materials which exhibited lower water-biomaterial interfacial tensions adsorbed proteins in smaller amounts, and less firmly, than materials which exhibited higher interfacial tensions.

The wetting properties of a solid are defined as the degree to which a liquid spreads over the solid surface and the degree to which a liquid

adheres to the solid (Baier et al., 1968). The contact angle (θ) is a measure of the surface energy. The contact angle, as determined by the sessile drop technique, is obtained by placing a drop of liquid on a solid substrate and measuring the angle θ, where θ is the angle of a line tangent to the drop surface at the region of solid (S), liquid (L), and vapor (V) equilibrium. The Young-Dupree equation, or contact angle equation, is $\gamma_{SV} = \gamma_{SL} + \gamma_{LV}\cos\theta$, where γ_{SV} = the interfacial energy at the solid-vapor interface, γ_{SL} = the interfacial energy at the solid-liquid interface, and γ_{LV} = the interfacial energy at the liquid-vapor interface. The contact angle is a useful inverse measure of wettability (Andrade, 1973). For a contact angle of 0, the liquid is completely spread. Clearly, the contact angle is influenced by the properties of the solid substrate. The contact angle is also used as a measure of hydrophilicity and hydrophobicity. A hydrophilic surface has a contact angle of less than 90°, and a hydrophobic surface has a contact angle of greater than 90° (Holly, 1979).

Solids that have a low surface free energy in air tend to have a high interfacial tension against water (Holly, 1979). However, this relationship is not the case with hydrogels. Hydrogels seem to be capable of changing their surface free energy by reorienting the polymer side chains, depending on the nature of the adjacent phase (Holly and Refojo, 1975). For example, hydrogels can have a low surface free energy in air by orienting their most hydrophobic groups (methyl groups) outward and a low interfacial tension while immersed in water by orienting their most hydrophilic groups (hydroxyl groups) outward (Holly, 1979). The large contact angle hysteresis observed for hydrogels when the contact angle is obtained

by advancing and receding techniques, instead of the sessile drop method explained earlier, is a result of these orientational and conformational changes (Holly and Refojo, 1975; Holly, 1979).

Critical surface tension (γ_c), like interfacial free energy, is a surface energy parameter used to predict blood compatibility. Critical surface tension can be defined as the surface tension of a liquid which just wets the surface of a particular solid (Bagnall, 1977). Zisman (1964) has established an empirical linear relationship between the cosine of the contact angle and the surface tension (γ_L) for a homologous series of organic liquids. The value of the intercept of the horizontal line $\cos\theta = 1$ is the critical surface tension for wetting for that series of liquids. Baier (1972) proposed a "hypothetical zone of biocompatibility" for polymers that possessed a critical surface tension of between 20 to 30 dynes/cm. Baier determined this range from a variety of ancillary studies. From studies that correlated the critical surface tension with the actual outermost atomic constitution, Baier found that the critical surface tension range of 20 to 30 dynes/cm represents surfaces almost totally dominated by closely packed methyl groups.

Hydrogels

Hydrogels, which were first introduced as possible candidates for biological use in 1960 by Wichterle and Lim, are cross-linked polymeric networks capable of absorbing and holding large quantities of water without dissolution of the polymer network (Bruck, 1972, 1973). The physical properties of hydrogels resemble those of living tissue more so than any other class of synthetic biomaterial (Ratner and Hoffman, 1976).

There are two major advantages of hydrogels according to Ratner and Hoffman (1976). The first advantage is that the expanded nature and permeability of the hydrogel structure to small molecules allows for extraneous material from the polymerization process to be extracted before placing the hydrogel in contact with a living system. The second advantage of hydrogels is that the soft and rubbery consistency of the gels decreases the mechanical irritation to surrounding cells and tissues, contributing to the biocompatibility of the gel. Ratner and Hoffman (1976) also state that a low interfacial tension may be exhibited between a hydrogel surface and an aqueous solution, which should reduce the tendency of proteins in body fluids to adsorb and to denature upon adsorption. However, there is one important disadvantage to hydrogels. The high water content of hydrogels renders them mechanically weak. The mechanical weakness of the hydrogel can be easily overcome by either radiation grafting the hydrogel onto a substrate (Ratner and Hoffman, 1974) or impregnating a substrate with the hydrogel (Predecki, 1974). These techniques allow for the combination of the desirable biocompatibility properties of the hydrogel with the good mechanical properties of the substrate polymer.

HEMA (2-hydroxyethyl methacrylate) and NVP (N-vinyl-2-pyrrolidone), the hydrogels used in this study, are both hydrophilic polymers. However, HEMA is somewhat more hydrophilic than NVP based upon contact angle measurements reported by Vale and Greer (1982) for samples prepared in a similar way. NVP can be used for preparing gels which will exhibit high water contents (Ratner and Hoffman, 1976). When HEMA and NVP are radiation grafted onto silicone rubber, a series of surfaces varying in hydrophilicity

can be produced by controlling the HEMA to NVP ratio in an appropriate solvent such as methanol. The NVP graft has been shown to penetrate the silicone rubber matrix, whereas the HEMA graft apparently localizes on the surface of the silicone rubber matrix (Horbett and Hoffman, 1975; Ratner et al., 1975; Ratner and Hoffman, 1975).

Radiation grafted HEMA and NVP hydrogels on silicone rubber (Silastic ®) were found to be resistant to thrombus accumulation by renal embolus ring results (Ratner et al., 1979). However, analysis of the kidneys after the ring test revealed that these grafts caused numerous infarcts. In the same report, the Cr-labeled platelet consumption due to HEMA grafted Silastic ® on a baboon arteriovenous shunt was observed to be relatively low.

NVP was radiation grafted onto 2 mm I.D. silicone rubber tubes and implanted in lamb carotid arteries for 3 to 7 days (Chapiro et al., 1981). Thrombus accumulation as a function of grafting ratio was followed over a range of 0 to 50% grafts. The grafting ratio was defined as $(W-W_o/W_o)x100$ where W = the weight of the silicone rubber tube plus graft and W_o = the initial weight of the silicone rubber tube. The grafting ratio was varied as a function of irradiation time in 70% NVP/30% toluene mixtures. For the 3 day implantation, implants with grafting ratios in excess of 25% were found to be significantly more blood compatible than implants with grafting ratios below 25%. However, a significant improvement in blood compatibility for the 7 day implantation was seen in implants with grafting ratios above 30 to 40%. Upon examination of the brains, very few or no thrombi were observed in the cases where the implant tubes remained clear. Under

the grafting conditions used, NVP diffused freely into the silicone rubber tubes (toluene behaved as a swelling agent), which led to a more homogenous grafting. However, tubes with grafting in excess of 30% were observed to become brittle.

The relative rates of consumption of fibrinogen and platelets by implant surfaces were measured in vivo using an arteriovenous baboon shunt model to determine quantitatively the rates of thrombus formation (Hanson et al., 1980). HEMA, which was radiation grafted to Silastic®, and Silastic® alone, were two implant materials tested. Silastic® was found to be relatively nonconsumptive towards platelets. Three other implant materials were studied for the detection of platelet microemboli in the kidneys of the baboons, and it was suggested that the production of significant numbers of platelet microemboli result from platelet consumption.

MATERIALS AND METHODS

Techniques

Sample preparation

Filler free silicone rubber was produced by filtering a solution of Silastic® 382 Medical Grade Elastomer (Dow Corning, Lot HHO82361) diluted with spectrophotometric grade hexane through filter material (Metricel Membrane Filters, 0.2 μm pores, Lot 3603072).[1] This pore size was smaller than the silica filler. The filtration was accomplished by using a vacuum pump.

Silicone rubber (SR) tubing (Dow Corning, Silastic® Medical Grade Tubing, Lot HHO63212, 0.078 in. inside diameter x 0.125 in. outside diameter) was first rinsed with approximately 10 ml of a 1:1 solution of ethanol and distilled water. This was followed by a profuse rinsing with distilled water, and the tubing was then air-dried. The interior surfaces of 2 foot sections were coated with either a 0% filler SR monomer or a 24% filler SR monomer solution (3.5 ml Silastic® with 12 ml hexane). Six 0% filler SR coated tubes were made by mixing 3.5 ml of filler free SR with 12 ml of hexane. One drop of stannous octoate (Dow Corning Catalyst M, Lot HH111094) was mixed in, and the fluid mixture was immediately drawn up the six SR tubes with a syringe and allowed to drip out freely. The samples were hung in a vertical position and allowed to vulcanize overnight. Six 24% filler SR coated tubes were made in the same manner except

---

[1] Gelman Sciences, Inc., Ann Arbor, Michigan.

that 0.6 ml of filler free SR was mixed with 2.9 ml of Silastic® 382 and 12 ml of hexane. The Silastic® 382 was determined to contain 28.9% filler by volume.

Five 2 foot sections of the 0% filler SR and of the 24% filler SR tubular substrates were filled with hydrogel monomer solutions in a solvent of 15% methanol and 65% water. The five monomer solutions used were 20% HEMA,[1] 15% HEMA/5% NVP,[2] 10% HEMA/10% NVP, 5% HEMA/15% NVP, and 20% NVP. The monomer solutions were de-oxygenated (to minimize oxidative reactions) by bubbling nitrogen gas through the solution for a minimum of 30 minutes. The tubes which were filled with monomer solutions were crimped at both ends and were then irradiated (0.25 Mrad dose) using a ^{60}Co source for polymerization purposes.

After being irradiated, the tubes were flushed with approximately 25 ml of a 1:1 solution of ethanol and distilled water to remove traces of any unpolymerized polymer. The tubes were then flushed with about an equal amount of distilled water, filled with distilled water, and then placed in a jar filled with distilled water. This flushing procedure was performed each day for several days, and then the tubes were kept in jars of distilled water. The tubes were filled with saline 24 hours prior to surgery.

A total of 13 sample types were exposed to blood: commercial Silastic®, 0% filler SR coated Silastic® (0% filler SR), 24% filler SR

---

[1] HEMA purchased from Alcolac, Lot 8763E8.

[2] NVP purchased from Monomer-Polymer and Dajak Labs, Inc., Lot 236-12.

coated Silastic® (24% filler SR), 0% filler SR/20% HEMA, 0% filler SR/15% HEMA/5% NVP, 0% filler SR/10% HEMA/10% NVP, 0% filler SR/5% HEMA/15% NVP, 0% filler SR/20% NVP, 24% filler SR/20% HEMA, 24% filler SR/15% HEMA/5% NVP, 24% filler SR/10% HEMA/10% NVP, 24% filler SR/5% HEMA/15% NVP, and 24% filler SR/20% NVP.

General

Mongrel dogs weighing 17-27 kilograms were obtained from Laboratory Animal Resources, Iowa State University, Ames, Iowa, and were used for the experiments. The weight, sex, and description of each dog were recorded before each experiment, and the following data were recorded before and after each surgery: blood flow rate, activated coagulation time (ACT), platelet count, and hematocrit (HCT). The flow rate was determined by measuring the volume of arterial blood pumped out in a given time period.

Activated coagulation time was determined by filling a vacuum tube containing 12 mg of siliceous earth (Vacutainer #6522)[1] with venous blood and recording the time until the first clot appeared.

Venous blood collected in a vacuum tube containing 7.5 mg of the anticoagulant sodium ethylenediaminetetraacetic acid (EDTA; Vacutainer #6453)[1] was used to determine the hematocrit and platelet counts. Capillary tubes filled with venous blood were centrifuged, and then a Spirocrit Microhematocrit Tube Reader was used to read the percent hematocrit. Platelet counts were determined using the Platelet Unopette[1] method. A sample of

---

[1]Becton-Dickinson of Becton, Dickinson and Co., Rutherford, NJ.

the EDTA venous blood which was diluted in an ammonium oxalate solution was used to charge a hematocytometer. The charged hematocytometer was incubated for 10 minutes, and then the platelets in the center square were counted. The result was multiplied by 1000 for the platelet count.

Surgery

The dogs, which had been fasted overnight, were anesthetized with an intravenous injection of sodium pentobarbital (29 mg/Kg body weight), and then presurgery blood values were determined. A nonsterile surgical technique was used.

With the animals placed in a supine position, a 12-14 cm incision was made parallel to the femoral artery and vein. Approximately 2 inches of the artery and vein were exposed. An *ex vivo* arteriovenous shunt with a flushing system was constructed by cannulating the femoral artery, femoral vein, and a branch off of the femoral artery. A 2 inch portion of the 2 foot section of tubing was inserted into the artery and vein, tightly ligated on the arterial side, and loosely ligated on the venous side. A 6 cm piece of polyethylene tubing with a saline filled syringe attached was inserted into a side branch off of the artery just above the arterial cannulation site so that the experimental tubing could be gently flushed with 35 ml of saline after various blood exposure periods. The experimental tubing was exposed for 0.25, 0.5, 5, 15, and 75 minutes. At the end of each time period (after the tubing was gently flushed with saline), the venous end was removed, and sample sizes ranging from 1.5 to 5 cm for both SEM and FT-IR analysis were cut. The sample for SEM analysis was fixed in

2% glutaraldehyde, while the sample for FT-IR analysis was placed in saline. The venous end of the tubing was cannulated and loosely ligated again. For the short blood exposure periods (0.25 and 0.5 minute), the venous end of the tubing was directed into a graduated cylinder to determine the starting flow rate. After the 75 minute blood exposure period was complete, post-surgical blood specimens were drawn, and the tube flow rate was determined as before. The animal was then euthanized with a dose of Sleepaway ®. After surgery, samples for SEM and FT-IR analysis were cut in half longitudinally with a scalpel blade, and the ends of the samples were cut off in order to attain the proper size sample. The sample sizes attained for SEM were 1 cm long and 0.31 cm wide, and the sample sizes attained for FT-IR analysis were 1 cm long and 0.31 cm wide for the first nine experiments and 1.5 cm long and 0.31 cm wide for the last four experiments.

Scanning electron microscopy

Microstructural information was obtained using scanning electron microscopy. The blood exposed samples were dehydrated in a series of acetone rinses (30, 60, 75, 90, 100, 100% v/v; 15 minutes each) following glutaraldehyde fixation. These samples were then air dried and mounted on carbon stubs with "dag" dispersion No. 154.[1] The mounted samples were sputter coated with 300 Å of gold prior to examination. The samples were examined in a JEOL-U3[2] scanning electron microscope at 15-25 Kev.

---

[1] Acheson Colloids Co., Port Huron, Michigan.

[2] Japanese Electron Optics, Tokyo, Japan.

Micrographs made from 40x to 1000x were used to study cellular deposition and to characterize surface buildup. Control samples not exposed to blood were taken through the same fixation and dehydration steps, mounted, coated with 300 Å of gold, and examined.

SEM micrograph analysis

Percentage of thrombus coverage was calculated for each sample type. The inside area (A) of the tube was calculated using the formula $A = 2\pi Rh$ where R = inside radius and h = 1 cm (the length of the sample). The area of the thrombi was estimated from SEM micrographs and use of a light microscope (both at a magnification of at least 120x). The percentage of area covered by thrombus was calculated by the equation (total area of thrombus/ total inside area of tube)*100 = % area covered by thrombus.

FT-IR spectroscopy

FT-IR evaluation of the blood exposed surfaces was performed using an IBM IR-98 FT-IR spectrometer[1] with a 45° germanium crystal and ATR solid sample holder. The sample length for FT-IR analysis was 1 cm for the first nine experimental tubes exposed. Half of the longitudinally bisected sample was placed on each side in the center of a 45° germanium crystal and firmly held in place by a solid sample holder. The flattened out sample dimensions were 1 cm by 0.31 cm. For the last four experiments, the sample length for FT-IR analysis was 1.5 cm. Two 1.5 cm samples were staggered on each side of the crystal so as to cover as much of the face of the crystal

[1] IBM Instruments, Inc., Danbury, Connecticut.

as possible. The infrared spectra collected using this sample size and number were more intense than the spectra collected using a single 1 cm sample on each side of the crystal.

Since water vapor is present in the atmosphere, and it does absorb infrared radiation, there was a problem with water vapor bands interfering with the spectra. It was determined that if the sample chamber was purged with nitrogen gas for a long period of time (approximately 23 minutes) before collecting a spectrum, the problem of water vapor interference could be eliminated. The long purging time was implemented after seven experimental tubes had already been studied. In Appendix A, the parameters used to collect, store, and plot the spectra are listed.

A reference spectrum of a clean crystal was collected before each sample spectrum was collected. After a sample spectrum was collected, the crystal was taken out of the crystal holder and cleaned with a cotton ball soaked in Micro cleaner diluted with distilled water. The crystal was then wiped with methanol and hexane to remove the Micro cleaner residue.

Spectral subtraction

Spectral subtraction of the blood exposed polymer spectrum was necessary because bands from saline, silicone rubber, the hydrogels, and, in some cases, water vapor interfered with the protein bands. A spectrum of each of the various samples tested which had not been exposed to blood, a spectrum of saline, and a spectrum of water vapor were collected for subtraction purposes. The saline infrared spectrum was collected by placing a few drops of saline in an air tight ATR liquid cell containing a

germanium crystal and purging for 23 minutes before collecting the spectrum. The water vapor spectrum was collected as soon as the crystal was placed in the path of the beam, allowing for little nitrogen gas purging of the sample chamber. The subtraction routines were provided by IBM.

One spectral subtraction routine was utilized for the necessary subtractions. Since reference files of the clean crystal were collected for each sample file (i.e., water vapor, "wet" protein coated polymer, and "wet" polymer), the first step was to convert these single-beam files into absorbance files by ratioing each sample file with the appropriate reference file. The absorbance files are created by setting the parameters AFN (arithmetic function) equal to AB, AFA equal to the appropriate sample file (e.g., TF20H30S),[1] and AFB equal to the appropriate reference file (e.g., GERT50).[2] The AB equation creates the absorbance files by using the equation $-\log_{10}[SCA*AFA)/(SCB*AFB)]$, where SCA and SCB are scaling factors set equal to one. The resultant absorbance files were stored (e.g., T2H30S). The next step, depending upon whether or not there was water vapor interference in the spectrum, was to subtract the water vapor absorbance file (VAPOS) from the "wet" protein coated polymer absorbance files (T2H30S) using the SAM (subtract absorbance manual) command with AFN set to AS.

The AS equation performs the subtraction by the following equation: SCA*AFA-CON*SCB*AFB. The subtraction factor (CON) is kept track of by the program while the absorbance file assigned to AFB is subtracted from the absorbance file assigned to AFA in real time and is stored automatically in

---

[1] TF20H30S = 24% filler SR/20% HEMA composite, 30 sec. exposure.

[2] GERT50 = germanium crystal.

the computer memory by the software routine. The absorbance files resulting from the subtraction of water vapor from the "wet" protein coated polymer were stored (e.g., T2H30SV) so that other subtractions could be performed on these files in the same manner. The next subtractions performed were the subtraction of the saline absorbance file (WATERS) from the water vapor subtracted "wet" protein coated polymer files (e.g., T2H30SV). The resultant files were the "dry" protein coated polymer files (e.g., T2H30SS), since the water vapor (if needed) and the saline had been subtracted from these files. Water vapor (if needed) and saline were subtracted in the same manner from the "wet" polymers to produce the "dry" polymer absorbance files (e.g., TWF02HS).[1]

The final step was to subtract the "dry" polymer absorbance files from the "dry" protein coated polymer files to obtain spectra of just the protein adsorbed onto the polymers. These last two files were then plotted with AFN set to AS. In a few cases, better spectra were obtained if water vapor was again subtracted from the final protein spectra (the spectra were made as smooth as possible with this technique). Figure 2 shows in equation form the subtractions necessary to obtain a spectrum of only the protein coat adsorbed onto the polymer.

After the subtractions were completed, a peak area routine provided by IBM was utilized to find the area underneath the 1550 cm^{-1} band of the protein spectra, since this band has been shown to be linearly related to the total amount of protein adsorbed (Gendreau et al., 1982). The

---

[1] TWF02HS = 24% filler SR/20% HEMA, unexposed.

SAM#	T2H30S-VAPOS	AFN = AS	Stored as T2H30SV
SAM#	T2H30SV-WATERS	AFN = AS	Stored as T2H30SS
SAM#	TWFO2H-VAPOS	AFN = AS	Stored as TWFO2HV
SAM#	TWFO2HV-WATERS	AFN = AS	Stored as TWFO2HS
SAM#	T2H30SS-TWFO2HS	AFN = AS	Plotted

Figure 2. Spectral subtractions depicted in equation form

integration is performed as follows: the integration limits (integer wavenumbers) are input into the peak area routine, and then a linear baseline is drawn from one integration limit to the other. The resulting area is then integrated.

RESULTS AND DISCUSSION

Results

Blood data

The blood data for the 13 dogs used for experimentation purposes are reported in Table 1. These values are within the normal range for healthy dogs.

Hemodynamic calculations

Reynolds number calculations were made for the flow conditions encountered in this investigation in order to assess if laminar or turbulent flow occurred. Also, it was of interest to determine if fully developed flow occurred along most of the tubing specimens. Once flow is fully established, it does not change any further with distance (Caro et al., 1978). The Reynolds number (Re) is defined as $Re = \rho DV/\mu$, where ρ= density of blood (1060 Kg/m^3), μ = viscosity of blood (0.004 N-s/m), V = velocity (m/s), and D = diameter of the tubing specimen (m). The relationships Q = VA, where A = area and Q = flow rate, and $A = \pi r^2$ then allow for the determination of Re. The Re for a 1.73 ml/sec flow rate is 296, and the Re for a 4.0 ml/sec flow rate is 689. It is known that turbulent flow occurs for a Re>2000, and laminar flow occurs for an Re<2000. Therefore, we had laminar flow for all of the cases studied.

The entrance length beyond the arterial side was calculated from the equation X = 0.03*D*Re (Caro et al., 1978), where X = the entrance length. It is known that beyond the entrance length, fully developed flow occurs. The X calculated for the 1.73 ml/sec flow rate is 1.8 cm, and for the

Table 1. Canine blood data

Dog number	Formulation	HCT before/ after	ACT (sec.) before/ after	Platelets/ $mm^3 \times 10^3$ before/after	Flow (ml/sec) before/after
4093	Commercial Silastic ®	39/39	102/130	475/465	2.33/3.0
4097	0% filler SR	44/42	101/159	267/253	2.33/3.33
4131	24% filler SR	37/36	115/107	261/250	2.81/4.0
4186	0% filler SR/ 20% H[a]	43/42	115/125	424/392	3.47/4.2
4210	0% filler SR/ 15% H/5% N[b]	45/42	112/100	424/405	3.33/4.67
4239	0% filler SR/ 10% H/10% N	37/37	104/134	350/440	1.87/2.67
4238	0% filler SR/ 5% H/15% N	41/42	120/125	312/346	2.27/3.75
4182	0% filler SR/ 20% N	46/39	96/98	294/324	2.67/2.86
4141	24% filler SR/ 20% H	44/43	112/93	365/302	3.07/2.73
4193	24% filler SR/ 15% H/5% N	45/46	146/103	559/453	1.73/3.0
4212	24% filler SR/ 10% H/10% N	38/36	99/102	327/422	2.67/4.0
4139	24% filler SR/ 5% H/15% N	47/43	109/139	250/277	2.67/4.0
4180	24% filler SR/ 20% N	35/37	125/123	469/410	4.0/3.73

[a] H = HEMA.

[b] N = NVP.

4.0 ml/sec flow rate case, X is 4.1 cm. Since sampling was done from the venous end, fully developed flow had occurred over the sampling length.

SEM observations

Microstructural information based on SEM observations of the 13 sample types will be presented in the following order: The "control" group (no hydrogel present) which consists of commercial Silastic®, 0% filler SR coated Silastic® (0% filler SR), and 24% filler SR coated Silastic® (24% filler SR); the hydrogel compositions 20% HEMA, 15% HEMA/5% NVP, 10% HEMA/10% NVP, 5% HEMA/15% NVP, and 20% NVP each grafted onto 0% filler SR; and finally the same above hydrogel compositions each grafted onto 24% filler SR.

The thickness of the 0% filler and 24% filler SR coating on the Silastic® substrates was determined in order to assess if an adequate coating was attained. The cross sectional views of the 0% filler SR and 24% filler SR substrates at low magnification and high magnification are shown in Figures 3a and 3b for the 0% filler SR substrate and 4a and 4b for the 24% filler SR substrate. The 0% filler SR coating thickness is 0.0035 mm, and the 24% filler SR coating thickness is 0.043 mm. The 0% filler SR coating along the Silastic® substrate was found to be relatively uniform, varying from 0.005 mm to 0.0035 mm in thickness. This indicates that the coating technique used was adequate.

The relative buildup of cellular material with respect to time on the 13 varieties was characterized with SEM. Microstructural features of thrombi (i.e., composition, porosity, shape) were studied since these

Figure 3a. Cross sectional view of 0% filler SR coated Silastic®. (S) designates Silastic®, (Z) designates 0% filler SR coating. 0% filler SR coating thickness is 0.0035 mm (scale bar = 250 μm)

Figure 3b. Higher magnification of Figure 3a showing the 0% filler SR coating (scale bar = 10 μm)

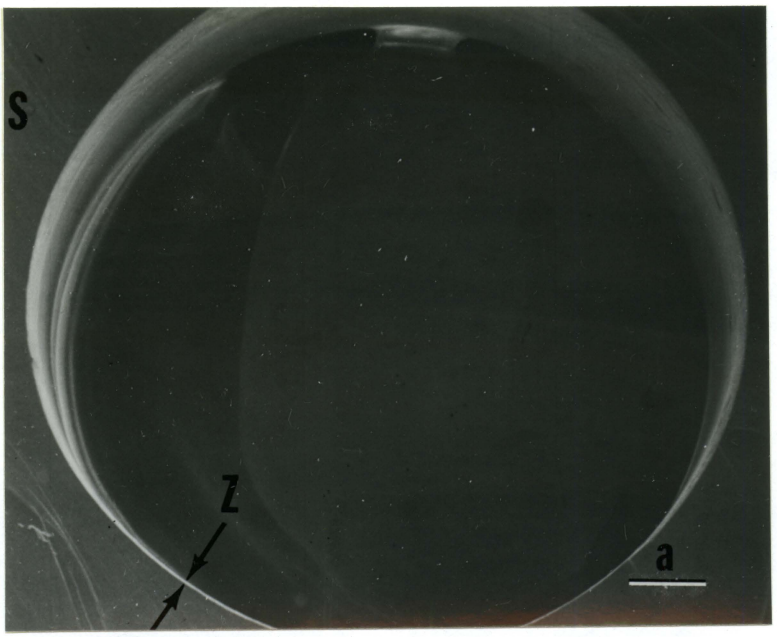
S
Z
a

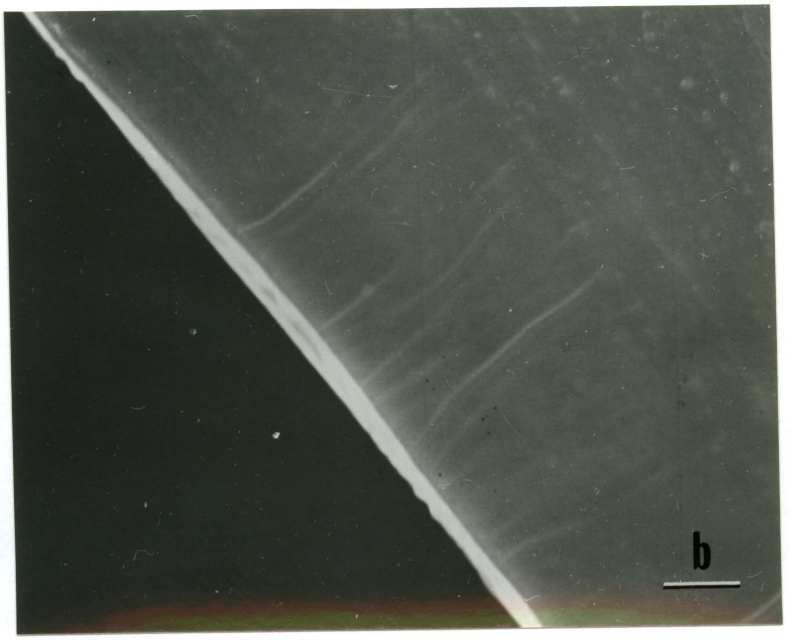
b

Figure 4a. Cross sectional view of 24% filler SR coated Silastic®. (S) designates Silastic®, (T) designates 24% filler SR coating. 24% filler SR coating thickness is 0.043 mm (scale bar = 250 μm)

Figure 4b. Higher magnification of Figure 4a showing the 24% filler SR coating (scale bar = 30 μm)

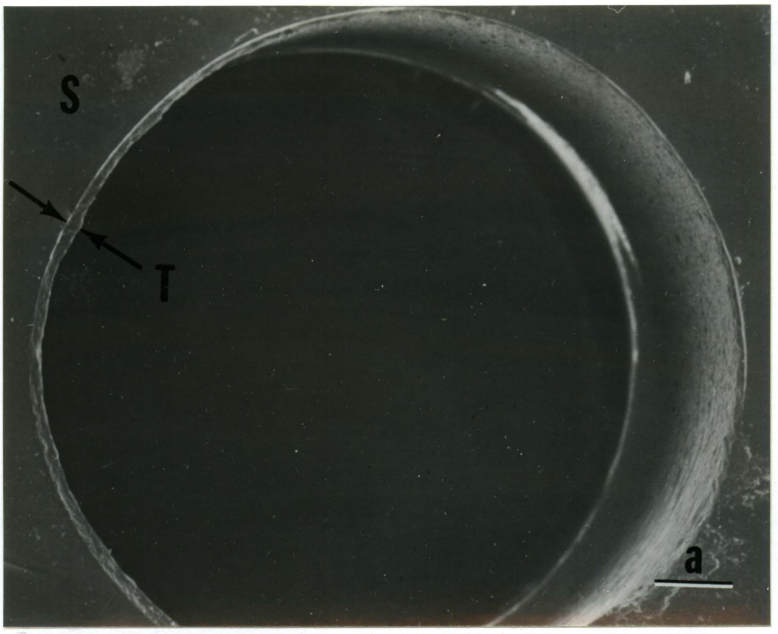
S
T
a

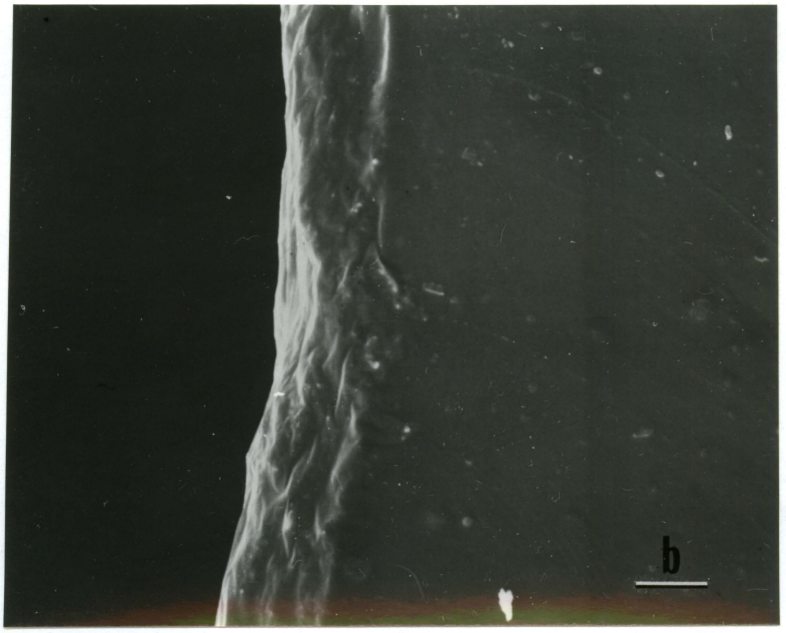
b

features may relate to protein adherence and embolization. SEM observations of each individual formulation with respect to time will be presented first. Then, comparisons will be made among samples based on the effects of the hydrogel formulations and the 0 and 24% filler SR-hydrogel combinations. Table 2 is a summary of thrombus deposition and release on the 13 sample types. The components of the thrombi as seen by SEM are also noted for each sample type in Table 2. SEM micrographs of the 13 varieties are shown in Figures 5a through 25c. The first set of six micrographs for each sample type shows sequentially the unexposed surface and the general blood response to that surface for the exposure times of 0.25, 0.5, 5, 15, and 75 minutes. For some varieties, an additional set of micrographs follow which depict the buildup of thrombi with time.

Controls (no hydrogel present) The response of blood to the sample types commercial Silastic®, 0% filler SR, and 24% filler SR, and the corresponding unexposed surfaces are presented in Figures 5a through 8f.

Commercial Silastic® The analysis of the commercial substrate (Figures 5b through 5f) shows a relatively light reaction, with platelet activity being the main cellular event. At 15 minutes (Figure 5e), the platelet activity has peaked (extensive aggregation), and at 75 minutes (Figure 5f), the cellular activity has subsequently decreased. It should be noted that platelets (some activated) were deposited as early as 0.25 minute (Figure 5b) on the commercial substrate.

0% filler SR The 0% filler SR substrate shows no obvious major cellular activity (Figures 6b through 6f). The surface imperfections, which are present in all the micrographs (Figures 6a through 6f), in

Table 2. Thrombus deposition and release

Formulation	Thrombus components[a]	Maximum thrombus coverage (%)/ time occurred	Thrombus coverage (%) 75 min.	% emboli-zation[b]
Commercial Silastic®	-	-	-	-
0% filler SR	Platelets, fibrin	.03/5	-	100
24% filler SR	-	-	-	-
0% filler SR/ 20% H	Platelets	3.4/15	0	100
0% filler SR/ 15% H/5% N	Platelets, some leuko-cytes, red blood cells	100/75	100	-
0% filler SR/ 10% H/10% N	-	-	-	-
0% filler SR/ 5% H/15% N	Platelets, fibrin, leukocytes, red blood cells	.9/15	.6	33
0% filler SR/ 20% N	-	-	-	-
24% filler SR/ 20% H	Platelets, some red blood cells, leukocytes	1.0/15	.82	18
24% filler SR/ 15% H/5% N	Platelets	.04/5	0	100
24% filler SR/ 10% H/10% N	-	-	-	-
24% filler SR/ 5% H/15% N	Platelets	1.46/15	.14	90
24% filler SR/ 20% N	Platelets	.4/15	.06	85

[a] A thrombus was considered to be a cell or cell-fibrin aggregate of 50 μm or more in its greatest dimension.

[b] % embolization = $(1 - \frac{\text{thrombus coverage at 75 min.}}{\text{maximum thrombus coverage}})*100$, as introduced by Barber et al. (1978).

Figure 5a. Scanning electron micrograph of Silastic®, unexposed (scale bar = 10 μm)

Figure 5b. Silastic® at 0.25 minute of blood exposure (scale bar = 10 μm)

Figure 5c. Silastic® at 0.5 minute of blood exposure (scale bar = 10 μm)

Figure 5d. Silastic® at 5 minutes of blood exposure (scale bar = 10 μm)

Figure 5e. Silastic® at 15 minutes of blood exposure (scale bar = 10 μm)

Figure 5f. Silastic® at 75 minutes of blood exposure (scale bar = 10 μm)

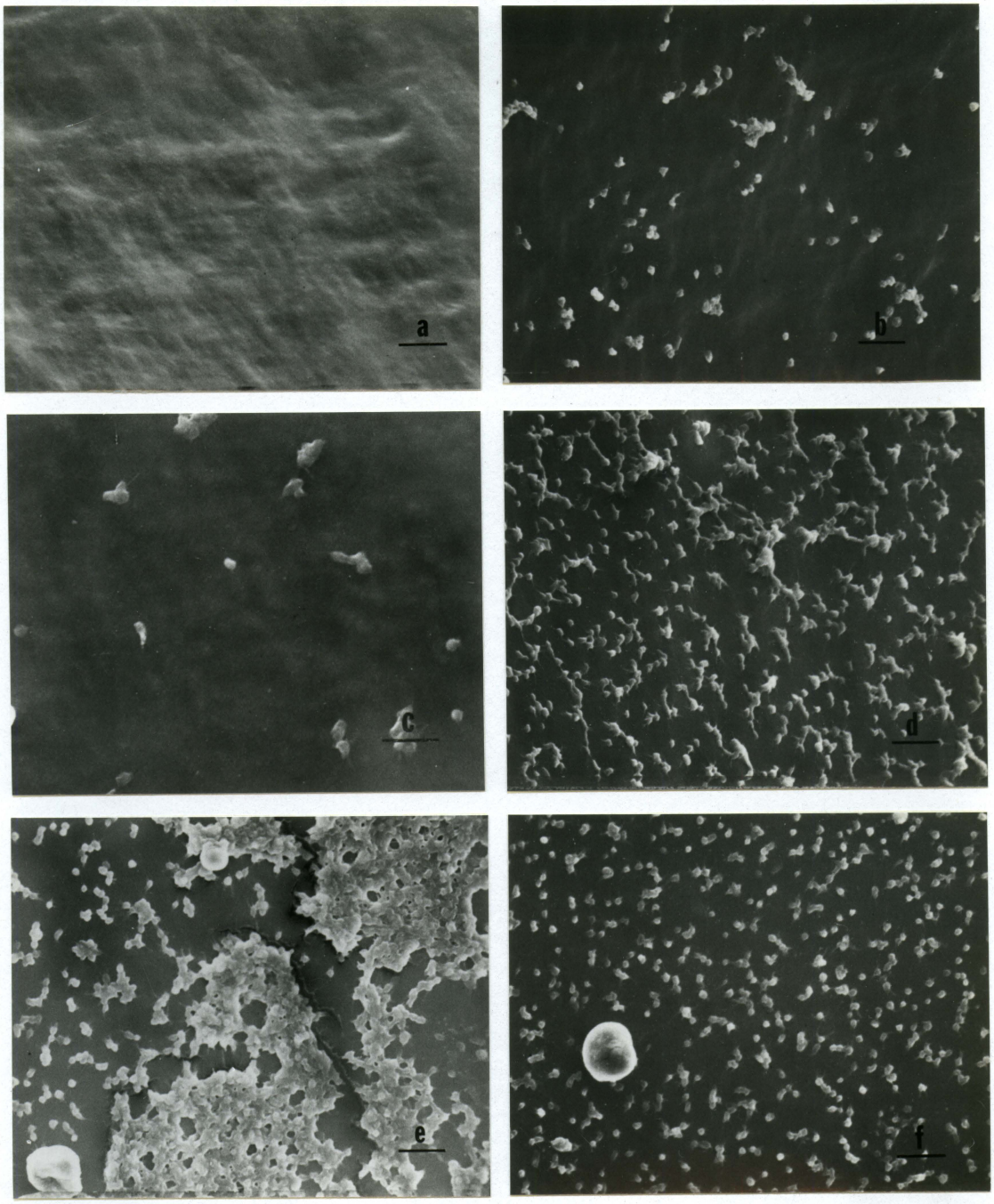
a
b
c
d
e
f

Figure 6a. Scanning electron micrograph of the 0% filler SR substrate, unexposed (scale bar = 10 μm)

Figure 6b. 0% filler SR substrate at 0.25 minute of blood exposure (scale bar = 10 μm)

Figure 6c. 0% filler SR substrate at 0.5 minute of blood exposure (scale bar = 10 μm)

Figure 6d. 0% filler SR substrate at 5 minutes of blood exposure (scale bar = 10 μm)

Figure 6e. 0% filler SR substrate at 15 minutes of blood exposure (scale bar = 10 μm)

Figure 6f. 0% filler SR substrate at 75 minutes of blood exposure (scale bar = 10 μm)

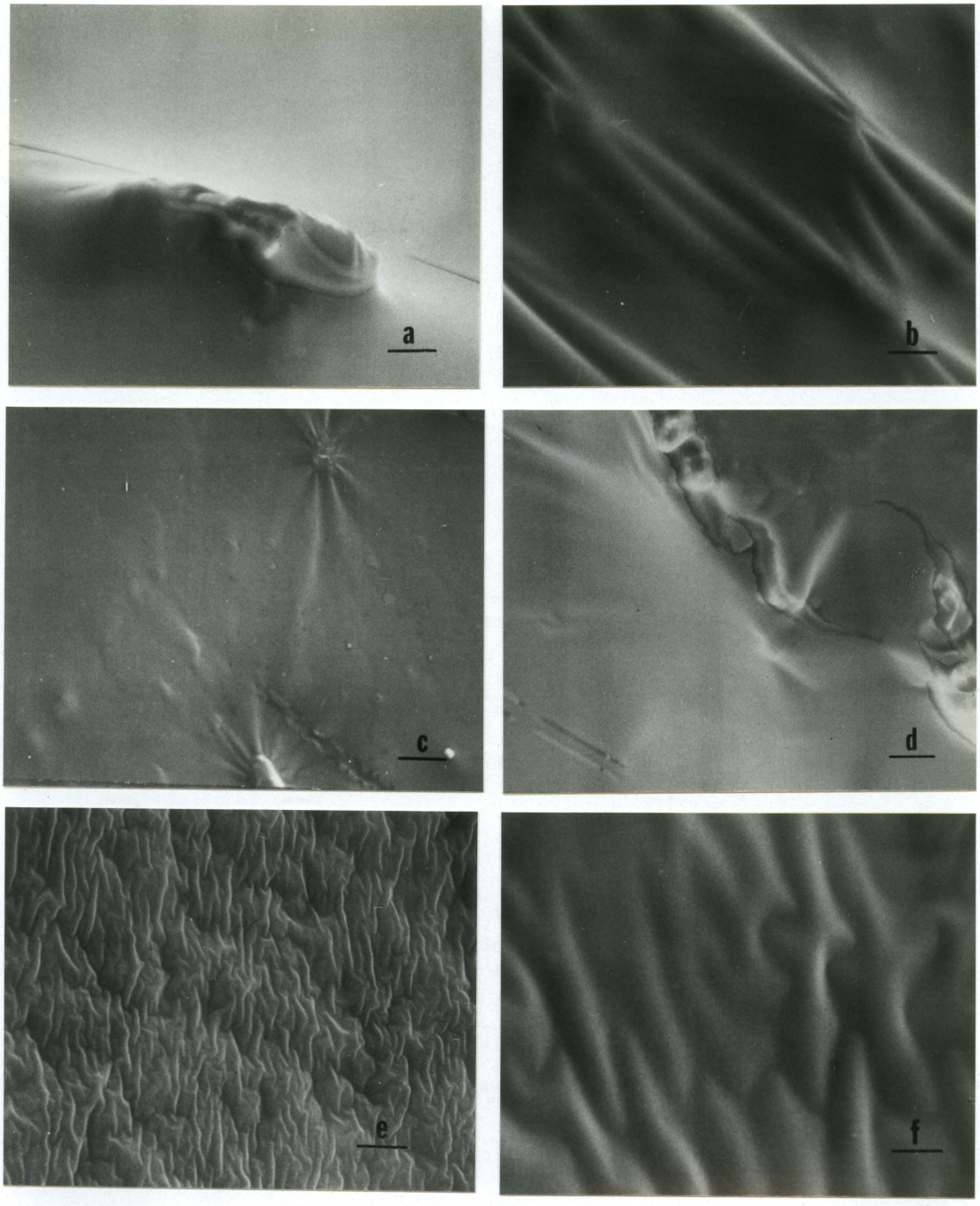
a
b
c
d
e
f

a few cases appear to cause limited cellular activity at 5 and 75 minutes (Figures 7a and 7b, respectively). These imperfections are believed to be due to filler particles (alone and possibly agglomerated) that were not filtered from the Silastic® 382 Medical Grade Elastomer. The number of imperfections in the particular sample type varied from area to area. At certain points, there were quite a few imperfections, and along other areas of the sample type, few imperfections were evident. Another 0% filler SR coated Silastic® tube was prepared in order to assess the frequency of silica filler occurrence along the tube. It was found that approximately the bottom three-fourths of the tube was essentially filler free. The bottom end of each sample type was where the samples were taken from. An isolated platelet thrombus in Figure 7a, as well as a fibrin mat in Figure 7b, appear to rest on surface imperfections. The fibrin mat is possibly what was left after a thrombus had embolized.

24% filler SR The blood response of the 24% filler SR substrate as seen in Figures 8b through 8f appears to indicate no deposition of formed blood elements. Silica filler is visible beneath the surface in all the micrographs (Figures 8a through 8f). Possibly, some platelets are present in a masked form. This special appearance of the platelets will be discussed in detail when the 0% filler SR/20% HEMA sample type is discussed. There appears to be a gradual buildup of platelets up to 15 minutes exposure (Figure 8e), with a subsequent decrease at 75 minutes of blood exposure (Figure 8f).

In general, these control varieties caused a minimal blood response with time, with the exception of the commercial substrate which caused extensive platelet activity up to 15 minutes of blood exposure.

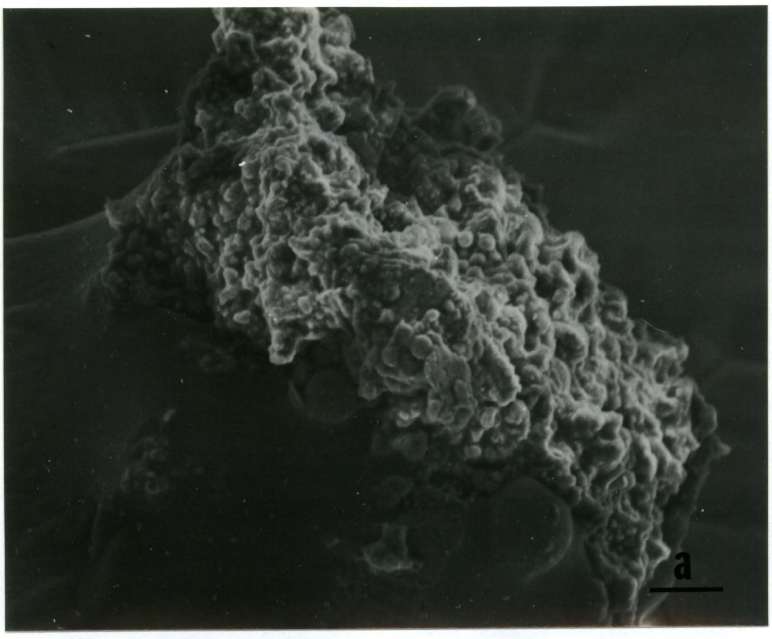

Figure 7a. Scanning electron micrograph of the 0% filler SR substrate, 5 minutes exposure to blood (scale bar = 20 μm)

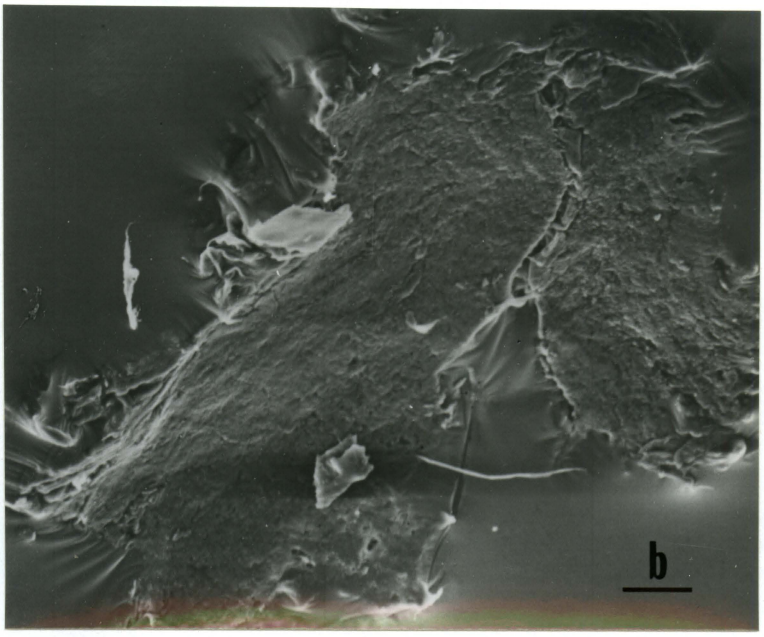

Figure 7b. 0% filler SR substrate at 75 minutes exposure to blood (scale bar = 30 μm)

Figure 8a. Scanning electron micrograph of the 24% filler SR substrate, unexposed (scale bar = 10 μm)

Figure 8b. 24% filler SR substrate at 0.25 minute of blood exposure (scale bar = 10 μm)

Figure 8c. 24% filler SR substrate at 0.5 minute of blood exposure (scale bar = 10 μm)

Figure 8d. 24% filler SR substrate at 5 minutes of blood exposure (scale bar = 10 μm)

Figure 8e. 24% filler SR substrate at 15 minutes of blood exposure (scale bar = 10 μm)

Figure 8f. 24% filler SR substrate at 75 minutes of blood exposure (scale bar = 10 μm)

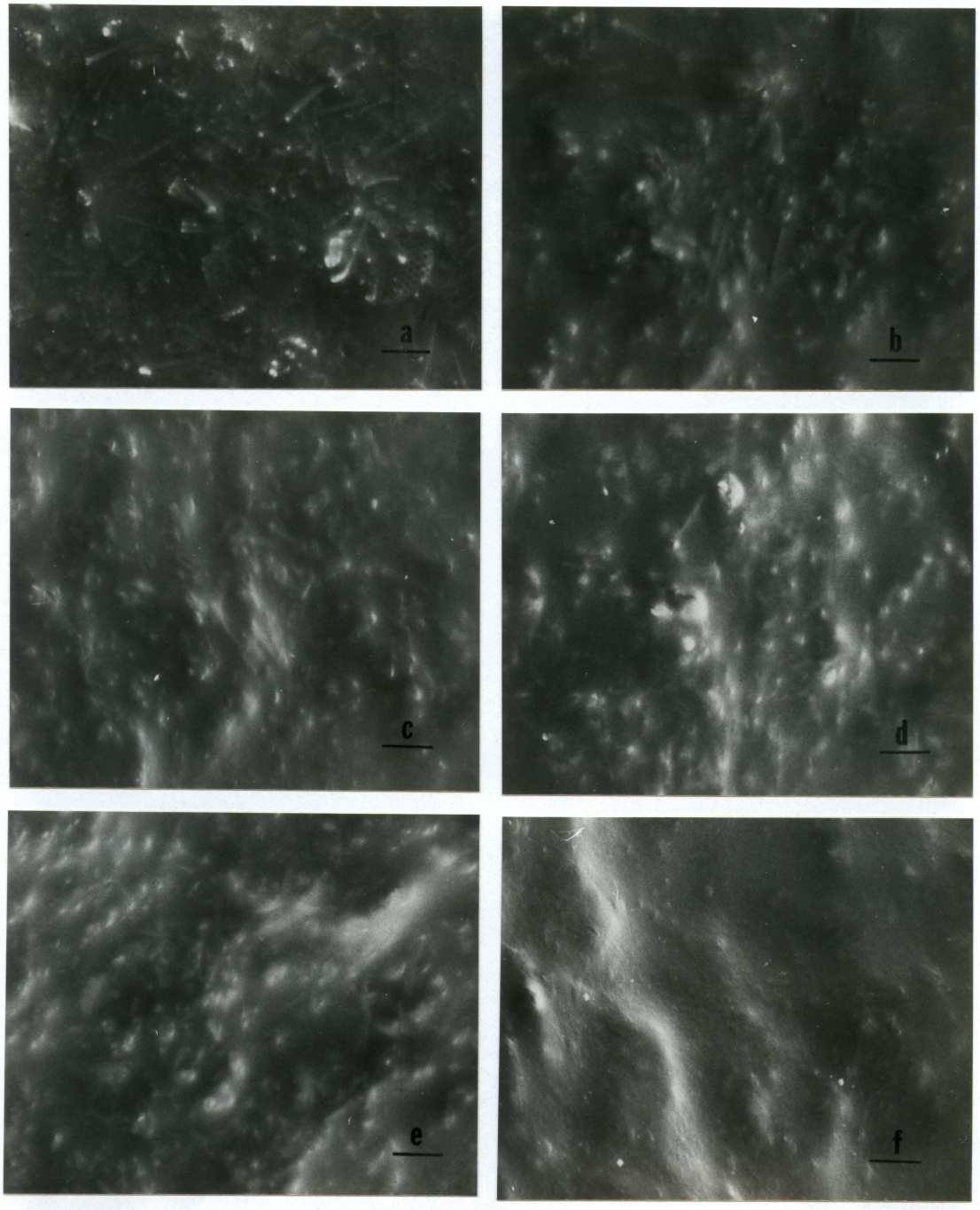
a
b
c
d
e
f

0% filler SR-hydrogel formulations SEM micrographs indicating the response of blood to the 0% filler SR-hydrogel formulations are shown in Figures 9a through 16f.

0% filler SR/20% HEMA The analysis of the 0% filler SR/20% HEMA composite shows an appearance of platelets comparable to the platelet appearance on the 24% filler SR SEM images (Figures 9b through 9f). The masked platelets could possibly be covered by a noncellular material (for instance, plasma). The possibility that these particles are silica filler, and not platelets, was dismissed since the unexposed surface (Figure 9a) shows no evidence of filler. The platelets appear activated (a shape change occurred) by 5 minutes of exposure (Figure 9d), and this activated state is maintained through 75 minutes of blood exposure (Figure 9f). Figures 10a and 10b show a low and high magnification (respectively) of a very large flat platelet thrombus that developed by 15 minutes. It is possible that parts of this thrombus had embolized earlier, leaving this flat base. The thrombus is quite porous in nature. As noted in Table 2, 100% embolization occurred by 75 minutes of blood exposure.

0% filler SR/15% HEMA/5% NVP Figures 11b through 12c show the blood-0% filler SR/15% HEMA/5% NVP composite interaction. The vessel with this formulation occluded by 75 minutes of blood exposure. However, the clot was pushed through with saline. The general response to blood as seen in Figures 11b through 11f is a uniform coating of platelets (note that the surface pictured at 75 minutes (Figure 11f) is the surface which resulted after the plug had been washed away). Platelet pillars developed by 15 minutes (Figure 12a). The particular platelet pillar pictured in

Figure 9a. Scanning electron micrograph of the 0% filler SR/20% HEMA formulation, unexposed (scale bar = 10 μm)

Figure 9b. 0% filler SR/20% HEMA formulation at 0.25 minute of blood exposure (scale bar = 10 μm)

Figure 9c. 0% filler SR/20% HEMA formulation at 0.5 minute of blood exposure (scale bar = 10 μm)

Figure 9d. 0% filler SR/20% HEMA formulation at 5 minutes of blood exposure (scale bar = 10 μm)

Figure 9e. 0% filler SR/20% HEMA formulation at 15 minutes of blood exposure (scale bar = 10 μm)

Figure 9f. 0% filler SR/20% HEMA formulation at 75 minutes of blood exposure (scale bar = 10 μm)

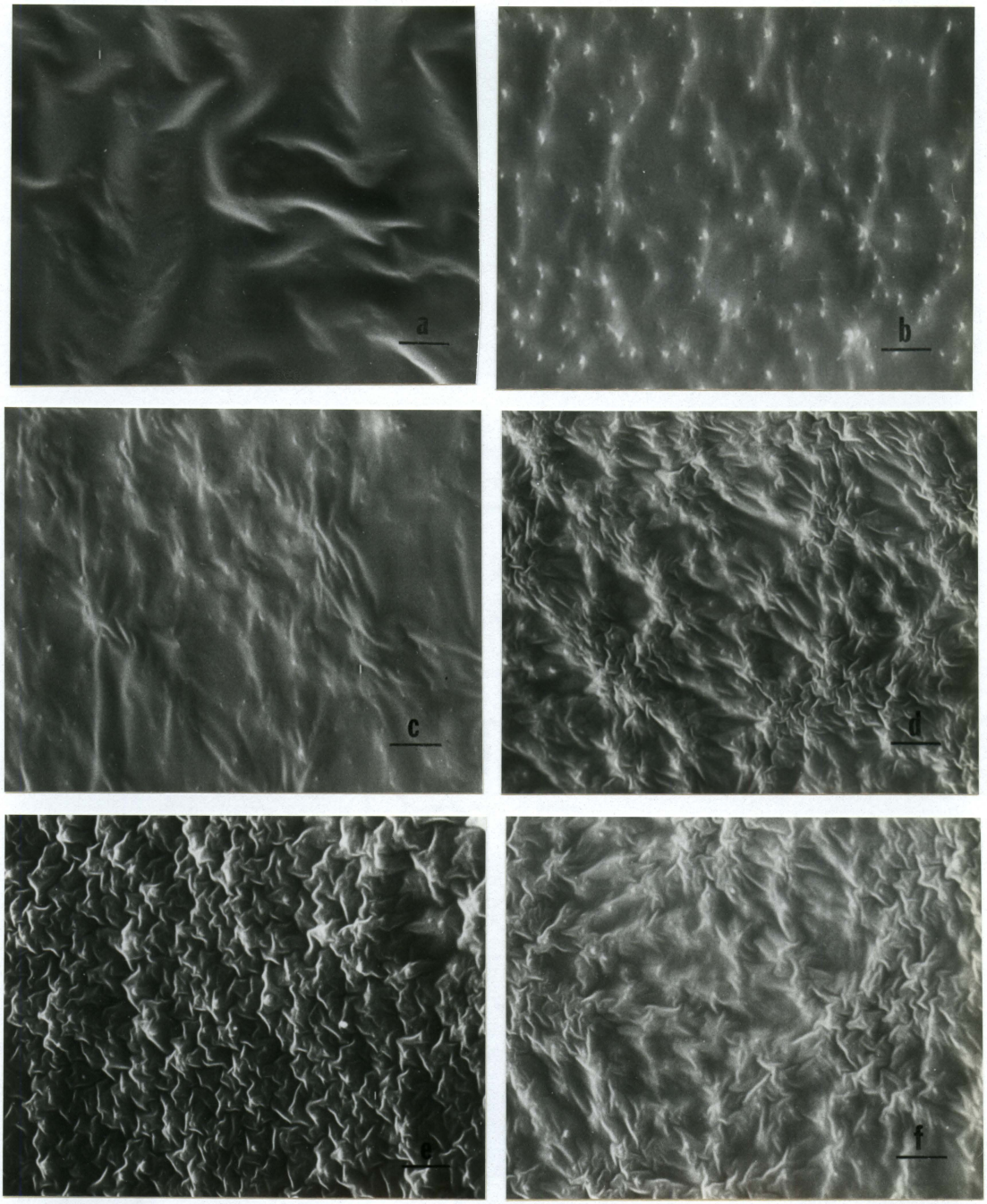
a
b
c
d
e
f

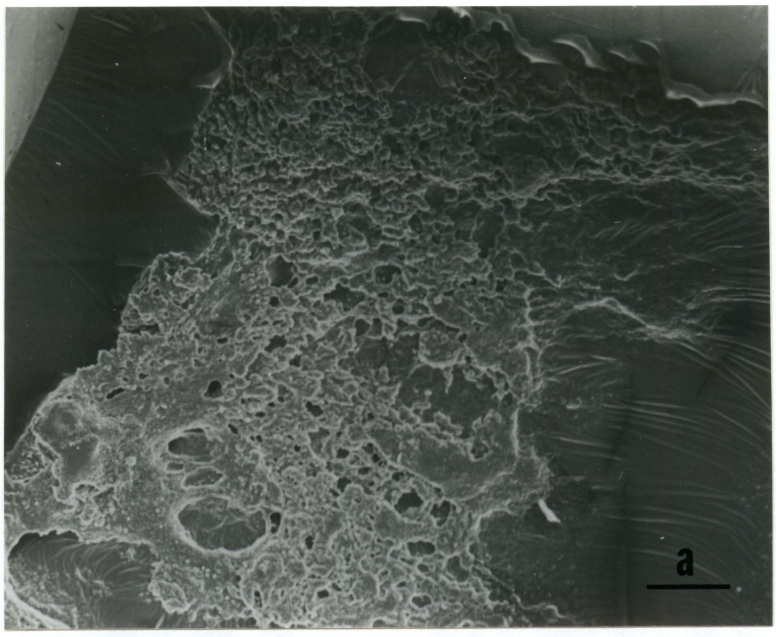

Figure 10a. Scanning electron micrograph of the 0% filler SR/20% HEMA formulation at 15 minutes of blood exposure (scale bar = 170 μm)

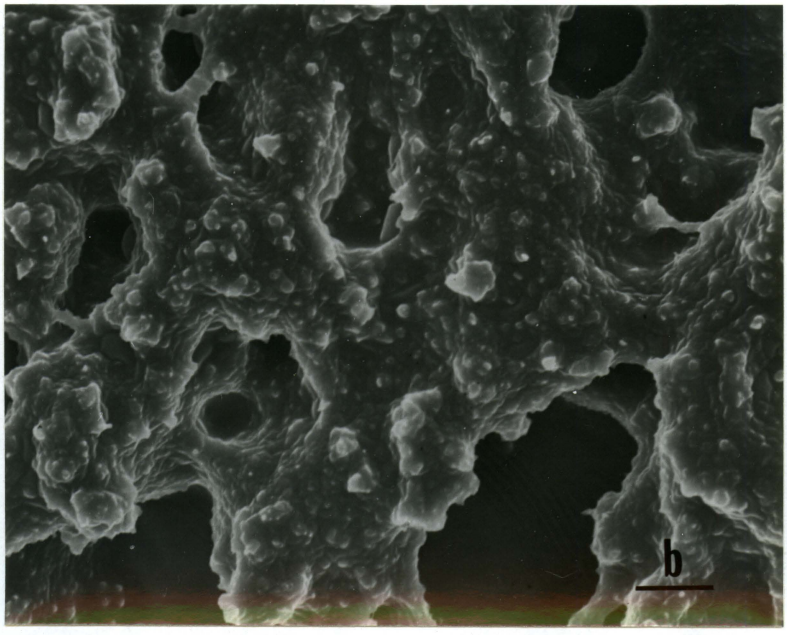

Figure 10b. Higher magnification of Figure 10a (scale bar = 10 μm)

Figure 11a. Scanning electron micrograph of the 0% filler SR/15% HEMA/ 5% NVP formulation, unexposed (scale bar = 10 μm)

Figure 11b. 0% filler SR/15% HEMA/5% NVP formulation at 0.25 minute of blood exposure (scale bar = 10 μm)

Figure 11c. 0% filler SR/15% HEMA/5% NVP formulation at 0.5 minute of blood exposure (scale bar = 10 μm)

Figure 11d. 0% filler SR/15% HEMA/5% NVP formulation at 5 minutes of blood exposure (scale bar = 10 μm)

Figure 11e. 0% filler SR/15% HEMA/5% NVP formulation at 15 minutes of blood exposure (scale bar = 10 μm)

Figure 11f. 0% filler SR/15% HEMA/5% NVP formulation at 75 minutes of blood exposure (scale bar = 10 μm)

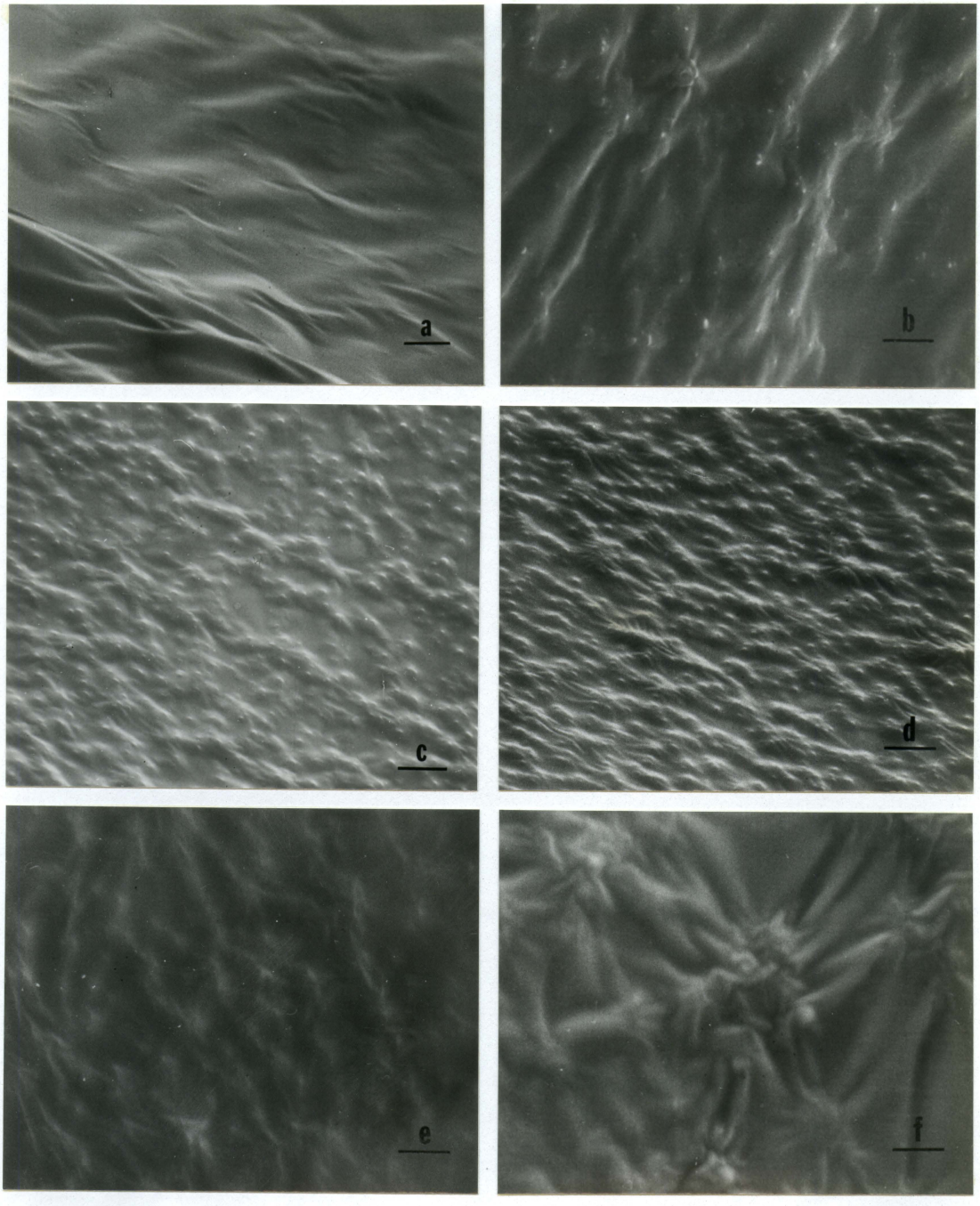
a
b
c
d
e
f

Figure 12a is porous in nature, protrudes into the lumen, and is surrounded by an area devoid of cellular material. These observations were typical of all of the thrombi formed on this particular surface. Figure 12b is a high magnification view of a platelet-leukocyte pillar formed on this surface at 15 minutes. Figure 12c is a micrograph of the resultant surface after the plug was stripped away, and the structure is probably the base of a thrombus.

0% filler SR/10% HEMA/10% NVP The 0% filler SR/10% HEMA/10% NVP blood response is shown in Figures 13b through 13f. Again, a uniform cover of platelets occurs at 0.5 minute (Figure 13c), and the deposit of material is seen to increase slightly at 5 minutes (Figure 13d). No further increase in platelet deposition is seen as time of blood exposure increases (Figures 13e and 13f).

0% filler SR/5% HEMA/15% NVP Platelet deposition is the primary event of the general blood response sequence as seen in Figure 14b. Platelet deposition appears to peak at 5 minutes (Figure 14d). Well-developed white thrombi were seen on this surface at 5 and 15 minutes (Figures 15a through 15c). The shapes of the thrombi are both string-like (Figure 15a) and clump-like (Figure 15b). The string-like thrombi are parallel to the direction of flow. These thrombi are somewhat porous (perhaps not as porous as the high % HEMA types) and are surrounded by a cell free layer (Figures 15a and 15b). The bulk of the thrombus in Figure 15b appears to be preparing to detach. Few leukocytes were found on the thrombi. However, Figure 15c shows numerous red blood cells (some entrapped in a fibrin mesh) on the surface of a thrombus at 15 minutes.

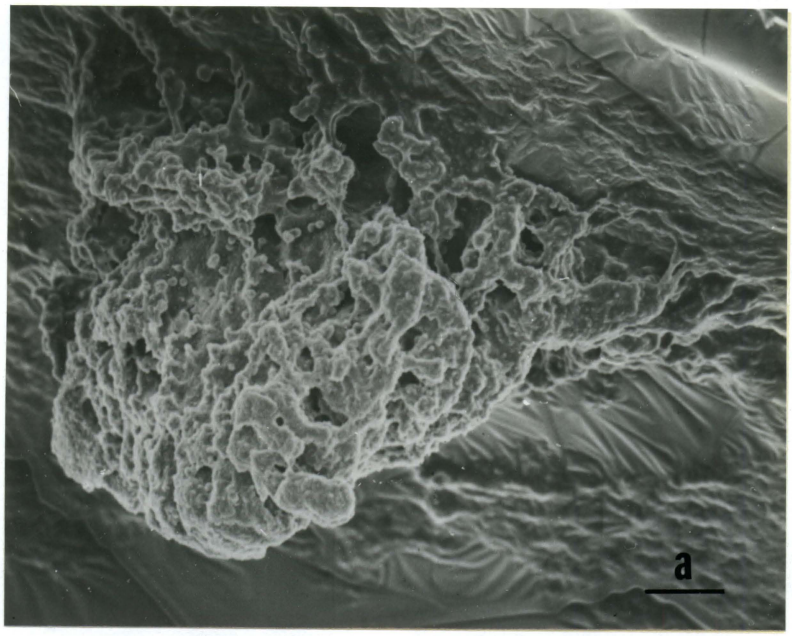

Figure 12a. Scanning electron micrograph of the 0% filler SR/15% HEMA/ 5% NVP formulation at 15 minutes of blood exposure (scale bar = 50 μm)

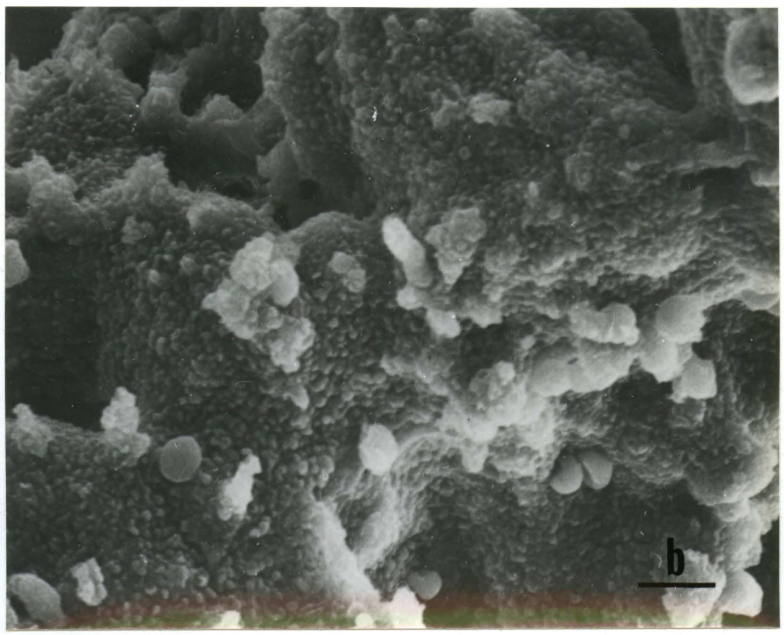

Figure 12b. 0% filler SR/15% HEMA/5% NVP formulation at 15 minutes of blood exposure (scale bar = 10 μm)

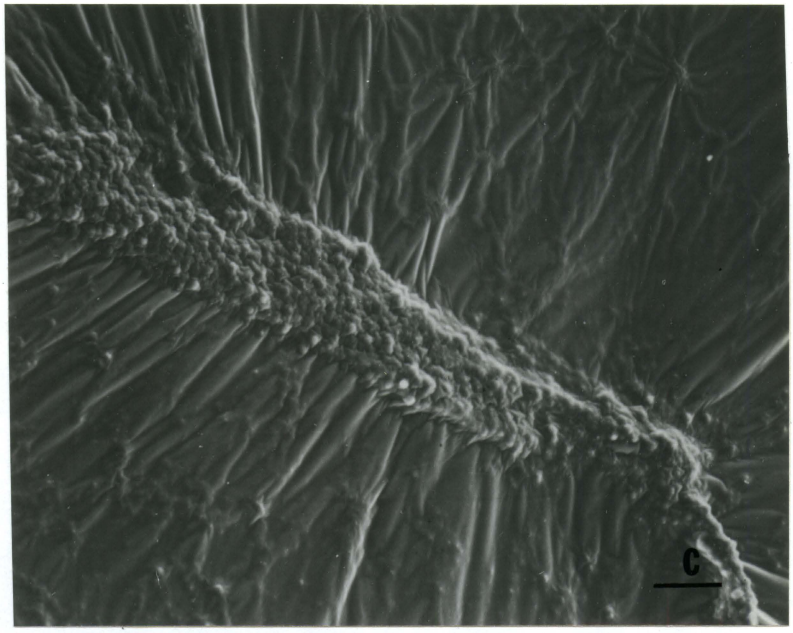

Figure 12c. 0% filler SR/15% HEMA/5% NVP formulation at 75 minutes of blood exposure (scale bar = 30 μm)

Figure 13a. Scanning electron micrograph of the 0% filler SR/10% HEMA/ 10% NVP formulation, unexposed (scale bar = 10 μm)

Figure 13b. 0% filler SR/10% HEMA/10% NVP formulation at 0.25 minute of blood exposure (scale bar = 10 μm)

Figure 13c. 0% filler SR/10% HEMA/10% NVP formulation at 0.5 minute of blood exposure (scale bar = 10 μm)

Figure 13d. 0% filler SR/10% HEMA/10% NVP formulation at 5 minutes of blood exposure (scale bar = 10 μm)

Figure 13e. 0% filler SR/10% HEMA/10% NVP formulation at 15 minutes of blood exposure (scale bar = 10 μm)

Figure 13f. 0% filler SR/10% HEMA/10% NVP formulation at 75 minutes of blood exposure (scale bar = 10 μm)

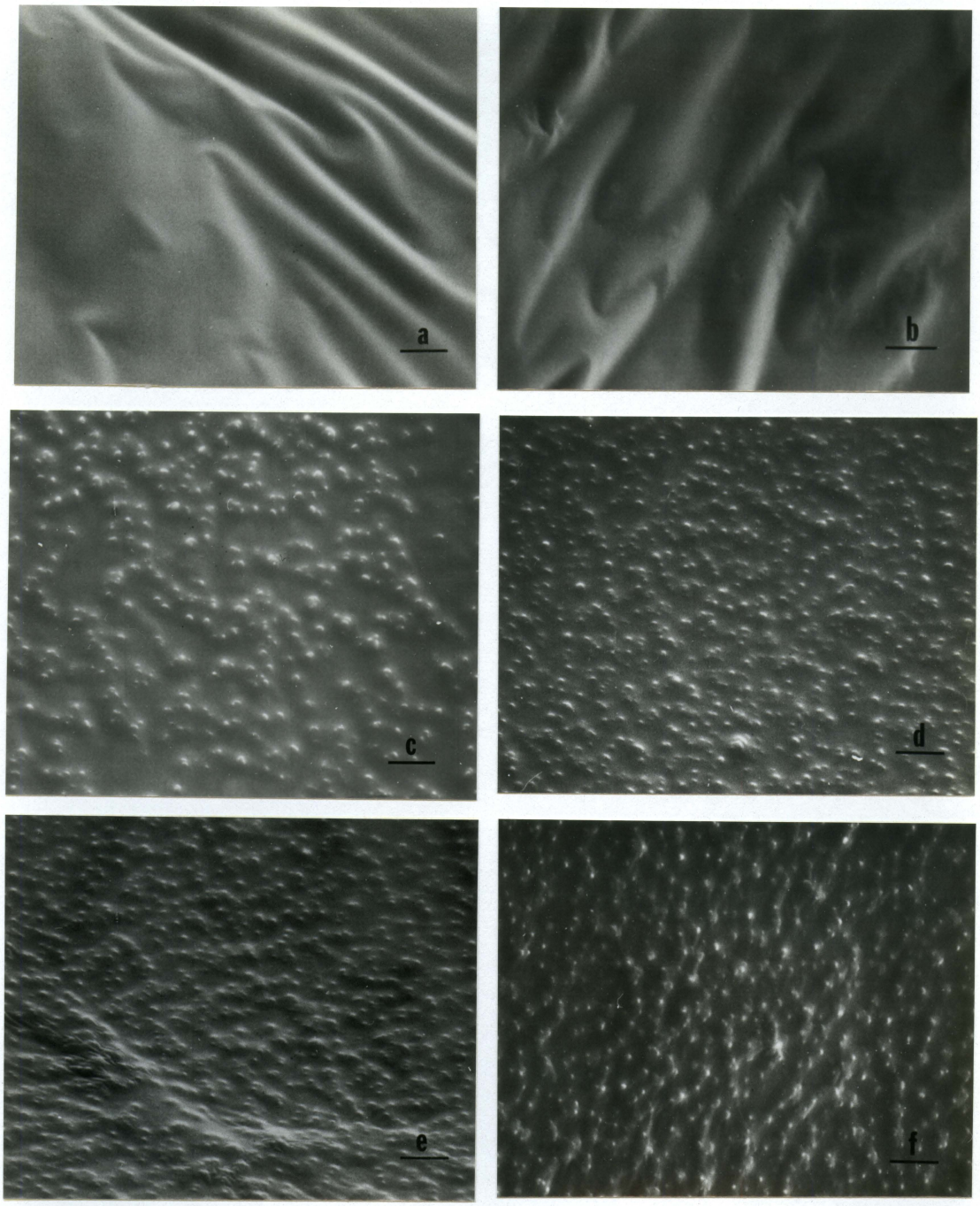
a
b
c
d
e
f

Figure 14a. Scanning electron micrograph of the 0% filler SR/5% HEMA/ 15% NVP formulation, unexposed (scale bar = 10 μm)

Figure 14b. 0% filler SR/5% HEMA/15% NVP formulation at 0.25 minute of blood exposure (scale bar = 10 μm)

Figure 14c. 0% filler SR/5% HEMA/15% NVP formulation at 0.5 minute of blood exposure (scale bar = 10 μm)

Figure 14d. 0% filler SR/5% HEMA/15% NVP formulation at 5 minutes of blood exposure (scale bar = 10 μm)

Figure 14e. 0% filler SR/5% HEMA/15% NVP formulation at 15 minutes of blood exposure (scale bar = 10 μm)

Figure 14f. 0% filler SR/5% HEMA/15% NVP formulation at 75 minutes of blood exposure (scale bar = 10 μm)

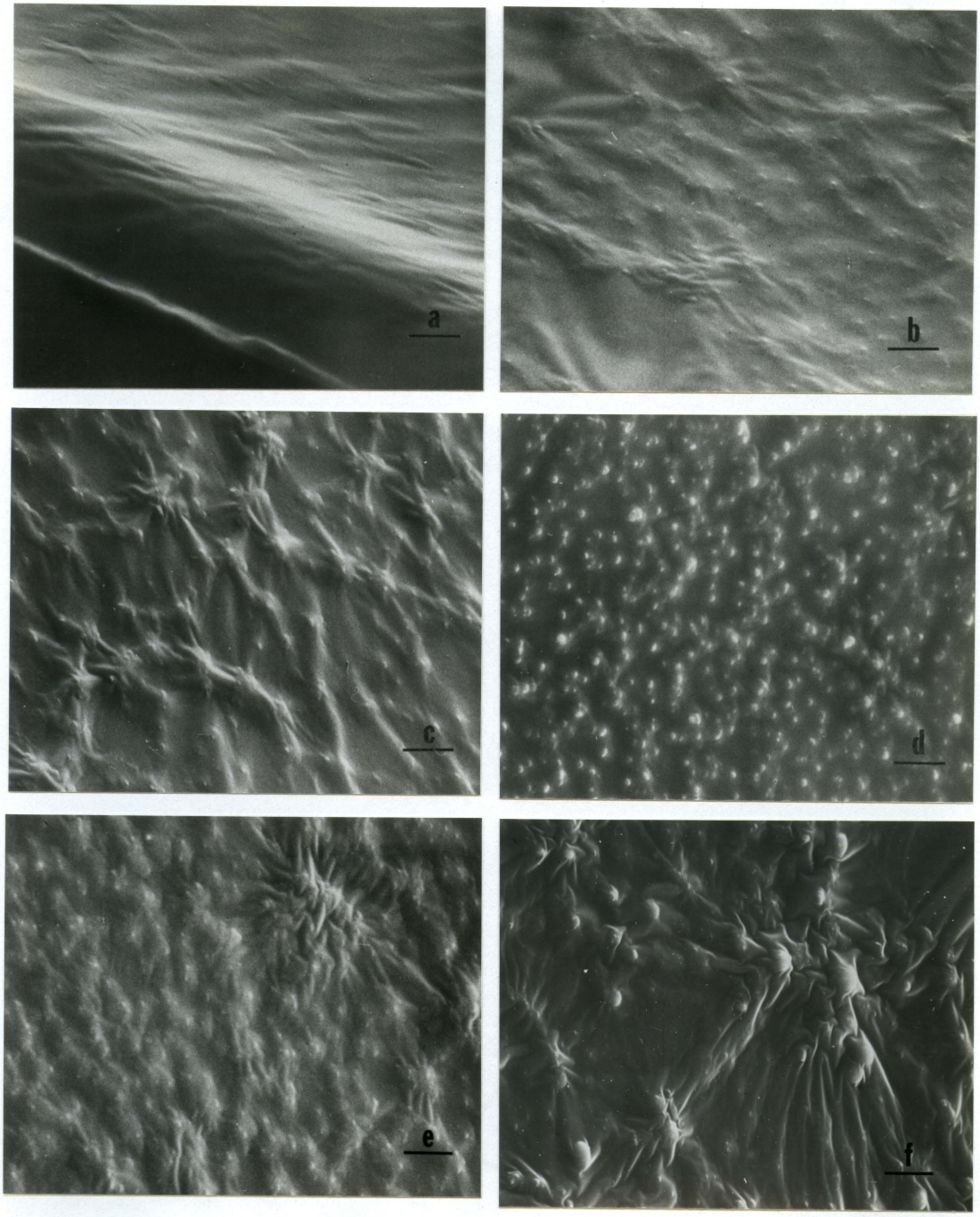
a
b
c
d
e
f

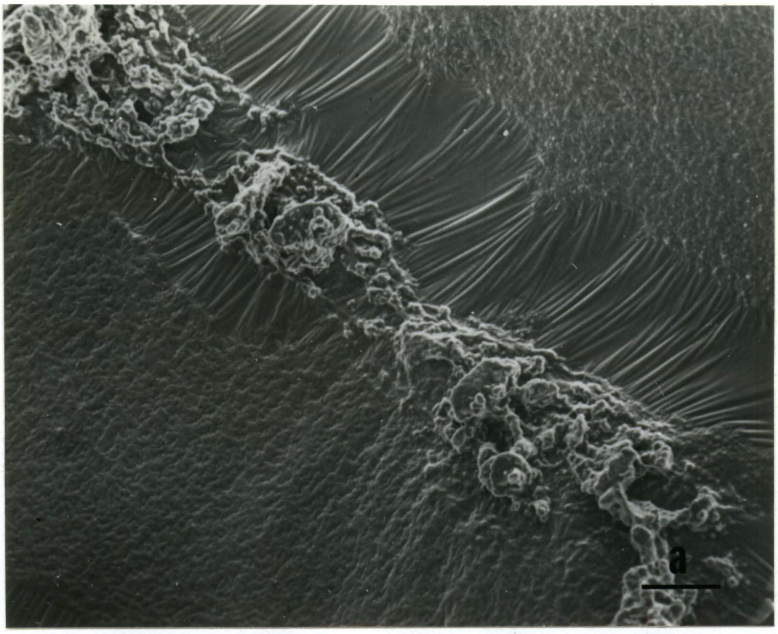

Figure 15a. Scanning electron micrograph of the 0% filler SR/5% HEMA/ 15% NVP formulation at 5 minutes of blood exposure (scale bar = 100 μm)

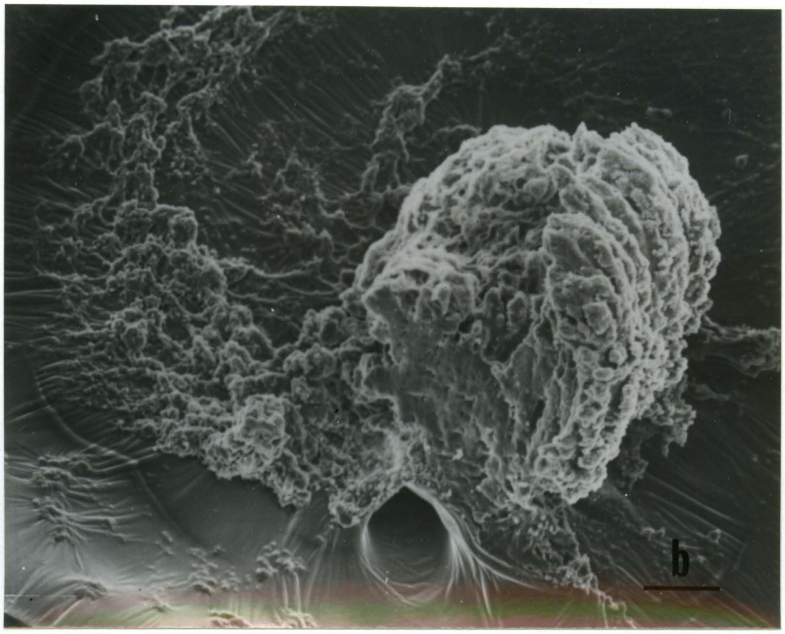

Figure 15b. 0% filler SR/5% HEMA/15% NVP formulation at 15 minutes of blood exposure (scale bar = 100 μm)

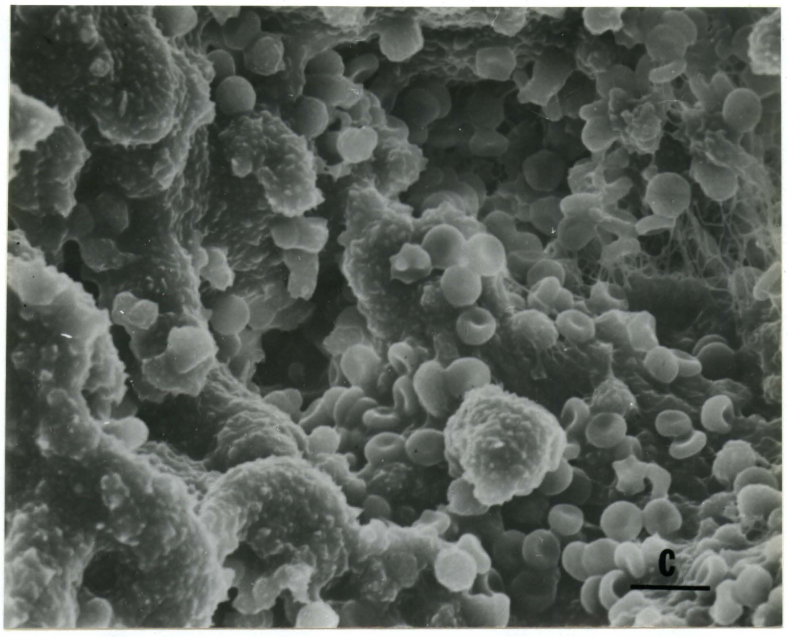

Figure 15c. 0% filler SR/5% HEMA/15% NVP formulation at 15 minutes of blood exposure (scale bar = 10 μm)

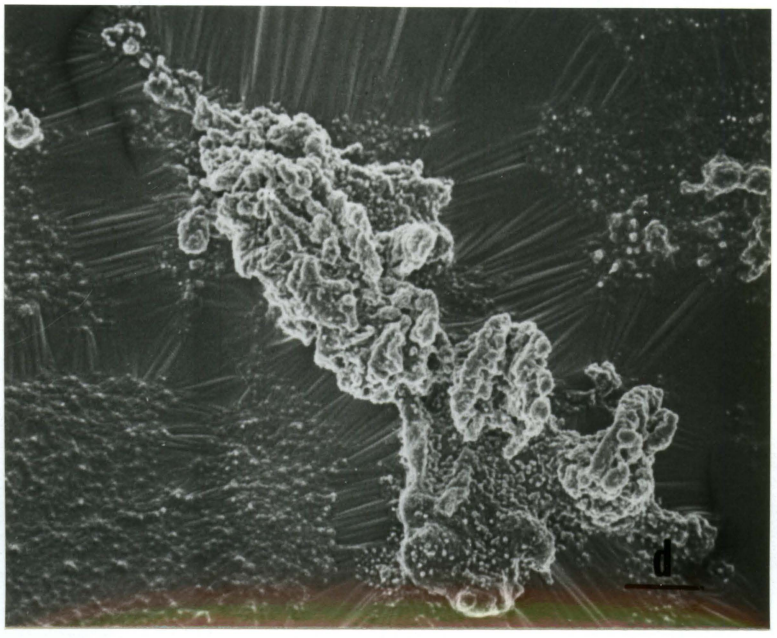

Figure 15d. 0% filler SR/5% HEMA/15% NVP formulation at 75 minutes of blood exposure (scale bar = 100 μm)

The response after 75 minutes is the buildup of platelet thrombi similar to those seen at 15 minutes (Figure 15d). As is indicated in Table 2, the maximum thrombus coverage occurred at 15 minutes, and 33% embolization occurred by 75 minutes. The appearance of all the thrombi on this surface is such that it seems likely that parts of the thrombi could embolize. The thrombi seem to be made out of loosely held agglomerates of material.

0% filler SR/20% NVP The response of blood to the 0% filler SR/20% NVP formulation is shown in Figures 16b through 16f. Surface imperfections also appear on this sample type and seem to be due to agglomerated filler as seen by the size and appearance of the imperfections pictured in Figures 16a and 16b. Platelets appear at 0.5 minute (Figure 16c). Extensive platelet aggregation is seen at 5 minutes (Figure 16d), and a subsequent decrease in the amount of material on the surface is seen at 15 minutes (Figure 16e). The platelets in Figures 16d and 16e are clearly visible, but at 75 minutes (Figure 16f), the platelets again appear covered by a thin film.

In general, the 0% filler SR/20% HEMA, the 0% filler SR/15% HEMA/5% NVP, and the 0% filler SR/5% HEMA/15% NVP formulations showed the most severe response to blood of all the 0% filler SR-hydrogel series.

24% filler SR-hydrogel formulations SEM micrographs indicating the blood response of the 24% filler SR-hydrogel formulations are shown in Figures 17a through 25c.

24% filler SR/20% HEMA The primary event of the general blood response sequence shown in Figures 17b through 17f is the appearance of thin film coated platelets at 0.25 minute (Figure 17b). Platelet deposition

Figure 16a. Scanning electron micrograph of the 0% filler SR/20% NVP formulation, unexposed (scale bar = 10 μm)

Figure 16b. 0% filler SR/20% NVP formulation at 0.25 minute of blood exposure (scale bar = 10 μm)

Figure 16c. 0% filler SR/20% NVP formulation at 0.5 minute of blood exposure (scale bar = 10 μm)

Figure 16d. 0% filler SR/20% NVP formulation at 5 minutes of blood exposure (scale bar = 10 μm)

Figure 16e. 0% filler SR/20% NVP formulation at 15 minutes of blood exposure (scale bar = 10 μm)

Figure 16f. 0% filler SR/20% NVP formulation at 75 minutes of blood exposure (scale bar = 10 μm)

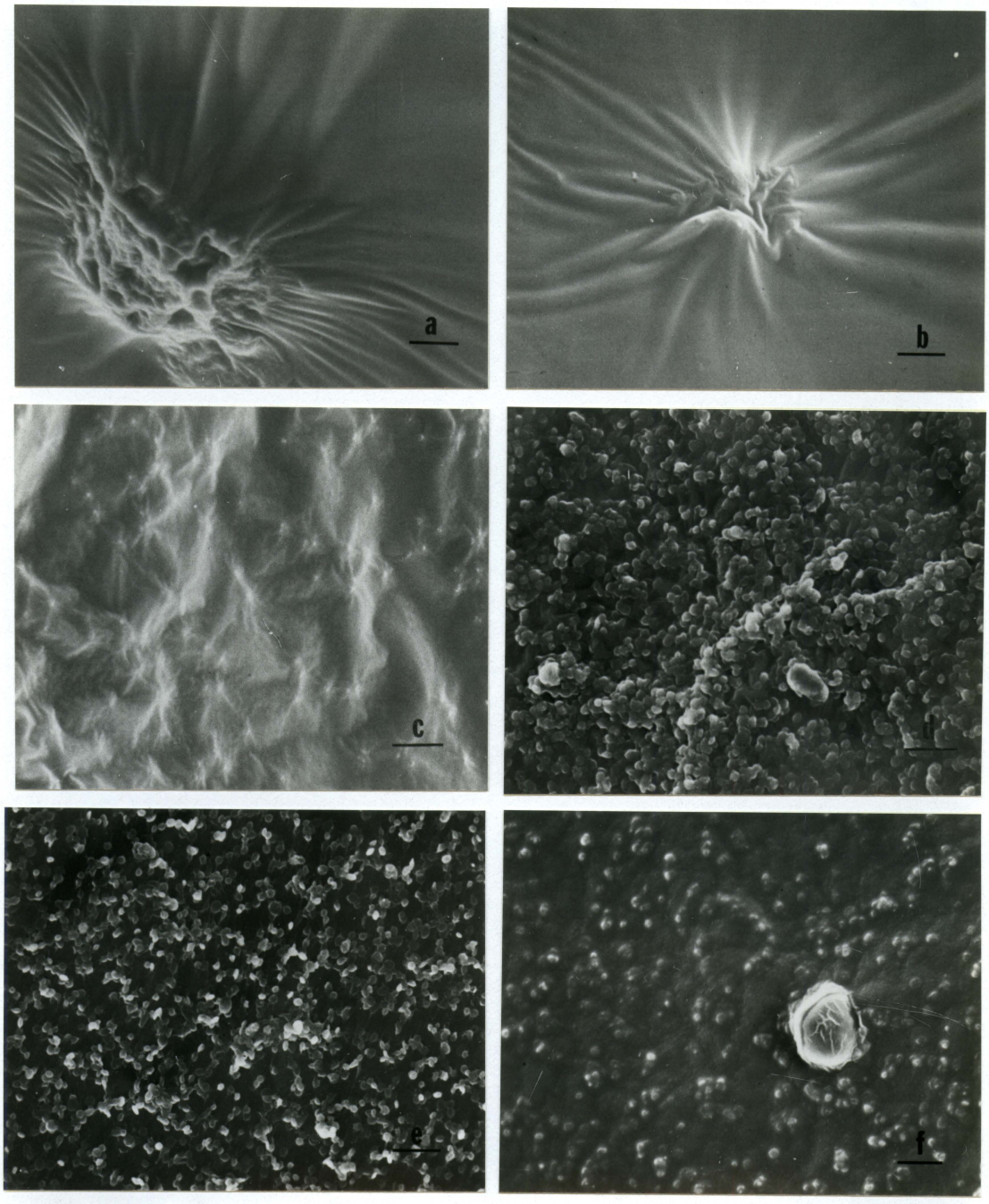
a
b
c
d
e
f

Figure 17a. Scanning electron micrograph of the 24% filler SR/20% HEMA formulation, unexposed (scale bar = 10 μm)

Figure 17b. 24% filler SR/20% HEMA formulation at 0.25 minute of blood exposure (scale bar = 10 μm)

Figure 17c. 24% filler SR/20% HEMA formulation at 0.5 minute of blood exposure (scale bar = 10 μm)

Figure 17d. 24% filler SR/20% HEMA formulation at 5 minutes of blood exposure (scale bar = 10 μm)

Figure 17e. 24% filler SR/20% HEMA formulation at 15 minutes of blood exposure (scale bar = 10 μm)

Figure 17f. 24% filler SR/20% HEMA formulation at 75 minutes of blood exposure (scale bar = 10 μm)

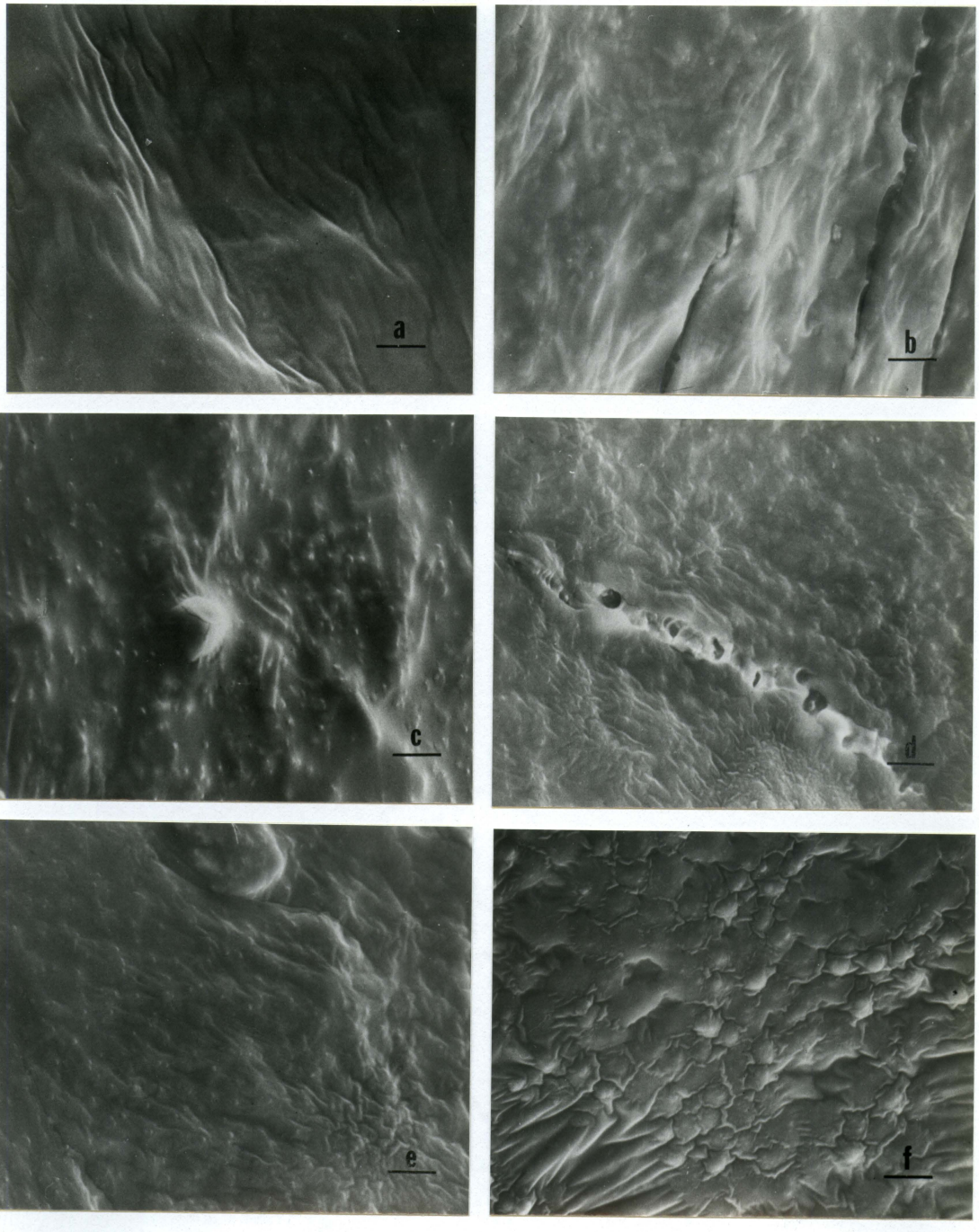
a
b
c
d
e
f

increases up to 15 minutes (Figure 17e), and then the surface takes on a different appearance at 75 minutes exposure (Figure 17f). Groups of platelets appear to be walled off by a thin film coating at 75 minutes exposure. Part of the surface appears to pull apart at 5 minutes. This surface defect shows that quite a buildup of material has occurred on the underlying Silastic® surface. The buildup is due to the coating of 24% filler SR and HEMA on the Silastic® surface plus the deposition of noncellular and cellular material on the surface. Thrombi are formed as early as 5 minutes on this particular formulation substrate (Figure 18a). The thrombi are primarily composed of platelets (5, 15, and 75 minutes; Figures 18a, 18b, and 18c, respectively). Some leukocytes are seen on the surface of the thrombi at 75 minutes (Figure 18c). As has been typical on many of the formulations tested, these thrombi are generally porous and are either clump-like or string-like in shape. Only 18% of the thrombi embolized by 75 minutes, and the maximum thrombus coverage occurred at 15 minutes (Table 2).

24% filler SR/15% HEMA/5% NVP Figures 19b through 19f show the general blood-24% filler SR/15% HEMA/5% NVP formulation interaction. The initial surface (before any blood exposure) is very rough (Figure 19a), and platelets appear coated by a thin film deposit at 0.5 minute (Figure 19c). Some platelets at 0.5 and 5 minutes (Figures 19c and 19d, respectively) appear activated (a shape change occurred). Further platelet buildup is not evident as time of blood exposure increases (Figures 19d through 19f). However, one clump-like platelet pillar is formed by 5 minutes (Figure 20). This platelet pillar is somewhat porous near the

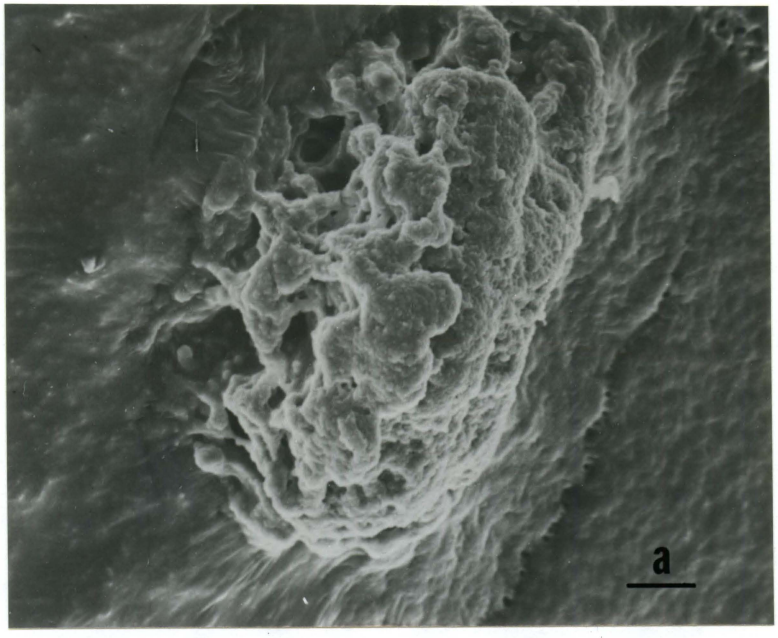

Figure 18a. Scanning electron micrograph of the 24% filler SR/20% HEMA formulation at 5 minutes of blood exposure (scale bar = 30 μm)

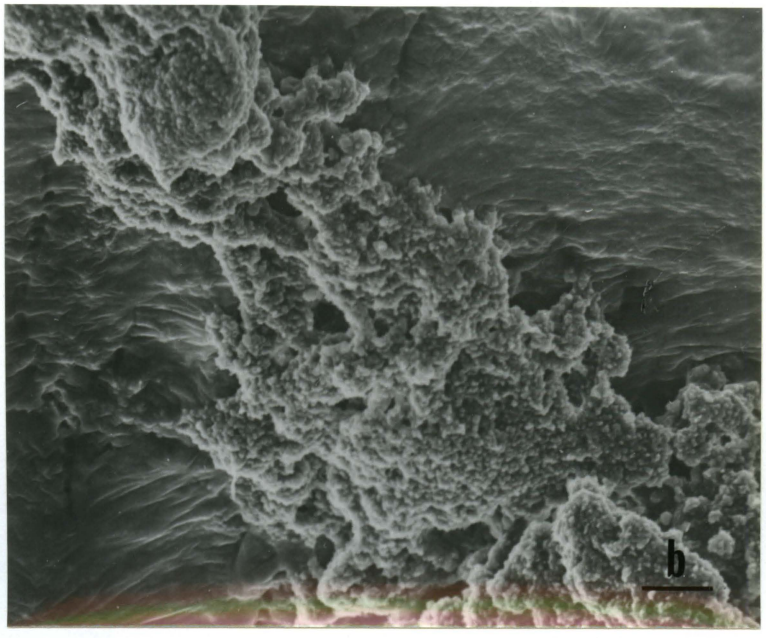

Figure 18b. 24% filler SR/20% HEMA formulation at 15 minutes of blood exposure (scale bar = 30 μm)

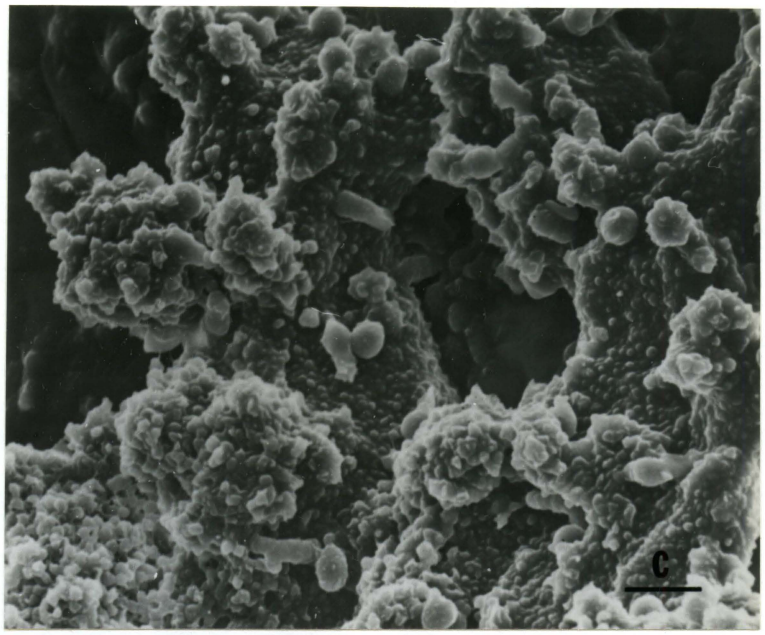

Figure 18c. 24% filler SR/20% HEMA formulation at 75 minutes of blood exposure (scale bar = 10 μm)

Figure 19a. Scanning electron micrograph of the 24% filler SR/15% HEMA/ 5% NVP formulation, unexposed (scale bar = 10 μm)

Figure 19b. 24% filler SR/15% HEMA/5% NVP formulation at 0.25 minute of blood exposure (scale bar = 10 μm)

Figure 19c. 24% filler SR/15% HEMA/5% NVP formulation at 0.5 minute of blood exposure (scale bar = 10 μm)

Figure 19d. 24% filler SR/15% HEMA/5% NVP formulation at 5 minutes of blood exposure (scale bar = 10 μm)

Figure 19e. 24% filler SR/15% HEMA/5% NVP formulation at 15 minutes of blood exposure (scale bar = 10 μm)

Figure 19f. 24% filler SR/15% HEMA/5% NVP formulation at 75 minutes of blood exposure (scale bar = 10 μm)

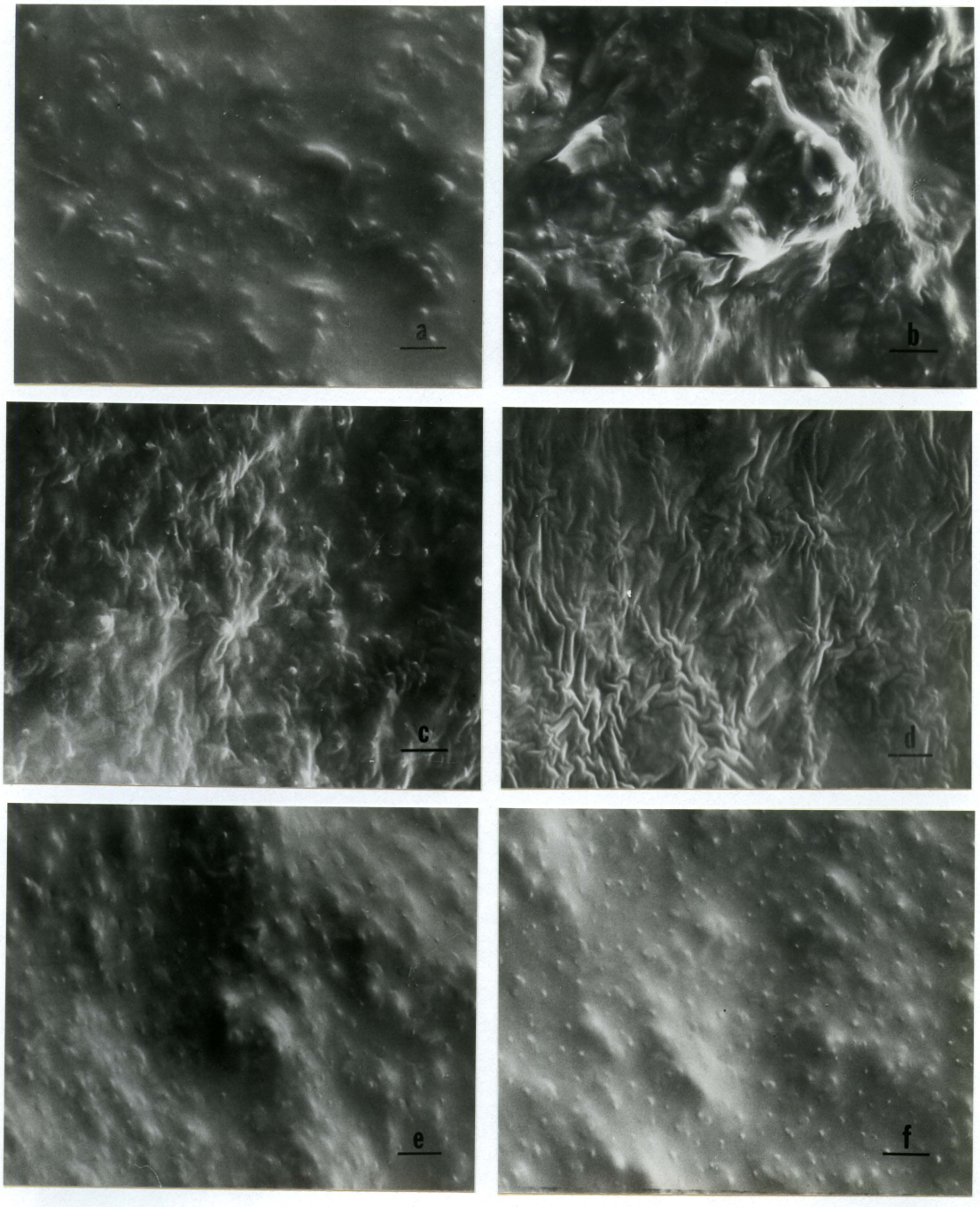
a
b
c
d
e
f

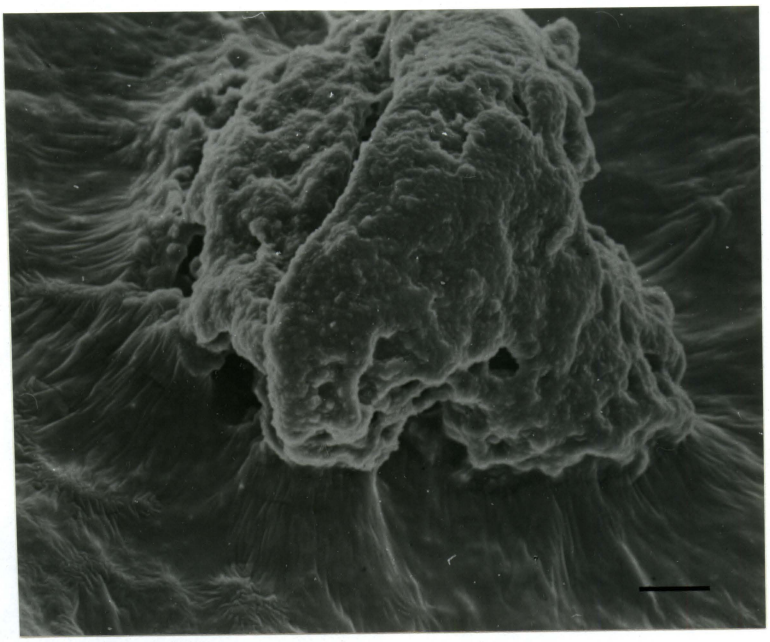

Figure 20. Scanning electron micrograph of the 24% filler SR/15% HEMA/ 5% NVP formulation at 5 minutes of blood exposure (scale bar = 30 μm)

bottom of the pillar, suggesting that the thrombus was preparing to detach, and the area surrounding the pillar is essentially cell free and apparently under tension. No thrombi were found at 15 and 75 minutes on this formulation.

24% filler SR/10% HEMA/10% NVP Platelets (seen with a thin film coating) appear at 0.25 minute (Figure 21b). An increase in platelet deposition is seen up to 15 minutes (Figures 21c through 21e), with a subsequent decrease in platelet adherence at 75 minutes (Figure 21f). The platelets appear activated underneath the thin film coating in some of the micrographs (Figures 21c through 21f). Pseudopodia appear to be protruding from the platelets.

24% filler SR/5% HEMA/15% NVP The general blood response of the 24% filler SR/5% HEMA/15% NVP formulation is shown in Figures 22b through 22f. The unexposed surface (Figure 22a) is rough in appearance. Substantial amounts of filler particles are evident within the silicone rubber coating on the surface which has been exposed to blood for 0.25 minute (Figure 22b), but it is not clear that there is any cellular material on the surface at this time. However, platelets (which are seen to be coated by a thin film) do appear by 0.5 minute of exposure (Figure 22c). Thrombi, which formed at 5, 15, and 75 minutes of blood exposure, are shown in Figures 23a, 23b, and 23c, respectively. In general, the clots are porous in nature and appear to be composed of platelets. The thrombi pictured at 5 and 75 minutes (Figures 23a and 23c, respectively) are partially surrounded by a cell free area. As is seen in Figure 23b, this particular thrombus at 15 minutes had a flat top and is relatively

Figure 21a. Scanning electron micrograph of the 24% filler SR/10% HEMA/ 10% NVP formulation, unexposed (scale bar = 10 μm)

Figure 21b. 24% filler SR/10% HEMA/10% NVP formulation at 0.25 minute of blood exposure (scale bar = 10 μm)

Figure 21c. 24% filler SR/10% HEMA/10% NVP formulation at 0.5 minute of blood exposure (scale bar = 10 μm)

Figure 21d. 24% filler SR/10% HEMA/10% NVP formulation at 5 minutes of blood exposure (scale bar = 10 μm)

Figure 21e. 24% filler SR/10% HEMA/10% NVP formulation at 15 minutes of blood exposure (scale bar = 10 μm)

Figure 21f. 24% filler SR/10% HEMA/10% NVP formulation at 75 minutes of blood exposure (scale bar = 10 μm)

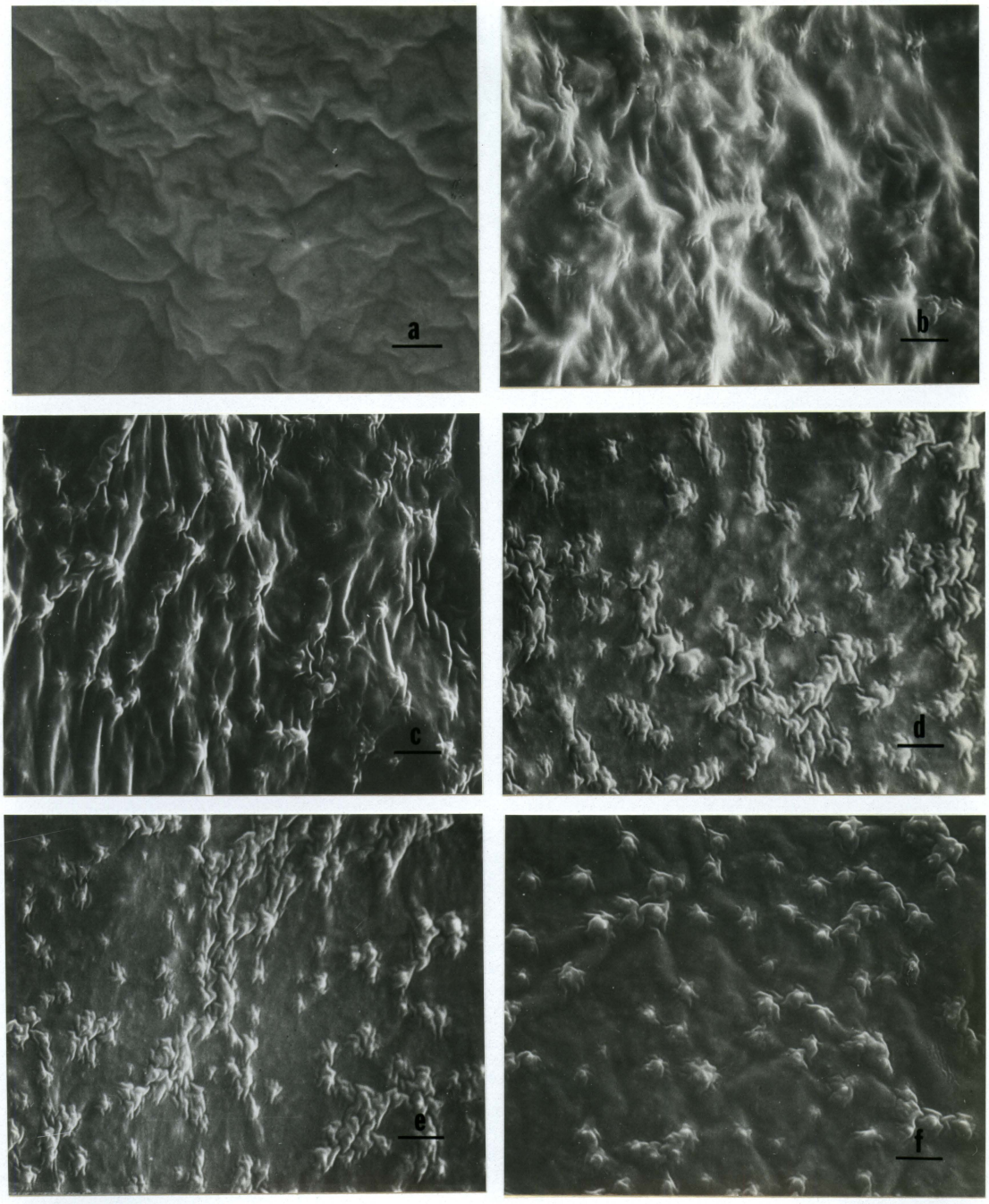
a
b
c
d
e
f

Figure 22a. Scanning electron micrograph of the 24% filler SR/5% HEMA/ 15% NVP formulation, unexposed (scale bar = 10 μm)

Figure 22b. 24% filler SR/5% HEMA/15% NVP formulation at 0.25 minute of blood exposure (scale bar = 10 μm)

Figure 22c. 24% filler SR/5% HEMA/15% NVP formulation at 0.5 minute of blood exposure (scale bar = 10 μm)

Figure 22d. 24% filler SR/5% HEMA/15% NVP formulation at 5 minutes of blood exposure (scale bar = 10 μm)

Figure 22e. 24% filler SR/5% HEMA/15% NVP formulation at 15 minutes of blood exposure (scale bar = 10 μm)

Figure 22f. 24% filler SR/5% HEMA/15% NVP formulation at 75 minutes of blood exposure (scale bar = 10 μm)

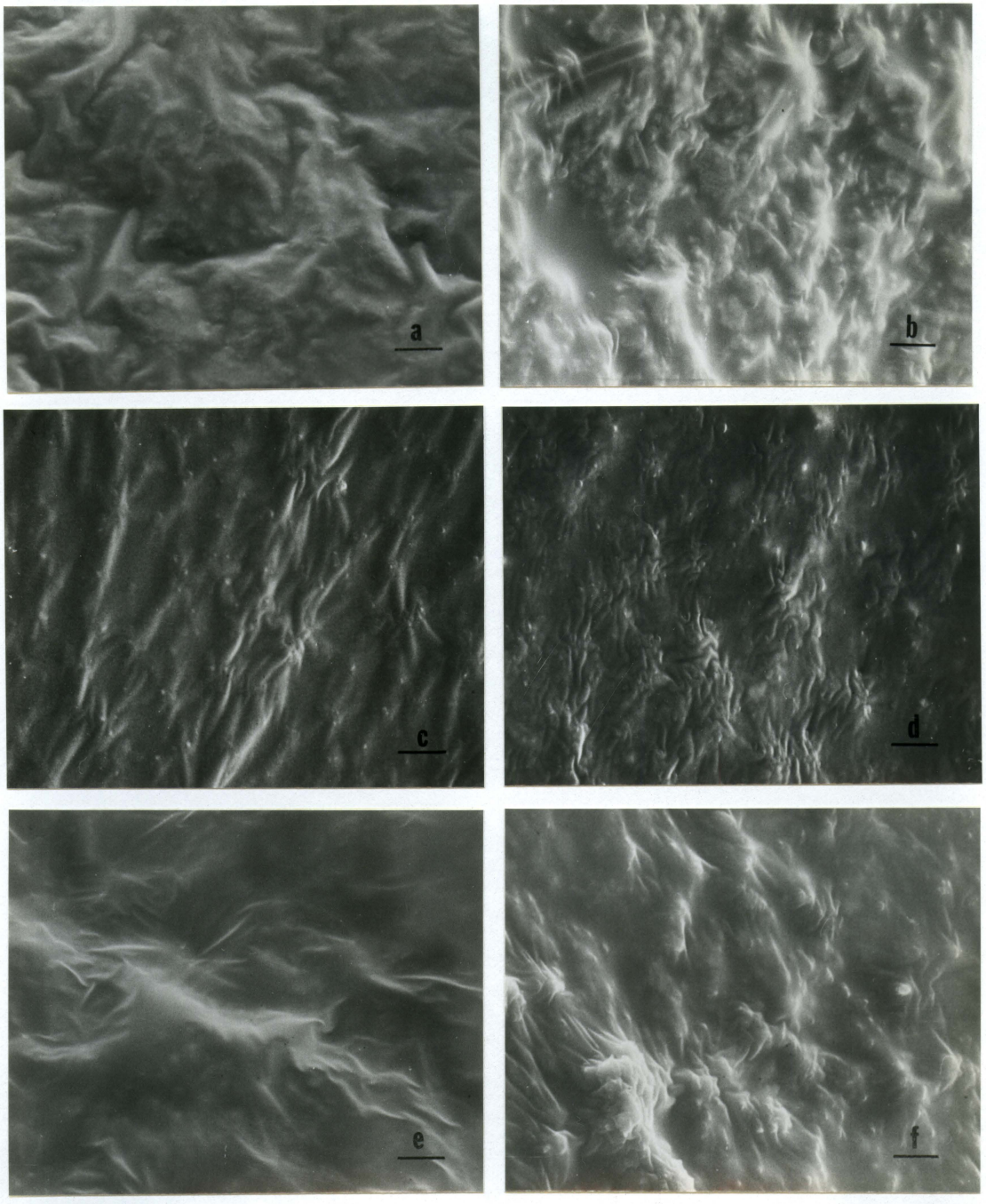
a
b
c
d
e
f

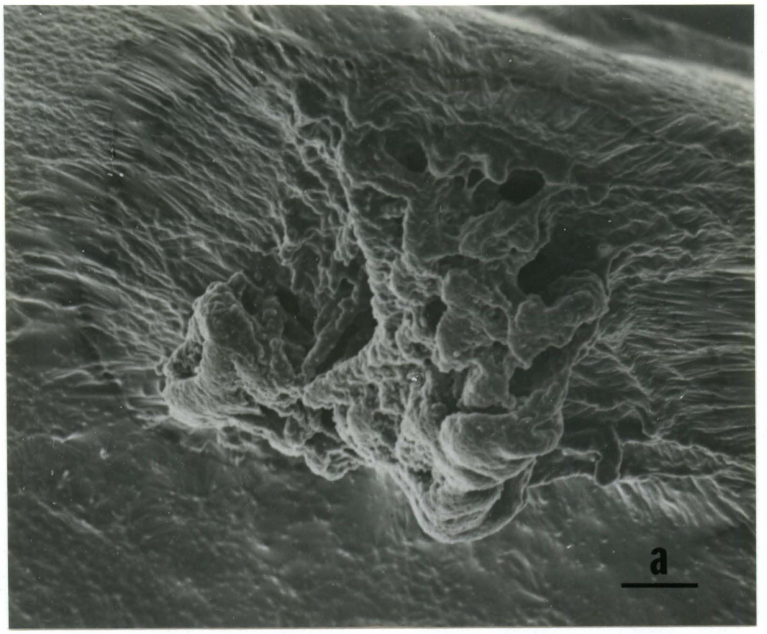

Figure 23a. Scanning electron micrograph of the 24% filler SR/5% HEMA/ 15% NVP formulation at 5 minutes of blood exposure (scale bar = 50 μm)

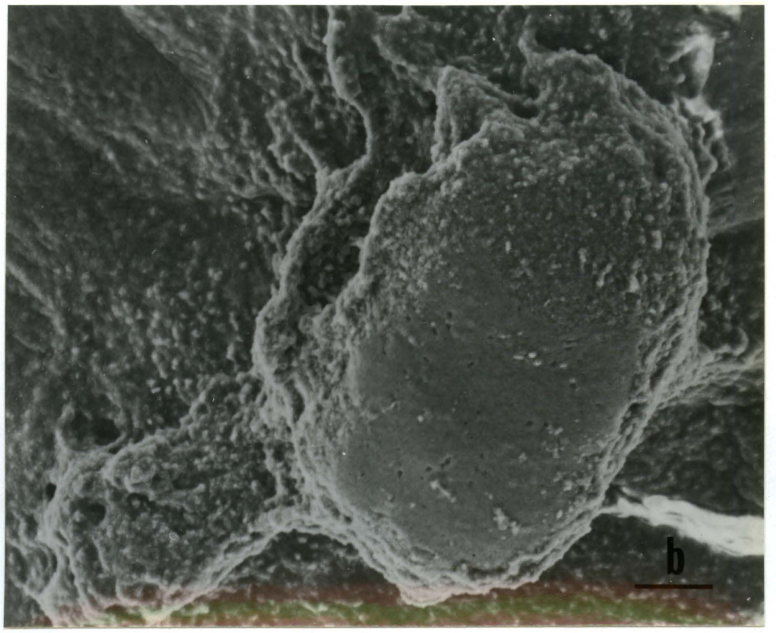

Figure 23b. 24% filler SR/5% HEMA/15% NVP formulation at 15 minutes of blood exposure (scale bar = 50 μm)

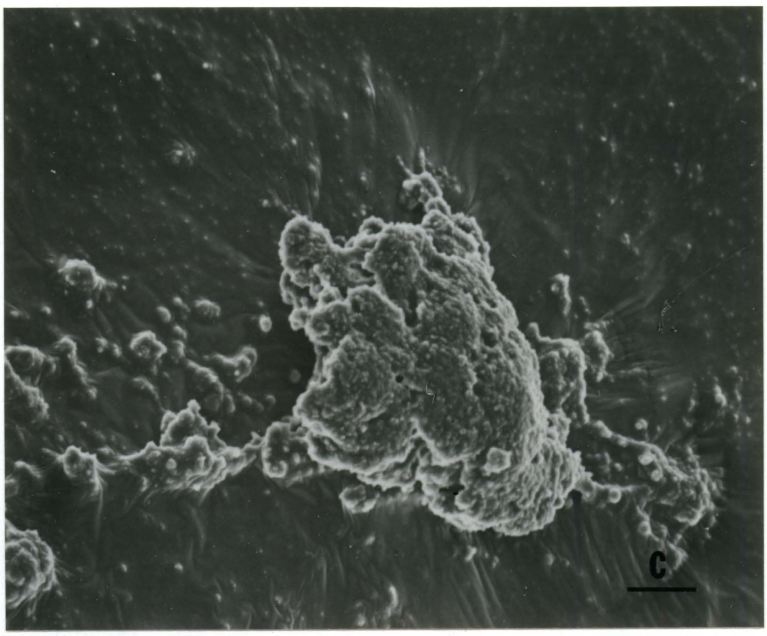

Figure 23c. 24% filler SR/5% HEMA/15% NVP formulation at 75 minutes of blood exposure (scale bar = 30 μm)

nonporous. There was a maximum buildup of thrombi by 15 minutes and a subsequent major decrease in thrombi by 75 minutes of blood exposure (see Table 2).

24% filler SR/20% NVP The result of blood exposure to the 24% filler SR/20% NVP surface is shown in Figures 24b through 25c. Filler can be seen just below the surface for the original surface (Figure 24a) and at 0.25 and 0.5 minute of blood exposure (Figures 24b and 24c, respectively). Platelets (with a thin film coating) are present by 5 minutes blood exposure (Figure 24d) and appear to decrease in number by 75 minutes blood exposure (Figure 24e and 24f). Thrombi develop by 15 minutes of exposure (Figure 25a), and at this time the thrombus formation is at its maximum (Table 2). The thrombi at this time of sampling are clump-like and relatively nonporous in nature. The cell free zone surrounding a thrombus is also apparent (Figure 25a). By 75 minutes of blood exposure, substantial embolization has occurred (85%). In Figures 25b and 25c, a thrombus is shown in a stage just prior to embolization.

The 24% filler SR/20% HEMA and 24% filler SR/5% HEMA/15% NVP formulations showed the most severe response to blood of the 24% filler SR-hydrogel series.

Both the 0 and 24% filler SR substrates caused minimal blood responses. The 10% HEMA/10% NVP formulation caused the least amount of cellular reactivity of all the formulations. The 20% HEMA formulation caused a relatively severe cellular reaction as did the 5% HEMA/15% NVP formulation. For the remaining two hydrogel formulations, the severity of the cellular reaction depended upon the underlying substrate. The 0%

Figure 24a. Scanning electron micrograph of the 24% filler SR/20% NVP formulation, unexposed (scale bar = 10 μm)

Figure 24b. 24% filler SR/20% NVP formulation at 0.25 minute of blood exposure (scale bar = 10 μm)

Figure 24c. 24% filler SR/20% NVP formulation at 0.5 minute of blood exposure (scale bar = 10 μm)

Figure 24d. 24% filler SR/20% NVP formulation at 5 minutes of blood exposure (scale bar = 10 μm)

Figure 24e. 24% filler SR/20% NVP formulation at 15 minutes of blood exposure (scale bar = 10 μm)

Figure 24f. 24% filler SR/20% NVP formulation at 75 minutes of blood exposure (scale bar = 10 μm)

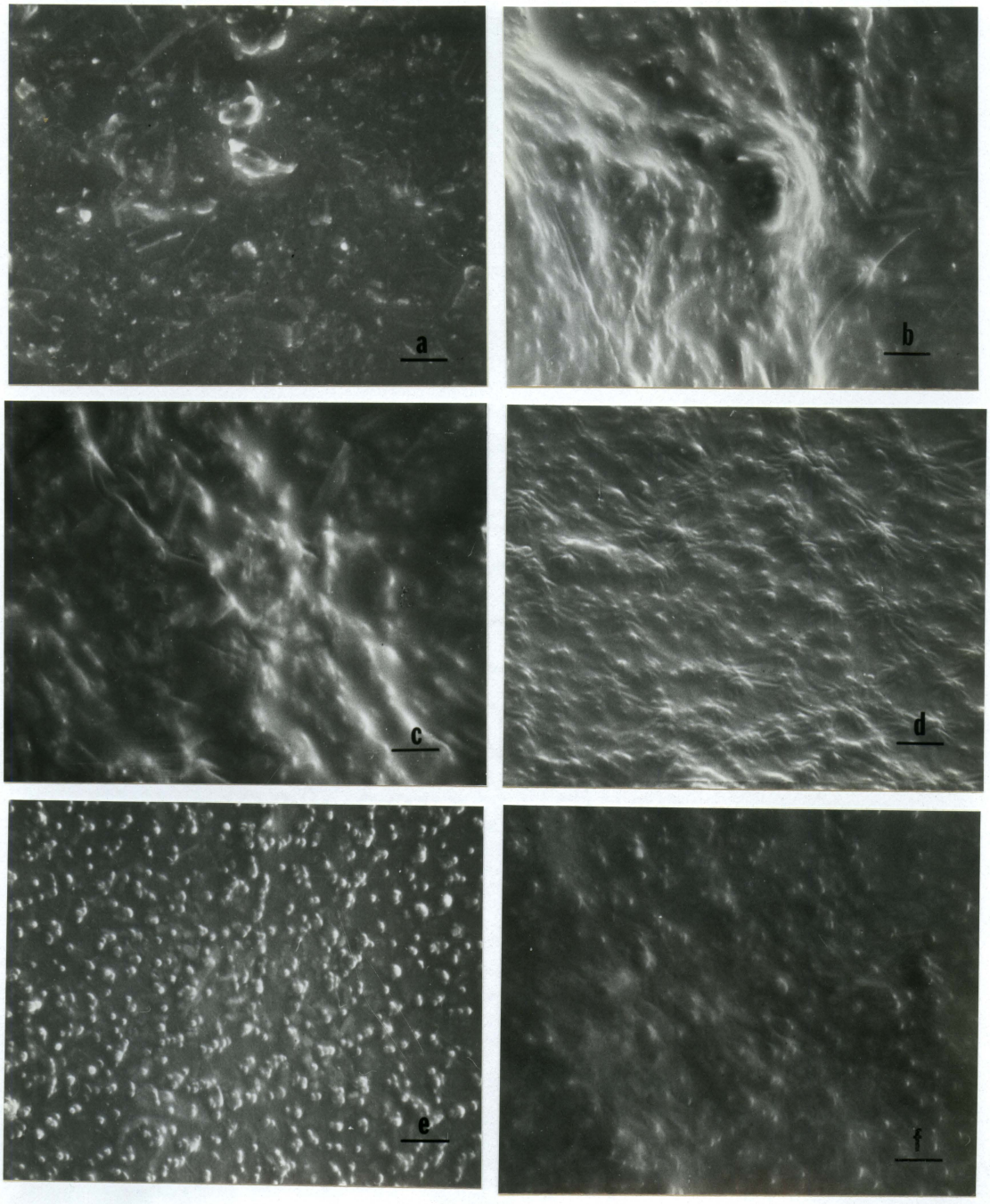
a
b
c
d
e
f

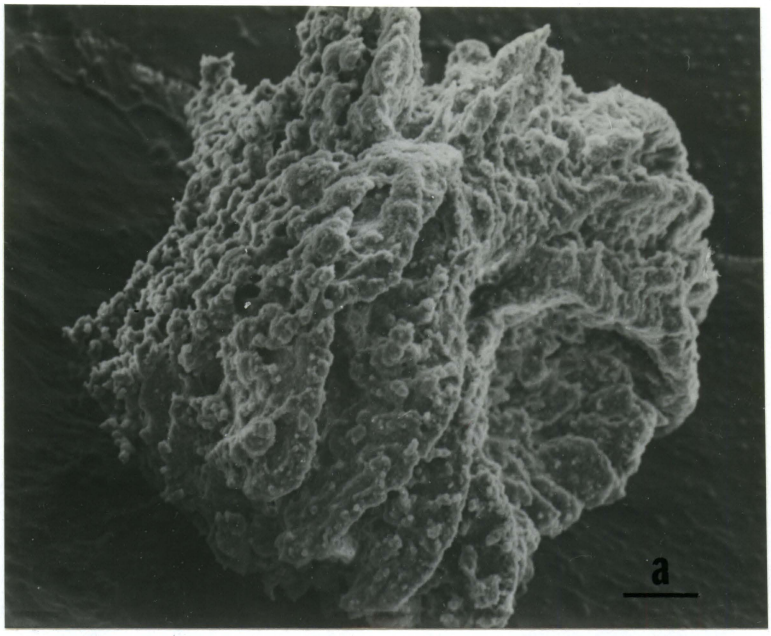

Figure 25a. Scanning electron micrograph of the 24% filler SR/20% NVP formulation at 15 minutes of blood exposure (scale bar = 50 μm)

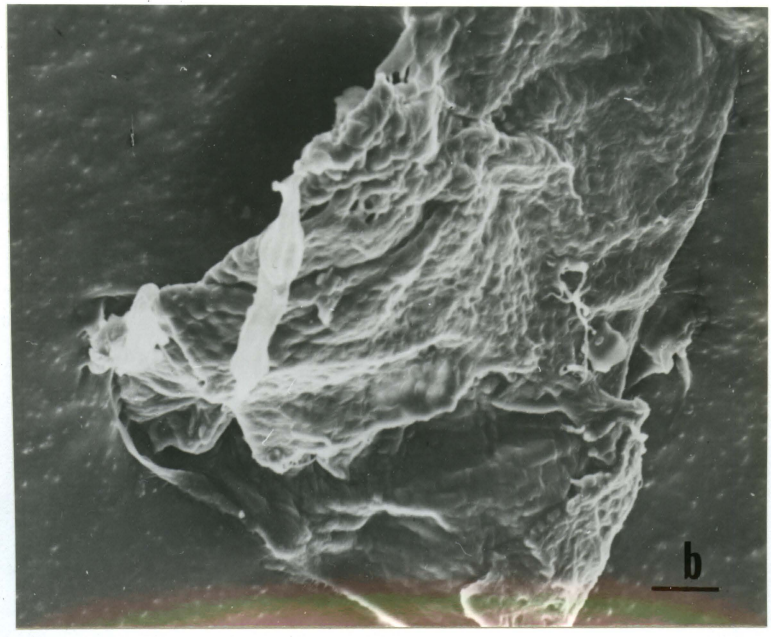

Figure 25b. 24% filler SR/20% NVP formulation at 75 minutes of blood exposure (scale bar = 30 μm)

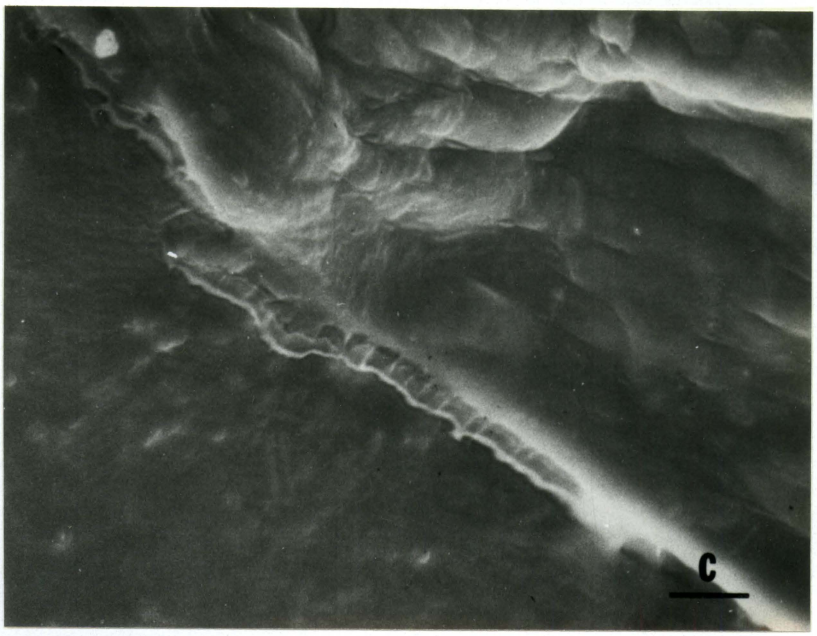

Figure 25c. Higher magnification of Figure 25b (scale bar = 10 μm)

filler SR/15% HEMA/5% NVP composite occluded by 75 minutes of blood exposure, whereas the 24% filler SR/15% HEMA/5% NVP composite caused only a minimal amount of cellular activity. The 0% filler SR/20% NVP composite caused only platelet activity, whereas the 24% filler SR/20% NVP composite caused some thrombotic activity. This difference in activity (in this case) could possibly be due to the relatively high surface roughness of the 24% filler content substrates compared with that of the 0% filler substrates.

Differences between the cellular reaction of the 0% filler content substrates and the 24% filler content substrates were seen to depend upon the formulation of hydrogel on the surface as observed in the two cases mentioned previously. Otherwise, little difference was seen between the cellular reactivity of the 0 and 24% filler content substrates. The appearance of imperfections on the 0% filler SR and 0% filler SR/20% NVP surfaces were most likely due to filler (SiO_2 particles, typically 1 to 30 μm in diameter) not caught in the filtering process and did not seem to adversely affect the blood-material interaction. These two surfaces had relatively little cellular reactivity.

FT-IR results

The spectral collection parameters are listed in Appendix A. The spectral coding designations are tabulated in Appendix B. The complete spectrally subtracted spectra for the 13 varieties tested are in Appendix C. The spectral range of interest is 1900 to 1000 cm^{-1} since most of the protein, hydrogel, and SR bands fall within this range. The bulk of the

information obtained from the FT-IR spectra came from the 1550 cm^{-1} infrared band, as this infrared band has been shown to be linearly related to the total amount of protein adsorbed and is, therefore, of primary interest. Table 3 shows the spectral features in the spectral range of 1620 to 1450 cm^{-1} with increased time of blood exposure (five sampling periods) for each of the 13 sample types. The actual areas underneath the 1550 cm^{-1} bands depicted in Table 3 as calculated by the IBM peak area routine are listed for each variety in Table 4.

In some of the spectra, other bands which provide useful information (besides the 1550 cm^{-1} band) became visible. These bands are the 1400 cm^{-1} band which is also linearly related to the total amount of protein adsorbed and the 1080 cm^{-1} band which has been speculated to be due to a blood plasma species of high carbohydrate content as stated previously. The relative buildup of the total amount of protein (as monitored by the 1550 cm^{-1} band) and release of protein with respect to time on the 13 sample types were characterized with FT-IR spectroscopy. It is difficult to interpret the FT-IR spectroscopy results in detail because of the complexity of the system studied. For most of the time periods studied, since platelet adhesion was observed as early as 0.25 minute, not only is the directly adsorbed layer of protein to the surface being detected, but the protein from the cellular elements is being detected, as well.

Protein deposition information for the 13 sample types based on FT-IR spectroscopy observations will be presented in the same order as the microstructural information was presented. The FT-IR spectroscopy observations of each individual formulation with respect to time will be presented

Table 3. 1550 cm^{-1} bands[a]; grouped as SR-substrates, 0% filler content-hydrogel substrates, and 24% filler content-hydrogel substrates

Formulation[b]	Time (minutes) 0.25	0.5	5	15	75
Commercial Silastic ®					
0% filler SR	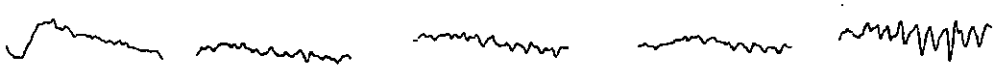				
24% filler SR					
0% filler SR/20% H					
0% filler SR/15% H/ 5% N[c]	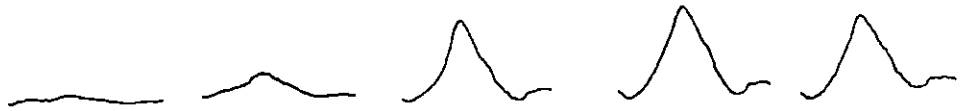				
0% filler SR/10% H/ 10% N[c]					
0% filler SR/5% H/ 15% N[c]					
0% filler SR/20% N					

[a]Spectral range of 1620 to 1450 m^{-1}; detailed spectra are in Appendix C.

[b]H = HEMA; N = NVP. This also applies to Tables 4 and 5.

[c]Samples taken from these formulations were three times as large as the samples taken from other formulations so these particular peaks were scaled down by a factor of 3 for comparison purposes since the 1550 cm^{-1} band is linearly related to total protein adsorption.

Table 3. (continued)

Formulation	Time (minutes) 0.25	0.5	5	15	75
24% filler SR/20%H		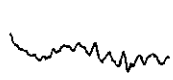			
24% filler SR/15% H/ 5% N					
24% filler SR/10% H/ 10% N[c]					
24% filler SR/5%H/ 15% N		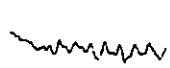		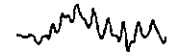	
24% filler SR/20% N					

first. Comparison of the results for the SR substrates (0% filler SR, 24% filler SR, and commercial Silastic®) and for different hydrogel formulations (20% HEMA, 15% HEMA/5% NVP, 10% HEMA/10% NVP, 5% HEMA/15% NVP, and 20% NVP) on the 0% and 24% silica filler content substrates will be made. The overall best sample type based on FT-IR observations will also be noted.

Controls (no hydrogel present) Spectra (wavenumber range of 1900 to 1000 cm^{-1}) for the sample types commercial Silastic®, 0% filler SR, and 24% filler SR can be found in Appendix C, Figures 26a through 28f. The total amount of protein adsorbed onto the commercial Silastic® substrate

Table 4. 1550 cm^{-1} band areas (absorbance units·cm^{-1}); grouped as SR substrates, 0% filler content-hydrogel substrates, and 24% filler content-hydrogel substrates

Formulation	Time of blood exposure (minutes)				
	0.25	0.5	5	15	75
Commerical Silastic®	0.306	n.d.[a]	0.205	0.084	0.422[b]
0% filler SR	0.402[b]	n.d.	n.d.	0.060	n.d.
24% filler SR	0.022	0.048	0.281[b]	0.242	0.168
0% filler SR/20% H	n.d.	0.073	0.275	0.379[b]	0.336
0% filler SR/ 15% H/5% N[c]	0.049	0.312	0.877	1.029[b]	0.843
0% filler SR/ 10% H/10% N[c]	n.d.	0.170	0.738[b]	0.594	0.242
0% filler SR/ 5% H/15% N[c]	n.d.	0.162	0.381	0.577[b]	0.058
0% filler SR/20% N	n.d.	n.d.	0.332	0.362[b]	.235
24% filler SR/20% H	n.d.	0.220	0.572[b]	0.323	0.474
24% filler SR/ 15% H/5% N	0.041	0.280	0.625	0.610	.792[b]
24% filler SR/ 10% H/10% N[c]	0.033	0.128	0.319	0.453[b]	0.214
24% filler SR/ 5% H/15% N	n.d.	n.d.	0.404[b]	0.396	0.307
24% filler SR/20% N	n.d.	n.d.	0.327[b]	0.197	n.d.

[a]None determined by the integration measurement.

[b]Indicates maximum peak area for the particular sample type.

[c]Samples from these formulations were three times as large as the samples taken from the other formulations, when the FT-IR spectra were obtained; therefore, these tabulated values represent one-third of 1550 cm^{-1} band area since the 1550 cm^{-1} band is linearly related to total protein adsorption, and the spectra utilized are those of Appendix C.

(Table 4) varied from exposure time to exposure time. As can be seen by looking at Table 3, the total protein adsorption based on areas for the 1550 cm^{-1} band as a function of time begins relatively high at 0.25 minute exposure but then drops off substantially by 0.5 minute exposure. The total amount of protein adsorbed increases again by 5 minutes, decreases at 15 minutes, and finally reaches a maximum for the time exposures studied by 75 minutes of blood exposure. The maximum amount of protein adsorption on the 0% filler SR substrate occurred at 0.25 minute of blood exposure (Table 4) and subsequently dropped to zero until 15 minutes of exposure where a slight adsorption was detected. By 75 minutes blood exposure, the protein adsorption had again dropped to zero. The relative amount of protein adsorption on the 24% filler SR substrate increased to a maximum sharply from 0.5 minute to 5 minutes, after which it gradually fell off.

In general, the 24% filler SR substrate adsorbed the least amount of protein of this series.

0% filler SR-hydrogel series Detailed spectra (1900 cm^{-1} to 1000 cm^{-1}) for the 0% filler SR-hydrogel formulations are in Appendix C, Figures 29a through 33f. It can be seen in Table 3 that the amount of protein adsorption on the 0% filler SR/20% HEMA formulation increases to a maximum at the 15 minute sampling period and then decreases somewhat at 75 minutes of exposure. The total protein adsorption on the 0% filler SR/ 15% HEMA/5% NVP composite was substantially higher at its maximum, which occurred at 15 minutes, than on any other sample type. The detailed spectra (Figures 30b through 30f) for this variety show that the 1400 cm^{-1} band increases with exposure to blood, along with the 1550 cm^{-1} band. By

75 minutes of blood exposure, the 1550 cm^{-1} infrared band decreases in area. A 1550 cm^{-1} band does occur on the unexposed sample (Figure 30a).

The total amount of protein adsorption is also relatively high on the 0% filler SR/10% HEMA/10% NVP formulation and reaches a maximum by 5 minutes of exposure, after which the 1550 cm^{-1} band area decreases (Table 4). It can be seen from the detailed spectra of this composite (Figures 31b through 31f) that the 1086 cm^{-1} band appears which indicates that a blood plasma species of high carbohydrate content is present. This band is present from 0.25 minute to 75 minutes of blood exposure. The 1400 cm^{-1} infrared band is also visible at 5 and 15 minutes (Figures 31d and 31e, respectively). A very slight 1550 cm^{-1} band occurs on the unexposed sample (Figure 31a).

The 1400 cm^{-1} infrared band also seems to track the 1550 cm^{-1} band on the 0% filler SR/5% HEMA/15% NVP sample type (Figures 32b through 32f). The 1550 cm^{-1} band reaches an intermediate maximum at the 15 minute sampling period of blood exposure (Table 4) and decreases substantially by 75 minutes. There is the occurrence of a slight 1550 cm^{-1} band on the unexposed 0% filler SR/5% HEMA/15% NVP sample which is unexpected (Figure 32a). The 0% filler SR/20% NVP composite adsorbs relatively little protein. The total protein adsorption on this sample peaks at the 15 minute sampling period and decreases by 75 minutes. In general, the 0% filler SR/20% NVP sample type adsorbed the least amount of protein of the 0% filler SR-hydrogel series, and the 0% filler SR/15% HEMA/5% NVP sample type adsorbed the most protein.

24% filler SR-hydrogel series The subtracted spectra of the 24% filler SR-hydrogel series are pictured in Appendix C, Figures 34a through 38f. As is seen in Table 4, an intermediate amount of protein is adsorbed onto the 24% filler SR/20% HEMA formulation; the buildup peaks at 5 minutes and subsequently decreases. The amount of protein adsorbed onto the 24% filler SR/15% HEMA/5% NVP formulation is relatively large, and the maximum value for the time exposures studied occurred by 75 minutes (Table 4). The 1400 cm^{-1} band also appears to track the 1550 cm^{-1} band on this sample type (Figures 35b through 35f). A 1550 cm^{-1} band occurred on the unexposed sample (Figure 35a). The 24% filler SR/10% HEMA/10% NVP composite adsorbed a moderate amount of protein which was a maximum at 15 minutes (Table 4). As can be seen in Figures 36d through 36f, a small 1400 cm^{-1} band also became visible. Also, a very slight 1550 cm^{-1} band occurred on the unexposed sample (Figure 36a).

No occurrence of protein adsorption was detected on the 24% filler SR/5% HEMA/15% NVP sample type until 5 minutes of blood exposure had passed, and at this time the maximum adsorption occurred for the time span studied (Table 4). Figure 37a shows the occurrence of a 1550 cm^{-1} band on the unexposed sample. The 24% filler SR/20% NVP composite spectra also indicated that no protein adsorption had occurred until 5 minutes of blood exposure, and at this time the 1550 cm^{-1} band was at its maximum (Table 4). A 1550 cm^{-1} band appeared on the unexposed sample for this formulation which was not expected (Figure 38a).

The 24% filler SR/20% NVP formulation adsorbed the least amount of protein of the 24% filler SR-hydrogel series, and the 24% filler SR/15%

HEMA/5% NVP composite adsorbed the most. In general, the maximum buildup of protein occurred by 5 to 15 minutes of blood exposure, and then this was followed by a release of material (Table 4).

A relative thrombogenicity index (defined as the area under the absorbance curve anywhere between 1620 cm^{-1} to 1479 cm^{-1} (depending upon the sample type) collected under identical conditions of sensitivity) was determined for the sample types based on the following 1550 cm^{-1} band area levels of buildup. Three levels of buildup are considered: first, an area of 0 to 0.36 is taken to indicate a nonthrombogenic surface; second, an area value of 0.37 to 0.57 is taken to indicate a surface relatively intermediate in thrombogenicity; and third, an area greater than 0.57 is taken as an indication of a relatively thrombogenic surface. The maximum value of the 1550 cm^{-1} band area for each sample type (Table 4) was used to rank the 13 varieties according to this thrombogenicity index. It can be seen from Table 4 that the 24% filler SR substrate, 0% filler SR/20% NVP composite, and the 24% filler SR/20% NVP composite are relatively nonthrombogenic; the Silastic ® substrate, 0% filler SR substrate, 0% filler SR/20% HEMA formulation, 24% filler SR/20% HEMA formulation, 24% filler SR/10% HEMA/10% NVP composite, and the 24% filler SR/5% HEMA/15% NVP formulation are more intermediate in their thrombogenicity; and the 0% filler SR/15% HEMA/5% NVP, 0% filler SR/10% HEMA/10% NVP, 0% filler SR/5% HEMA/15% NVP, and 24% filler SR/15% HEMA/5% NVP composites are all relatively thrombogenic based on these three levels of protein buildup.

Of the SR substrates, the 24% filler SR substrate adsorbed the least amount of protein, and the commercial Silastic ® substrate adsorbed the

most amount of protein. The 15% HEMA/5% NVP formulation had the largest amount of protein adsorption not only of the 0 and 24% filler SR substrates but also of the 13 sample types. The 20% NVP formulation caused the least amount of protein adsorption of all the formulations. The 20% HEMA and 5% HEMA/15% NVP formulations in general caused an intermediate amount of protein adsorption. The 10% HEMA/10% NVP formulation caused a variable response depending upon the underlying substrate material (0 or 24% filler SR). The 0% filler SR/10% HEMA/10% NVP variety caused a relatively large amount of protein adsorption, whereas the 24% filler SR/10% HEMA/10% NVP variety caused a relatively intermediate amount of protein adsorption. There was not much difference between the reaction of the 0% filler content substrates and the 24% filler content substrates, except for the response of the 10% HEMA/10% NVP formulation as stated previously. The overall best variety based on FT-IR spectroscopic observations is the 24% filler SR substrate, as this sample type had the lowest "maximum" 1550 cm^{-1} band area.

A trend for the occurrence of a very weak 1550 cm^{-1} band on the unexposed samples is evident in that on all of the sample types that this band became visible, the composite contained some percentage of NVP. The structure for poly(NVP) is the following:

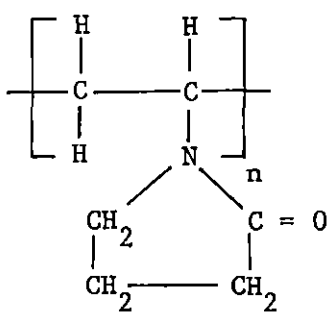

The band at 1550 cm^{-1} for NVP containing sample types could be due to the bending of -NH bands (Koenig and Tabb, 1980) or from general structural units such as -NH and CN (Alpert et al., 1970). Possible sources for the band include the following: a) impurities, b) effects of irradiation, or 3) an unknown source. The spectrum of the monomer NVP used (Appendix C, Figure 39) shows no evidence of a major band at 1550 cm^{-1}; there is a very weak band at 1550 cm^{-1} for NVP, but the intensities of the bands at 1703 and 1626 cm^{-1} for NVP, compared with the intensity of the 1546 cm^{-1} band, are approximately 26:1. Thus, the weak 1550 cm^{-1} band that is seen in the unexposed spectra for formulations containing NVP is probably not due to NVP alone. It may be possible that during irradiation, the pyrrolidone ring hydrolyzes (water is used in the polymerization process), allowing for the formation of -NH bonds (the free hydrogen could come from the irradiation process), which would contribute to the -NH bending. The spectrum for bulk polymerized NVP is shown in Figure 40 (Appendix C). For this spectrum, the spectral region of 1550 cm^{-1}, compared with 1664-1621 cm^{-1} region, shows an intensity difference of approximately 9:1 for the smaller 1621 cm^{-1} band and an intensity difference of about 13:1 for the larger 1664 cm^{-1} band. Therefore, the possibility that the irradiation procedure contributed to the formation of -NH bonds exists since the 1550 cm^{-1} band intensity appears to be larger after irradiation. That the 1550 cm^{-1} band on the unexposed samples is due entirely to -NH bending from NVP is still questionable, however.

The 1550 cm^{-1} band on the unexposed surfaces could also be due to protein residues left on the crystal at different stages of accumulating

reference spectra or exposed sample spectra. The amounts seen on the individual spectra for unexposed surfaces (Figures 30a, 31a, 32a, 35a, 36a, 37a, and 38a) are entered in Table 5. These integrated values may be added to appropriate formulation values given in Table 4 as an additional spectral adjustment. However, as the complete understanding of the source of this band is not fully understood, these values are listed separately.

If we compare the spectra of some unexposed formulations, which were dried prior to FT-IR/ATR analysis, with the spectra (of the same formulations) adjusted by spectral subtraction of the saline spectrum (e.g., Figure 41), some differences are apparent and are of value in interpreting the FT-IR spectra representing exposed hydrogel formulations. The particular spectra representative of certain formulations dried prior to FT-IR/ATR analyses are shown in Figure 42 through 49. These figures provide a basis for locating the HEMA band (approximately 1730 cm^{-1}) and a primary NVP band (approximately 1650 cm^{-1}). It should be emphasized that the presence of NVP complicates spectral interpretation, especially in the band regions of 1650 cm^{-1} (i.e., with water subtraction at 1640 cm^{-1} and with the appearance of a protein band at about 1640 cm^{-1} on exposed samples) and of 1550 cm^{-1} (i.e., with the protein band used as an indicator of the amount of protein present). The comparison of the 0% filler SR/20% HEMA composite spectrum in Figure 29a with the spectrum of the same composite in Figure 42 (which was dried) shows a shift of the HEMA band (expected to occur around 1754 cm^{-1}) in Figure 29a.

A 1550 cm^{-1} band occurs on the spectrum of the 0% filler SR/10% HEMA/10% NVP formulation for this investigation (Figure 31a), but it does not

Table 5. Absorbance values[a] representing the area under 1550 cm^{-1} bands seen for unexposed formulations (absorbance units·cm^{-1})

Formulation	Integrated area[a]
Commercial Silastic®	n.d.[b]
0% filler SR	n.d.
24% filler SR	n.d.
0% filler SR/20% H	n.d.
0% filler SR/15% H/5% N	0.198
0% filler SR/10% H/10% N	0.149
0% filler SR/5% H/15% N	0.265
0% filler SR/20% N	n.d.
24% filler SR/20% H	n.d.
24% filler SR/15% H/5% N	0.478
24% filler SR/10% H/10% N	0.083
24% filler SR/5% H/15% N	0.301
24% filler SR/20% N	1.162

[a]These factors may be added to the various exposed formulation band areas in Table 4 for the appropriate formulations in efforts to further correct spectra for an indication of the amount of protein buildup.

[b]None determined by the integration measurement.

appear on the spectrum of the same formulation for the dried case (Figure 43). The spectrum for the unexposed 0% filler SR/5% HEMA/15% NVP composite (Figure 30a) shows a 1550 cm^{-1} band, and the spectrum of the same formulation for the dried case (Figure 44) shows no 1550 cm^{-1} band.

The spectrum of the unexposed 24% filler SR/20% HEMA composite (Figure 34a) shows a shift in the HEMA band when compared to the HEMA band seen for the same formulation for the dried case (Figure 45). It is possible that water (Figure 41) was not subtracted properly from the 24% filler SR/20% HEMA formulation in Figure 34a. The HEMA band appears to be masked,

and there is a 1550 cm^{-1} band occurring on the spectrum of the unexposed 24% filler SR/15% HEMA/5% NVP formulation (Figure 35a). In contrast, the spectrum for the dried sample (Figure 46) shows a strong HEMA band at 1724 cm^{-1} and no obvious 1550 cm^{-1} band. Another possible explanation for this may be sample polymerization heterogeneity (i.e., from point-to-point, the amount of polymer may vary on a surface). The large variation in contact angle measurements for similar formulations may be indicative of heterogeneity (Vale and Greer, 1982).

The unexposed 24% filler SR/10% HEMA/10% NVP formulation spectrum (Figure 36a) shows a very weak 1550 cm^{-1} band. However, the spectrum of the same formulation for the dried case (Figure 47) shows no evidence of a 1550 cm^{-1} band. No HEMA, NVP, or 1550 cm^{-1} bands appear on the spectrum of the dried 24% filler SR/5% HEMA/15% NVP composite (Figure 48). In contrast, both a 1550 cm^{-1} band and a relatively large 1649 cm^{-1} band occur (probably due to NVP and some water) on the unexposed sample for this same formulation (Figure 37a). No NVP or 1550 cm^{-1} band is visible on the spectrum for the dried 24% filler SR/20% NVP composite (Figure 49). In contrast, 1550 cm^{-1} and 1650 cm^{-1} bands are apparent on the spectrum for the same unexposed sample type (Figure 38a).

Comparison of the SEM and FT-IR spectroscopy results The SEM and FT-IR spectroscopy results will be compared in terms of the relative thrombogenicity determined for each composite, which is based on the relative protein buildup and cellular buildup that occurred on each sample type.

In general, similar patterns were observed in the FT-IR spectroscopy and SEM results. The 0% filler SR/15% HEMA/5% NVP formulation completely occluded by 75 minutes and also adsorbed the greatest amount of protein of all the sample types. The 0% filler SR/20% HEMA, 0% filler SR/5% HEMA/15% NVP, 24% filler SR/20% HEMA, and 24% filler SR/5% HEMA/15% NVP sample types were all relatively thrombogenic based on the SEM results (Table 2) and were intermediate in thrombogenicity to relatively thrombogenic based on the FT-IR spectroscopy results (Table 4). The 0% filler SR/10% HEMA/10% NVP, 24% filler SR/10% HEMA/10% NVP, and 24% filler SR/15% HEMA/5% NVP varieties showed little cellular deposition but an intermediate to high amount of protein adsorption. The commercial Silastic®, 0% filler SR, 24% filler SR, 0% filler SR/20% NVP, and 24% filler SR/20% NVP sample types showed relatively little to no cellular deposition based on SEM and were intermediately thrombogenic to nonthrombogenic based on the FT-IR spectroscopy results.

There are some apparent discrepancies between the FT-IR spectroscopy and SEM findings. No protein adsorption was indicated on the commercial Silastic® variety at the 0.5 minute exposure time by the FT-IR spectroscopy results, but Figure 5c (the SEM micrograph of the commercial Silastic® substrate exposed for 0.5 minute) shows some platelet aggregation. It is well-agreed upon that protein adsorption occurs before platelet adhesion, and the platelet membrane does contain protein, so some protein adsorption would have been expected. It is possible that the FT-IR spectrometer used was not capable of monitoring very small amounts of protein adsorption that may have occurred. Discrepancies of the same

nature also occurred on other sample types. The 0% filler SR/20% HEMA, 0% filler SR/5% HEMA/15% NVP, and 24% filler SR/20% HEMA sample types obviously have thin film coated platelets present at 0.25 minute (Figures 9b, 14b, and 17b, respectively), but no protein adsorption was detected at this exposure time by FT-IR spectroscopy (Table 4).

Discussion

In general, a peak and a subsequent decline were seen in both the amount of protein adsorbed (as determined by FT-IR spectroscopy) and the cellular reaction (as determined by SEM) during the course of the 75 minutes of blood exposure. Vale and Greer (1982) and Lelah et al. (1983) also saw a similar trend in cellular reactivity as determined by SEM for approximately the same time period.

String-like thrombi (parallel to the direction of flow) were observed on the 0% filler SR/15% HEMA/5% NVP, 0% filler SR/5% HEMA/15% NVP, and 24% filler SR/20% HEMA sample types. Most of the thrombi formed on all samples were surrounded by an area devoid of platelets. The exceptions were a few cases on the relatively high percent NVP formulations. The cases for the relatively high NVP formulations may be related to the concept that NVP in this grafted form is less hydrophilic than the high HEMA formulations (see contact angle data of Vale and Greer (1982)), and thus the deposits (although less) are more tightly held. Lelah et al. (1983) have suggested that this platelet retraction appears to be an important mechanism for embolization. Lelah et al. (1983) speculated that shear forces (produced by the flowing blood) also aid in the detachment process.

Hanson et al. (1980) and Ratner et al. (1979) found that HEMA radiation grafted silicone rubber was relatively nonconsumptive towards platelets and that this surface accumulated minor amounts of thrombi. In the present study, the 0% filler SR/20% HEMA and 24% filler SR/20% HEMA composites were found to accumulate relatively large amounts of thrombi, and it appeared that embolization would be continuous and extensive (from the numerous string-like, porous thrombi). Thus, such a surface may throw off numerous emboli, although thick deposits might not buildup. Relative to NVP surfaces, the amounts on high HEMA surfaces were greater.

NVP grafted to silicone rubber (above a particular grafting ratio) was found to be blood compatible by Chapiro et al. (1981) which is consistent with the results reported here. The 0% filler SR/20% NVP composite adhered no thrombus mass, and the 24% filler SR/20% NVP composite adhered relatively few thrombi.

A surface consisting of a high percentage of NVP grafted onto SR is less hydrophilic when compared with a surface which consists of a high percentage of HEMA grafted onto SR (Vale and Greer, 1982). It was found that the high percent NVP sample types adsorbed less protein and caused less cellular deposition to occur than the high percent HEMA sample types. The aspect of a hydrophilic surface strongly interacting with plasma proteins becomes of interest here. The high percent HEMA sample types caused relatively more platelet activation (shape change) than the high percent NVP composites, which subsequently led to further thrombus buildup. Perhaps the thrombi forming on a highly hydrophilic surface would be able to gather in material more easily than thrombi forming on a relatively less

hydrophilic or even a hydrophobic surface. As a result, the thrombi on the hydrophilic surface would be larger, which was the case seen in this study. One thrombus on the 0% filler SR/20% HEMA formulation covered 3.4% of the tube surface at 15 minutes. Emboli from the high percent HEMA sample type would be expected to be larger and thus more difficult to breakup by the body (i.e., cause infarcts) than the emboli coming off of high percent NVP sample types.

The thrombi on the high percent HEMA formulations tended to be more porous (i.e., less tightly held) than the thrombi on the high percent NVP formulations, indicating that perhaps more emboli could be coming off the high percent HEMA formulations.

In general, leukocytes were not found to be necessary in either thrombus formation or embolization. However, the surfaces they did occur on (the 0% filler SR/15% HEMA/5% NVP, 0% filler SR/5% HEMA/15% NVP, and 24% filler SR/20% HEMA formulations) were surfaces that showed relatively severe cellular reactivity (Table 2). Their occurrences on these sample types were in small numbers. Lelah et al. (1983) also found leukocytes to be unnecessary in thrombosis and embolization.

Similar trends were seen for the rougher 24% filler SR and the smoother 0% filler SR sample-formulations. This observation suggests that the filler particles were adequately covered by SR. Nyilas et al. (1970) suggest that if the SR covering of silica is imperfect, the relatively high energy nature of the silica could cause blood protein denaturation. The fact that the silica filler was not filtered out completely is apparent from the SEM 0% filler SR substrate and 0% filler SR/20% NVP substrate-

formulation results. However, as stated before, the presence of the filler in the "0% filler" SR substrate did not cause a particularly adverse effect when the surface was exposed to blood. In general, surface roughness on this micrometer size scale was not found to cause a noticeably negative effect on the blood interactions of the materials tested.

Baier (1972) stated that a material with a critical surface tension within 20 to 30 dynes/cm should be biocompatible. Critical surface tension values for the hydrogel-coated silicone rubber sample types were measured as part of an overall project objective (Table 6). Also, silicone rubber critical surface tension values are summarized in Table 7. From the SEM and FT-IR spectroscopy results for the 13 formulations studied at the five time periods, the commercial Silastic®, 0% filler SR, 0% filler SR/20% NVP, and the 24% filler SR/20% NVP sample types were all found to be "better" surfaces than the rest. As seen using information in Tables 6 and 7, this tends to agree with the Baier critical surface tension (γ_c) hypothesis. The 24% filler SR substrate, which has a γ_c lower than the "biocompatible range," was also found to be a relatively "good" surface based on SEM and FT-IR spectroscopy results. In general, the middle hydrogel formulations (15% HEMA/5% NVP to 5% HEMA/15% NVP) were not as biocompatible as the other sample types, as judged by relative buildup of material of a higher level at each time period studied. Also, as can be seen in Table 6, these formulations have higher critical surface tensions than those within the "biocompatible range."

Table 6. SR-hydrogel critical surface tension values[a] (dyne/cm)

Formulation	% filler SR	
	0	24
20% HEMA	32[b]	33
15% HEMA/5% NVP	35	35
10% HEMA/10% NVP	31	34
5% HEMA/15% NVP	30	32
20% NVP	28	29

[a]Personal communication, D. T. Zhang, visiting scientist, Department of Engineering Science and Mechanics, Iowa State University, Ames, IA.

[b]95% level of confidence; any contact angle values were within 4% of average value obtained for a particular liquid.

Table 7. Critical surface tension values of silicone rubbers[a] (dyne/cm)

	Values
Commercial Silastic®	20
0% filler	20
24% filler	17

[a]Literature values = 22 and 24 dyne/cm for commercial material.

CONCLUSION

Results from this examination can be grouped as follows: the characteristics of material, the techniques of analysis, and the resulting experimental findings.

This investigation allowed for the testing of materials that ranged in hydrophilicity, critical surface tension, and surface roughness. The effects of varying these parameters, which influence the characteristics of the materials, were investigated.

The techniques of analysis, FT-IR spectroscopy and SEM, provided the opportunity for both qualitative analysis (through SEM) and quantitative analysis (through FT-IR spectroscopy). However, as stated before, due to the complexity of the signal (from the multiple sample components) received by the detector, the FT-IR spectroscopy results were difficult to interpret. Platelets were seen as early as the first sampling period (0.25 minute) on some sample types, and the contribution to the protein band regions in the FT-IR spectra complicates attempts to quantitate initial protein buildup of a noncellular nature. Scanning electron microscopy permitted the morphological investigations of the materials to be conducted, both pre- and post-surgery. Information on surface roughness and cellular material adhesion was obtained utilizing SEM.

The resulting experimental findings can be summarized as follows: the trend of relative buildup, the relation of the chemical characteristics of the sample with the blood-biomaterial responses, and the effect of surface roughness on the blood-biomaterial responses.

Most of the formulations tested were found to exhibit similar patterns of buildups and declines in protein adsorption and cellular reactivity by 75 minutes of blood exposure. Buildups in material deposited were found to peak on most samples by 5 to 15 minutes. Samples that had a critical surface tension value in a range of 20 to 30 dynes/cm (i.e., 0% filler SR/20% NVP and 24% filler SR/20% NVP) had less material deposited on them for the maxima seen than samples that had values greater than this range. Those samples within the range may be more "biocompatible." However, additional studies are of interest in establishing the characteristics of emboli from these surfaces and the relative frequency of embolization. Also, the three nonhydrogel coated silicone rubber samples had values less than or within this range and had minimal protein deposit buildups similar to the 0% filler SR/20% NVP and 24% filler SR/20% NVP samples).

The more hydrophilic 20% HEMA composites were found to cause a more severe reaction in terms of protein and cellular buildup than the less hydrophilic 20% NVP sample types. Surface roughness on the micrometer scale was not found to contribute substantially to the amount of buildup of material when compared to the primary effect of changing formulation of hydrogel. In other words, for a particular formulation, major differences of the amount of deposits on the 0% filler content substrate compared with the 24% filler content substrate were not seen.

BIBLIOGRAPHY

Alpert, N. L., W. E. Keiser, and H. A. Szymanski. 1970. IR: Theory and practice of infrared spectroscopy. Plenum Press, New York.

Andrade, J. D. 1973. Interfacial phenomena and biomaterials. Medical Instrumentation 7(2):110-120.

Andrade, J. D., H. B. Lee, M. S. Jhon, S. W. Kim, and J. B. Hibbs, Jr. 1973. Water as a biomaterial. Trans. Am. Soc. Artif. Internal Organs 19:1-7.

Bagnall, R. D. 1977. Adsorption of plasma proteins on hydrophobic surfaces. I. Albumin and gamma globulin. J. Biomed. Mater. Res. 11: 947-978.

Baier, R. E. 1972. The role of surface energy in thrombogenesis. New York Academy of Medicine, Bulletin 48:257-272.

Baier, R. E. 1978a. Key events in blood interactions at nonphysiologic interfaces-a personal primer. Artif. Organs 2:422-426.

Baier, R. E. 1978b. Physical chemistry of the vascular interface: Composition, texture, and adhesive quality. Pages 76-107 in P. N. Sawyer and J. Kaplitt, eds. Vascular grafts. Appleton-Century-Crofts, New York.

Baier, R. E., E. B. Shafrin, and W. A. Zisman. 1968. Adhesion: Mechanisms that assist or impede it. Science 162:1360-1368.

Baier, R. E., G. I. Loeb, and G. T. Wallace. 1971. Role of an artificial boundary in modifying blood proteins. Fed. Proc. 30:1523-1538.

Barber, T. A., T. Mathis, J. V. Ihlenfeld, S. L. Cooper, and D. F. Mosher. 1978. Short-term interactions of blood with polymeric vascular graft materials: Protein adsorption, thrombus formation, and leukocyte deposition. Scanning Electron Microscopy 2:431-441.

Barber, T. A., L. K. Lambrecht, D. L. Mosher, and S. L. Cooper. 1979. Influence of serum proteins on thrombosis and leukocyte adherence on polymer surfaces. Scanning Electron Microscopy 3:881-890.

Brash, J. L. and D. J. Lyman. 1969. Adsorption of plasma proteins in solution to uncharged, hydrophobic polymer surfaces. J. Biomed. Mater. Res. 3:175-189.

Brash, J. L. and D. J. Lyman. 1971. Adsorption of proteins and lipids to nonbiological surfaces. Pages 177-232 in M. L. Hair, ed. Chemistry of biosurfaces. Marcel Dekker, Inc. New York.

Bruck, S. D. 1972. Biomaterials in medical devices. Trans. Am. Soc. Artif. Internal Organs 18:1-9.

Bruck, S. D. 1973. Polymeric materials: Current status of biocompatibility. Biomater. Med. Devices Artif. Organs 1:79-98.

Caro, C. G., T. J. Pedley, R. C. Schroter, and W. A. Seed. 1978. The mechanics of the circulation. Oxford University Press, New York.

Chapiro, A., D. Domurado, M. Foex-Millequant, and A. M. Jendrychowska-Bonamour. 1981. Radiation grafting of N-vinylpyrrolidone into silicone tubes. Synthesis of polymers with improved hemocompatibility and implantation tests in lambs. Radiat. Phys. Chem. 18(5-6):1203-1206.

Chawla, A. S. 1978. In vivo interactions between novel filler free silicone rubber and blood. Biomater. Med. Devices Artif. Organs 6(2):89-102.

Cottonaro, C. N., H. V. Roohk, G. Shimizu, and D. R. Sperling. 1981. Quantitation and characterization of competitive protein binding to polymers. Trans. Am. Soc. Artif. Internal Organs 27:391-395.

Cumming, R. D. 1980. Important factors affecting initial blood-material interactions. Trans. Am. Soc. Artif. Internal Organs 26:304-308.

De Haseth, J. A. 1982. Fourier Transform infrared spectrometry. Pages 387-420 in A. G. Marshall, ed. Fourier, Hadamard, and Hilbert Transforms in chemistry. Plenum Press, New York.

Dutton, R. C., A. J. Webber, S. A. Johnson, and R. E. Baier. 1969. Microstructure of initial thrombus formation on foreign materials. J. Biomed. Mater. Res. 3:13-23.

Elliot, A., and E. M. Bradbury. 1962. Infrared spectra of proteins and polypeptides and their conformations. J. Mol. Biol. 5:574-576.

Garcia, C., J. M. Anderson, and S. A. Barenberg. 1980. Hemocompatibility: Effect of structured water. Trans. Am. Soc. Artif. Internal Organs 26:294-298.

Gendreau, R. M. and R. J. Jakobsen. 1979. Blood-surface interactions: Fourier Transform infrared studies of protein surface adsorption from flowing blood plasma and serum. J. Biomed. Mater. Res. 13:893-906.

Gendreau, R. M., R. I. Leininger, S. Winters, and R. J. Jakobsen. 1982. Fourier Transform infrared spectroscopy for protein-surface studies. Adv. Chem. Ser. 199:371-394.

Gordon, J. L. 1976. Platelets in biology and pathology. North-Holland Pub. Co., New York.

Hanson, S. R., L. A. Harker, B. D. Ratner, and A. S. Hoffman. 1980. In vivo evaluation of artificial surfaces with a nonhuman primate model of arterial thrombosis. J. Lab. Clin. Med. 95:289-304.

Herzlinger, G. A., and R. D. Cumming. 1980. Role of complement activation in cell adhesion to polymer blood contact surfaces. Trans. Am. Soc. Artif. Internal Organs 26:165-171.

Hoffman, A. S. 1982. Blood-biomaterial interactions: An overview. Adv. Chem. Ser. 199:3-8.

Holly, F. J. 1979. Protein and lipid adsorption by acrylic hydrogels and their relation to water wettability. J. Polymer Science: Polymer Symposium 66:409-417.

Holly, F. J. and M. F. Refojo. 1975. Wettability of hydrogels. I. Poly (2-hydroxyethyl methacrylate). J. Biomed. Mater. Res. 9:315-326.

Horbett, T. A. 1982. Protein adsorption on biomaterials. Adv. Chem. Ser. 199:233-244.

Horbett, T. A. and A. S. Hoffman. 1975. Bovine plasma protein adsorption onto radiation-grafted hydrogels based on hydroxyethyl methacrylate and N-vinyl-pyrrolidone. Adv. Chem. Ser. 199:230-254.

Jakobsen, R. J. and R. M. Gendreau. 1978. Blood plasma/implant interfaces FT-IR studies of adsorption on polyethylene and heparin-treated polyethylene surfaces. Artif. Organs 2:183-188.

Jakobsen, R. J., S. Winters, and R. M. Gendreau. 1981. Biological applications of FT-IR and bloody FT-IR. Page 469 in H. Sakai, ed. Proceedings of the international conference on Fourier Transform Infrared Spectroscopy. Vol. 289. S.P.I.E. - The International Society for Optical Engineering, held at Columbia, S. Carolina.

Jhon, M. S. and J. D. Andrade. 1973. Water and hydrogels. J. Biomed. Mater. Res. 7:509-522.

Kim, S. W. and R. G. Lee. 1975. Adsorption of blood proteins onto polymer surfaces. Adv. Chem. Ser. 145:218-229.

Kim, S. W., R. G. Lee, H. Oster, D. Coleman, J. D. Andrade, D. J. Lentz, and D. Olsen. 1974. Platelet adhesion to polymer surfaces. Trans. Am. Soc. Artif. Internal Organs 20:449-455.

Kim, S. W., S. Wisniewski, E. S. Lee, and M. L. Winn. 1977. Role of protein and fatty acid adsorption on platelet adhesion and aggregation at the blood-polymer interface. J. Biomed. Mater. Res. 11:23-31.

Koenig, J. L. and D. L. Tabb. 1980. Infrared spectra of globular proteins in aqueous solution. NATO Adv. Study Inst. Series C. Math and Physical Sciences. Vol. 57. Anal. Applications of FT-IR to molecular and biological systems. Proceedings of the NATO Adv. Study Inst. held at Florence, Italy. D. Reidel Pub. Co., Boston.

Lee, R. G. and S. W. Kim. 1974. The role of carbohydrate in platelet adhesion to foreign surfaces. J. Biomed. Mater. Res. 8:393-398.

Lelah, M. D., C. A. Jordan, M. E. Pariso, L. K. Lembrecht, S. L. Cooper, and R. M. Albrecht. 1983. Morphological changes occurring during thrombogenesis and embolization on biomaterials in a canine ex vivo series shunt. Scanning Electron Microscopy 4:1983-1994.

Lindsay, R. M., R. G. Mason, S. W. Kim, J. D. Andrade, and R. M. Hakim. 1980. Blood surface interactions. Trans. Am. Soc. Artif. Internal Organs 26:603-610.

Lyman, D. J., J. L. Brash, S. W. Chaikin, K. G. Klein, and M. Carini. 1968. The effect of chemical structure and surface properties of synthetic polymers on the coagulation of blood. II. Protein and platelet interaction with polymer surfaces. Trans. Am. Soc. Artif. Internal Organs 14:250-255.

Lyman, D. J., L. C. Metcalf, D. Albo, Jr., K. F. Richards, and J. Lamb. 1974. The effect of chemical structure and surface properties of synthetic polymers on the coagulation of blood. III. In vivo adsorption of proteins on polymer surfaces. Trans. Am. Soc. Artif. Internal Organs 20:474-478.

Lyman, D. J., K. Knutson, B. McNeill, and K. Shibatani. 1975. The effects of chemical structure and surface properties of synthetic polymers on the coagulation of blood. IV. The relation between polymer morphology and protein adsorption. Trans. Am. Soc. Artif. Internal Organs 21: 49-53.

Madras, P. N., W. A. Morton, and H. E. Petschek. 1971. The dynamics of thrombus formation. Fed. Proc. 30:1665-1675.

Merrill, E. W. and E. W. Salzman. 1976. Properites of materials affecting the behavior of blood at their surfaces. Pages 119-129 in P. N. Sawyer and J. Kaplitt, eds. Vascular grafts. Appleton-Century-Crofts, New York.

Nakashima, T., K. Takakura, and Y. Komoto. 1977. Thromboresistance of graft-type copolymers with hydrophilic-hydrophobic microphase-separated structure. J. Biomed. Mater. Res. 11:787-798.

Niemetz, J. and K. Fani. 1973. Thrombogenic activity of leukocytes. Blood 42(1):47-59.

Nyilas, E., E. L. Kupski, P. Burnett, and R. M. Haag. 1970. Surface microstructural factors and the blood compatibility of a silicone rubber. J. Biomed. Mater. Res. 4:369-432.

Packham, M. A., G. Evans, M. F. Glynn, and J. F. Mustard. 1969. The effect of plasma proteins on the interaction of platelets with glass surfaces. J. Lab. Clin. Med. 73(4):686-697.

Predecki, P. 1974. A method for Hydron impregnation of silicone rubber. J. Biomed. Mater. Res. 8:487-489.

Ratner, B. D. 1982. Surface characterization of material for blood contact applications. Adv. Chem. Ser. 199:9-23.

Ratner, B. D. and A. S. Hoffman. 1974. The effect of cupric ion on the radiation grafting of N-vinyl-2-pyrrolidone and other hydrophilic monomers onto silicone rubber. J. Applied Polymer Science 18:3183-3204.

Ratner, B. D. and A. S. Hoffman. 1975. Radiation grafted hydrogels on silicone rubber as new biomaterials. Pages 159-171 in H. P. Gregor, ed. Biomedical applications of polymers. Plenum Pub. Corp., New York.

Ratner, B. D. and A. S. Hoffman. 1976. Synthetic hydrogels for biomedical applications. Pages 1-36 in J. D. Andrade, ed. Hydrogels for medical and related applications. American Chemical Society, Washington, D.C.

Ratner, B. D., A. S. Hoffman, and J. D. Whiffen. 1975. Blood compatibility of radiation-grafted hydrogels. Biomater. Med. Devices Artif. Organs 3(1):115-120.

Ratner, B. D., A. S. Hoffman, S. R. Hanson, L. A. Harker, and J. D. Wiffen. 1979. Blood-compatibility--water-content relationships for radiation-grafted hydrogels. J. Polymer Science 66:363-375.

Roohk, H. V., J. Pick, R. Hill, E. Yung, and R. H. Bartlett. 1976. Kinetics of fibrinogen and platelet adherence to biomaterials. Trans. Am. Soc. Artif. Internal Organs 22:1-7.

Roohk, H. V., M. Nakamura, R. L. Hill, E. K, Hung, and R. H. Bartlett. 1977. A thrombogenic index for blood contact materials. Trans. Am. Soc. Artif. Internal Organs 23:152-161.

Sasaki, T., B. D. Ratner, and A. S. Hoffman. 1976. Radiation induced co-graft polymerization of 2-hydroxyethyl methacrylate and ethyl methacrylate onto silicone rubber films. Adv. Chem. Ser. 31:283-294.

Vale, B. H. and R. T. Greer. 1982. Ex vivo shunt testing of hydrogel-silicone rubber composite materials. J. Biomed. Mater. Res. 16:471-500.

Van Kampen, C. L., D. F. Gibbons, and R. D. Jones. 1979. Effect of implant surface chemistry upon arterial thrombosis. J. Biomed. Mater. Res. 13:517-541.

Weathersby, P, K., T. A. Horbett, and A. S. Hoffman. 1977. Fibrinogen adsorption to surfaces of varying hydrophilicity. J. Bioeng. 1:395-410.

Whicher, S. J. and J. L. Brash. 1978. Platelet-foreign surface interactions: Release of granule constituents from adherent platelets. J. Biomed. Mater. Res. 12:181-201.

Wichterle, O. and D. Lim. 1960. Hydrophilic gels in biological use. Nature (London) 185:117-118.

Young, B. R., L. K. Lambrecht, S. L. Cooper, and D. F. Mosher. 1982. Plasma proteins: Their role in initiating platelet and fibrin deposition on biomaterials. Adv. Chem. Ser. 199:317-350.

Zisman, W. A. 1964. Relation of the equilibrium contact angle to liquid and solid constitution. Pages 1-51 in R. F. Gould, ed. Contact angle, wettability, and adhesion. American Chemical Society, Washington, D.C.

ACKNOWLEDGMENTS

I wish to express my appreciation to my major professor, Dr. Raymond T. Greer, for his support and guidance throughout my graduate work. I would also like to thank Drs. D. Carlson and F. Hembrough for serving on my committee. I sincerely thank Dr. Pam McAllister for her surgical and technical assistance and for her encouragement. I also wish to thank Randy Tweden for his suggestions, patience, and unending encouragement. Sincere thanks are extended to the American Heart Association Iowa Affiliate for funding this project.

APPENDIX A: PARAMETER SET

The following parameters were used to collect, store, and obtain a hardcopy plot of the infrared spectra.

ASE = NO	APF = HG	APT = 3	BMS = 6	CON = 1
COR = LO	CSU = IN	DLY = 40	DTC = MI	HFQ = 5000
HPF = 6	LAB = LN	LGO = NO	LPF = 2	LWN = 15800.0
NLV = 0.000625	NSR = 100	NSS = 100	OPF = 2	PLF = AB
PIP = 128	POP = DP	PTS = 1024	RES = 4	RGN = -1
SGN = -1	SMF = 0	SPZ = NO	SSP = -1	SVI = NO
TGD = 1	VEL = 5	WTM = 13800	XAU = WN	XAX = NO
XEP = 1000	XSP = 1900	XSL = 6.5	XST = 0	YHT = 0.5
YSL = 4.5	YST = 5.5	YTC = 3	ZFF = 2	LFQ = 0

APPENDIX B: SPECTRAL CODING

At the top of each FT-IR spectrum (Appendix C), designations are made as AFA (or FLS) = and AFB (or FLR) =. The coding for the particular entry is as follows:

WATERS	= saline
COM15S2	= commercial Silastic ®, 15 sec. exposure, adjusted with the vapor file a second time
VAPOS	= the water vapor absorbance file
COM30S2	= commercial Silastic ®, 30 sec. exposure, adjusted with the vapor file a second time
COMER5M	= commercial Silastic ®, 5 min. exposure
COMERUN, COMUV	= commercial Silastic ®, unexposed
COMER15M	= commercial Silastic ®, 15 min. exposure
COM75M2	= commercial Silastic ®, 75 min. exposure, adjusted with the vapor file a second time
ZER15S2	= 0% filler SR, 15 sec. exposure, adjusted with the vapor file a second time
ZER30SS	= 0% filler SR, 30 sec. exposure
ZEROUN, ZEROV	= 0% filler SR, unexposed
ZER5MS	= 0% filler SR, 5 min, exposure
ZER15MS	= 0% filler SR, 15 min. exposure
ZER75MS	= 0% filler SR, 75 min. exposure
TWF015SS	= 24% filler SR, 15 sec. exposure
TWEFOS, TWEFV	= 24% filler SR, unexposed
TWF030SS	= 24% filler SR, 30 sec. exposure
TWF05MS	= 24% filler SR, 5 min. exposure

TWFO15MS = 24% filler SR, 15 min. exposure

TWFO75MS = 24% filler SR, 75 min. exposure

Z20H15SS = 0% filler SR/20% HEMA, 15 sec. exposure

Z20HS, Z20H2V = 0% filler SR/20% HEMA, unexposed

Z20H30SS = 0% filler SR/20% HEMA, 30 sec. exposure

Z20H5MS = 0% filler SR/20% HEMA, 5 min. exposure

Z20H15MS = 0% filler SR/20% HEMA, 15 min. exposure

Z20H75MS = 0% filler SR/20% HEMA, 75 min. exposure

Z5N15SS = 0% filler SR/15% HEMA/5% NVP, 15 sec. exposure

Z5NS, Z5N = 0% filler SR/15% HEMA/5% NVP, unexposed

Z5N30SS = 0% filler SR/15% HEMA/5% NVP, 30 sec. exposure

Z5N5MS = 0% filler SR/15% HEMA/5% NVP, 5 min. exposure

Z5N15MS = 0% filler SR/15% HEMA/5% NVP, 15 min. exposure

Z5N75MS = 0% filler SR/15% HEMA/5% NVP, 75 min. exposure

Z1N15SS = 0% filler SR/10% HEMA/10% NVP, 15 sec. exposure

Z1NS, Z1N = 0% filler SR/10% HEMA/10% NVP, unexposed

Z1N30SS = 0% filler SR/10% HEMA/10% NVP, 30 sec. exposure

Z1N5MS = 0% filler SR/10% HEMA/10% NVP, 5 min. exposure

Z1N15MS = 0% filler SR/10% HEMA/10% NVP, 15 min. exposure

Z1N75MS = 0% filler SR/10% HEMA/10% NVP, 75 min. exposure

Z5H15SS = 0% filler SR/5% HEMA/15% NVP, 15 sec. exposure

Z5HS, Z5H = 0% filler SR/5% HEMA/15% NVP, unexposed

Z5H30SS = 0% filler SR/5% HEMA/15% NVP, 30 sec. exposure

Z5H5MS = 0% filler SR/5% HEMA/15% NVP, 5 min. exposure

Z5H15MS = 0% filler SR/5% HEMA/15% NVP, 15 min. exposure

Z5H75MS = 0% filler SR/5% HEMA/15% NVP, 75 min. exposure

Z20N15SS = 0% filler SR/20% NVP, 15 sec. exposure

ZER20NS, ZE20NV = 0% filler SR/20% NVP, unexposed

Z20N30SS = 0% filler SR/20% NVP, 30 sec. exposure

Z20N5MS = 0% filler SR/20% NVP, 5 min. exposure

Z20N15MS = 0% filler SR/20% NVP, 15 min. exposure

Z20N75MS = 0% filler SR/20% NVP, 75 min. exposure

T2H15SS = 24% filler SR/20% HEMA, 15 sec. exposure

TWF02HS, TWF02HV = 24% filler SR/20% HEMA, unexposed

T2H30SS = 24% filler SR/20% HEMA, 30 sec. exposure

T2H5MS = 24% filler SR/20% HEMA, 5 min, exposure

T2H15M2 = 24% filler SR/20% HEMA, 15 min. exposure, adjusted with the vapor file a second time

T2H75MS = 24% filler SR/20% HEMA, 75 min. exposure

T5N15SS = 24% filler SR/15% HEMA/5% NVP, 15 sec. exposure

T5NS, T5N = 24% filler SR/15% HEMA/5% NVP, unexposed

T5N30SS = 24% filler SR/15% HEMA/5% NVP, 30 sec. exposure

T5N5MS = 24% filler SR/15% HEMA/5% NVP, 5 min. exposure

T5N15MS = 24% filler SR/15% HEMA/5% NVP, 15 min. exposure

T5N75MS = 24% filler SR/15% HEMA/5% NVP, 75 min. exposure

T1N15SS = 24% filler SR/10% HEMA/10% NVP, 15 sec. exposure

T1NS, T1N = 24% filler SR/10% HEMA/10% NVP, unexposed

T1N30SS = 24% filler SR/10% HEMA/10% NVP, 30 sec. exposure

T1N5MS = 24% filler SR/10% HEMA/10% NVP, 5 min. exposure

T1N15MS = 24% filler SR/10% HEMA/10% NVP, 15 min. exposure

T1N75MS = 24% filler SR/10% HEMA/10% NVP, 75 min. exposure

T5H15SS = 24% filler SR/5% HEMA/15% NVP, 15 sec. exposure

TF5HS, TF5HEV = 24% filler SR/5% HEMA/15% NVP, unexposed

T5H30SS = 24% filler SR/5% HEMA/15% NVP, 30 sec. exposure

T5H5MS = 24% filler SR/5% HEMA/15% NVP, 5 min. exposure

T5H15M2 = 24% filler SR/5% HEMA/15% NVP, 15 min. exposure, adjusted with the vapor file a second time

T5H75MS = 24% file SR/5% HEMA/15% NVP, 75 min. exposure

T2N15SS = 24% filler SR/20% NVP, 15 sec. exposure

T20NS, T20N = 24% filler SR/20% NVP, unexposed

T2N30SS = 24% filler SR/20% NVP, 30 sec. exposure

T2N5MS = 24% filler SR/20% NVP, 5 min. exposure

T2N15MS = 24% filler SR/20% NVP, 15 min. exposure

T2N75MS = 24% filler SR/20% NVP, 75 min. exposure

SALINE10 = saline

Z2000DRY = 0% filler SR/20% HEMA, dried and unexposed

R... = germanium crystal

Z1010DRY = 0% filler SR/10% HEMA/10% NVP, dried and unexposed

Z0515DRY = 0% filler SR/5% HEMA/15% NVP, dried and unexposed

W2000DRY = 24% filler SR/20% HEMA, dried and unexposed

W1505DRY = 24% filler SR/15% HEMA/5% NVP, dried and unexposed

W1010DA = 24% filler SR/10% HEMA/10% NVP, dried and unexposed

W0515DRY = 24% filler SR/5% HEMA/15% NVP, dried and unexposed

W0020DRY = 24% filler SR/20% NVP, dried and unexposed

NVP1 = the monomer N-vinyl-pyrrolidone

PVP1 = poly (N-vinyl-pyrrolidone)

WAT2 = saline

The detailed spectra follow in Appendix C and are presented in the sequence unexposed, 0.25 min., 0.5 min., 5 min., 15 min., and 75 min.

APPENDIX C: FT-IR SPECTRA

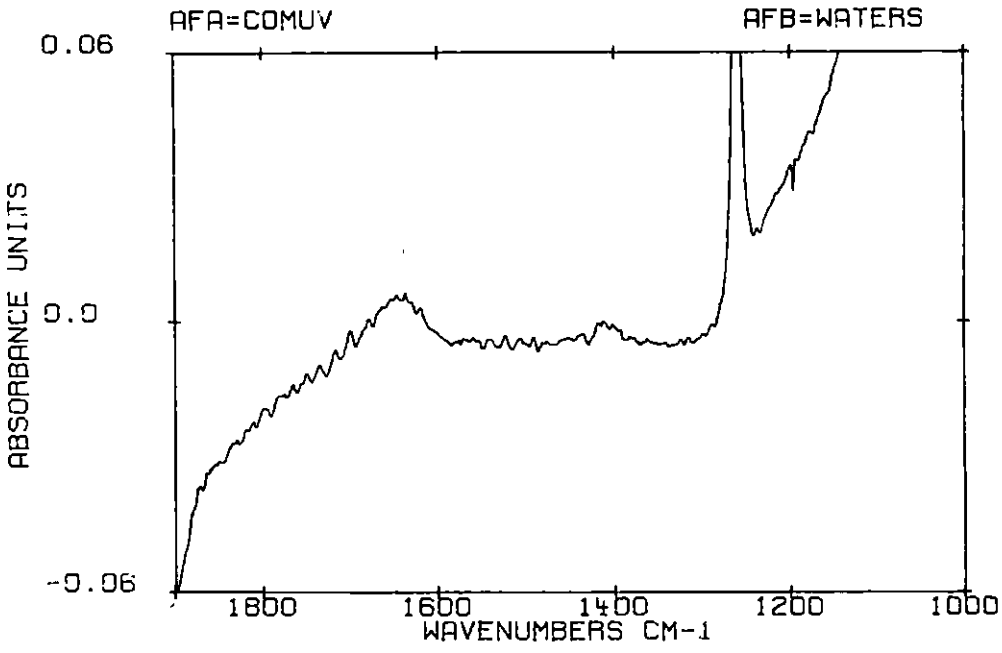

Figure 26a. Spectrum of water vapor and saline subtracted from commercial Silastic®

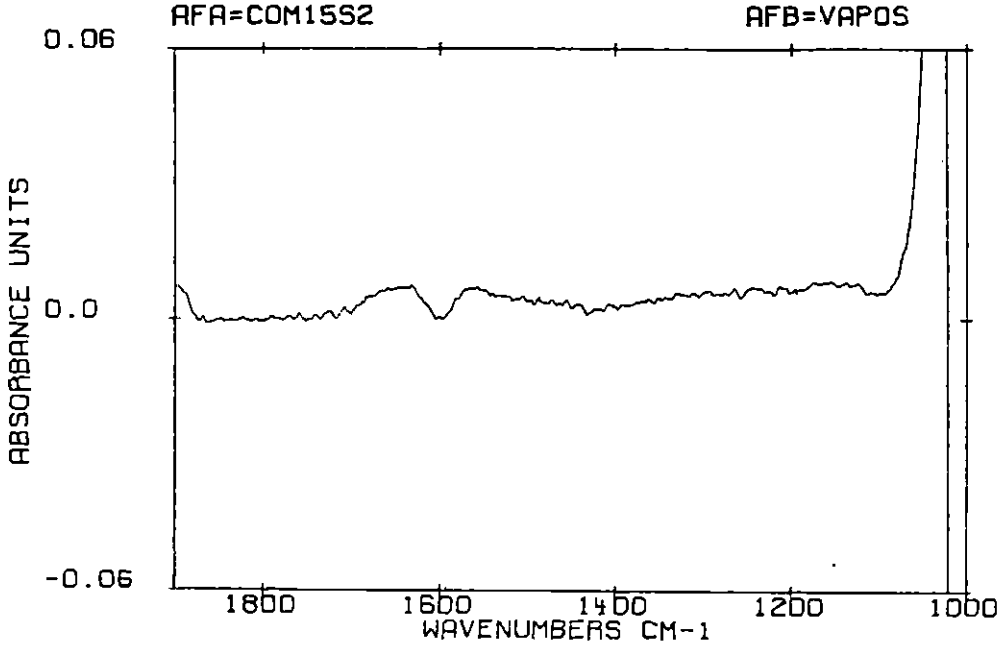

Figure 26b. Spectrum of protein adsorbed onto commercial Silastic® after 0.25 minute exposure to blood

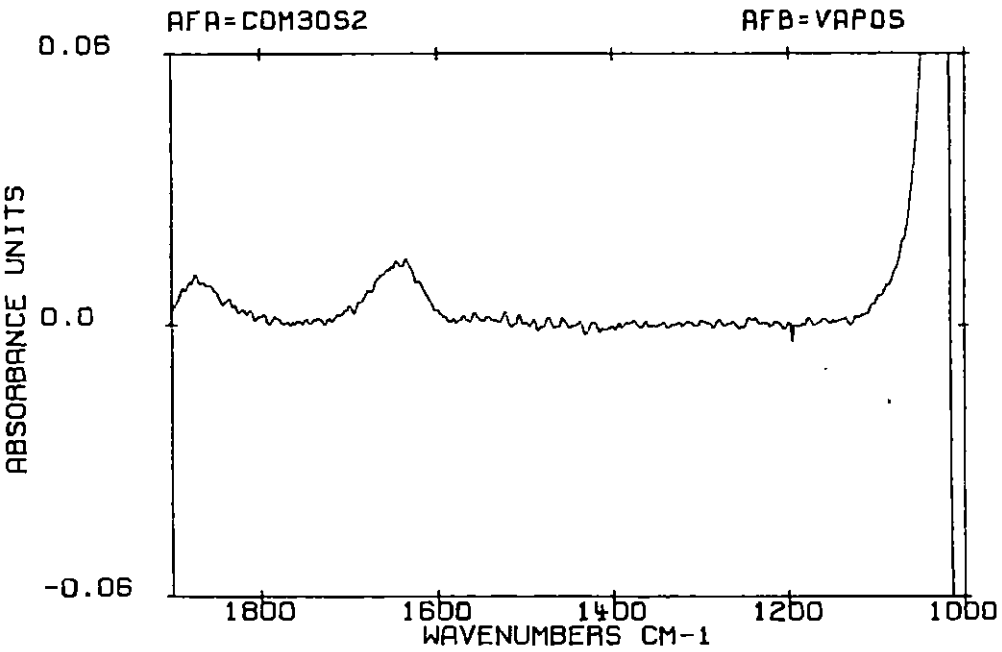

Figure 26c. Spectrum of protein adsorbed onto commercial Silastic® after 0.5 minute exposure to blood

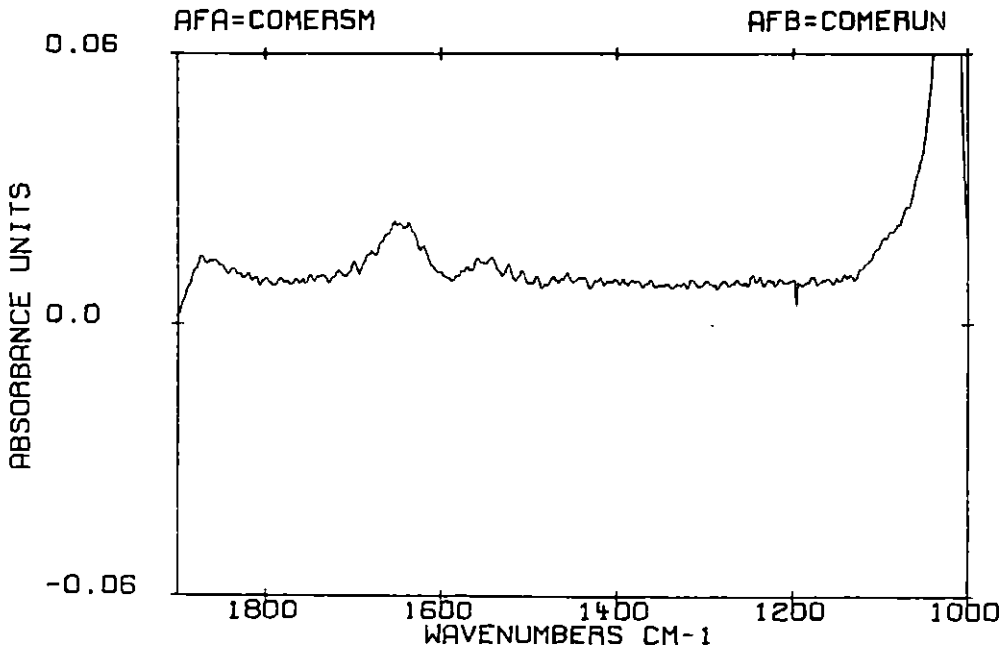

Figure 26d. Spectrum of protein adsorbed onto commercial Silastic® after 5 minutes exposure to blood

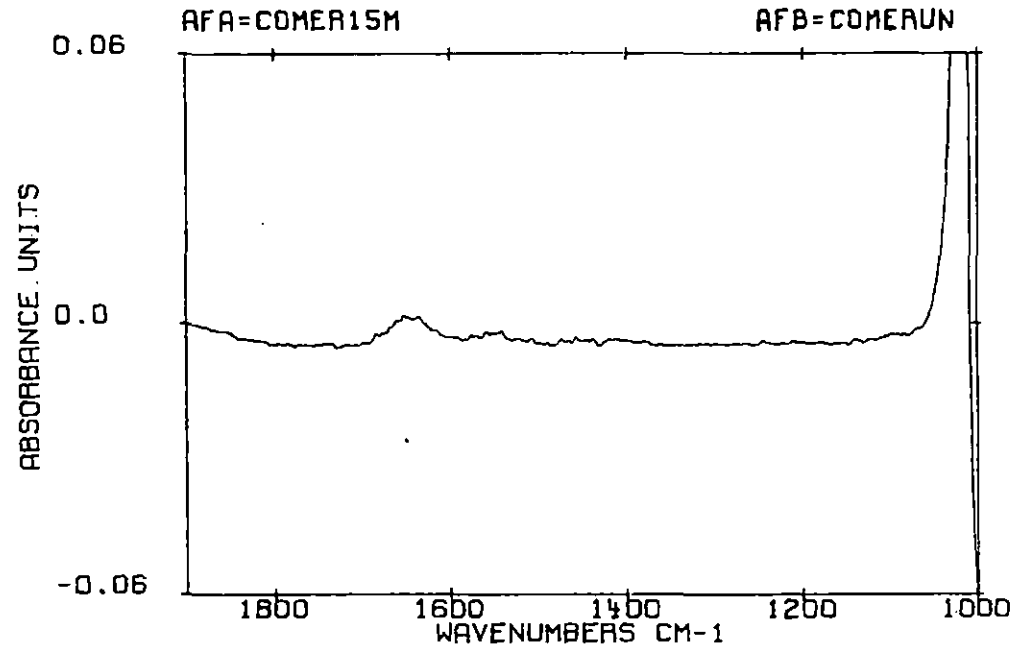

Figure 26e. Spectrum of protein adsorbed onto commercial Silastic® after 15 minutes exposure to blood

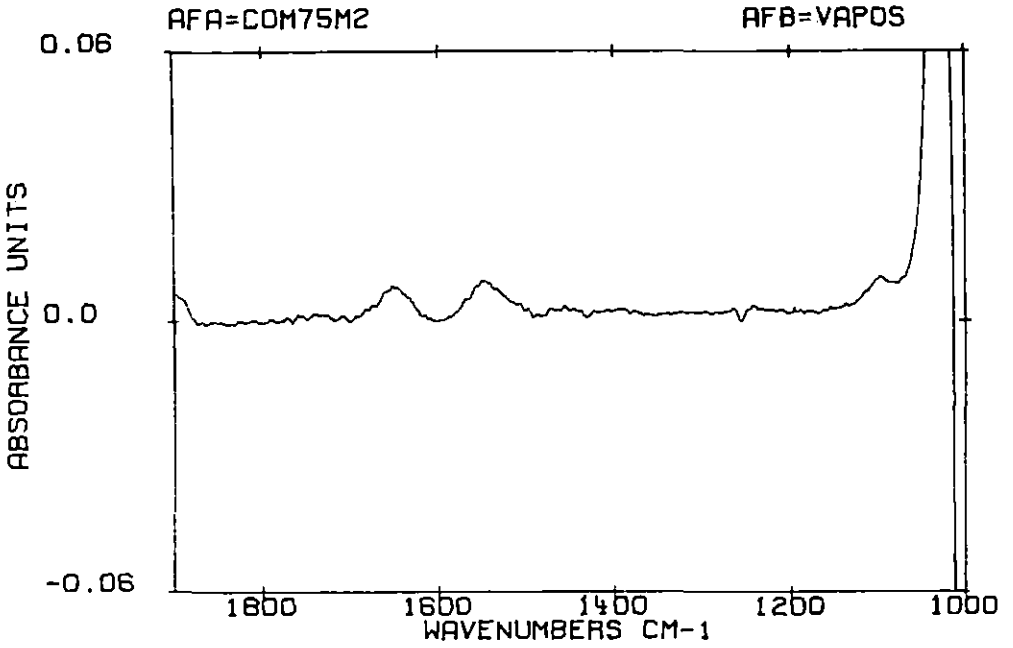

Figure 26f. Spectrum of protein adsorbed onto commercial Silastic® after 75 minutes exposure to blood

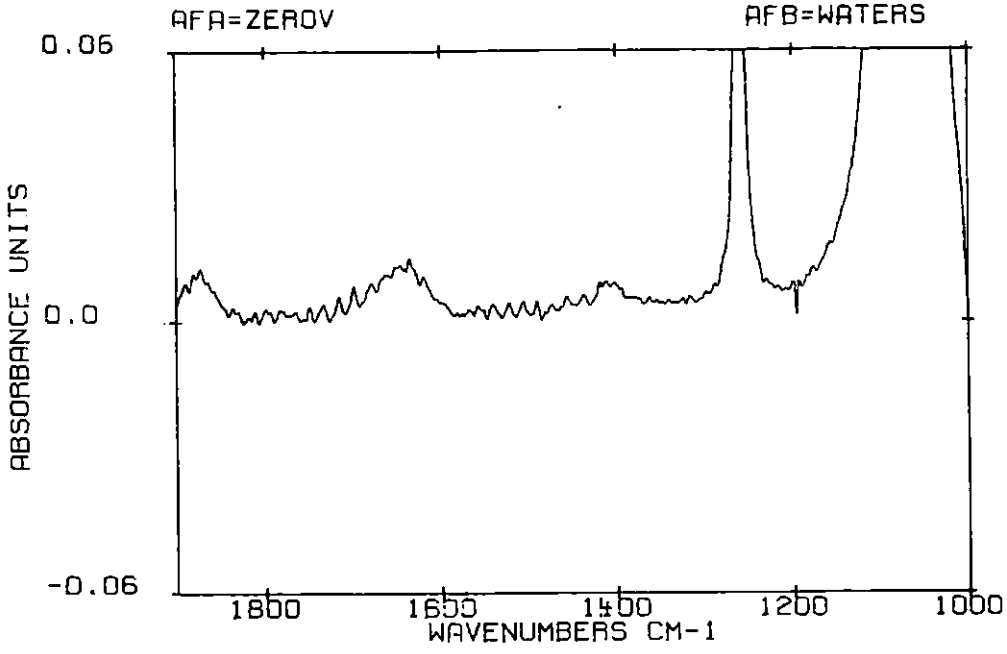

Figure 27a. Spectrum of water vapor and saline subtracted from the 0% filler SR substrate

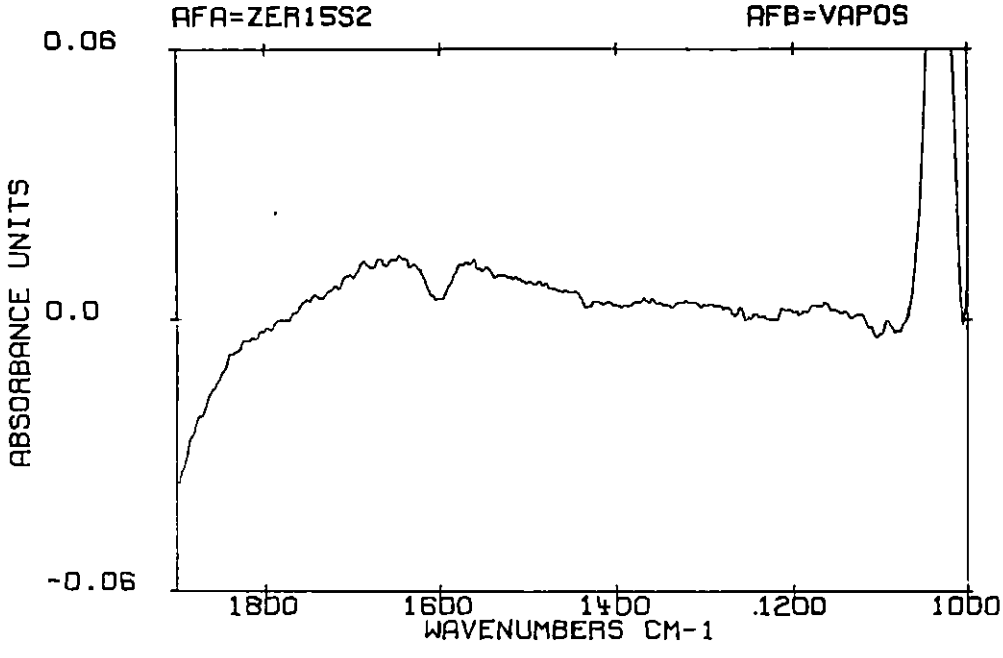

Figure 27b. Spectrum of protein adsorbed onto the 0% filler SR substrate after 0.25 minute exposure to blood

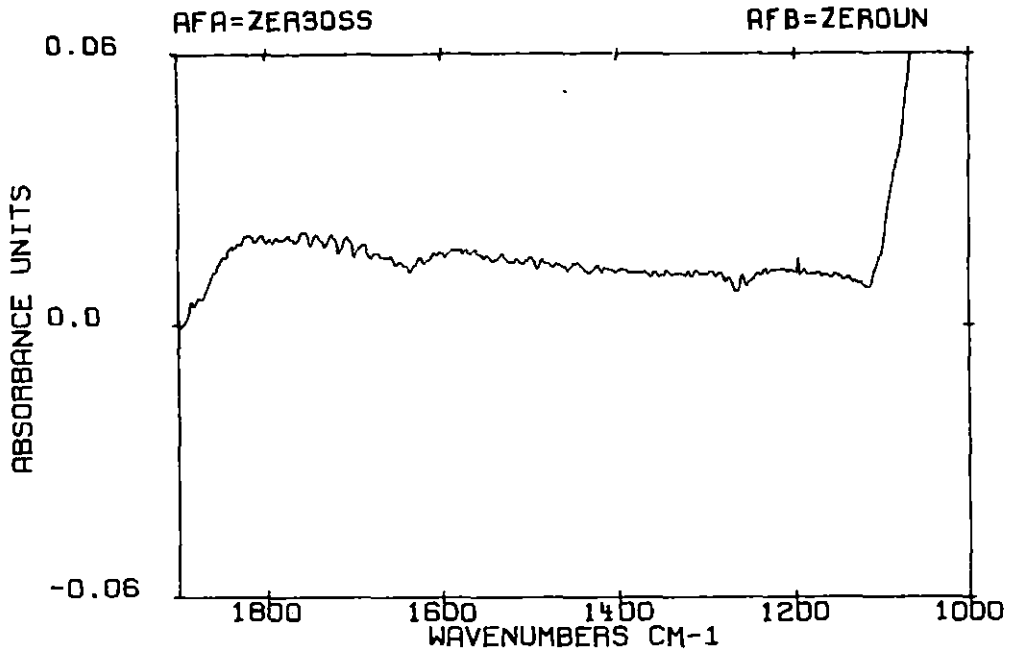

Figure 27c. Spectrum of protein adsorbed into the 0% filler SR substrate after 0.5 minute exposure to blood

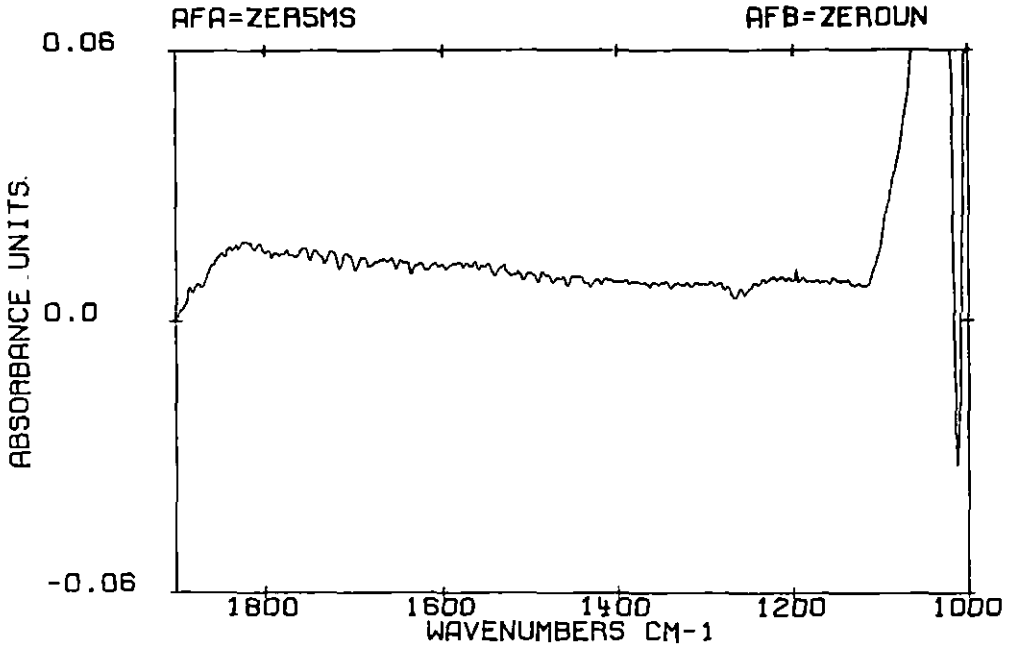

Figure 27d. Spectrum of protein adsorbed onto the 0% filler SR substrate after 5 minutes exposure to blood

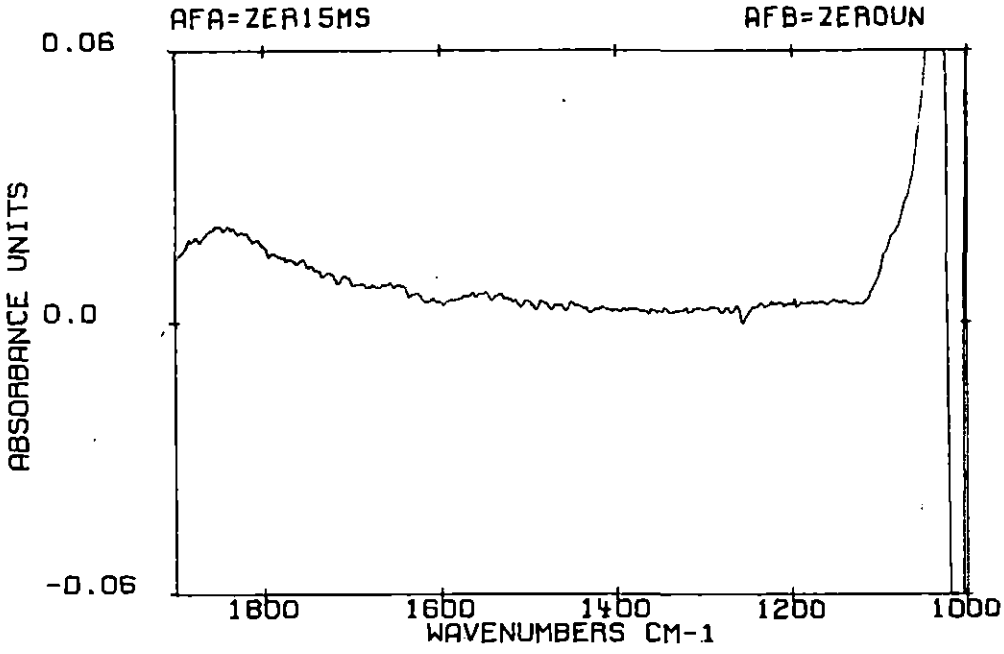

Figure 27e. Spectrum of protein adsorbed onto the 0% filler SR substrate after 15 minutes exposure to blood

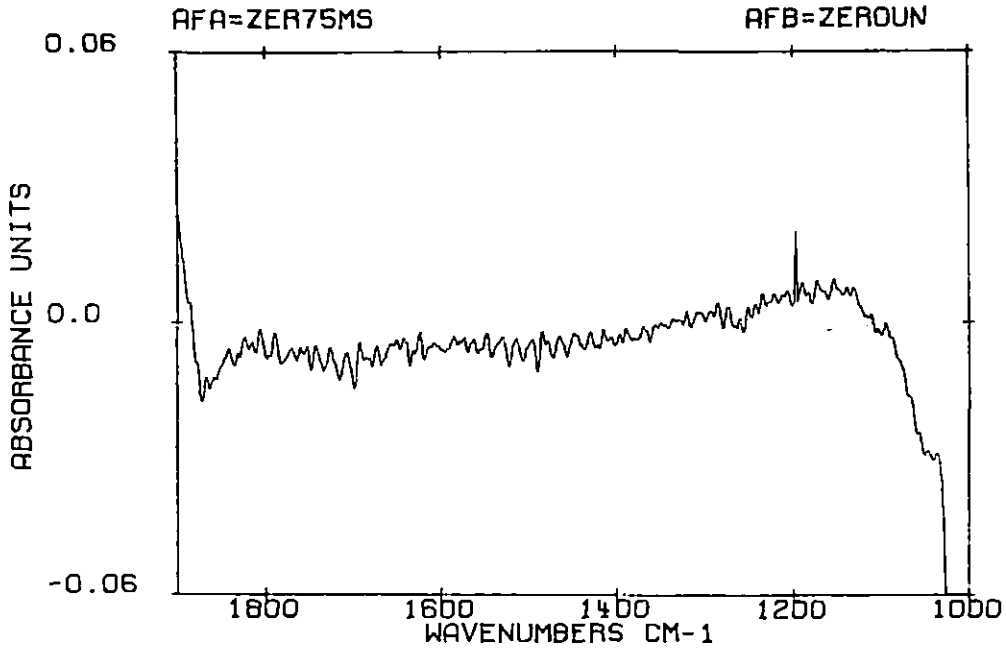

Figure 27f. Spectrum of protein adsorbed onto the 0% filler SR substrate after 75 minutes exposure to blood

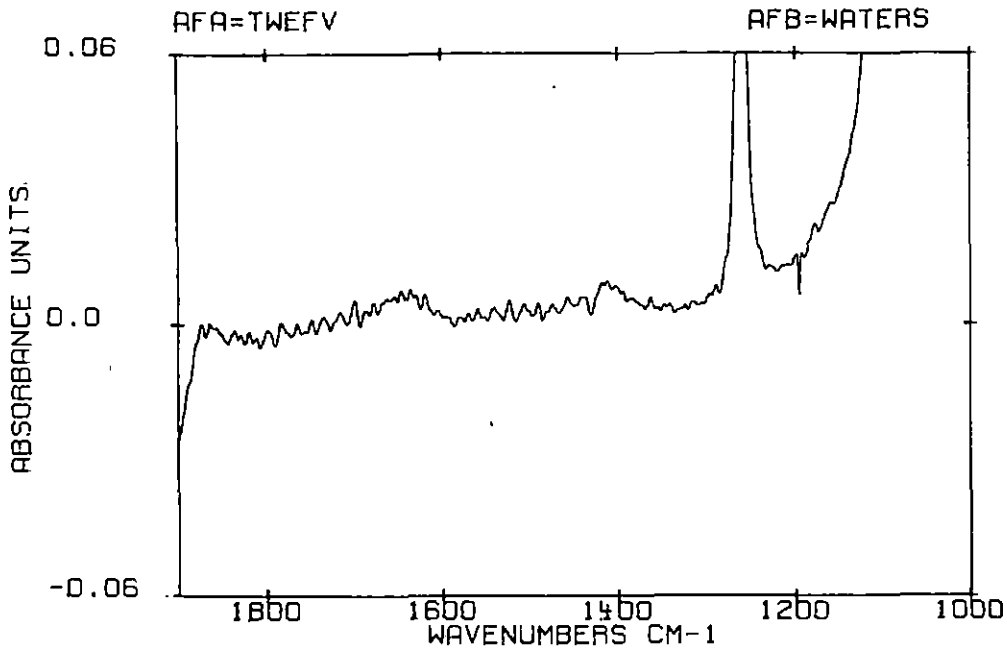

Figure 28a. Spectrum of water vapor and saline subtracted from the 24% filler SR substrate

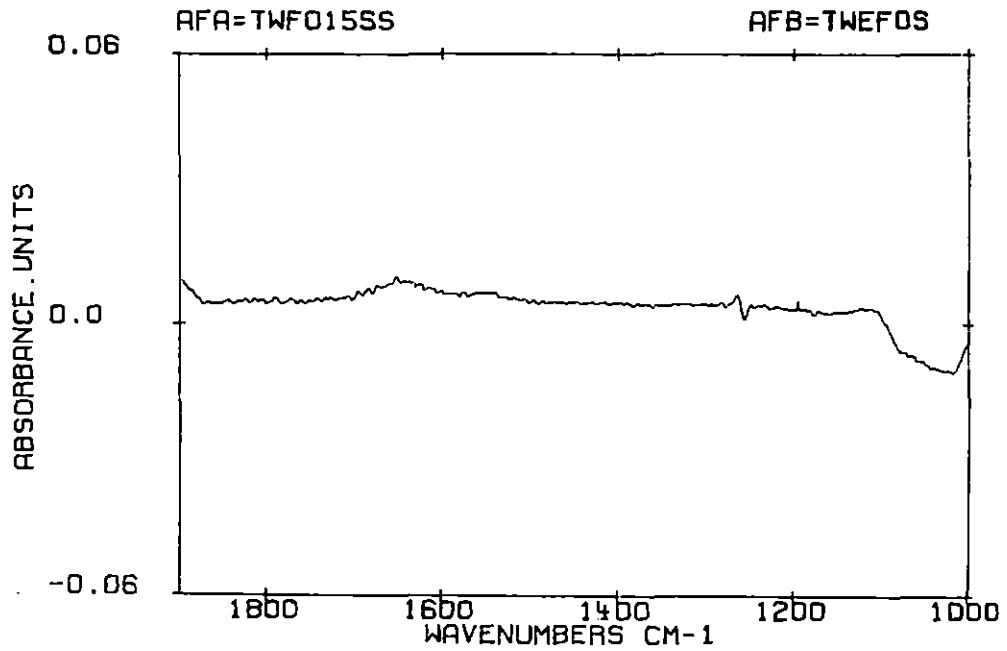

Figure 28b. Spectrum of protein adsorbed onto the 24% filler SR substrate after 0.25 minute of exposure to blood

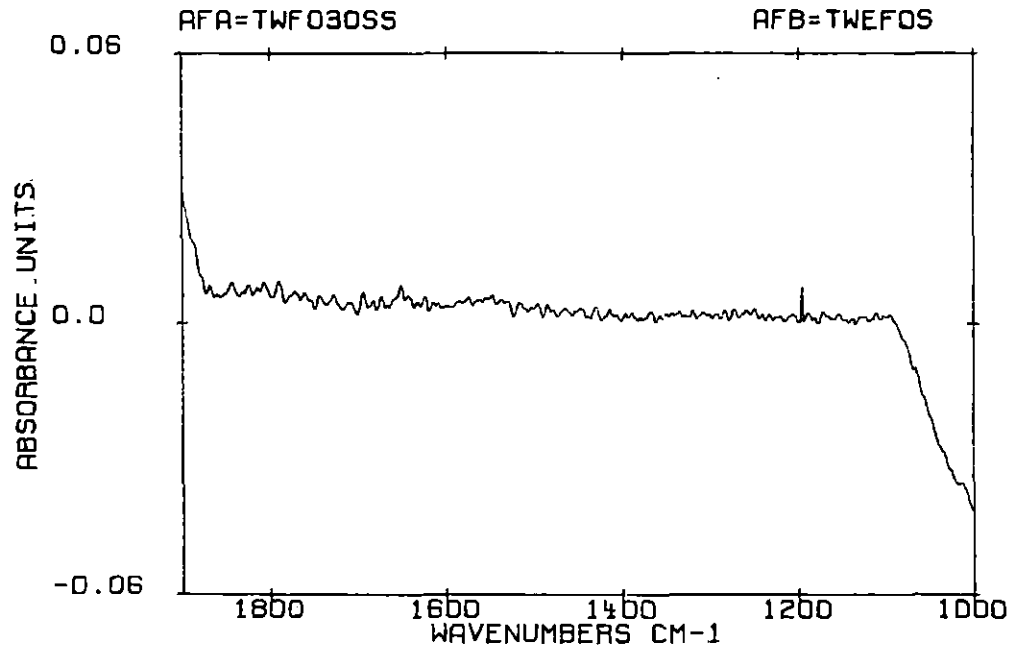

Figure 28c. Spectrum of protein adsorbed onto the 24% filler SR substrate after 0.5 minute of exposure to blood

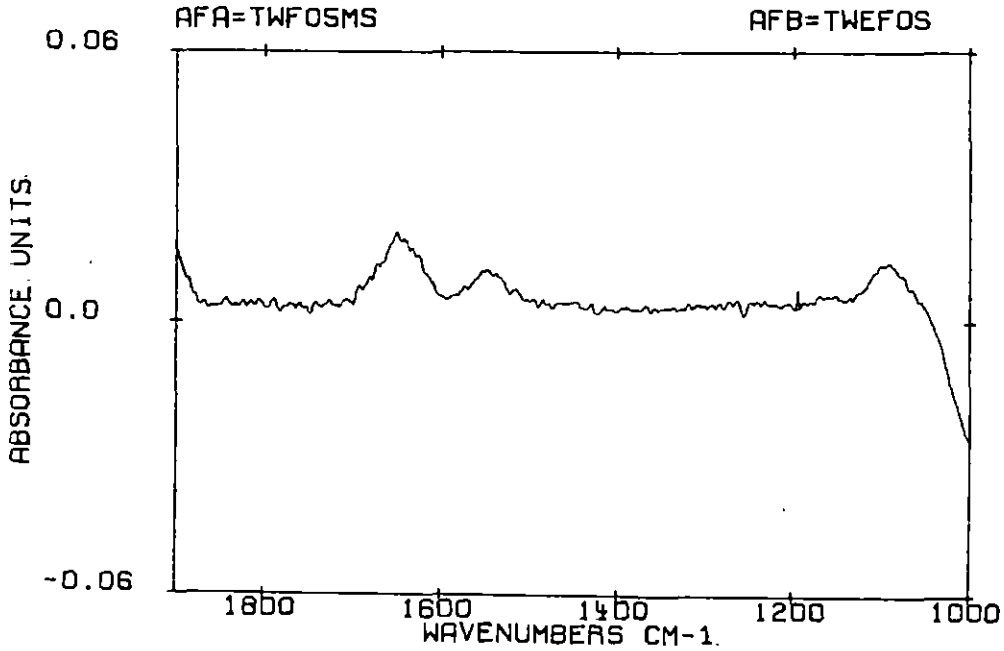

Figure 28d. Spectrum of protein adsorbed onto the 24% filler SR substrate after 5 minutes exposure to blood

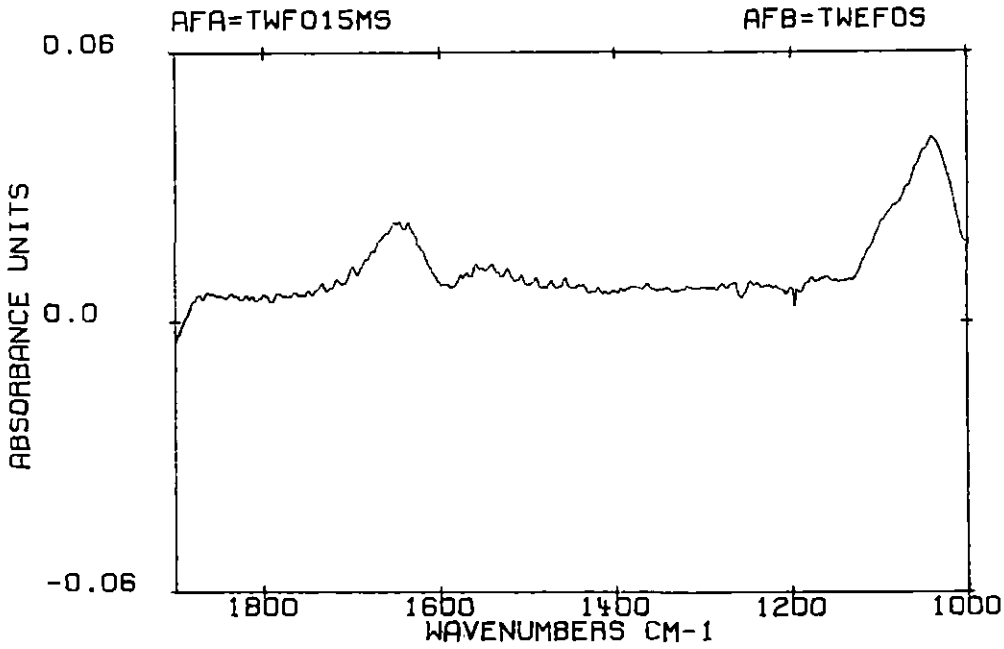

Figure 28e. Spectrum of protein adsorbed onto the 24% filler SR substrate after 15 minutes exposure to blood

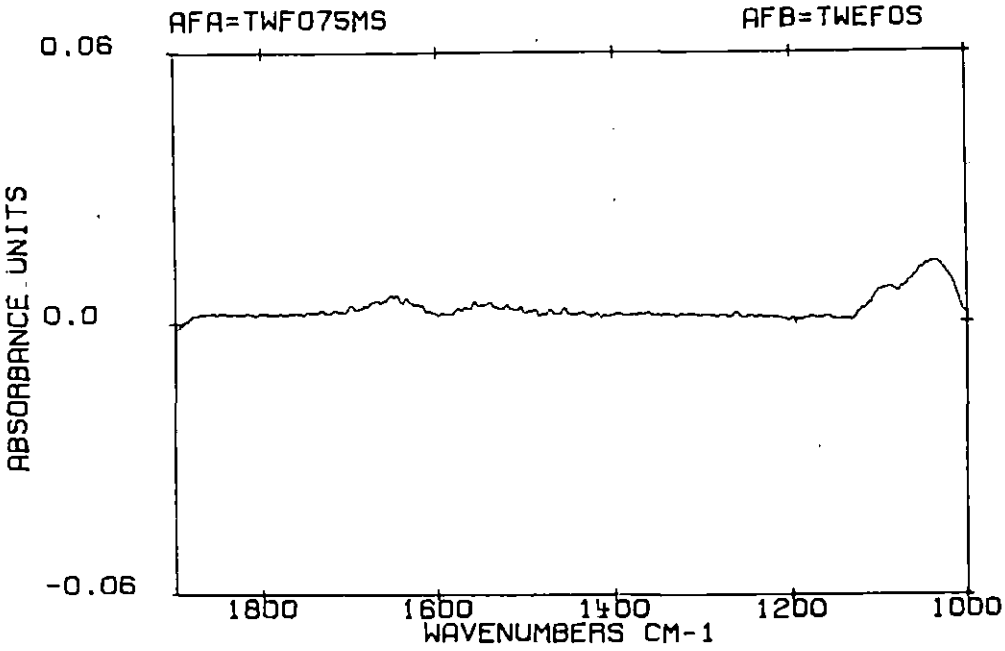

Figure 28f. Spectrum of protein adsorbed onto the 24% filler SR substrate after 75 minutes exposure to blood

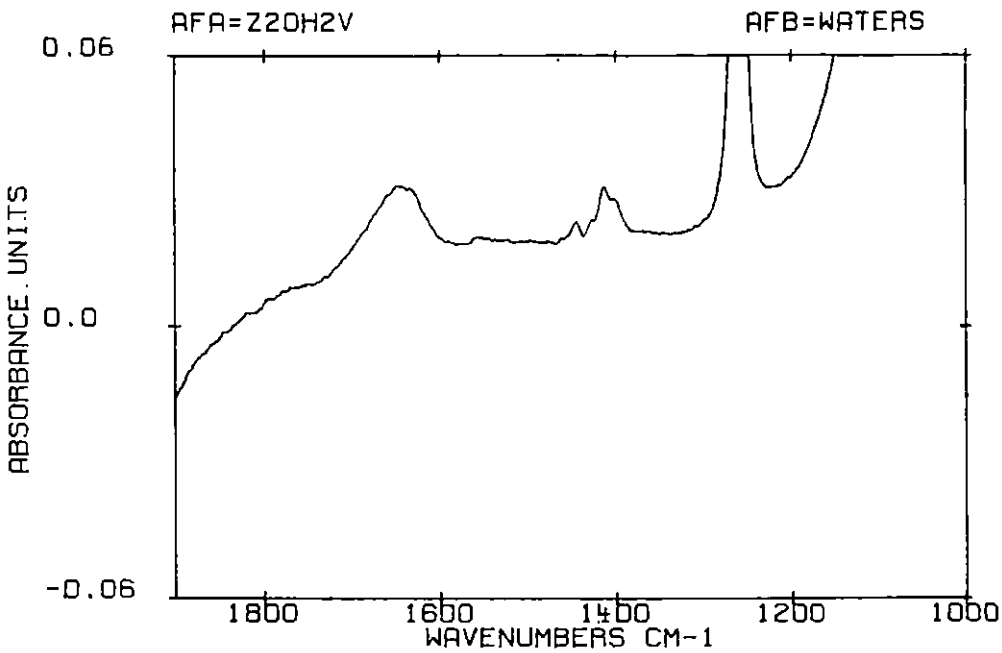

Figure 29a. Spectrum of water vapor and saline subtracted from the 0% filler SR/20% HEMA formulation

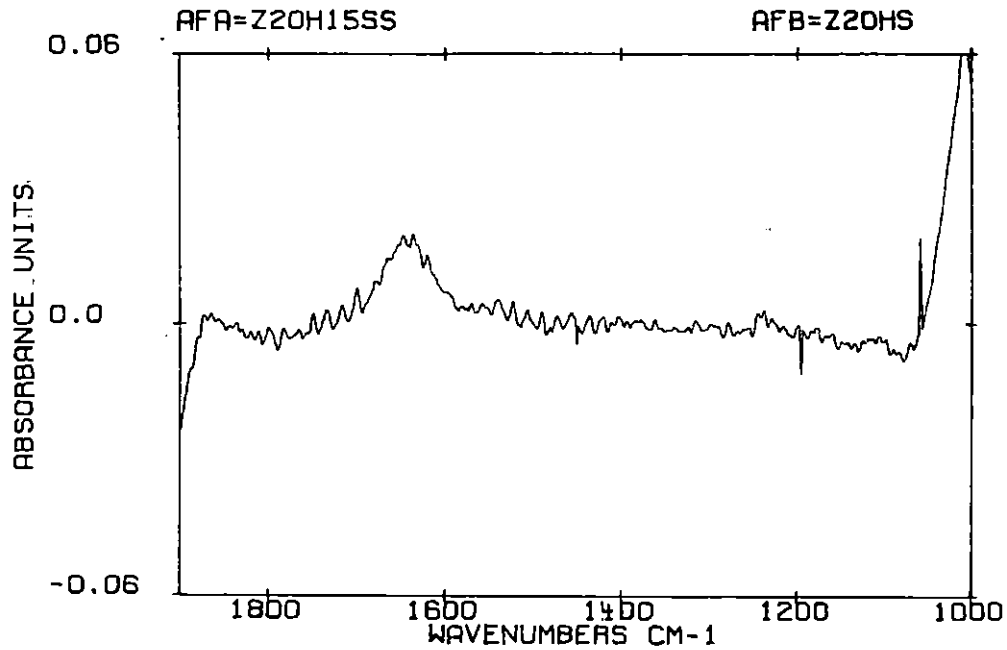

Figure 29b. Spectrum of protein adsorbed onto the 0% filler SR/20% HEMA formulation after 0.25 minute of blood exposure

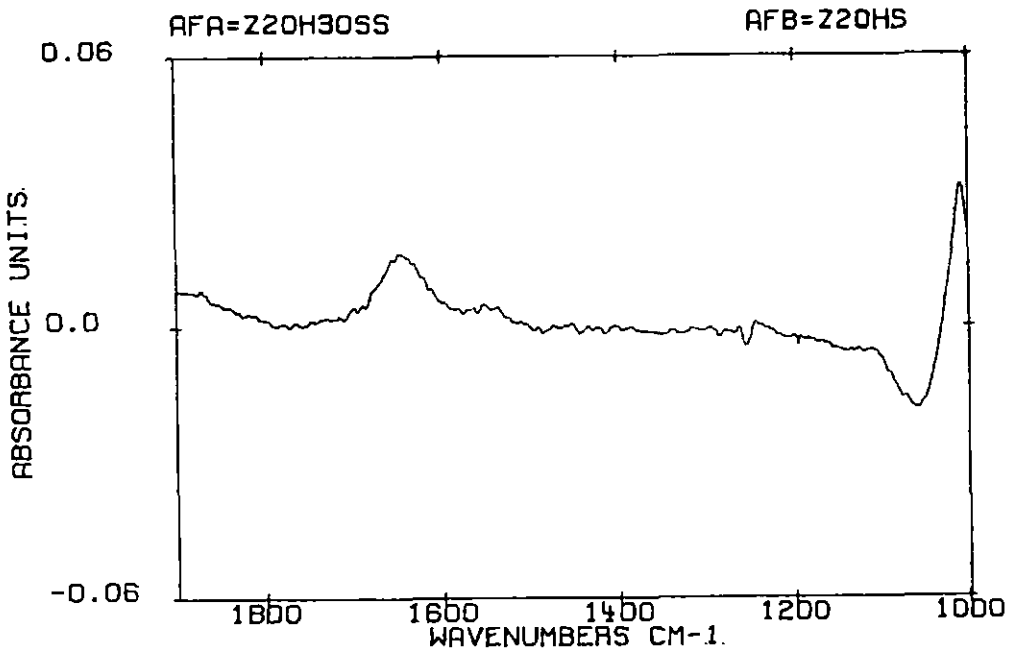

Figure 29c. Spectrum of protein adsorbed onto the 0% filler SR/20% HEMA formulation after 0.5 minute of blood exposure

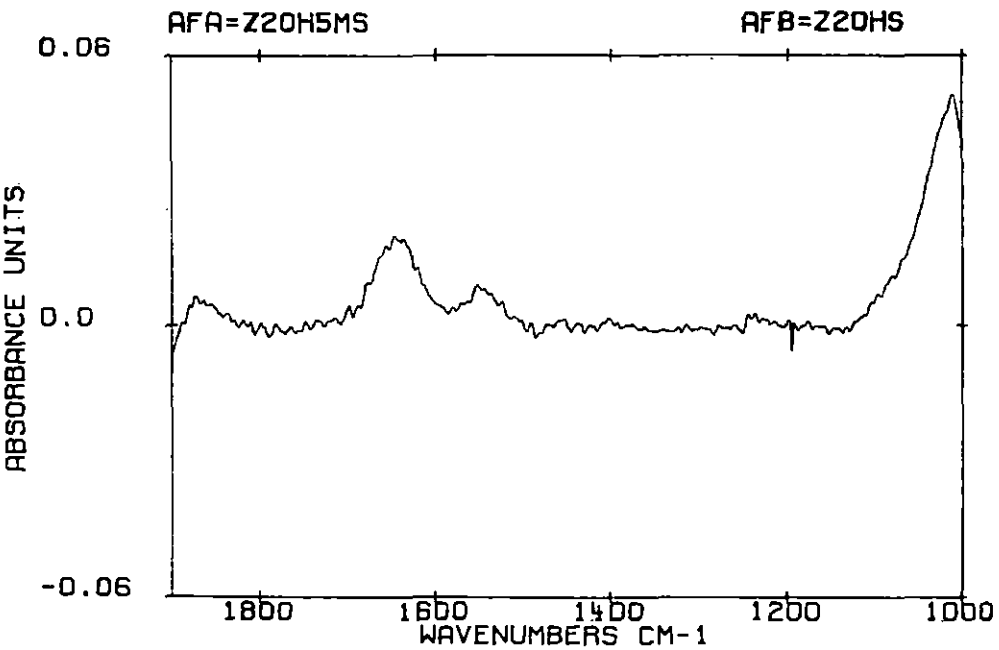

Figure 29d. Spectrum of protein adsorbed onto the 0% filler SR/20% HEMA formulation after 5 minutes of blood exposure

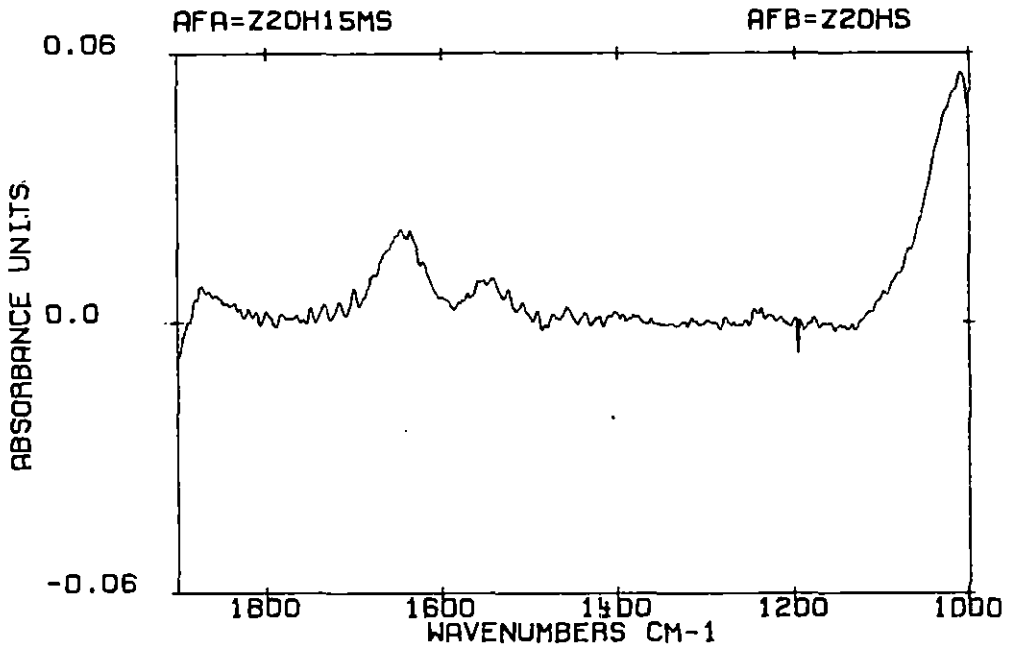

Figure 29e. Spectrum of protein adsorbed onto the 0% filler SR/20% HEMA formulation after 15 minutes of blood exposure

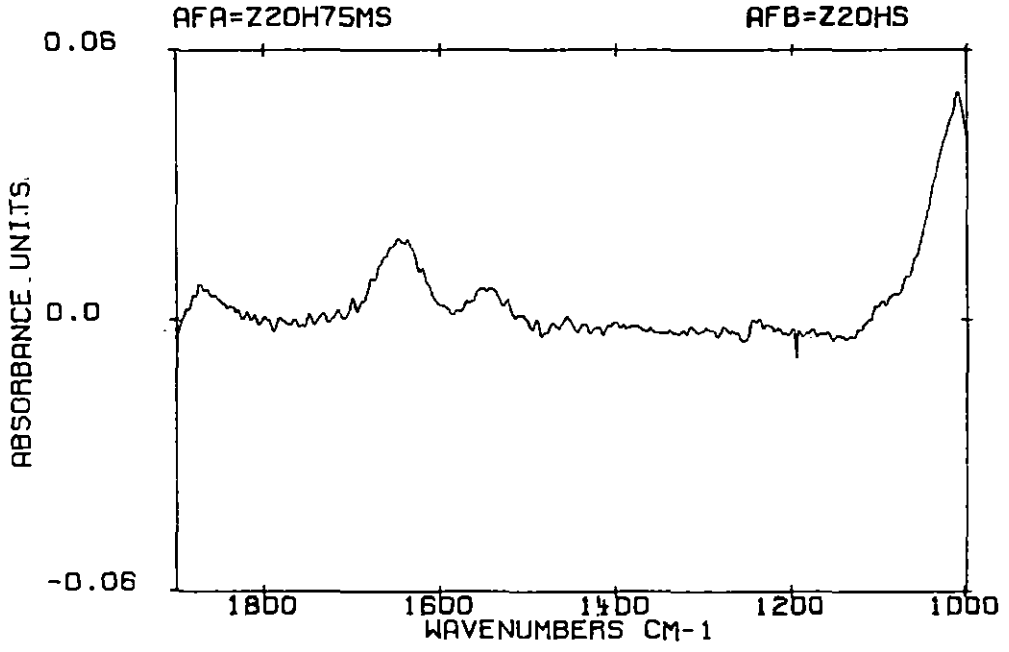

Figure 29f. Spectrum of protein adsorbed onto the 0% filler SR/20% HEMA formulation after 75 minutes of blood exposure

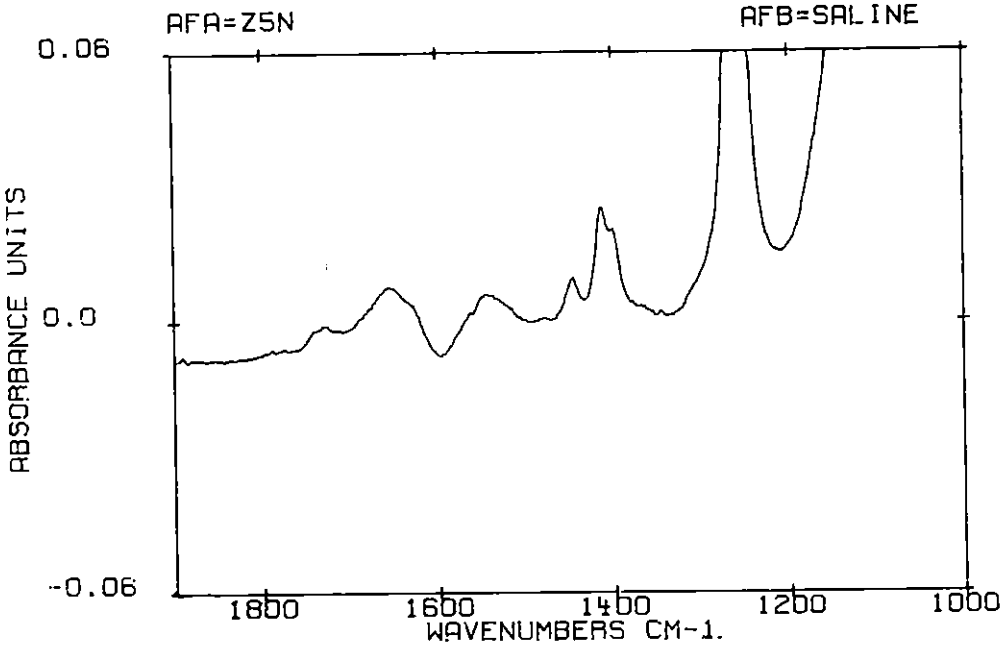

Figure 30a. Spectrum of saline subtracted from the 0% filler SR/15% HEMA/ 5% NVP formulation

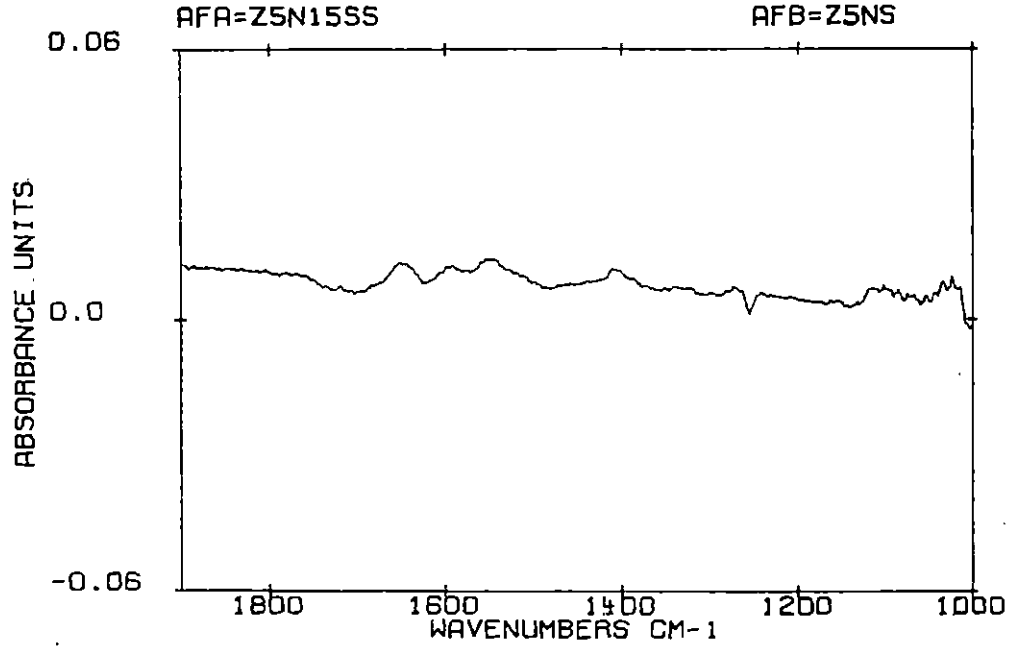

Figure 30b. Spectrum of protein adsorbed onto the 0% filler SR/15% HEMA/ 5% NVP formulation after 0.25 minute of blood exposure

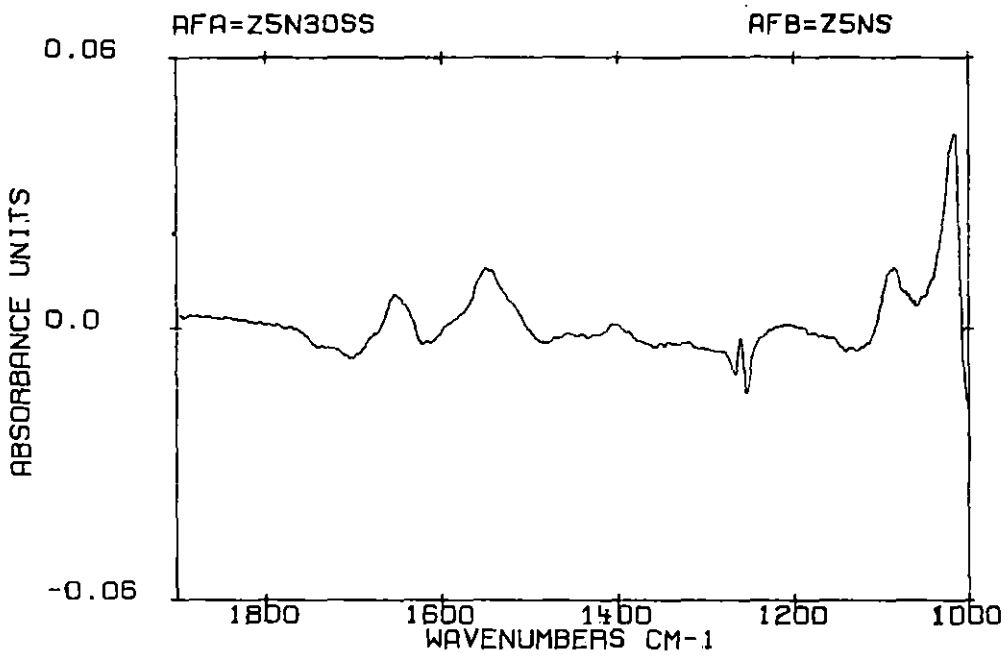

Figure 30c. Spectrum of protein adsorbed onto the 0% filler SR/15% HEMA/ 5% NVP formulation after 0.5 minute of blood exposure

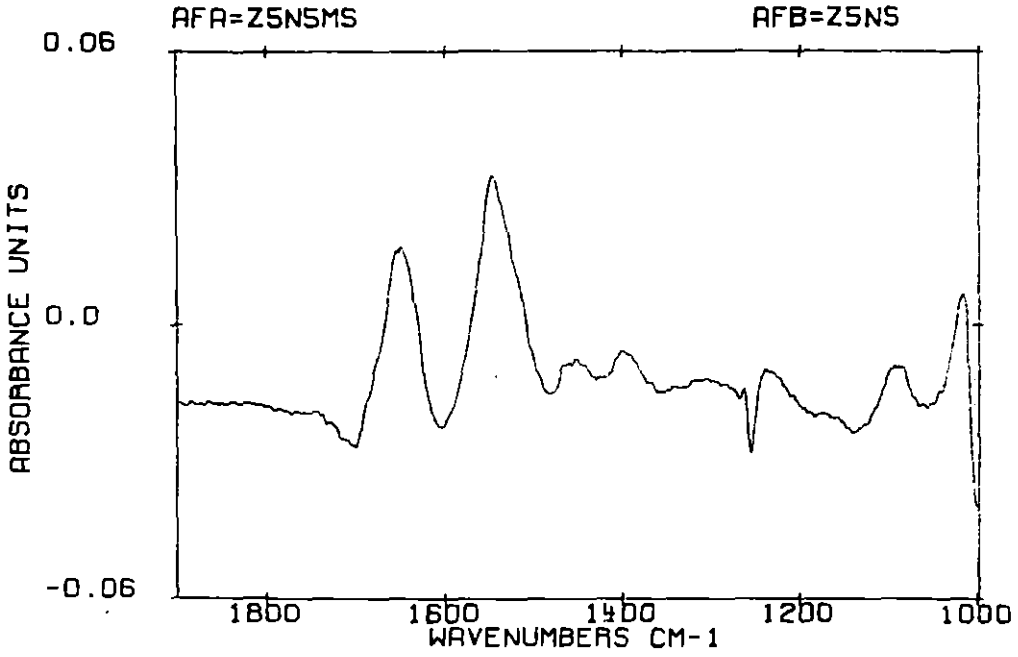

Figure 30d. Spectrum of protein adsorbed onto the 0% filler SR/15% HEMA/ 5% NVP formulation after 5 minutes of blood exposure

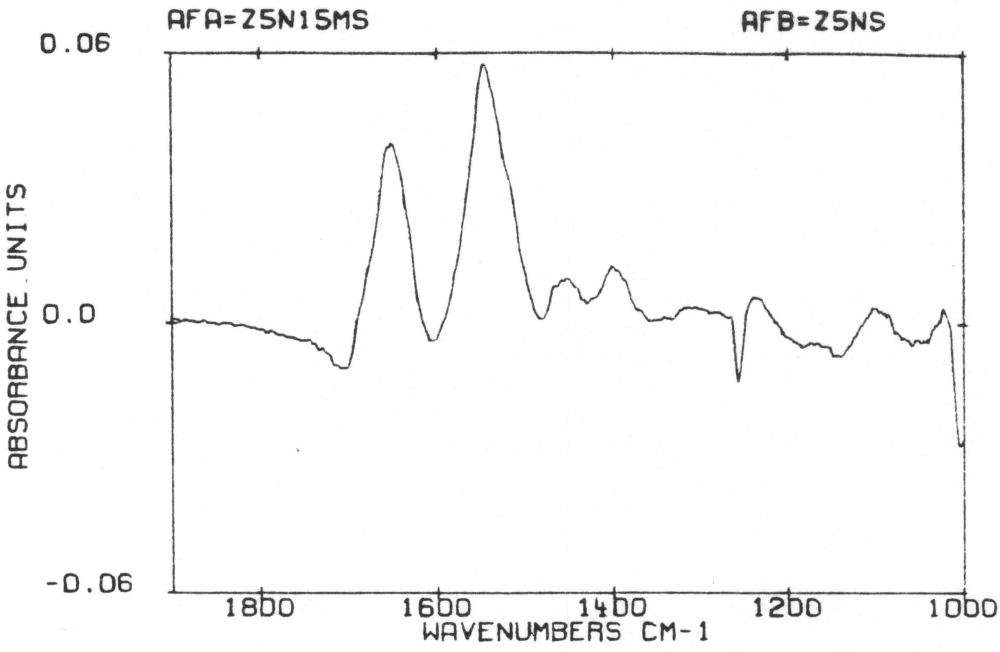

Figure 30e. Spectrum of protein adsorbed onto the 0% filler SR/15% HEMA/ 5% NVP formulation after 15 minutes of blood exposure

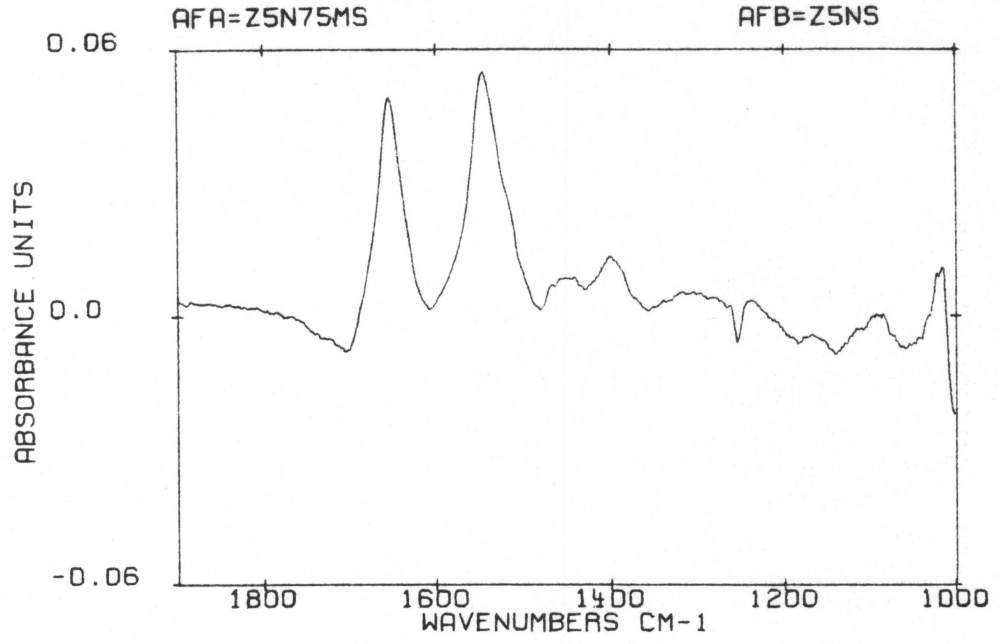

Figure 30f. Spectrum of protein adsorbed onto the 0% filler SR/15% HEMA/ 5% NVP formulation after 75 minutes of blood exposure

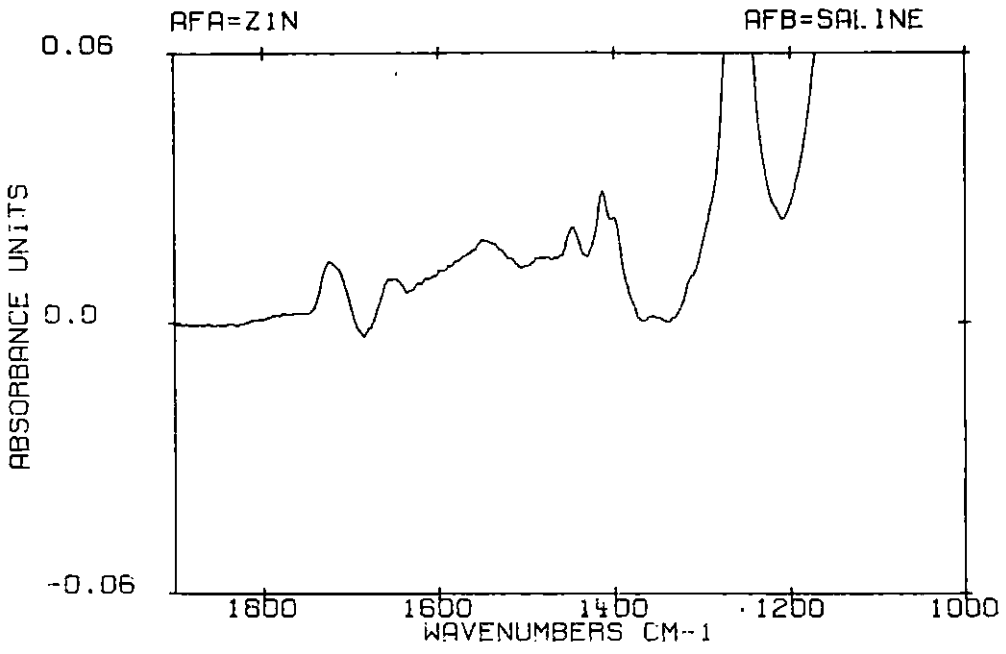

Figure 31a. Spectrum of saline subtracted from the 0% filler SR/10% HEMA/ 10% NVP formulation

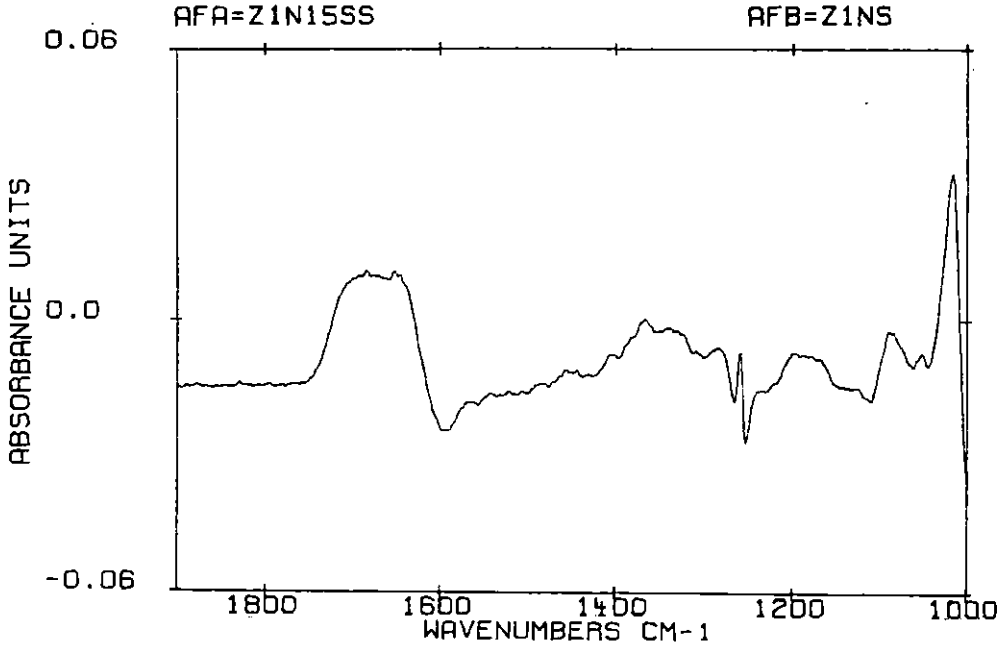

Figure 31b. Spectrum of protein adsorbed onto the 0% filler SR/10% HEMA/ 10% NVP formulation after 0.25 minute of blood exposure

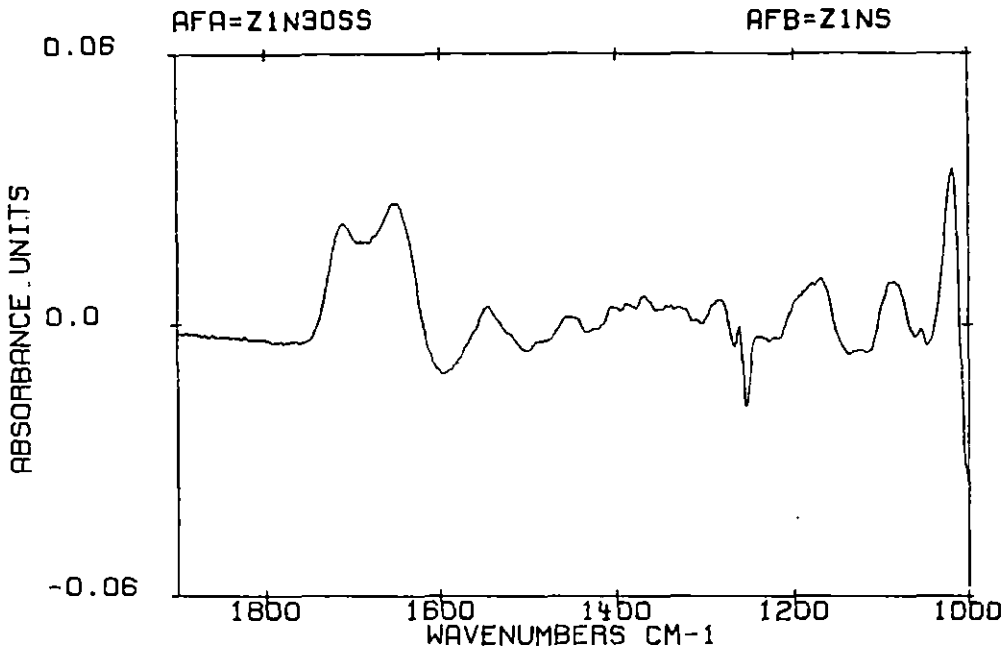

Figure 31c. Spectrum of protein adsorbed onto the 0% filler SR/10% HEMA/ 10% NVP formulation after 0.5 minute of blood exposure

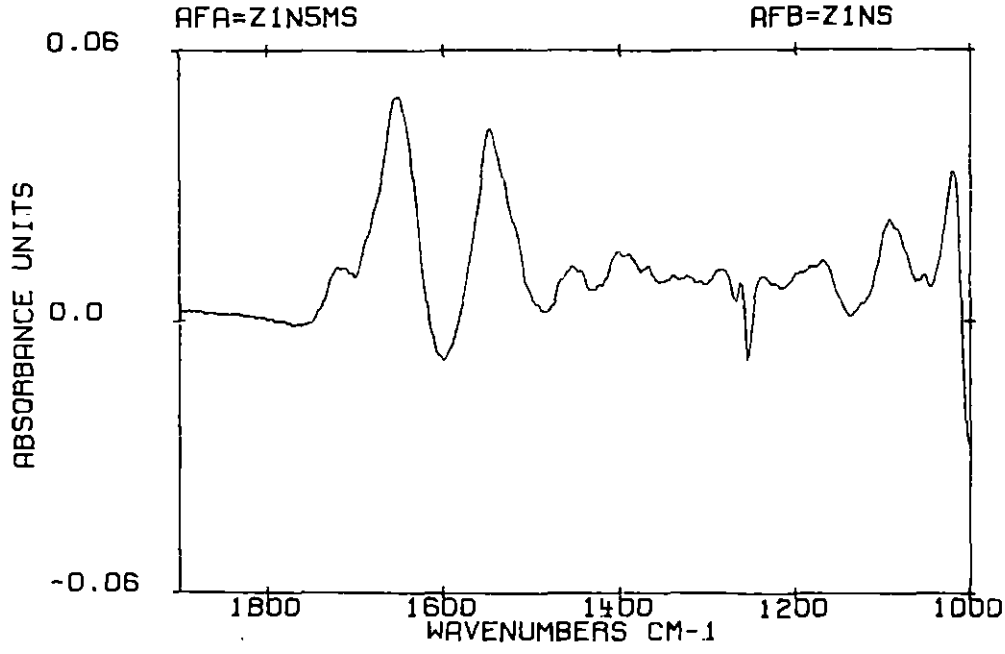

Figure 31d. Spectrum of protein adsorbed onto the 0% filler SR/10% HEMA/ 10% NVP formulation after 5 minutes of blood exposure

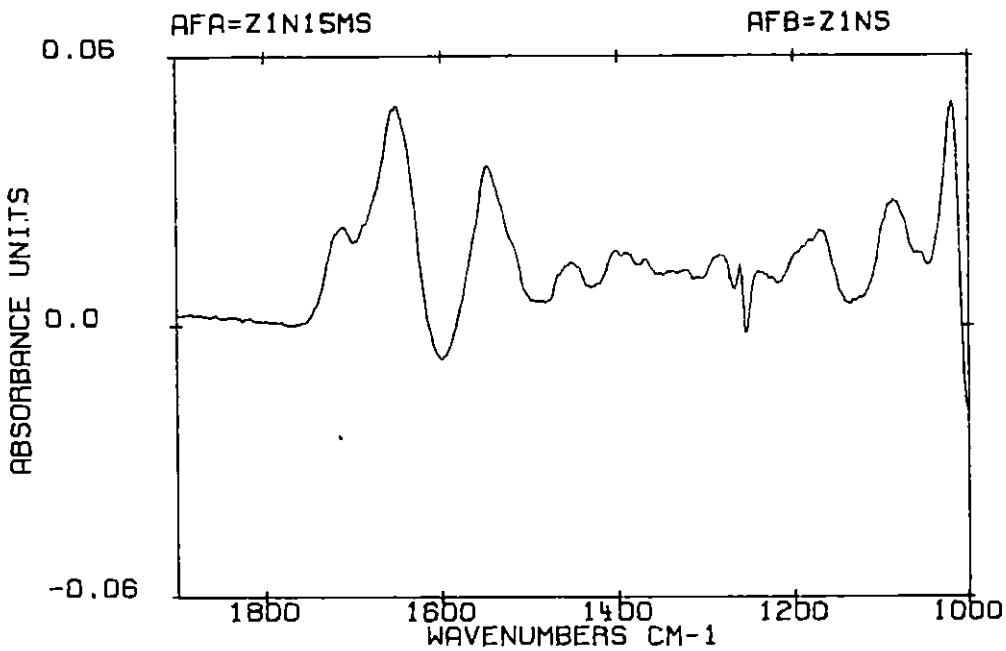

Figure 31e. Spectrum of protein adsorbed onto the 0% filler SR/10% HEMA/ 10% NVP formulation after 15 minutes of blood exposure

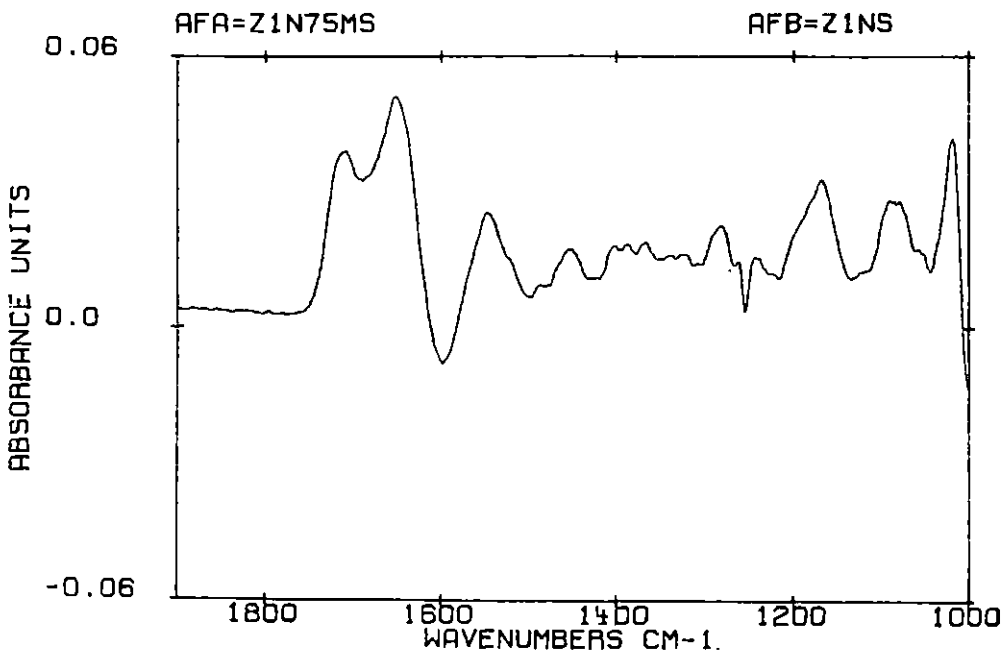

Figure 31f. Spectrum of protein adsorbed onto the 0% filler SR/10% HEMA/ 10% NVP formulation after 75 minutes of blood exposure

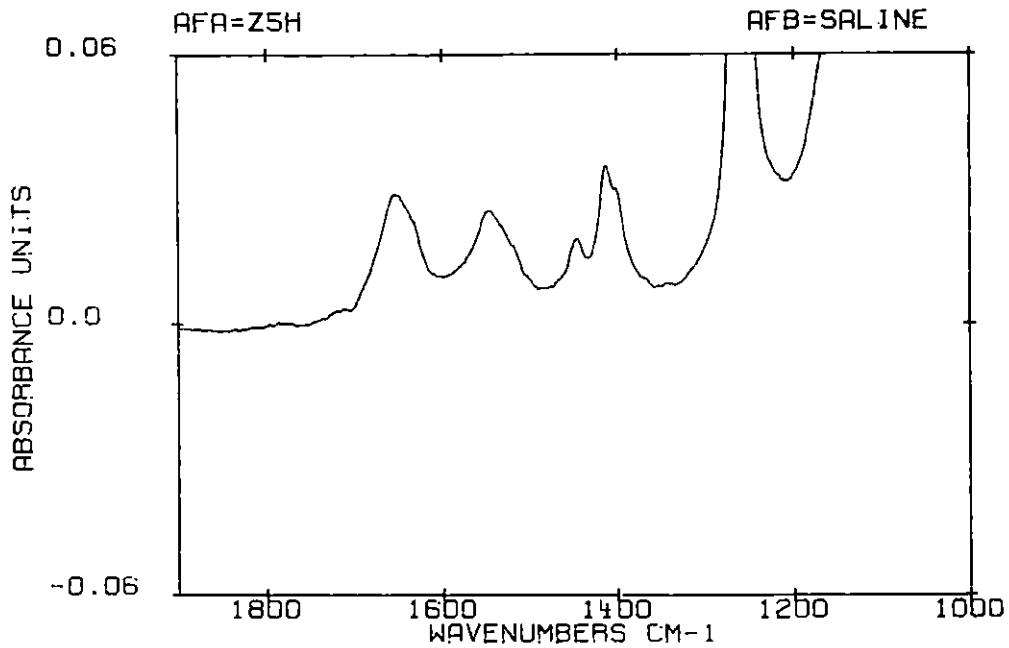

Figure 32a. Spectrum of saline subtracted from the 0% filler SR/5% HEMA/ 15% NVP formulation

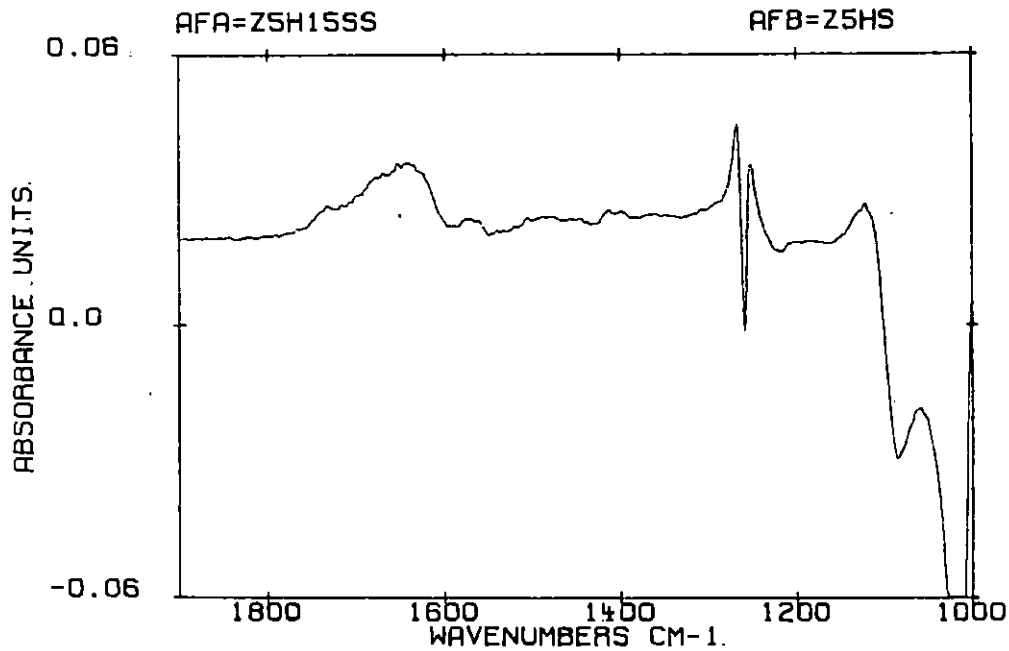

Figure 32b. Spectrum of protein adsorbed onto the 0% filler SR/5% HEMA/ 15% NVP formulation after 0.25 minute of blood exposure

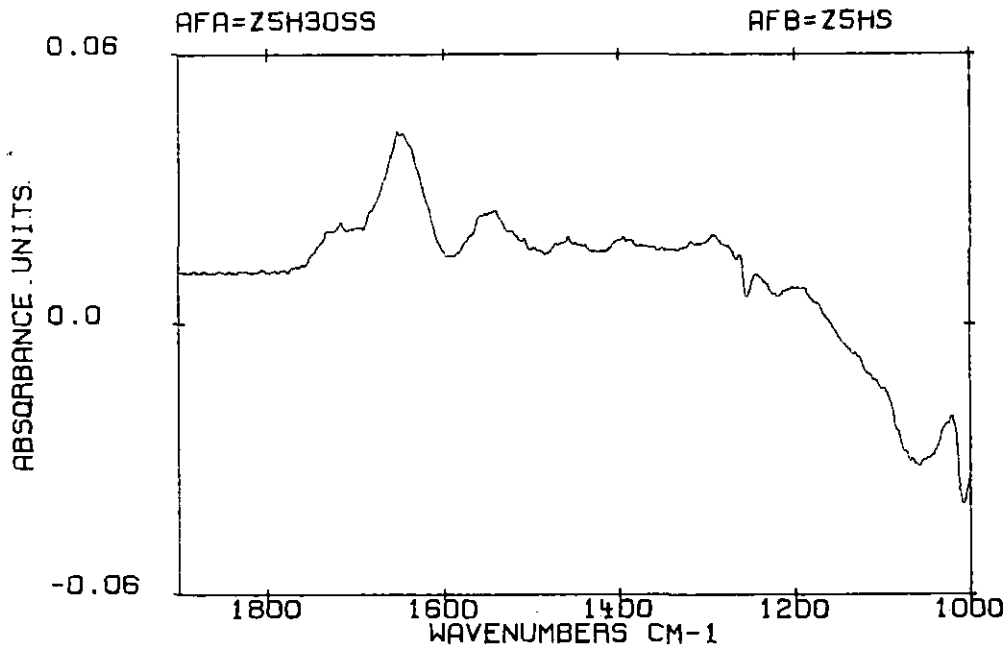

Figure 32c. Spectrum of protein adsorbed onto the 0% filler SR/5% HEMA/ 15% NVP formulation after 0.5 minute of blood exposure

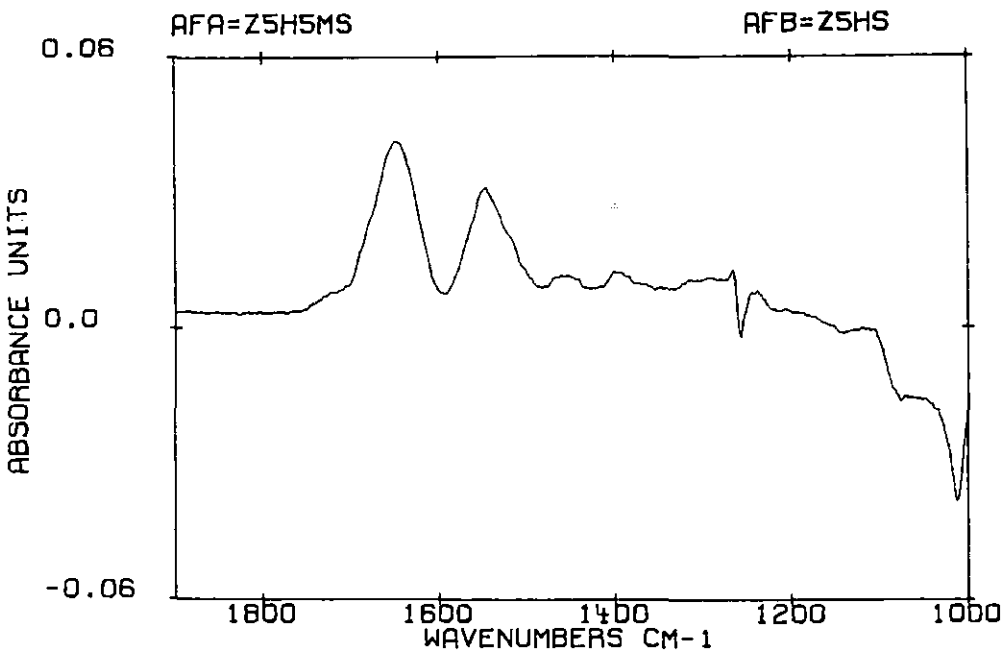

Figure 32d. Spectrum of protein adsorbed onto the 0% filler SR/5% HEMA/ 15% NVP formulation after 5 minutes of blood exposure

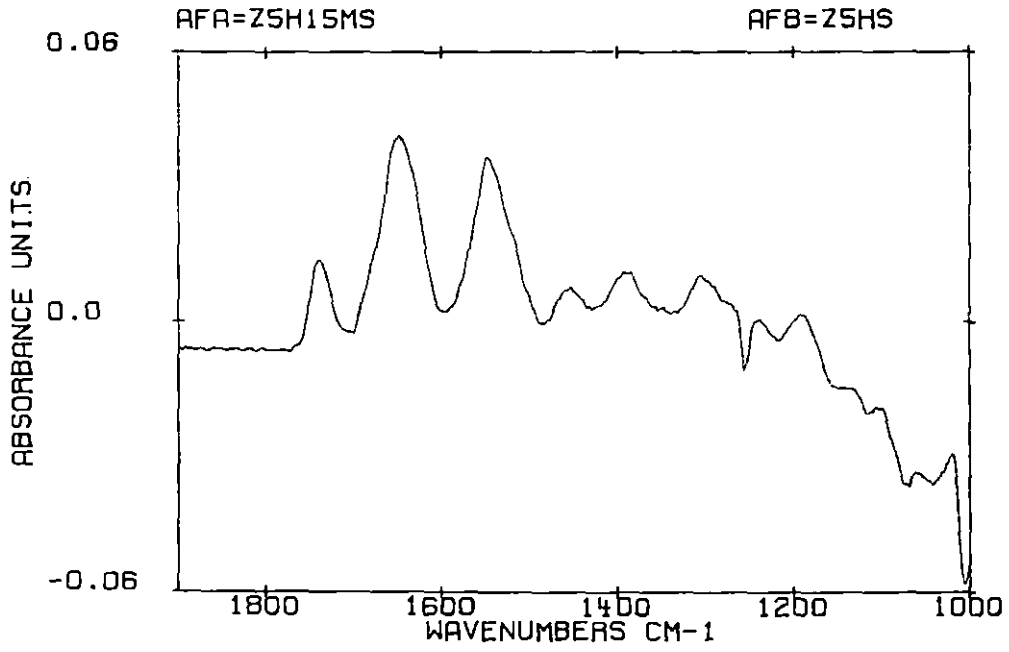

Figure 32e. Spectrum of protein adsorbed onto the 0% filler SR/5% HEMA/ 15% NVP formulation after 15 minutes of blood exposure

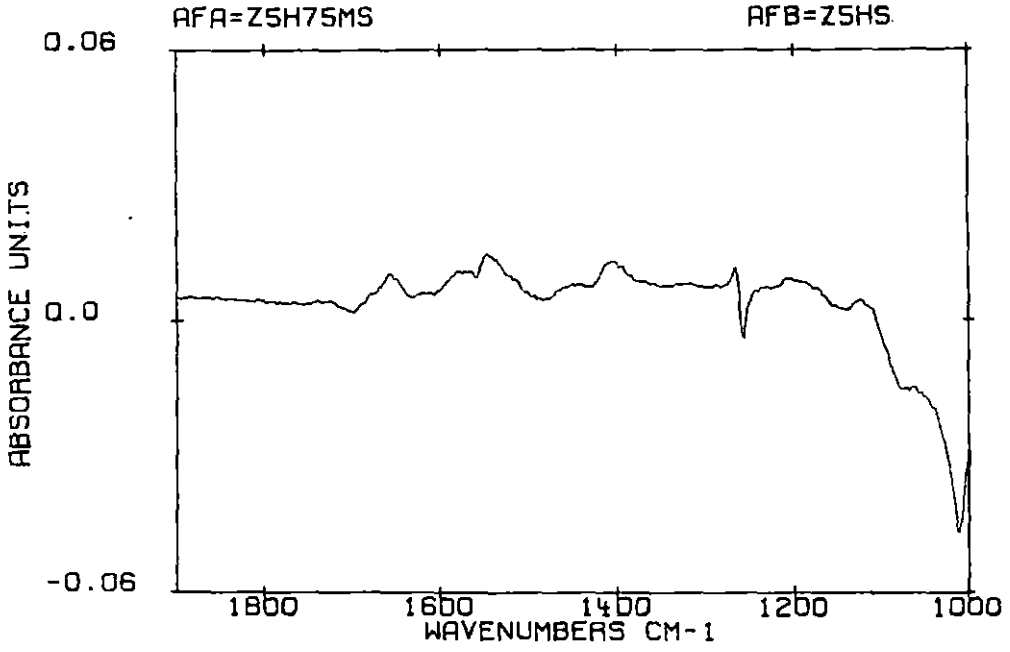

Figure 32f. Spectrum of protein adsorbed onto the 0% filler SR/5% HEMA/ 15% NVP formulation after 75 minutes of blood exposure

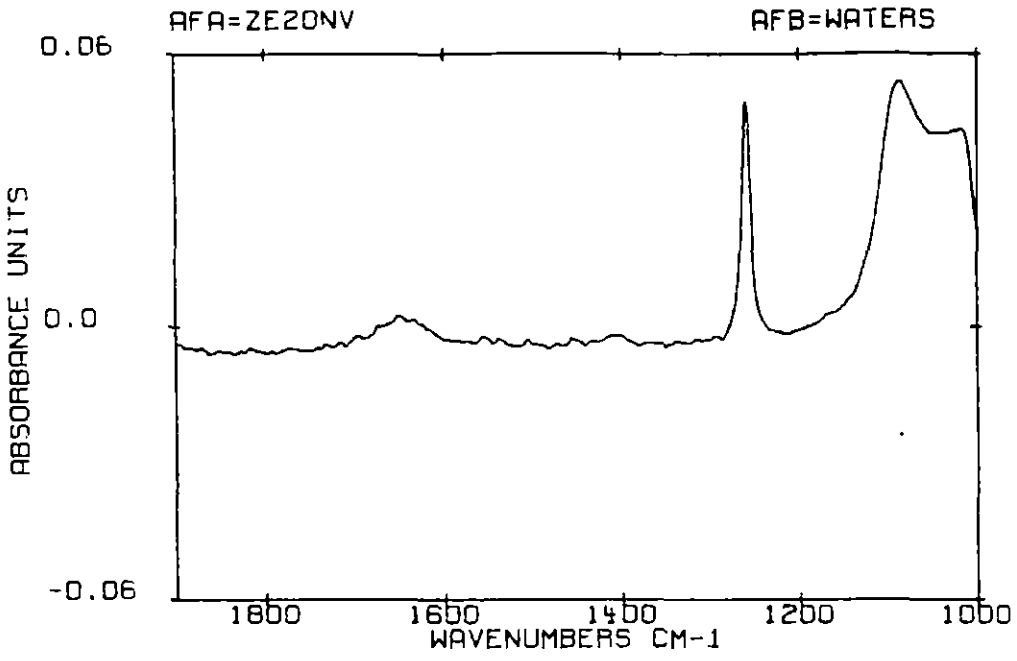

Figure 33a. Spectrum of water vapor and saline subtracted from the 0% filler SR/20% NVP formulation

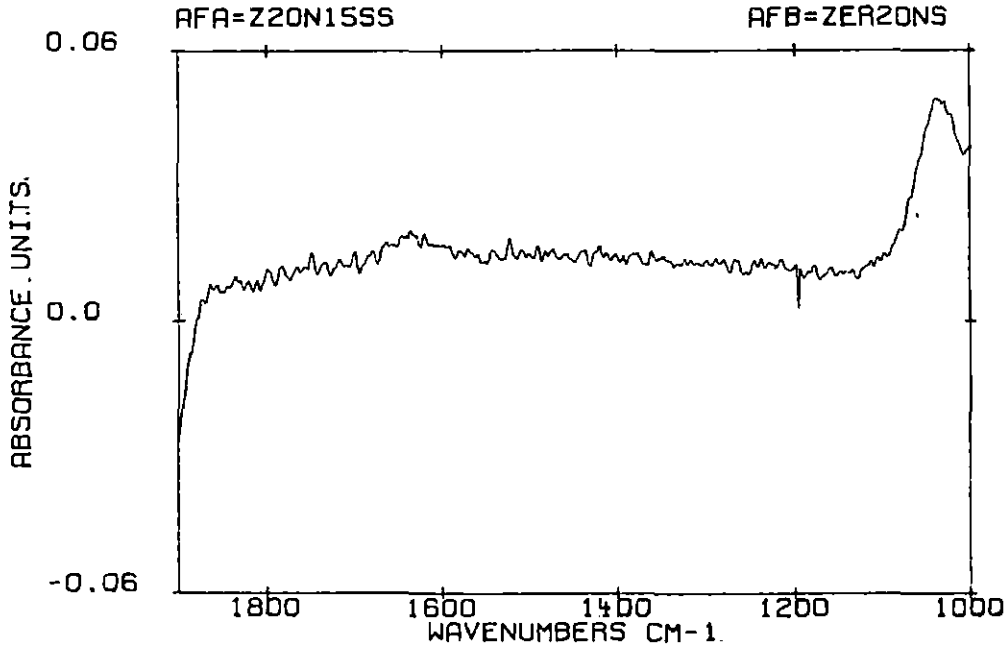

Figure 33b. Spectrum of protein adsorbed onto the 0% filler SR/20% NVP formulation after 0.25 minute of blood exposure

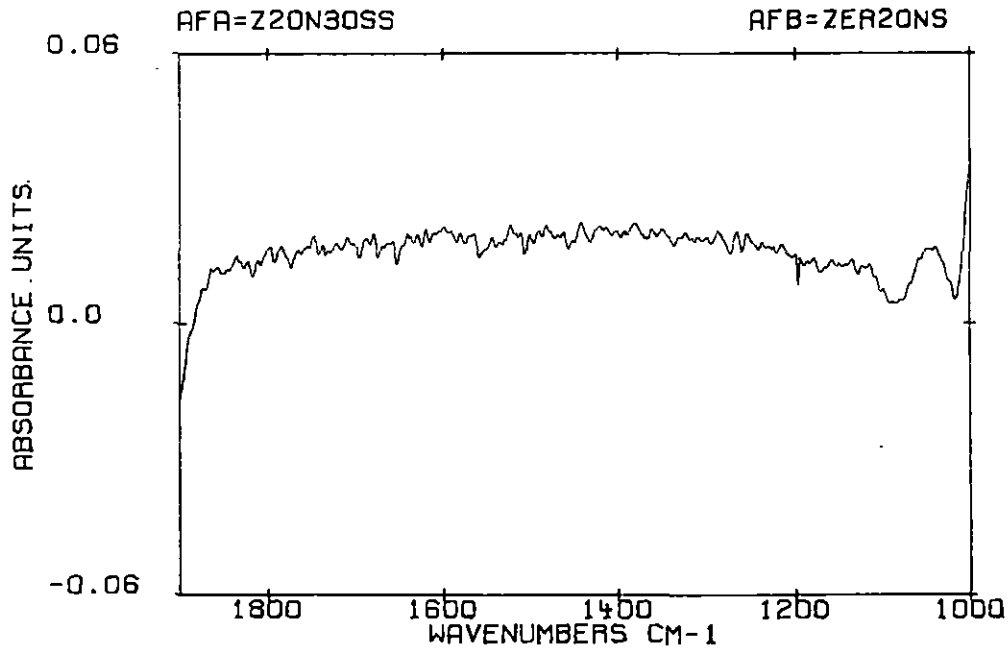

Figure 33c. Spectrum of protein adsorbed onto the 0% filler SR/20% NVP formulation after 0.5 minute of blood exposure

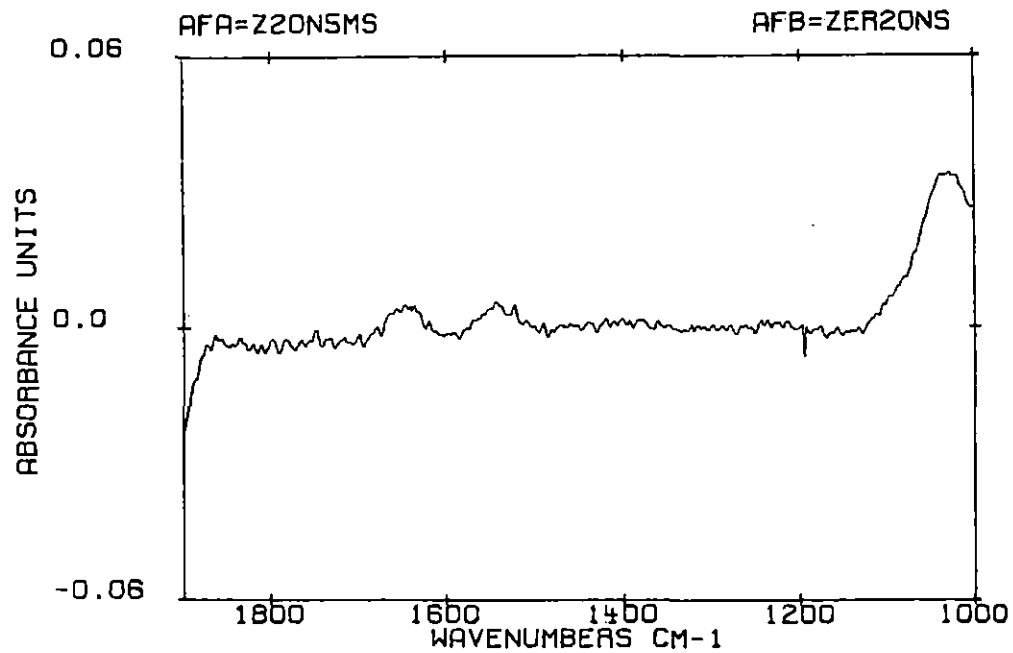

Figure 33d. Spectrum of protein adsorbed onto the 0% filler SR/20% NVP formulation after 5 minutes of blood exposure

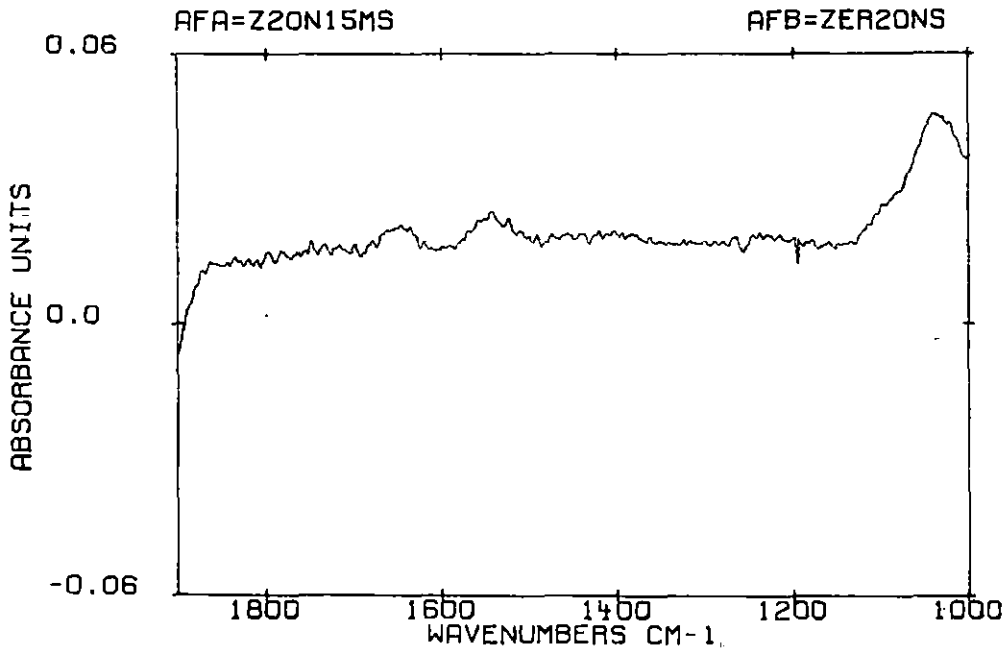

Figure 33e. Spectrum of protein adsorbed onto the 0% filler SR/20% NVP formulation after 15 minutes of blood exposure

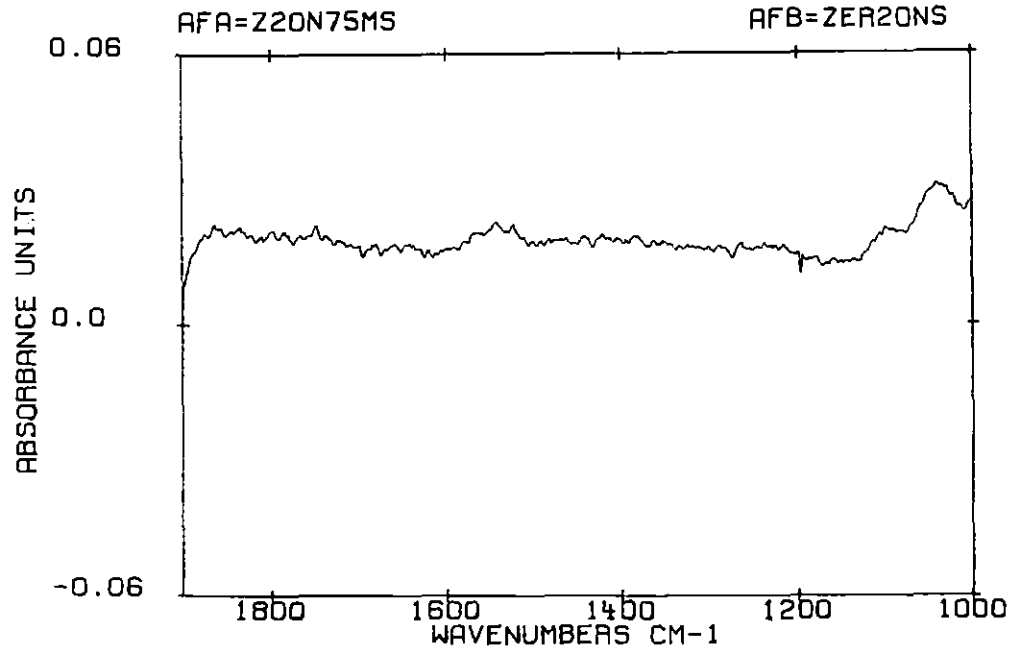

Figure 33f. Spectrum of protein adsorbed onto the 0% filler SR/20% NVP formulation after 75 minutes of blood exposure

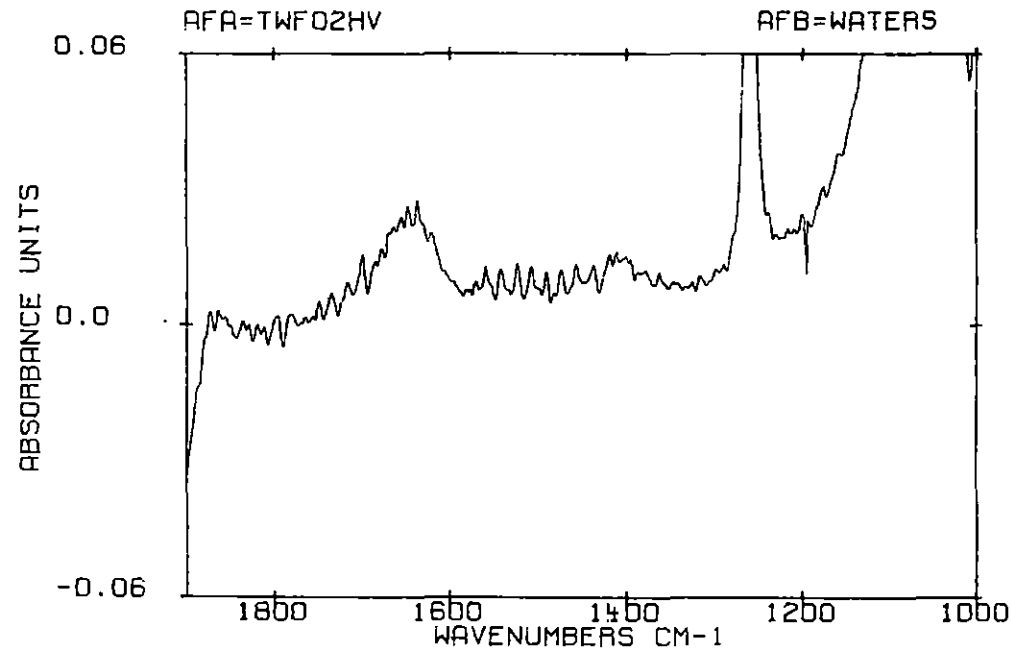

Figure 34a. Spectrum of water vapor and saline subtracted from the 24% filler SR/20% HEMA formulation

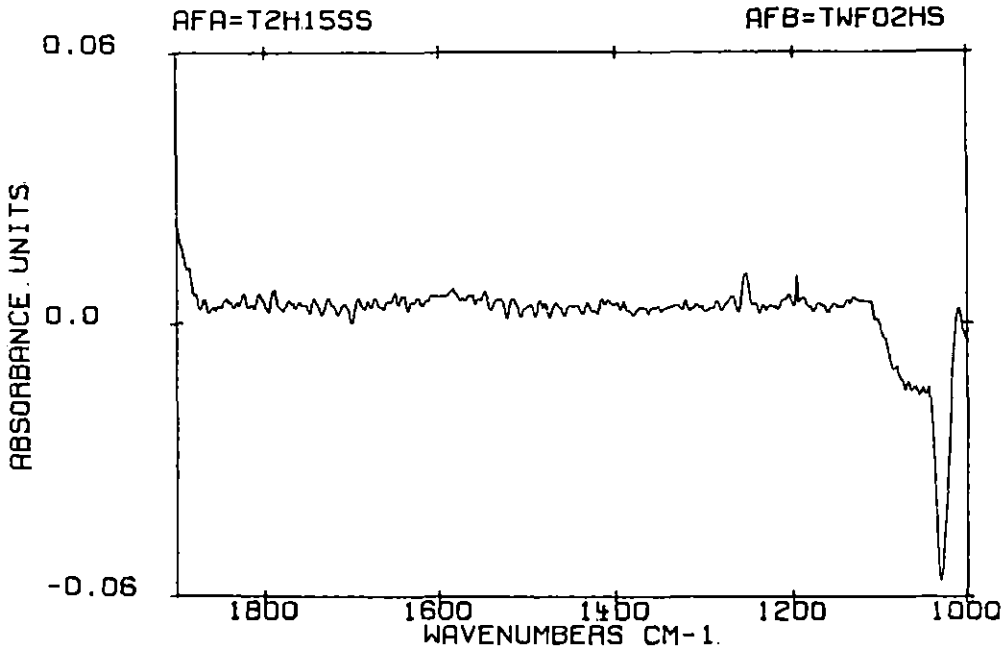

Figure 34b. Spectrum of protein adsorbed onto the 24% filler SR/20% HEMA formulation after 0.25 minute of blood exposure

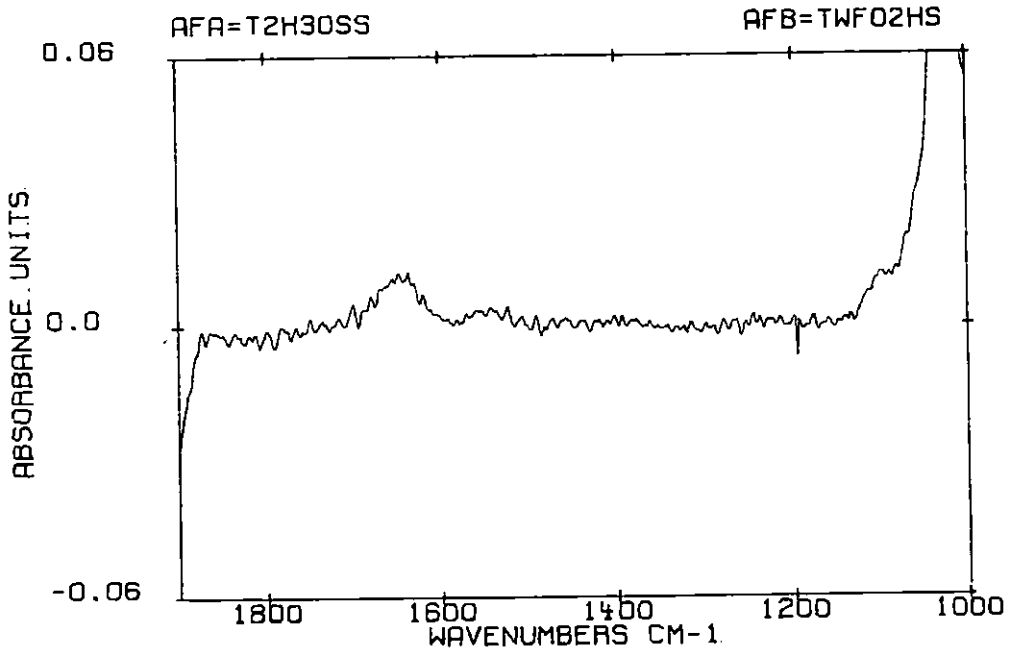

Figure 34c. Spectrum of protein adsorbed onto the 24% filler SR/20% HEMA formulation after 0.5 minute of blood exposure

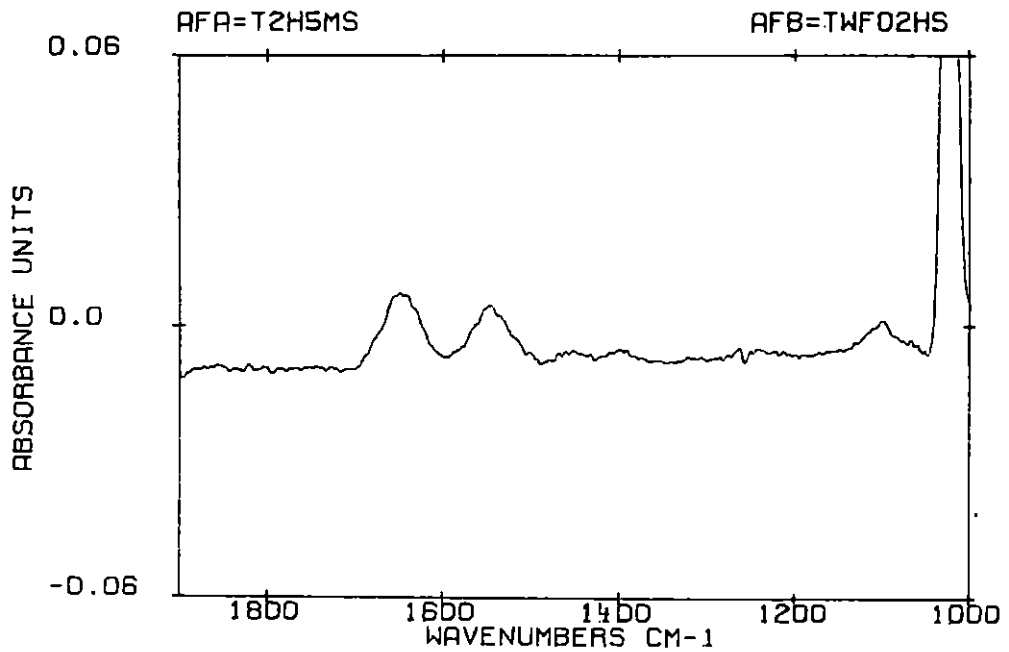

Figure 34d. Spectrum of protein adsorbed onto the 24% filler SR/20% HEMA formulation after 5 minutes of blood exposure

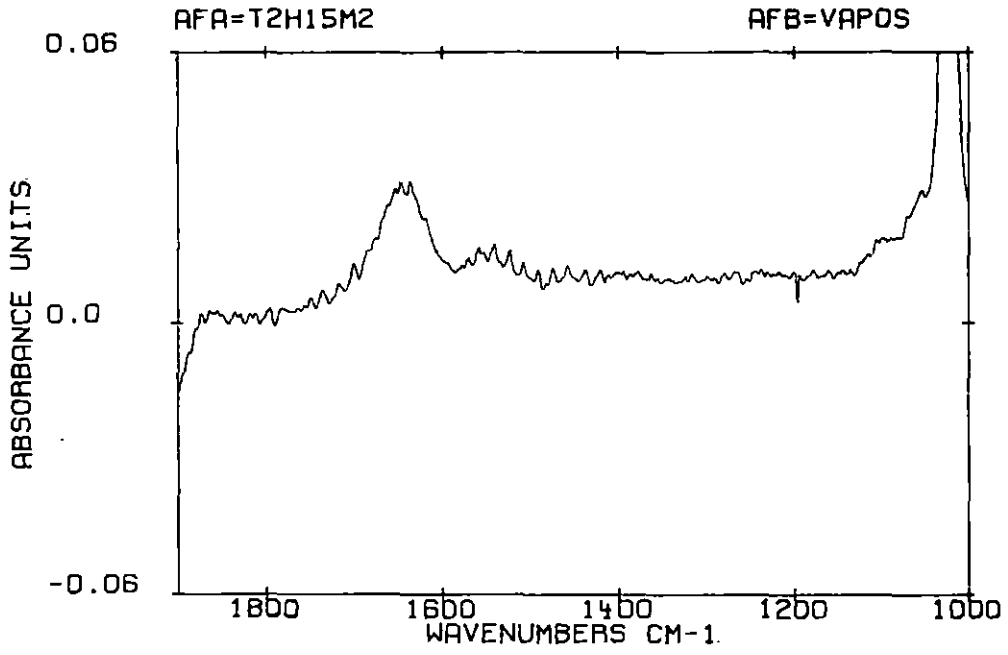

Figure 34e. Spectrum of protein adsorbed onto the 24% filler SR/20% HEMA formulation after 15 minutes of blood exposure

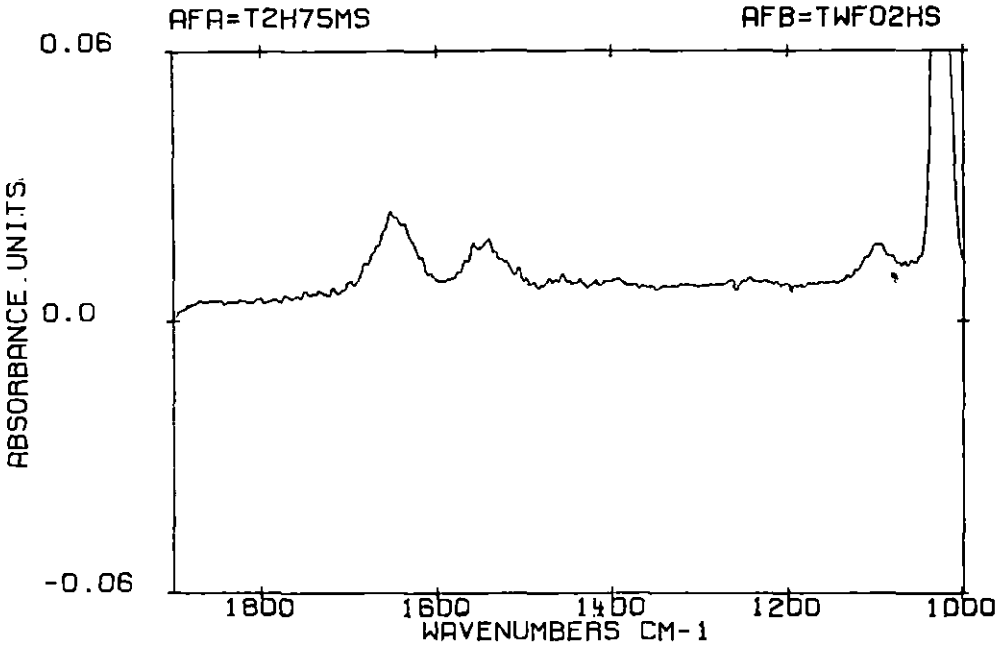

Figure 34f. Spectrum of protein adsorbed onto the 24% filler SR/20% HEMA formulation after 75 minutes of blood exposure

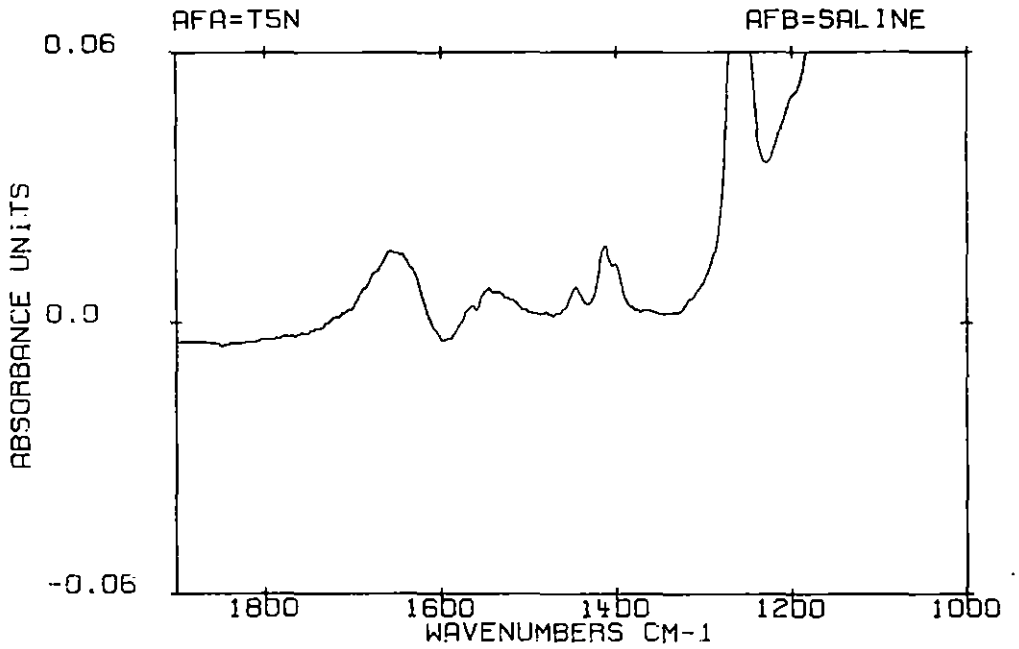

Figure 35a. Spectrum of saline subtracted from the 24% filler SR/15% HEMA/ 5% NVP formulation

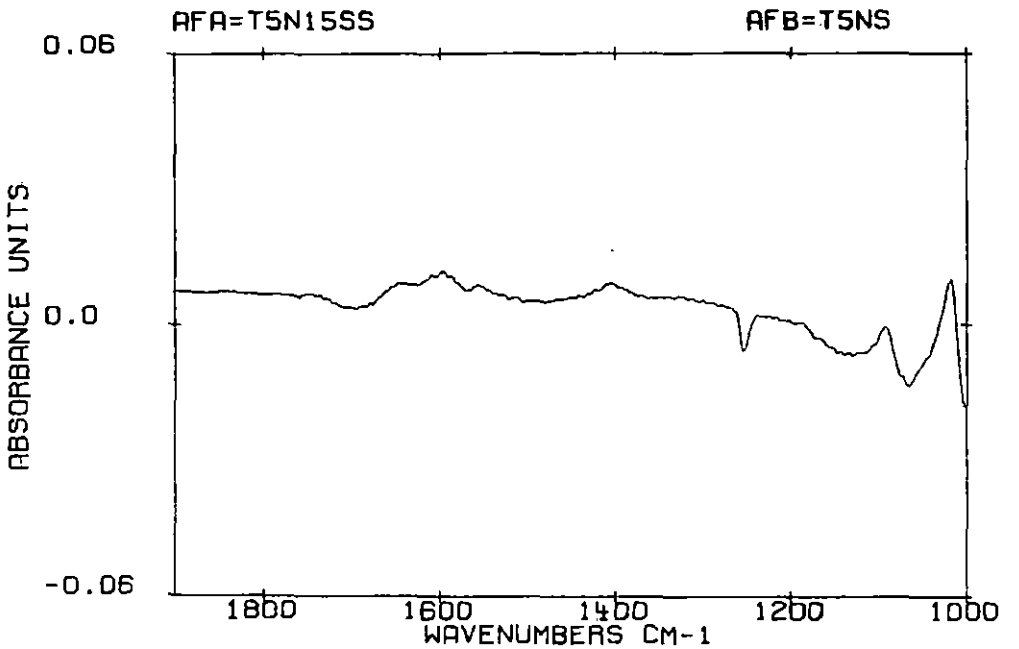

Figure 35b. Spectrum of protein adsorbed onto the 24% filler SR/15% HEMA/ 5% NVP formulation after 0.25 minute of blood exposure

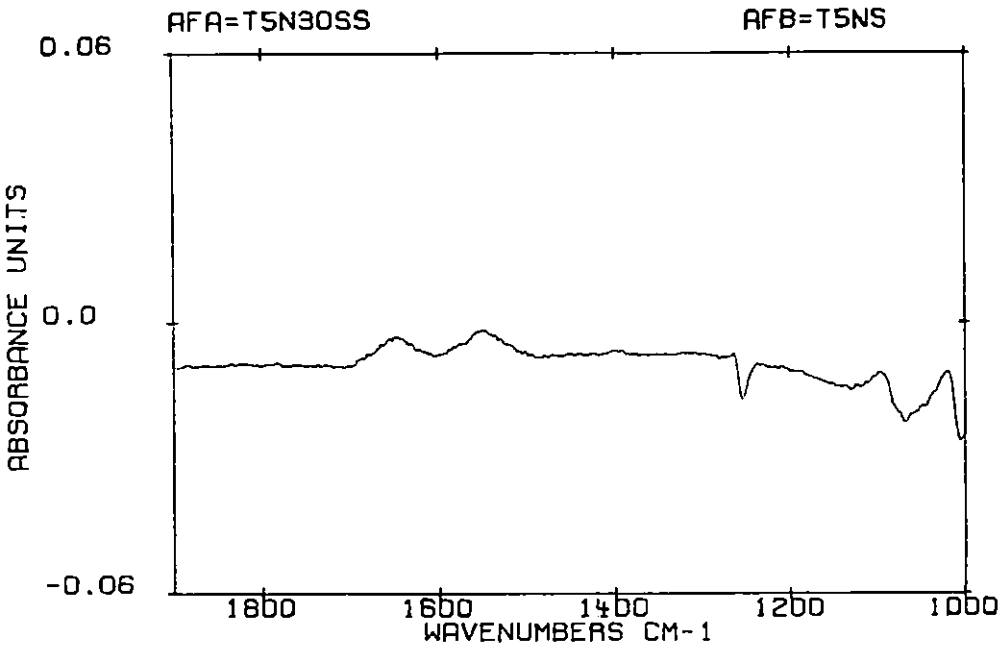

Figure 35c. Spectrum of protein adosrbed onto the 24% filler SR/15% HEMA/ 5% NVP formulation after 0.5 minute of blood exposure

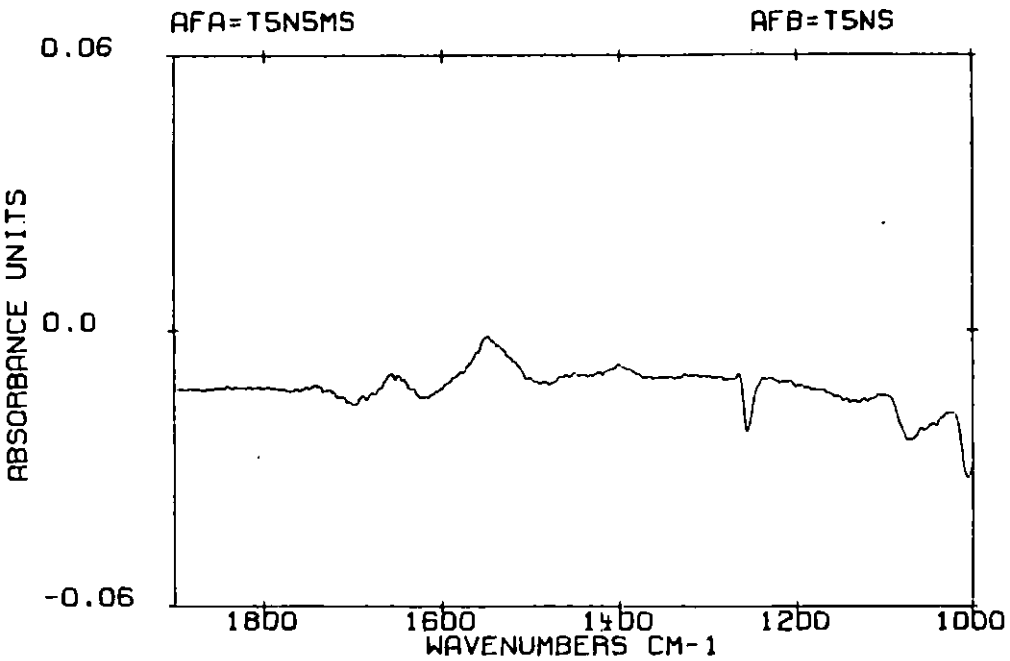

Figure 35d. Spectrum of protein adsorbed onto the 24% filler SR/15% HEMA/ 5% NVP formulation after 5 minutes of blood exposure

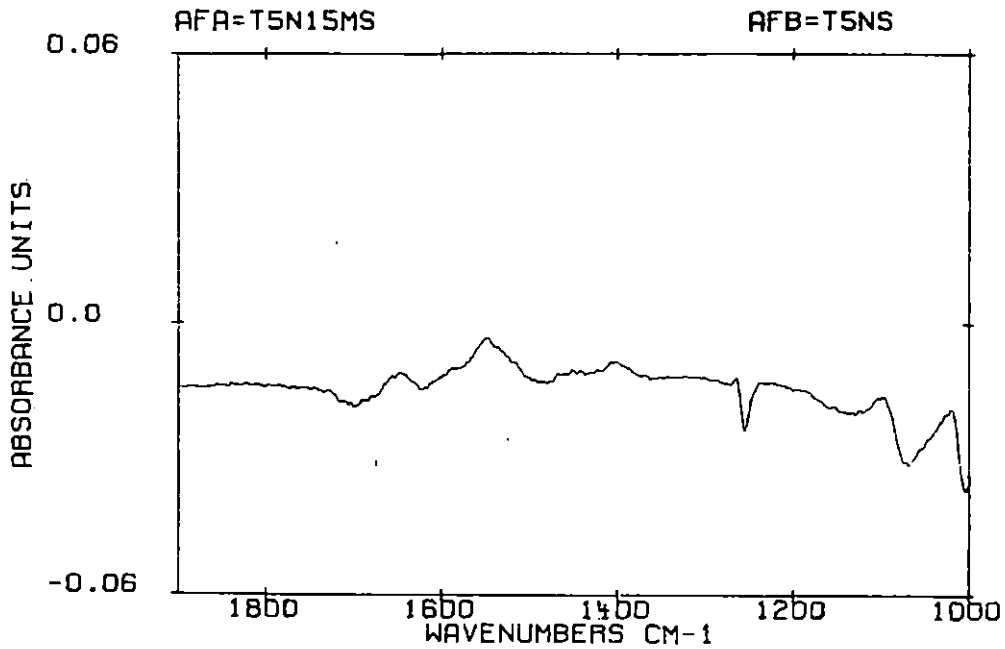

Figure 35e. Spectrum of protein adsorbed onto the 24% filler SR/15% HEMA/ 5% NVP formulation after 15 minutes of blood exposure

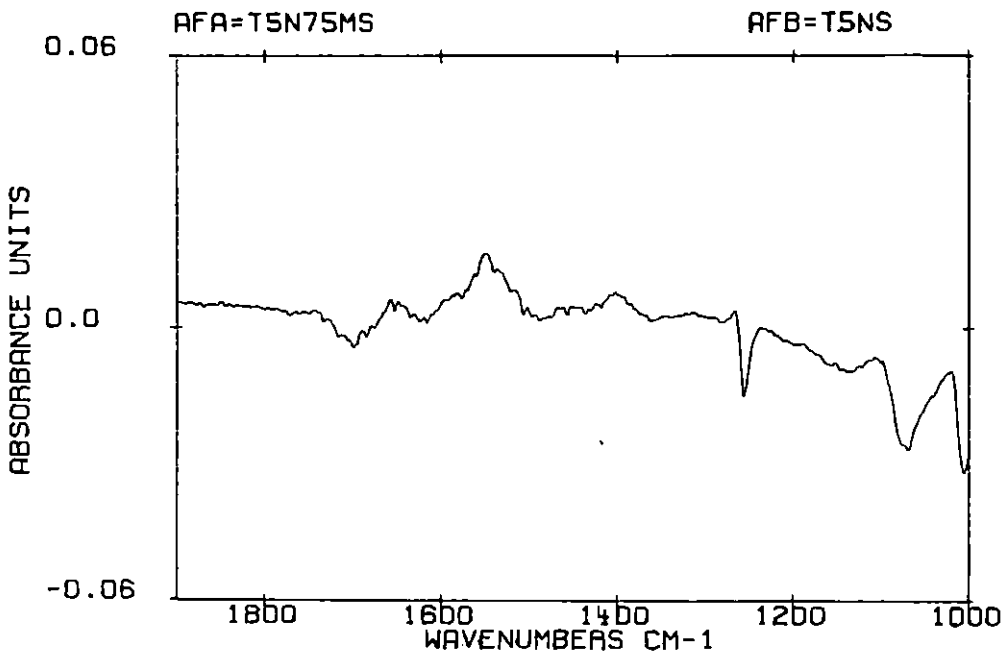

Figure 35f. Spectrum of protein adsorbed onto the 24% filler SR/15% HEMA/ 5% NVP formulation after 75 minutes of blood exposure

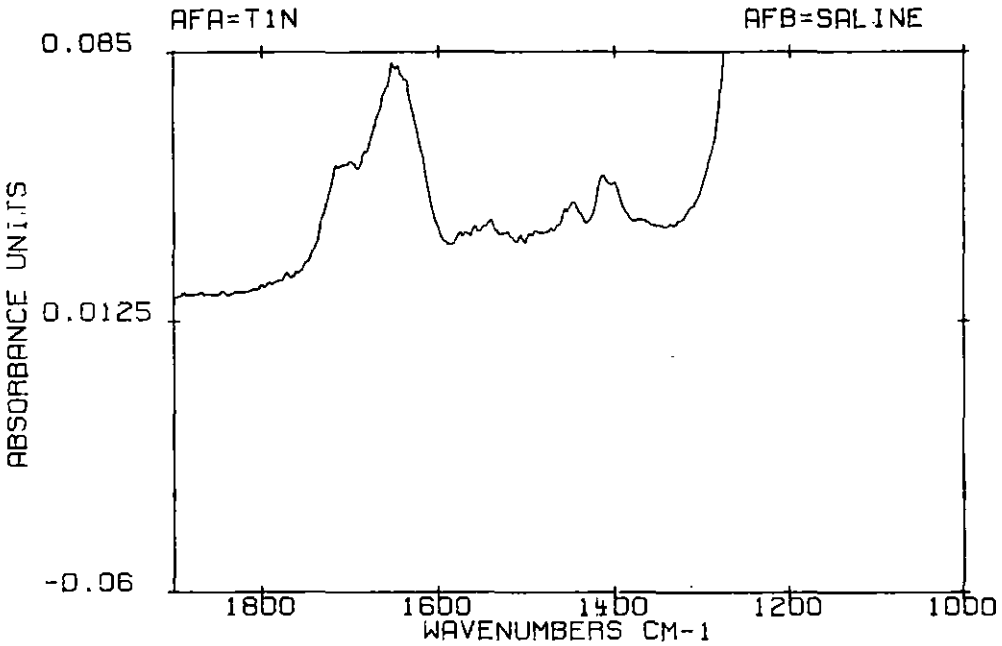

Figure 36a. Spectrum of saline subtracted from the 24% filler SR/10% HEMA/ 10% NVP formulation

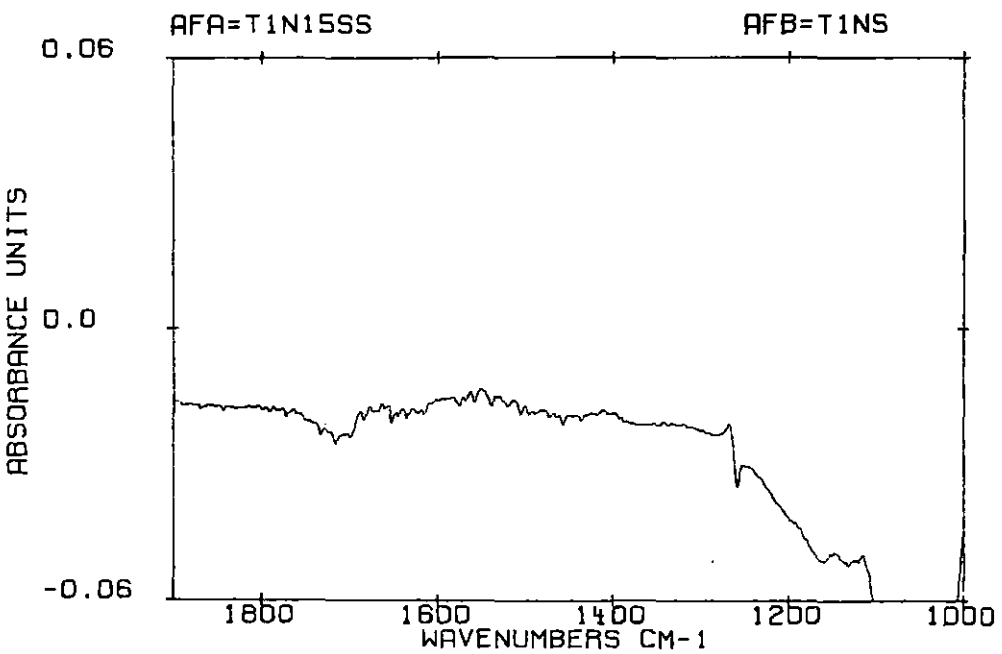

Figure 36b. Spectrum of protein adsorbed onto the 24% filler SR/10% HEMA/ 10% NVP formulation after 0.25 minute of blood exposure

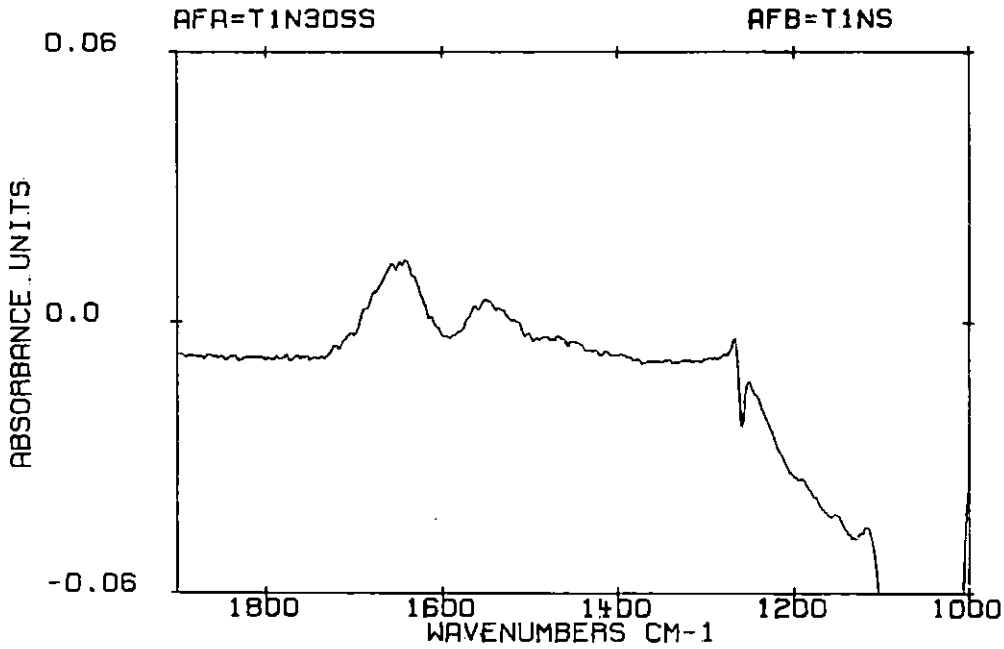

Figure 36c. Spectrum of protein adsorbed onto the 24% filler SR/10% HEMA/ 10% NVP formulation after 0.5 minute of blood exposure

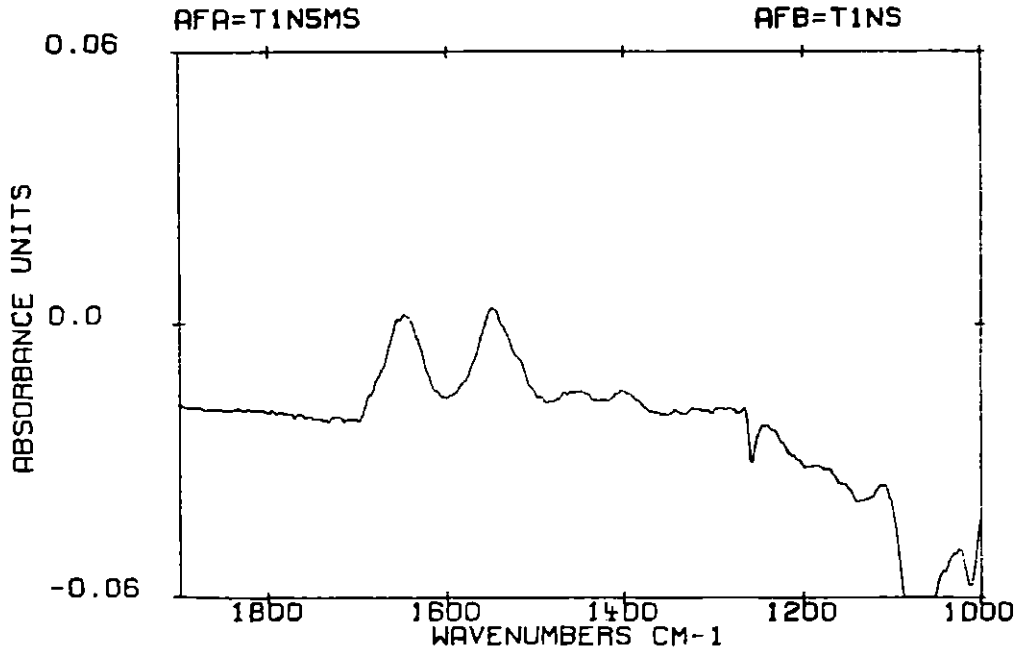

Figure 36d. Spectrum of protein adsorbed onto the 24% filler SR/10% HEMA/ 10% NVP formulation after 5 minutes of blood exposure

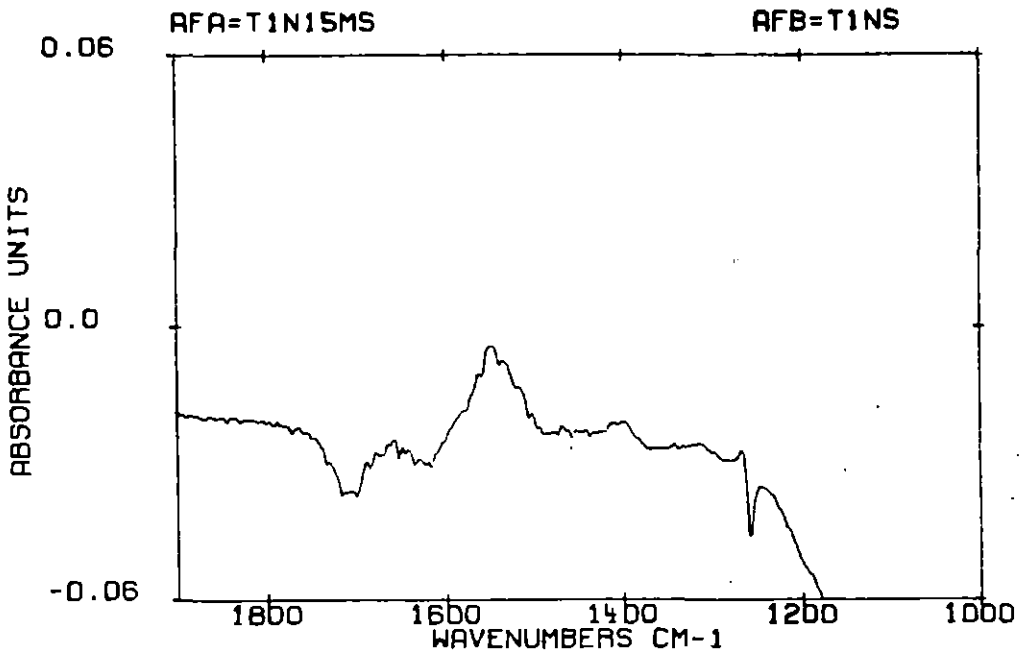

Figure 36e. Spectrum of protein adsorbed onto the 24% filler SR/10% HEMA/ 10% NVP formulation after 15 minutes of blood exposure

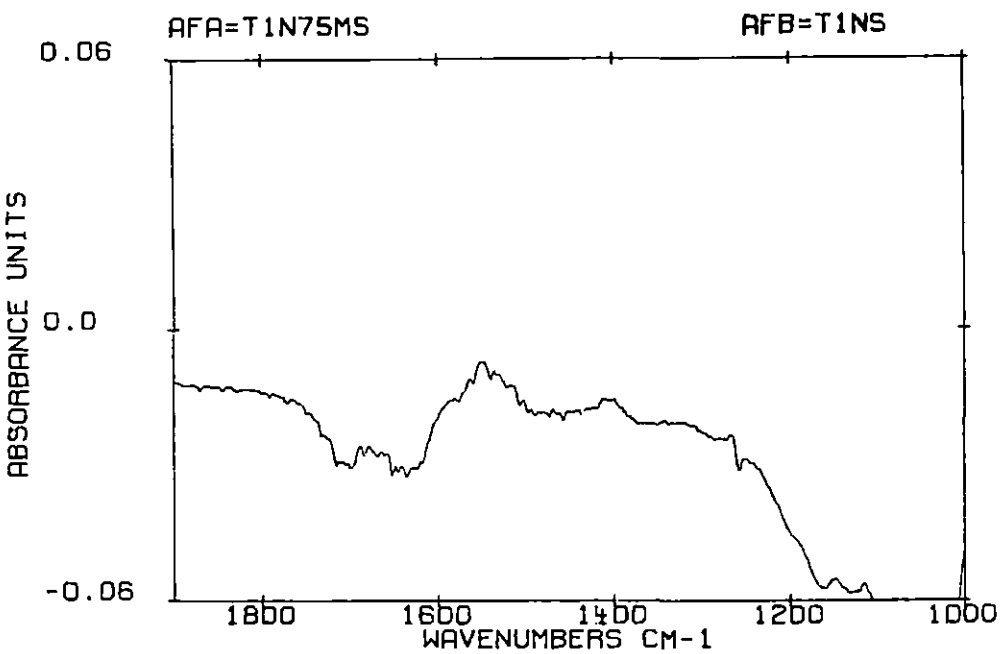

Figure 36f. Spectrum of protein adsorbed onto the 24% filler SR/10% HEMA/ 10% NVP formulation after 75 minutes of blood exposure

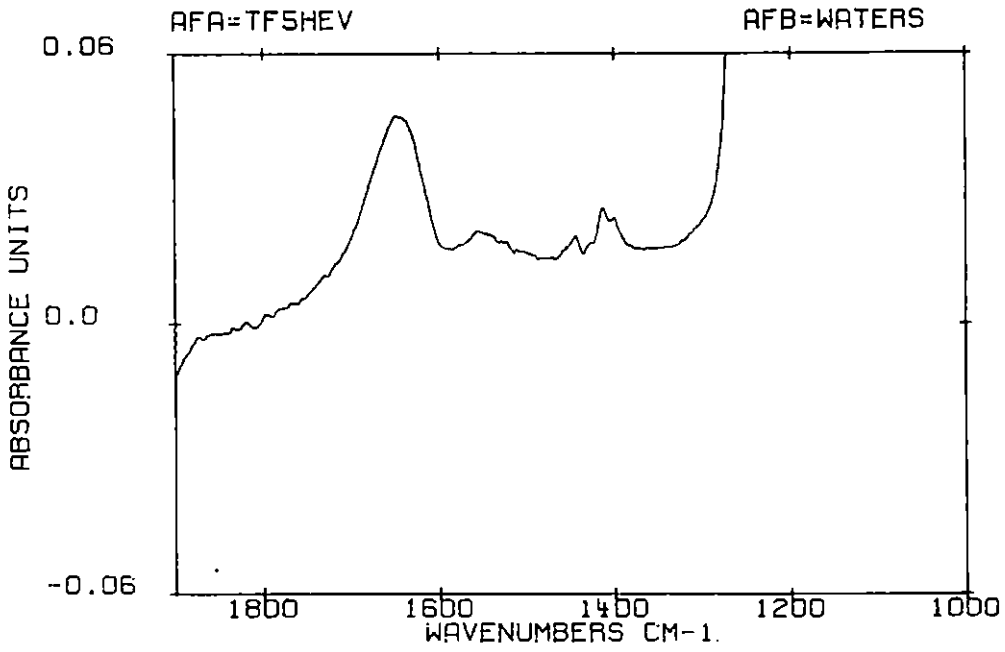

Figure 37a. Spectrum of water vapor and saline subtracted from the 24% filler SR/5% HEMA/15% NVP formulation

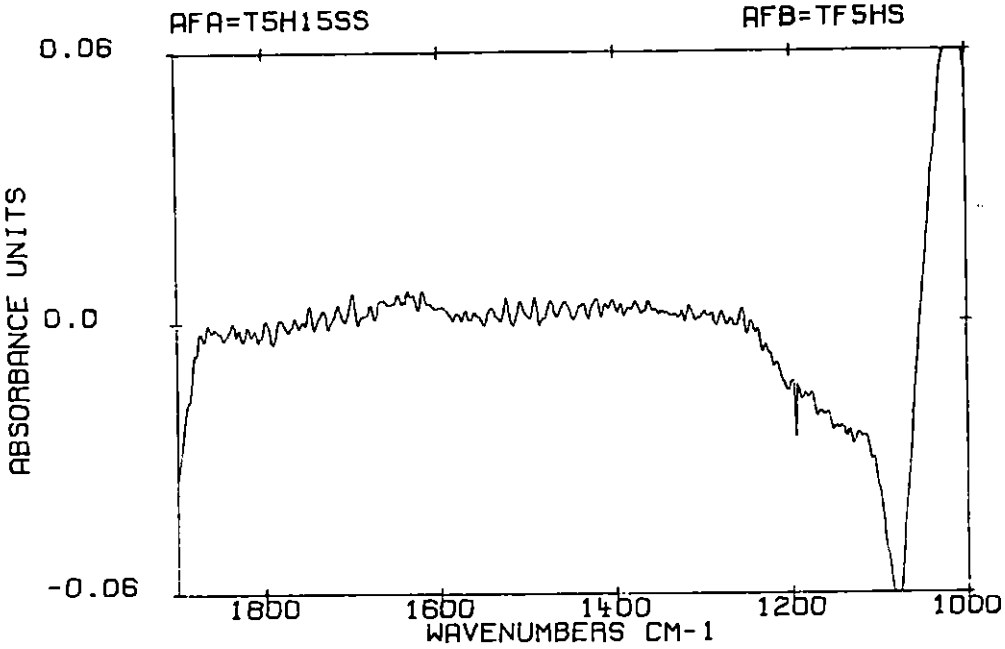

Figure 37b. Spectrum of protein adsorbed onto the 24% filler SR/5% HEMA/ 15% NVP formulation after 0.25 minute of blood exposure

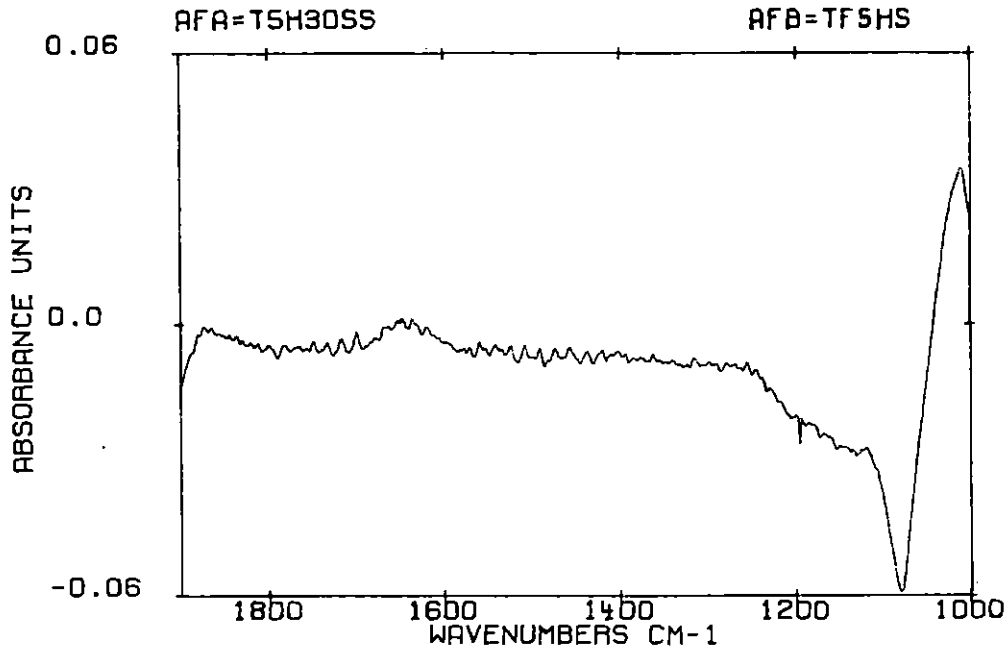

Figure 37c. Spectrum of protein adsorbed onto the 24% filler SR/5% HEMA/ 15% NVP formulation after 0.5 minute of blood exposure

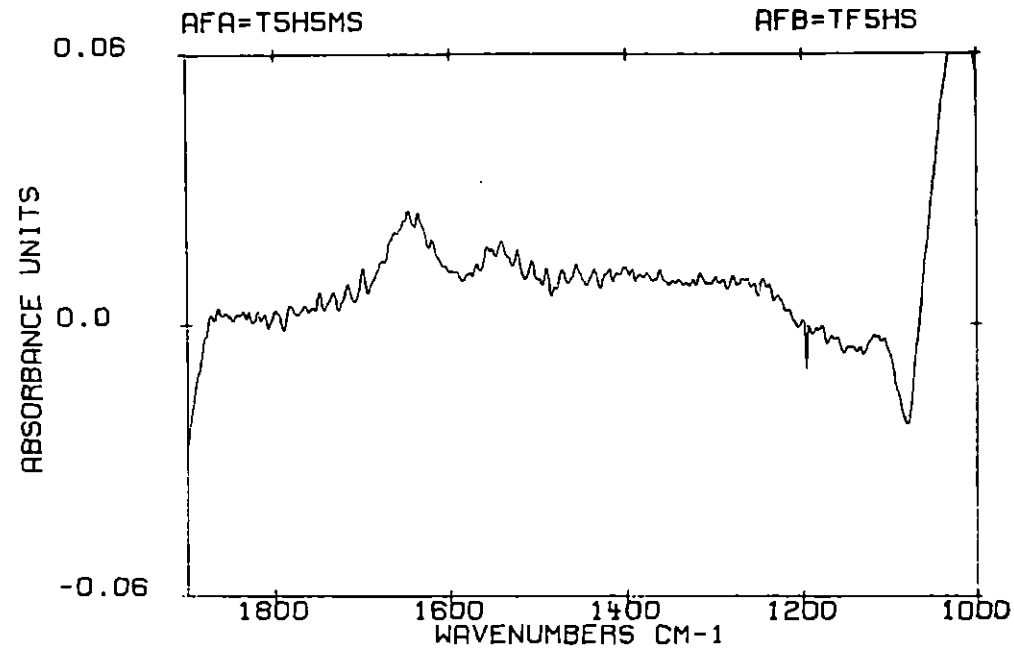

Figure 37d. Spectrum of protein adsorbed onto the 24% filler SR/5% HEMA/ 15% NVP formulation after 5 minutes of blood exposure

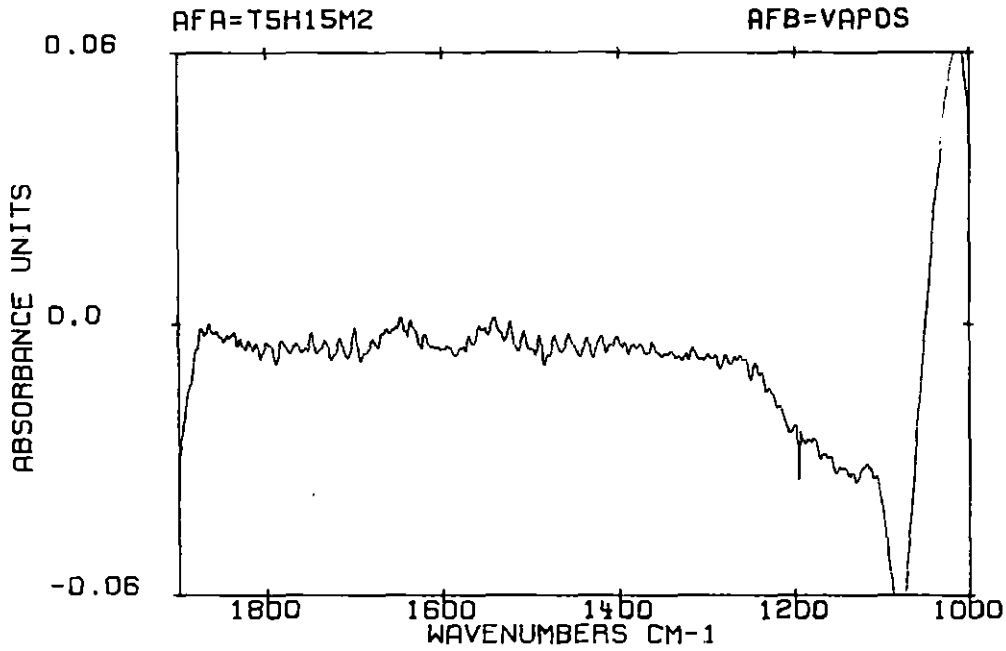

Figure 37e. Spectrum of protein adsorbed onto the 24% filler SR/5% HEMA/ 15% NVP formulation after 15 minutes of blood exposure

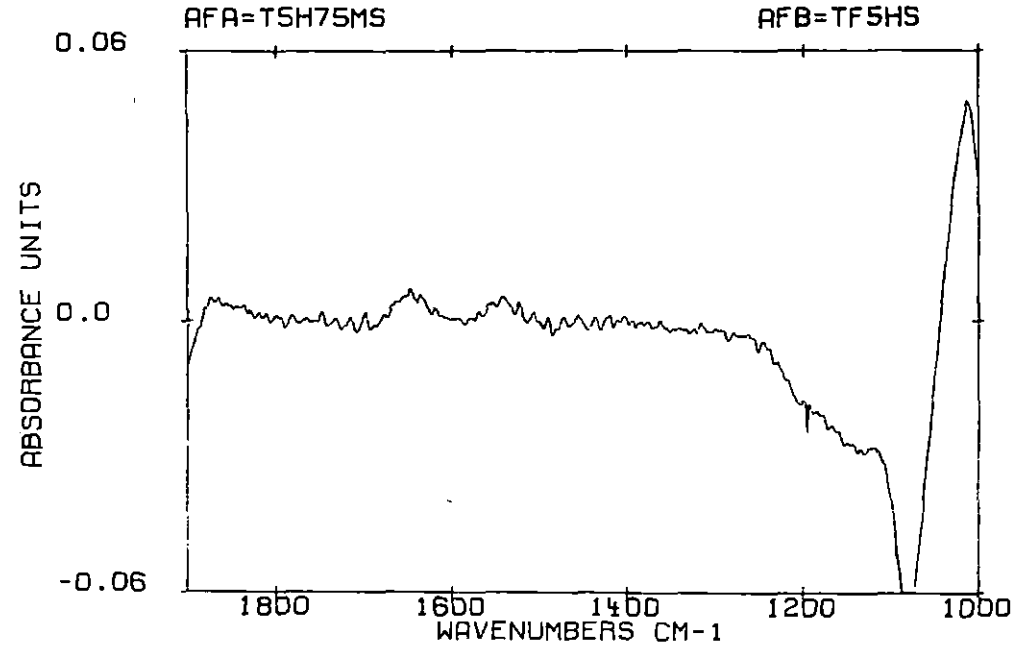

Figure 37f. Spectrum of protein adsorbed onto the 24% filler SR/5% HEMA/ 15% NVP formulation after 75 minutes of blood exposure

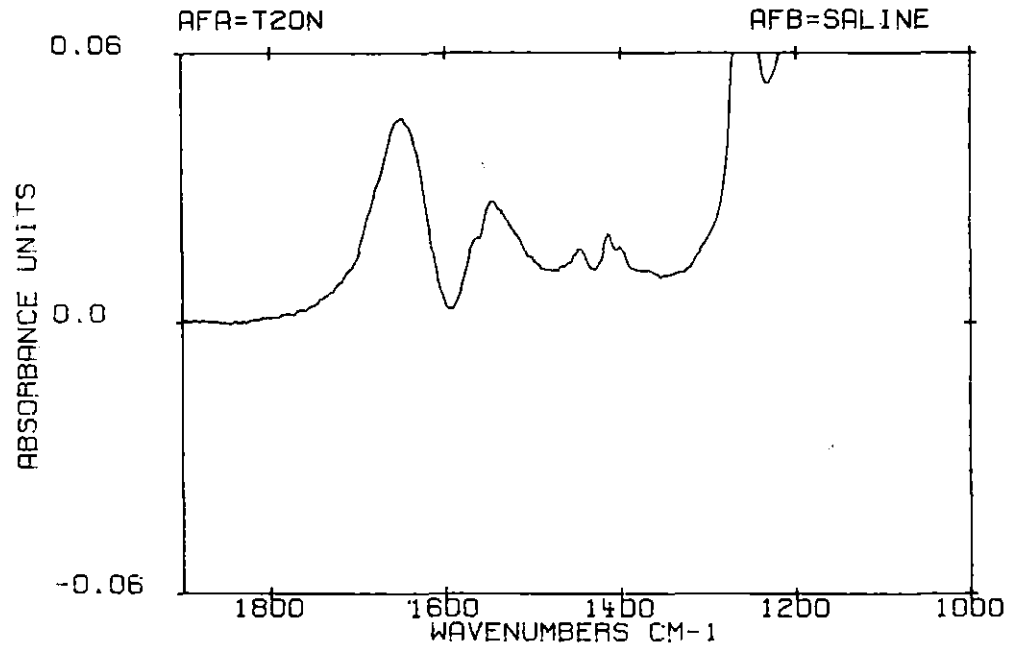

Figure 38a. Spectrum of saline subtracted from the 24% filler SR/20% NVP formulation

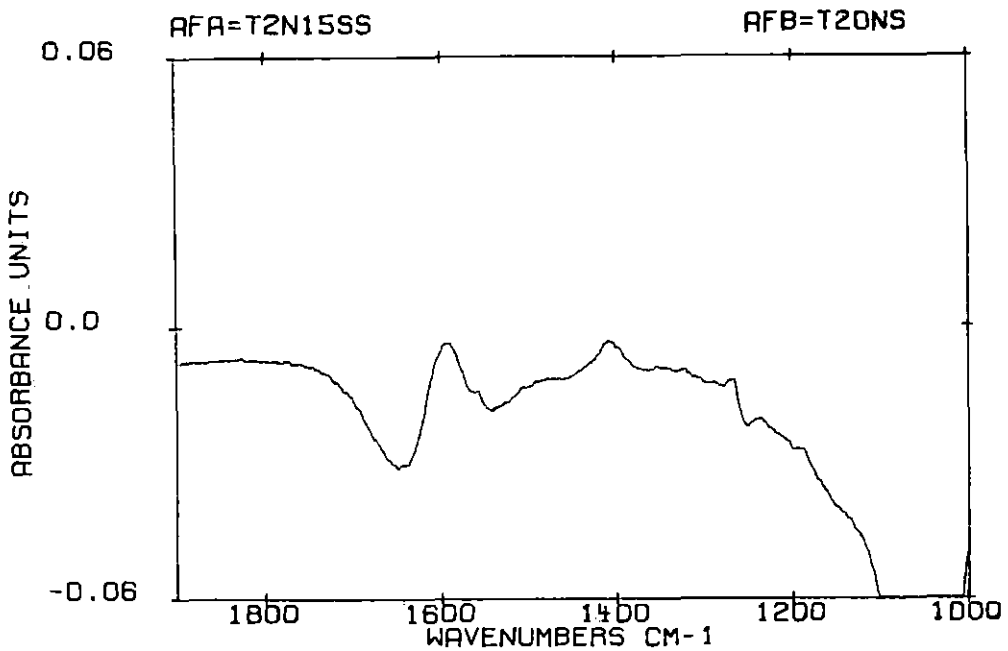

Figure 38b. Spectrum of protein adsorbed onto the 24% filler SR/20% NVP formulation after 0.25 minute of blood exposure

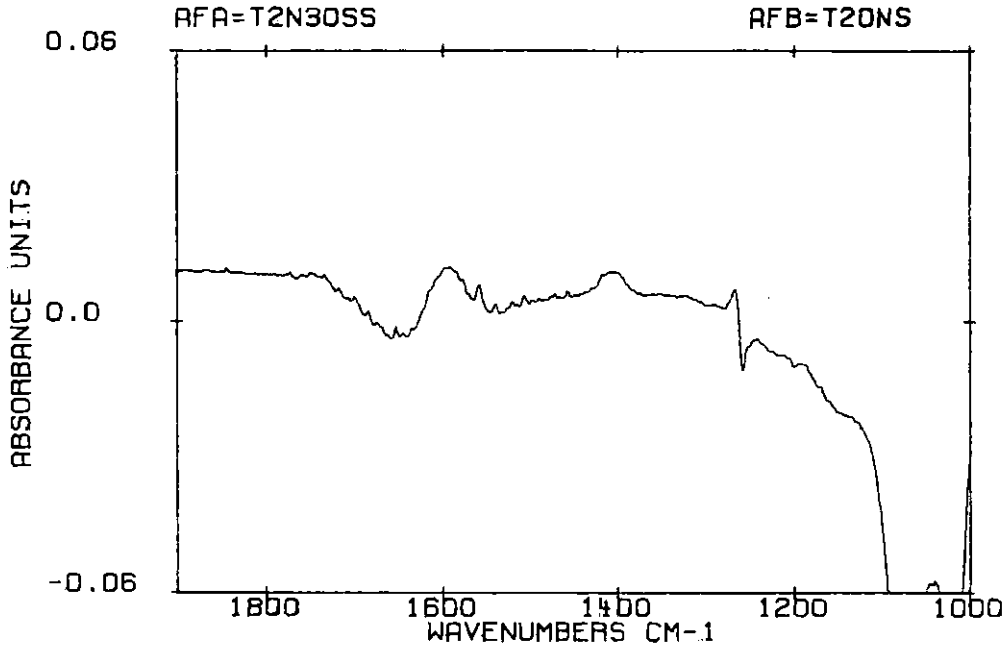

Figure 38c. Spectrum of protein adsorbed onto the 24% filler SR/20% NVP formulation after 0.5 minute of blood exposure

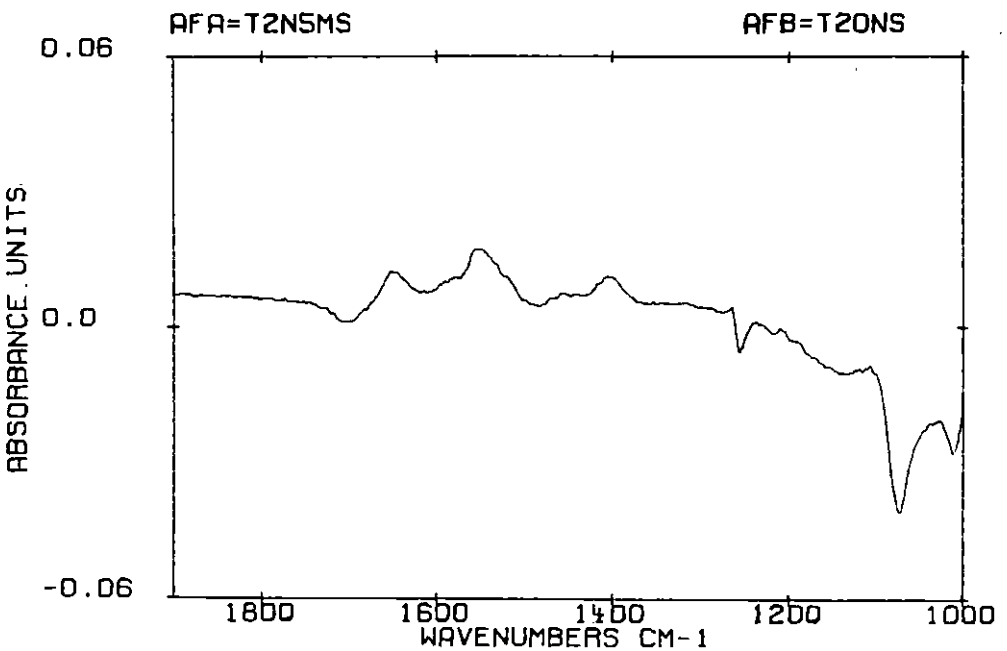

Figure 38d. Spectrum of protein adsorbed onto the 24% filler SR/20% NVP formulation after 5 minutes of blood exposure

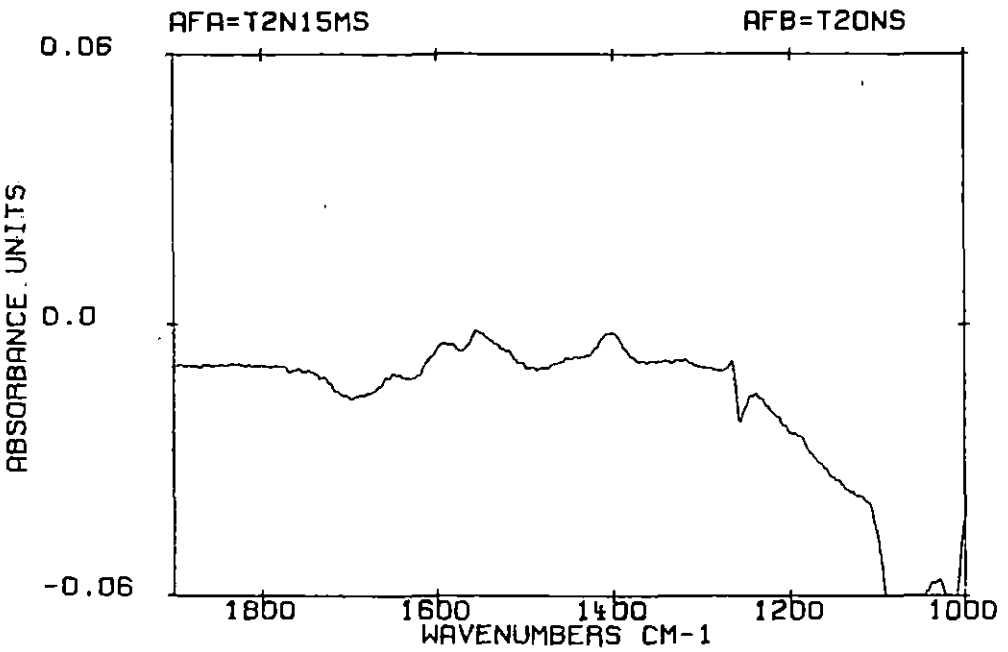

Figure 38e. Spectrum of protein adsorbed onto the 24% filler SR/20% NVP formulation after 15 minutes of blood exposure

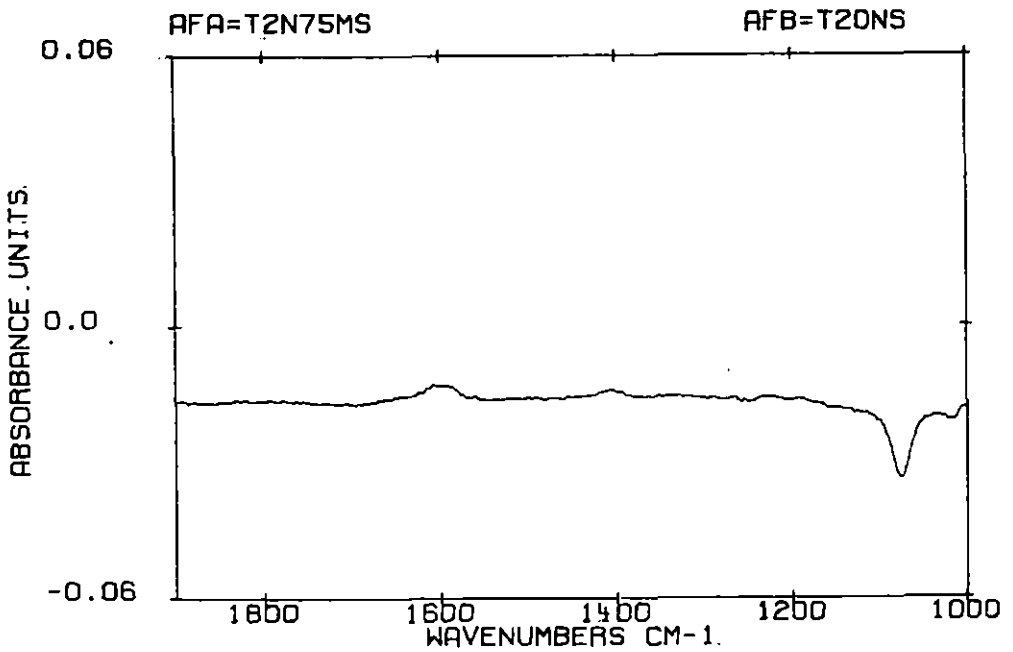

Figure 38f. Spectrum of protein adsorbed onto the 24% filler SR/20% NVP formulation after 75 minutes of blood exposure

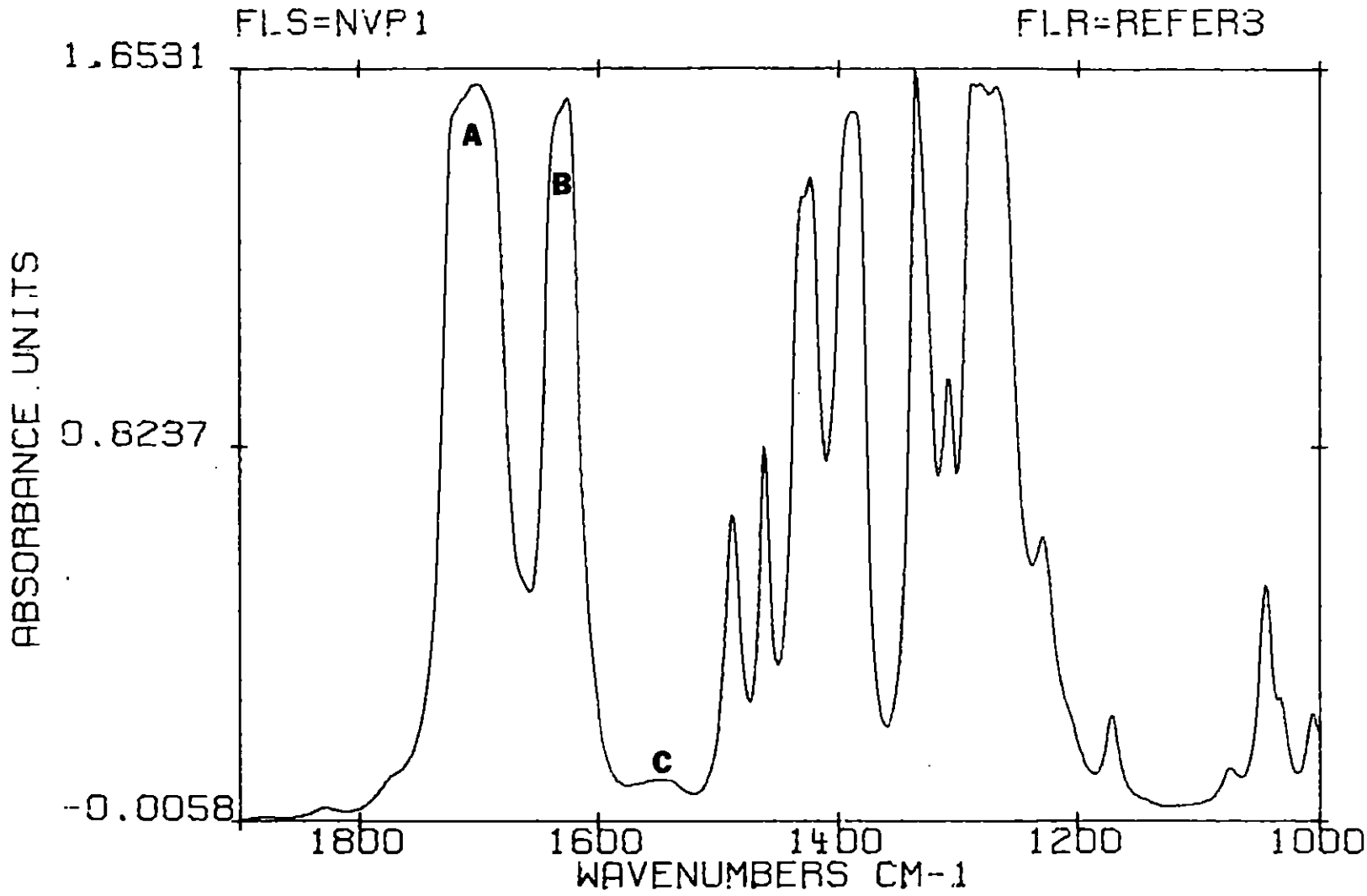

Figure 39. Spectrum of the monomer N-vinyl-pyrrolidone. (A) designates the 1703 cm^{-1} band, (B) designates the 1623 cm^{-1} band, and (C) designates the 1546 cm^{-1} band

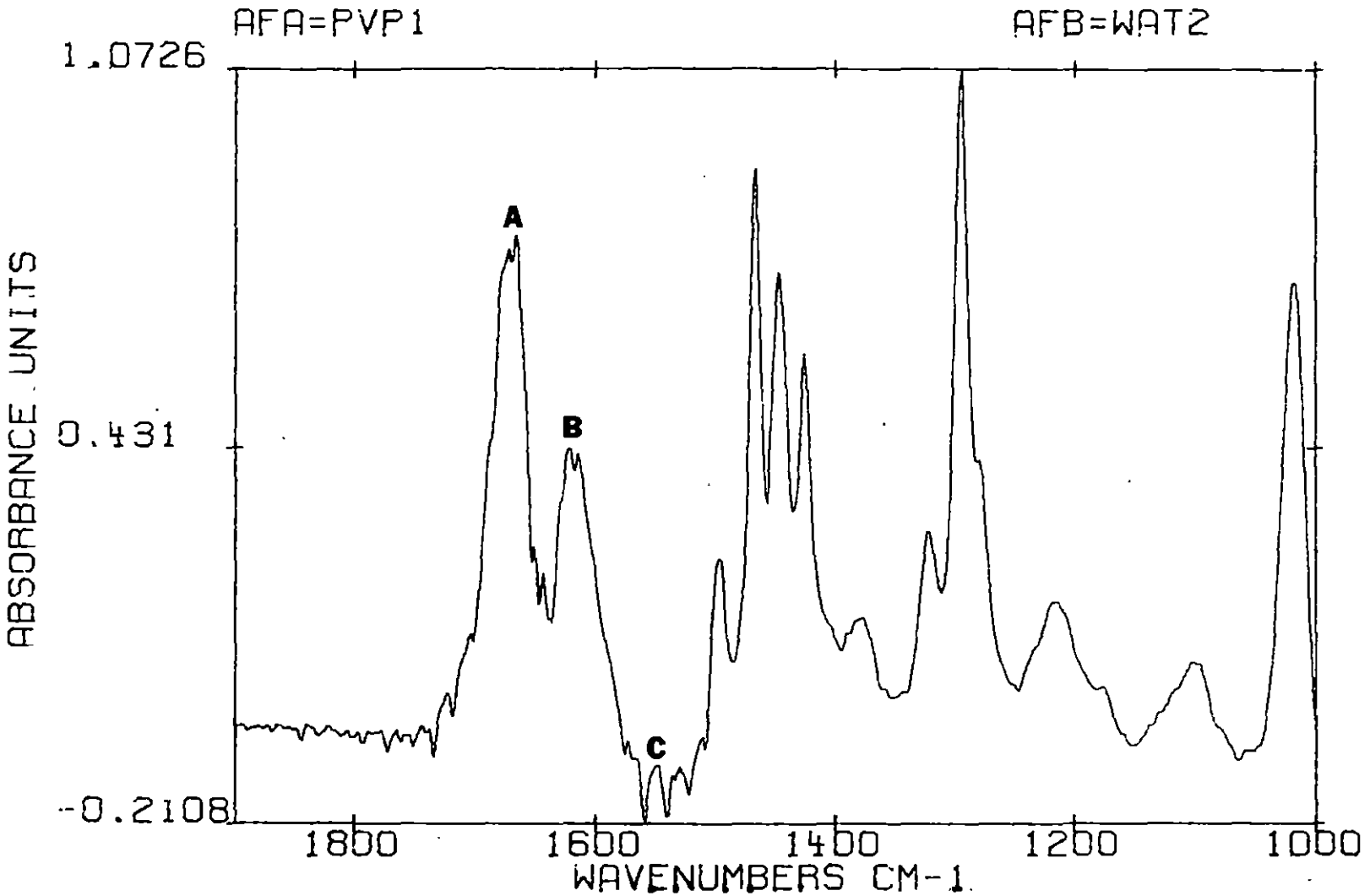

Figure 40. Spectrum of bulk polymerized N-vinyl-pyrrolidone. (A) designates the 1664 cm^{-1} band, (B) designates the 1621 cm^{-1} band, and (C) designates the 1546 cm^{-1} band

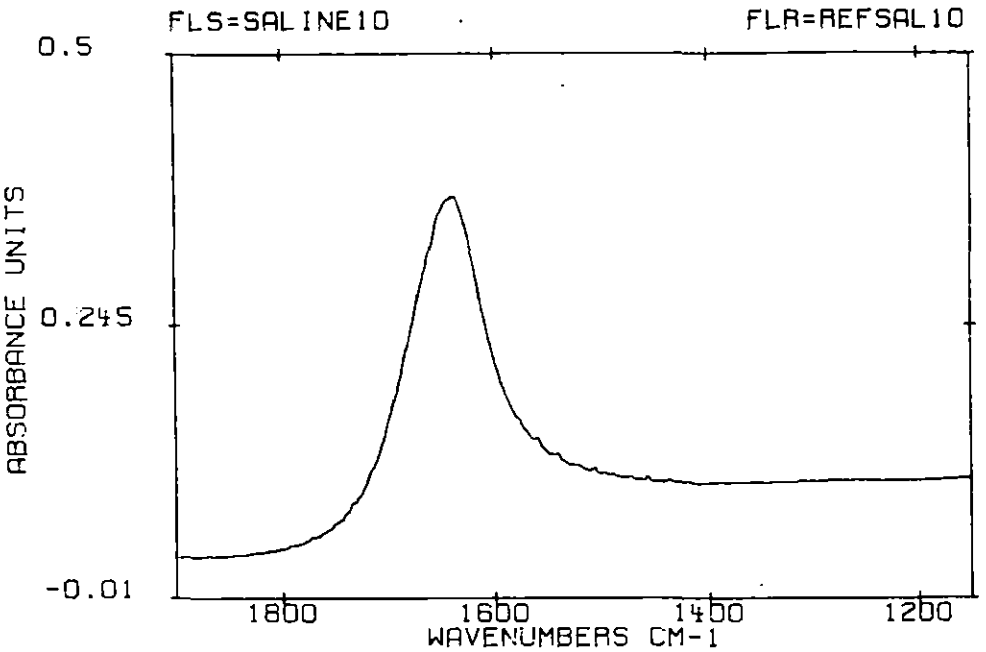

Figure 41. Spectrum of saline

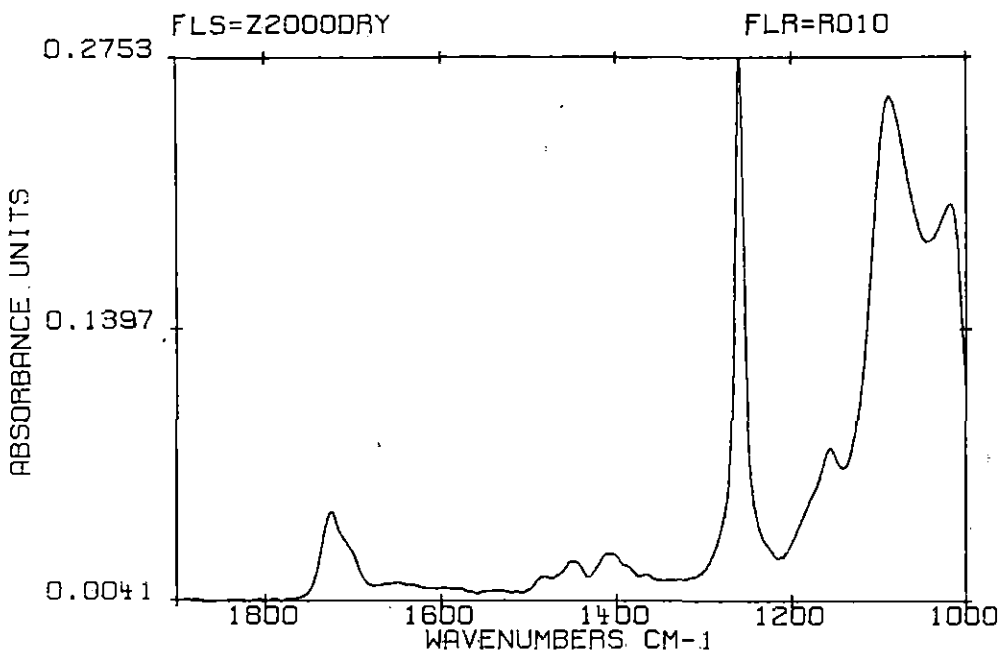

Figure 42. Spectrum of the 0% filler SR/20% HEMA composite, dried and unexposed

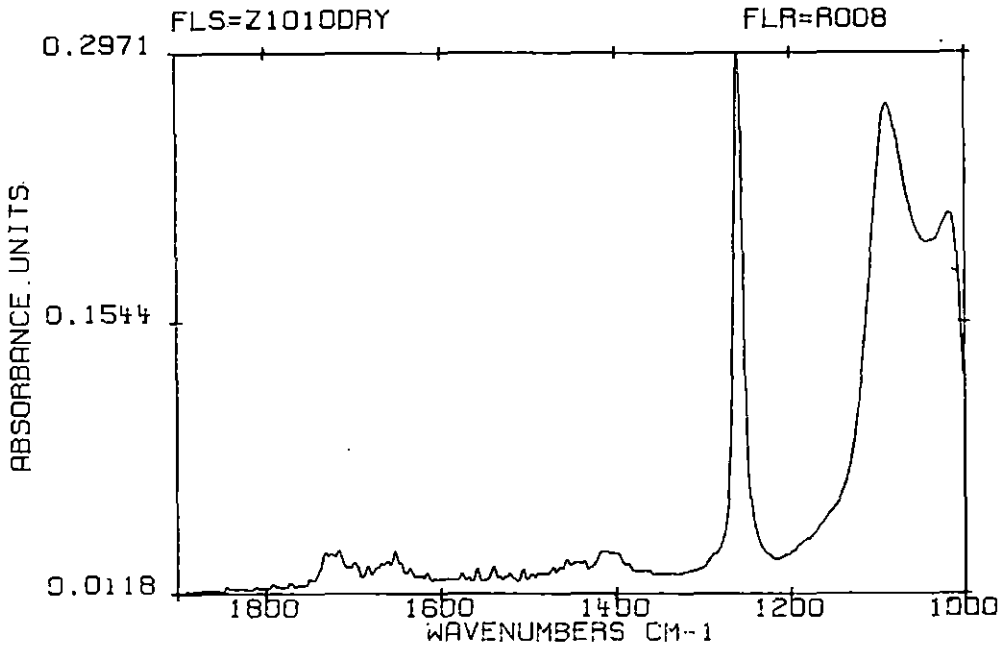

Figure 43. Spectrum of the 0% filler SR/10% HEMA/10% NVP composite, dried and unexposed

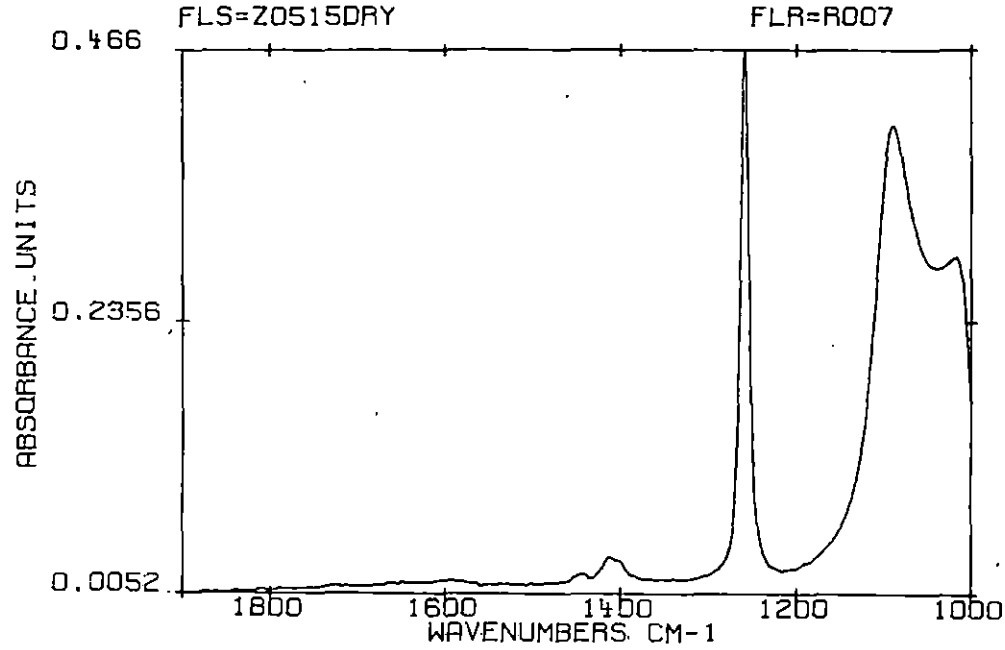

Figure 44. Spectrum of the 0% filler SR/5% HEMA/15% NVP composite, dried and unexposed

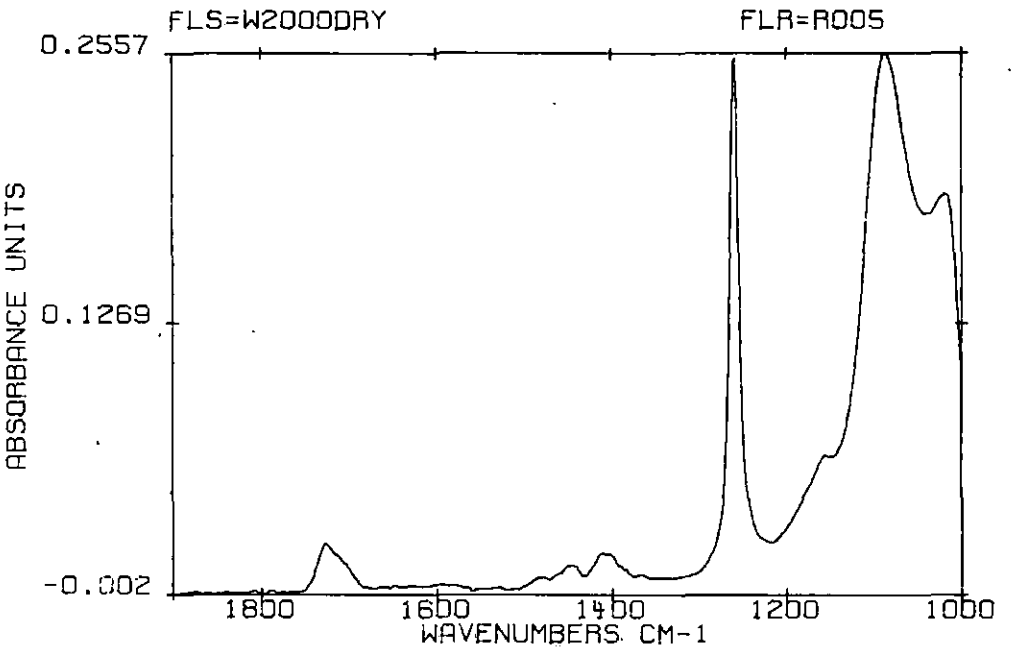

Figure 45. Spectrum of the 24% filler SR/20% HEMA composite, dried and unexposed

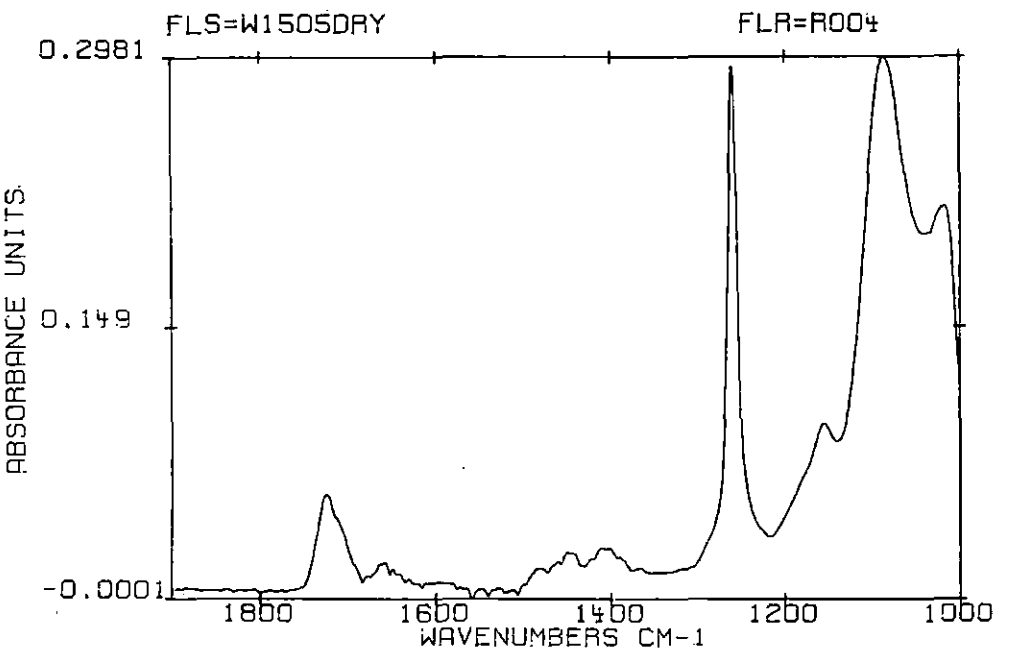

Figure 46. Spectrum of the 24% filler SR/15% HEMA/5% NVP composite, dried and unexposed

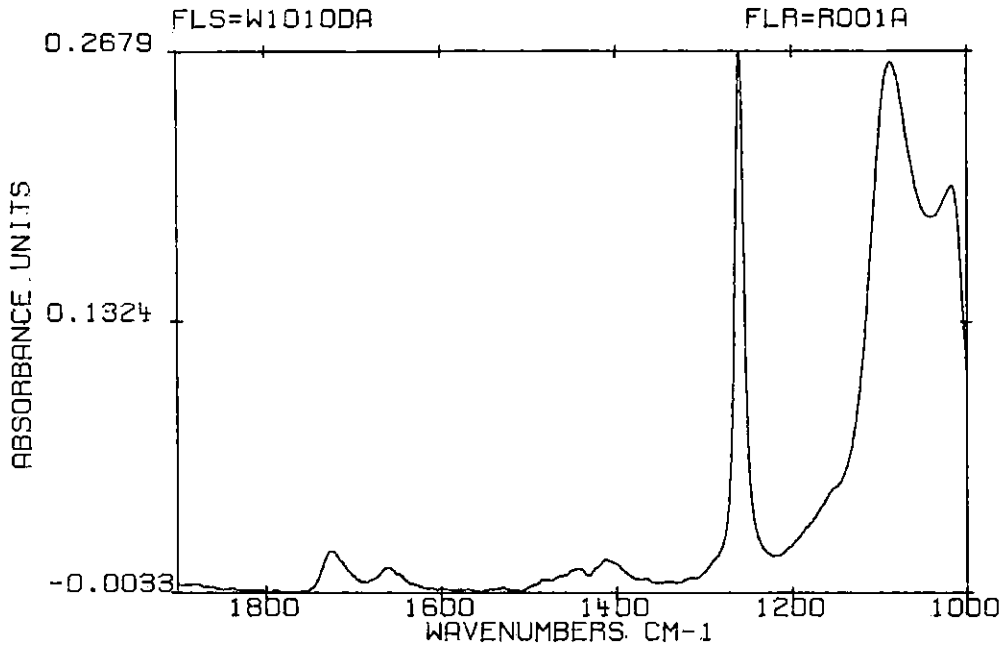

Figure 47. Spectrum of the 24% filler SR/10% HEMA/10% NVP composite, dried and unexposed

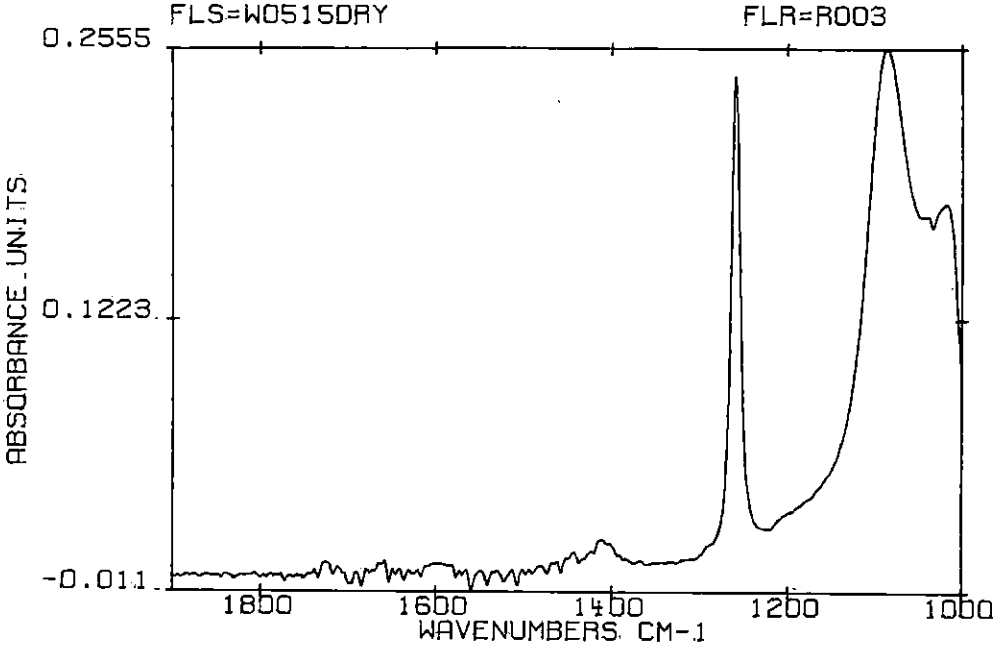

Figure 48. Spectrum of the 24% filler SR/5% HEMA/15% NVP composite, dried and unexposed

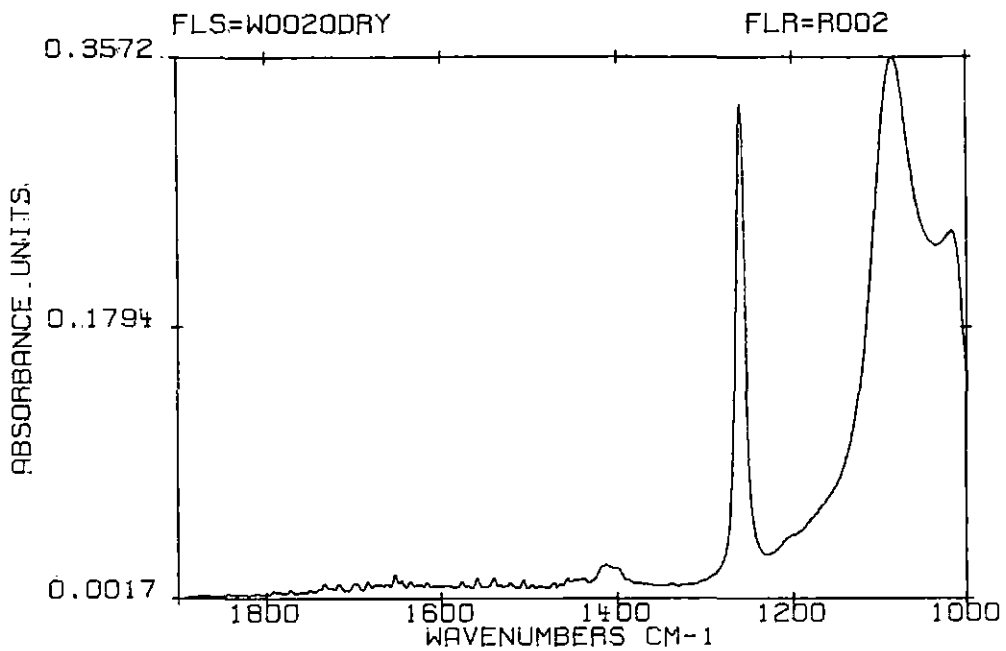

Figure 49. Spectrum of the 24% filler SR/20% NVP composite, dried and unexposed